Imperial College London

Life Cycle Assessment of Silica-derived Adsorbents for Wastewater Treatment

By

Ethan Errington

Department of Chemical Engineering
Imperial College London

Thesis submitted in fulfilment of the requirements for the degree of doctor of Philosophy and the Diploma of Imperial College London

Supervision

First supervisor: Prof. Jerry Yong Yew Heng

Second supervisor: Dr. Miao Guo

Industrial Supervisor: Tamsyn Kennedy

Statement of Originality

I hereby declare that the work presented in this thesis is the result of my own work and has not been submitted to any other university for any other degree. The work of other people used herein has been properly acknowledged and referenced.

Copyright Declaration

The copyright of this thesis rests with the author. Unless otherwise indicated, its contents are licensed under a Creative Commons Attribution-Non Commercial 4.0 International Licence (CC BY-NC).

Under this licence, you may copy and redistribute the material in any medium or format. You may also create and distribute modified versions of the work. This is on the condition that: you credit the author and do not use it, or any derivative works, for a commercial purpose.

When reusing or sharing this work, ensure you make the licence terms clear to others by naming the licence and linking to the licence text. Where a work has been adapted, you should indicate that the work has been changed and describe those changes.

Please seek permission from the copyright holder for uses of this work that are not included in this licence or permitted under UK Copyright Law.

Abstract

Current trends in wastewater pollution are inconsistent with long-term sustainable growth. This is being exacerbated by increases in the presence of emerging wastewater pollutants (EWPs), which existing treatment approaches are often not well-equipped to handle.

Silica-Based adsorbent materials (SBAMs) are one technological solution being investigated as a treatment for a range of environmental pollutants including EWPs. This is because of their desirable material properties, manufacturability, and capacity for surface chemistry modifications – which enable efficient and selective pollutant recovery. Nonethless, the environmental impact (EI) of producing and using SBAMs is still poorly understood.

This work addresses gaps in understanding for the EI associated with SBAM life cycles. This is done using a life cycle assessment (LCA) approach supported by material and energy use estimates developed from a mixture of approaches including literature review (academic and patent), process design modelling, and laboratory experimentation. It culminates in a demonstrative case-study assessing the EI of using SBAMs to recover vegetable oils (an example source of EWP).

Results of the work report EI estimates for a range of materials used in SBAM manufacture, including: 1) silica substrates, 2) silane coupling agents, 3) surface-modified SBAMs, and 4) associated intermediates (e.g. organic surfactants, silicon metals, and chlorosilanes). Findings suggest that silica precursor choice contributes significantly (e.g. 69 and 100%) to the EI of silica substrates produced commercially. Moreover, for emerging methods, silica precursor choice also drives wider changes in predicted SBAM EIs (e.g. 4 to 92 kg-CO_2eq/kg) due to its implications on process design constraints.

Findings suggest that silica precursor choice may be a key factor in reducing the impact of SBAMs produced via emerging methods if they are to compete with commercial manufacturing methods. Similar insights are also provided regarding intermediate materials in SBAM lifecycles (e.g. silica substrates, silane coupling agents, and organic surfactant materials).

Acknowledgements

The completion of this thesis would not have been possible without the support, guidance, and encouragement of many individuals and institutions, which I would like to acknowledge.

Firstly, no work would have been possible without the generous financial support provided by Scottish Water (EPSRC ICASE Award), the EPSRC (project references: EP/R513052/1, NE/W503198/1, and 2293053), the Grantham Institute for Climate Change (SSCP DTP), and Imperial College London's Transition to Zero Pollution initiative. The funding provided has not only allowed me to focus on my research but removed financial pressures during times of great uncertainty.

Secondly, I would like to express my sincere gratitude to my academic supervisors, Prof. Jerry Heng and Dr. Miao Guo, for their support, insights, and patience throughout our time together. Their trust and confidence has been pivotal in allowing me to shape this work in my own direction. I am honoured to have had the opportunity to meet you both and to have learned from you. I will not forget the opportunities that both have provided for me.

Thirdly, I am deeply grateful to many friends that I have made and kept during my study. This includes Jacqui and James for the levity that they have brought; Craig, for the grounding and perspective that he has always provided; and Alex, who has been a dear friend and sounding board throughout the whole experience. Thank you also to Liam and Kayleigh, and Ben and Emma, who have helped me selflessly in dire times.

Fourthly, I would like to acknowledge my family, who have been a constant source of strength during my journey. To Eileen, for her unconditional love; to Tracey, who has always held the unit together; and to Francis, without whom everything has changed.

Fifthly, I would like to acknowledge the many members of my research group, who have enriched my time at Imperial. Particularly to Vivek, Hamish, and Isha, who have had the (mis)fortune of listening to many rants on topics unrelated to their own work; Deniz, who has helped me find confidence in fields where I had none; Frederik, my original office buddy**;** and Ian, who made the whole journey possible.

Finally, I am deeply grateful to Kimberley, who has experienced much of the ups and downs, supported me through much of it, and helped me see beyond the technical detail.

For Francis,

Now I must learn to drive.

Publications from this Research

A list of all publications achieved throughout the time of study are published below. This includes some collaborations based on topics that have not made it into the thesis to ensure a clear narrative.

In this work

[1] Errington, E., Guo, M. and Heng, J.Y.Y. "Synthetic amorphous silica: Environmental impacts of current industry and the benefit of biomass-derived silica." *Green Chemistry* 25.11 (2023): 4244-4259.

[2] Errington, E, Guo, M. and Heng, J.Y.Y. "Environmental Impacts of Rice Husk-Derived Silica under Uncertainty: Is “Bio” better?" *Computer Aided Chemical Engineering*. Vol. 51. Elsevier, (2022). 1615-1620.

[3] Errington, E., Guo, M. and Heng, J.Y.Y. "Environmental Impacts of Bio-derived Silicon: Uncertainty in the Benefit of Industrial Transition." *Computer Aided Chemical Engineering*. Vol. 52. Elsevier, (2023). 2255-2260.

Beyond this work

[4] Guo M., Guo, Rosbottom, I., Zhou, L., Yong, C.W., Zhou, L., Yin, Q., Todorov, I.T., Errington, E. and Heng. J.Y.Y. "Triglycine (GGG) Adopts a Polyproline II (pPII) Conformation in Its Hydrated Crystal Form: Revealing the Role of Water in Peptide Crystallization." *The Journal of Physical Chemistry Letters* 12.34 (2021): 8416-8422.

[5] Link, F.J., Errington, E., Verma, V., and Heng, J.Y.Y. "The role of mixing and surface hydrophobicity on the operation of a continuous tubular slug flow crystalliser for lysozyme." *Chemical Engineering Journal* 471 (2023): 144363.

[6] Verma, V., Mitchell, H., Ethan Errington, Guo, M., and Heng, J.Y.Y. "Templated crystallization of glycine homopeptides: experimental and computational developments." *Chemical Engineering & Technology* 46.6 (2023): 1271-1278.

[7] Mitchell, H., Verma, V., Errington, E., Guo, M., Guinn, E.J., and Heng, J.Y.Y. "Experimental and Computational Insights into the Homogeneous and Heterogeneous Crystallisation Behaviour of Glycine Homopeptides." *2023 AIChE Annual Meeting*. AIChE, 2023.

Additionally, a number are also in some stage preparation. These are summarised as follows.

In Preparation

[8]Gosiamemang, T., Errington, E., Kalha, C., Etit, D., Regoutz, A. and Heng, J.Y.Y. Room temperature acid catalysed silanisation of silica nanoparticles in non-polar organic solvents.

[9] Errington, E., Guo, M., and Heng, J.Y.Y. “Sol-Gel Silica: Environmental Impacts and Green Metrics of Stöber, MCM, SBA and Bio-inspired Products”.

[10] Errington, E., Guo, M., and Heng, J.Y.Y. “Silane Coupling Agents: Environmental Impact of Trichlorosilane, Aminopropyltriethoxysilane (APTES), and Octyltrimethoxysilane (OTMS)”.

[11] Errington, E., Lorentz, C., Guo, M., and Heng, J.Y.Y. “At the INTERACE: The effect of water model and parameterization choice on Water Dynamics near the surface of silica predicted by the INTERFACE force-field”.

Presentations from this Research

A list of external presentations carried out throughout this work are provided below. This includes an invited talk to at the University of Cambridge (see [2]) and an award-winning poster presentation (see [5]). Info on additional presentations not included in the scope of the thesis is also provided.

In this work

[1] Errington, E., Guo, M., and Heng, J.Y.Y. "Environmental Impacts of Rice Husk-Derived Silica under Uncertainty: Is "Bio" better?". European Symposium on Computer Aided Process Engineering – ESCAPE 32. 2022.

[2] Errington, E., Guo, M., and Heng, J.Y.Y. "Environmental Impacts of Rice Husk-Derived Silica under Uncertainty: Is "Bio" better?". University of Cambridge (Invited Talk). 2022.

[3] Errington, E., Guo, M., and Heng, J.Y.Y. Rational Design of oil-in-water sorbents: Life cycle assessment, experimentation, and surface modelling. Imperial College London Department of Chemical Engineering PhD Symposium. 2023.

[4] Errington, E., Guo, M., and Heng, J.Y.Y. "Environmental Impacts of Bio-derived Silicon: Uncertainty in the Benefit of Industrial Transition". European Symposium on Computer Aided Process Engineering – ESCAPE 32. 2023.

[5] Errington, E., Guo, M., and Heng, J.Y.Y. "Effect of Surface Chemistry on the Performance of Silica-based Oil Sorbents, Oil Sorption Capacity, Carbon Footprint and Water use". ChemEngDayUK2023. 2023.

[6] Errington, E., Guo, M., and Heng, J.Y.Y. "Preparation of Silica by Sol-Gel Methods: How Sustainable are current research methods?" 2023 AIChE Annual Meeting. 2023.

Beyond this work

[7] Mitchell, H., Verma, V., Errington, E., Guo, M., Guinn, E.J., and Heng, J.Y.Y. "Experimental and Computational Insights into the Homogeneous and Heterogeneous Crystallisation Behaviour of Glycine Homopeptides". 2023 AIChE Annual Meeting. 2023

Table of Contents

Abstract 3
Acknowledgements 4
Publications from this Research 6
Presentations from this Research 8
Abbreviations 25
1. Introduction 26
1.1. Research Motivations 26
1.1.1. Upward Trends in Pollution to Natural Waters: Globally and in the UK 26
1.1.2. Fat, Oil and Grease as a Catalyst for Urban Sewer Overflows 26
1.1.3. Adsorbent Materials as Treatments for Emerging Pollutant Chemicals 27
1.1.4. Use of Silica in the Design of Novel Adsorbent Materials 27
1.1.5. Silica-Based Adsorbent Materials for Fat, Oil and Grease Pollution 29
1.1.6. Environmental Impact of Nanofabricated Silica-Based Adsorbent Materials .29
1.2. Research Aims 31
1.2.1. Overview 31
1.2.2. Relation to Sustainable Development Goals 31
1.1. Thesis Structure 33
2. Literature Review 34
2.1. Introduction 34
2.2. Fat, Oil and Grease as a Wastewater Pollutant 35
2.2.1. Overview 35
2.2.2. Chemical Composition 42
2.2.3. Deposit Formation and Characteristics 43
2.3. Life Cycle Assessment as an Impact Assessment Method 46
2.3.1. Overview 46
2.3.2. Assessment Framework 46
2.3.3. Use in Chemical Product Design 47
2.4. Process Modelling for Estimating Mass and Energy Use 49
2.4.1. Overview 49
2.4.2. Use in Process Design 49
2.4.3. Use of Process Optimization 50
2.4.4. Use in Life Cycle Assessment 52

2.5. Silica as an Adsorbent Substrate 54
2.5.1. Overview 54
2.5.2. Chemistry 54
2.5.3. Manufacture 55
2.5.4. Life Cycle Perspective 60
2.6. Organic Surfactants as Additives for Substrate Synthesis 67
2.6.1. Overview 67
2.6.2. Quaternary Ammonium Salts 67
2.6.3. Linear Triblock Copolymers 68
2.6.4. Poly(alkylamines) 69
2.6.5. Life Cycle Perspective 70
2.7. Silane Coupling Agents as Surface Chemistry Modifiers 72
2.7.1. Overview 72
2.7.2. Commercial Production 72
2.7.3. Use in Surface Chemistry Modification 76
2.7.4. Life Cycle Understanding 78
3. Research Approach 79
3.1. Introduction 79
3.2. Understanding Life Cycles using Prior Art 79
3.3. Process Modelling using the Aspen Plus Software 80
3.3.1. Property Estimation 80
3.3.2. Use of Shortcut Methods 80
3.4. Life Cycle Assessment using the openLCA Software 81
3.5. Advanced Modelling using Python Integration 81
3.5.1. Process Design Optimization 81
3.5.2. Monte-Carlo Modelling of Impact Uncertainty 82
3.6. A Note on Interpretation 82
4. Industrial Silica Products 83
4.1. Introduction 83
4.1.1. Background 83
4.1.2. Aims and Objectives 84
4.2. Methods 84
4.2.1. Inventory Modelling of Commercial Silica Substrates 85

4.2.2. Environmental Impact Assessment 86
4.2.3. Uncertainty Assessment 88
4.3. Results and Discussion 89
4.3.1. Environmental Impact Predictions 89
4.3.2. Product Impact Comparisons 94
4.3.3. Shortcomings of Inventory Models 95
Conclusions 98
5. Emerging Sol-Gel Silica Products 100
5.1. Introduction 100
5.1.1. Background 100
5.1.2. Aims and Objectives 101
5.2. Methods 102
5.2.1. Process Modelling 102
5.2.2. Inventory Modelling of Surfactant Products 106
5.2.3. Inventory Modelling of Emerging Silica Substrates 112
5.2.4. Environmental Impact Assessment 115
5.3. Results 117
5.3.1. Environmental Impacts of Surfactant Products 117
5.3.2. Environmental Impact of Emerging Sol-Gel Silica Products 125
5.4. Discussion 127
5.4.1. Silica Reagent Choice 127
5.4.2. Energy use 128
5.4.3. Additive Choice 128
5.4.4. Functional Unit 129
5.4.5. Waste Production 129
5.4.6. Shortcomings of Inventory Models 130
5.4.7. Uncertainty Modelling 131
Conclusions 132
6. Silane Coupling Agents 134
6.1. Introduction 134
6.1.1. Overview 134
6.1.2. Aims and Objectives 135
6.2. Methods 136

6.2.1. Process Modelling 136
6.2.2. Life Cycle Inventory Modelling of Trichlorosilane 145
6.2.3. Life Cycle Inventory Modelling of Silane Coupling Agents 147
6.2.4. Environmental Impact Assessment 151
6.3. Results 151
6.3.1. Process Optimization 151
6.3.2. Environmental Impact of Trichlorosilane 154
6.3.3. Environmental Impact of Silane Coupling Agents 157
6.4. Discussion 162
6.4.1. Process Modelling 162
6.4.2. Importance of Trichlorosilane Processing History 163
6.4.3. Importance of Desired Chemistry 163
6.4.4. Importance of Allocation Factor 164
6.4.5. Modelling Issues 165
Conclusions 166
7. Environmental Cost of Silica-Based Oil Adsorbents 168
7.1. Introduction 168
7.1.1. Background 168
7.1.2. Aims and Objectives 169
7.2. Methods 169
7.2.1. Materials 170
7.2.2. Adsorbent Characterisation 171
7.2.3. Adsorption Performance 173
7.2.4. Life Cycle Inventory Modelling of Silanized Powders 176
7.2.5. Life Cycle Inventory Modelling of Recovered Oil 178
7.2.6. Environmental Impact Assessment 181
7.3. Results 181
7.3.1. Experimental Results 181
7.3.2. Environmental Impact of Adsorbent-based Oil Recovery 192
Conclusions 196
8. Conclusions 198
8.1. Key Conclusions 198
8.2. Recommendations for Future Work 204

8.2.1. Research Themes 204
8.2.2. Cultural Changes 205
8.3. Contribution to knowledge 206
References 208
Appendix A: Life Cycle Assessment of Commercial Silicas 223
A.1. Data Quality Scores of Life Cycle Inventory Flows for Pyrogenic Silica 223
A.2. Data Quality Scores of Life Cycle Inventory Flows for Precipitated Silica 229
Appendix B: Process Modelling of Cetrimmonium Chloride 235
B.1. Production of cetyldimethylamine, CDMA 235
B.2. Production of cetrimmonium chloride, CTAC 238
Appendix C: Process Modelling of Pluronic 123 240
C.1. Production of poly(propylene oxide)$_{17}$, PPO_{70} 240
C.2. Production of poly(propylene oxide)$_{70}$, PPO_{70} 243
C.3. Production of Pluronic 123, P_{123} 246
Appendix D: Process Modelling of Trichlorosilane 249
D.1. Process Modelling 249
D.2. Process Optimization 253
D.3. More on Cost Calculation Parameters 254
Appendix E: Process Modelling of Aminopropyltriethoxysilane 257
E.1. Production of 3-chloropropyltrichlorosilane, APTCS 257
E.2. Production of 3-chloropropyltriethoxysilane, CPTES 261
E.3. Production of 3-aminopropyl triethoxysilane, APTES 263
Model Assumptions 263
Appendix F: Process Modelling of Octyltrimethoxysilane 265
F.1. Production of octyltrichlorosilane, OTCS 265
F.2. Production of octyltrimethoxysilane, OTMS 267

Table of Figures

Figure 1.1: Optimized adsorbent design focussed on mesoporous adsorbents with surface chemistry modification. 28

Figure 1.2: Applications of silica-based adsorbent materials (SBAMs) in addressing fat, oil and grease pollution in traditional municipal wastewater settings. Note: reduction pre-sewer includes consideration for application of SBAMs at sewage pumping stations which act to collect to sewage before entering a combined municipal sewer system. 30

Figure 1.3: Understanding for the impact of silica based adsorbent materials is lacking due to missing information in the stages of silica synthesis and surface chemistry modification. 30

Figure 1.4: A framework for sustainable decision making through manufacturing understanding, process modelling, and impact reporting....31

Figure 1.5: Illustration of major questions surrounding understanding the environmental impact of silica-based adsorbent material life cycles. 32

Figure 1.6: Relation of proposed research to 8 of the 17 UN Sustainable Development Goals for 2030. 32

Figure 2.1: General characteristics distinguishing fat, oil and grease materials. 35

Figure 2.2: Correlation of fat availability with degree of urbanization (top), and gross domestic product with(bottom). Based on data from [32]. 36

Figure 2.3: Overview of common approaches for FOG pollution treatment, the nature of their treatment of their approach, typical point of application, and potential for use of adsorbent materials. Pre-effluent relates to applications of treatments to wastewater prior to its introduction into a wastewater management system. In-line refers to any treatments applied to wastewater within lines carrying wastewater from the initial point of disposal to the sewer system (e.g. within wastewater pipes or within pumping stations where relevant). In-sewer represents all treatments applying to directly to wastewater present within sewer systems. 38

Figure 2.4: Relation of FOG deposit formation to interaction between metals, FOG-derived pollutants, and their relation to pollution source. 45

Figure 2.5: Relationship of major stages in the Life Cycle Assessment Framework according to ISO 14040 [69]. 46

Figure 2.6: Illustrative example of decision making for equipment networks present in process systems modelling. 49

Figure 2.7: Relationship between process system specification and process unit specification in a typical process design optimization problem. 50

Figure 2.8: Tetrahedral structure of the silicate anion. 54

Figure 2.9: Surface chemistry of unmodified silica surfaces including silanol (a-c) and siloxane (d) functional groups. 55

Figure 2.10: A summary of main conceptual stages in the synthesis of silica substrates according to surfactant templating approaches. 58

Figure 2.11: Schematic representation of an ABA triblock copolymer formed by a sequence three distinct polymer 'block' sections. 68

Figure 2.12: Major synthesis pathways for producing organosilane coupling agents depending on desired product chemistry. 73

Figure 2.13: Effect of functional group chemistry on hydrolysis rate. All rates displayed relative to methoxy only functional group chemistry. Adapted from [127]. 75

Figure 3.1: Use of computer algorithms scripted in the python language to call the execution of individual software simulations (Aspen Plus and OpenLCA) as part of investigations in computational experiments. 82

Figure 4.1: Schematic workflow of methods used to investigate the environmental impact of producing silica substrates according to commercial synthesis methods. 84

Figure 4.2: Scope associated with the production of precipitated and pyrogenic silica according to commercial methods. 85

Figure 4.3: Environmental impact predictions for producing 1 kilogramme of precipitated and pyrogenic silica products according to commercial methods 90

Figure 4.4: Contributions of foreground activities to environmental impact of producing 1 kilogramme of precipitated (top) and pyrogenic (bottom) silica products according to commercial methods. 91

Figure 4.5: Uncertainty in the impact of individual silica products relative to one-another based on pairwise comparison. Bars represent the 10, 50, 95, and 99 % prediction intervals in order of increasing bar width, diamond markers represent the position of impact predictions made without consideration of uncertainty (i.e. Section 4.3.1). The positive portion of the x axis reflect probability space where the impact of precipitated silica is larger than pyrogenic silica, the negative portion reflects the opposite. 97

Figure 5.1: Total annual publications discussing the production of silica substrates according to the Stöber, MCM, SBA and bio-inspired silica synthesis methods. Results are based on search data from the Web of Science search engine (June 20th, 2024), using the following search terms: "MCM-41 OR MCM-48", "Stöber", "SBA-15", and "bio-inspired silica". 100

Figure 5.2: Schematic workflow of methods used to investigate the environmental impact of silica substrates produced according to emerging synthesis methods. 102

Figure 5.3: Process flow diagram of processes modelled to estimate material and energy use associated with the production of cetyldimethylamine (CDMA, top) and cetrimmonium chloride (CTAC, bottom). 103

Figure 5.4: Major stages modelled in the production of Pluronic 123 according to the manufacture of PPO_{17} (top), PPO_{70} (middle), and Pluronic 123 (P_{123}, bottom). Each process is based on a one-pot synthesis approach, with three processing states. NaOH: sodium hydroxide, PO: propylene oxide, EO: ethylene oxide, H_3PO_4: Phosphoric acid, DMC: Double metal cyanide catalyst, PCO: polycarboxylate. 105

Figure 5.5: Illustration of system boundaries associated with life cycle inventory models reported on the production of cetyldimethlyamine (CDMA, top) and cetrimmonium chloride (bottom). 108

Figure 5.6: Illustration of system boundaries associated with life cycle inventories modelling the production poly(propylene oxide)$_{17}$ (PPO_{17}, top), poly(propylene oxide)$_{70}$ (PPO_{70}, middle), and Pluronic 123 (bottom).....111

Figure 5.7: Illustration of system boundaries associated with life cycle inventories modelling the production of silica powder according to the Stöber, MCM, SBA, and BI synthesis methods. 113

Figure 5.8: Environmental impact predictions for 1kg of Cetrimmonium Chloride (CTAC) and the associated amount of cetyldimethylamine (CDMA) produced during the CTAC product life cycle.....118

Figure 5.9: Effect of quaternization solvent choice on the impact prediction of 1 kilogramme of cetrimmonium chloride. 120

Figure 5.10: Environmental impact predictions for 1kg of Pluronic 123 (P123) and associated amount of PPO_{70} and PPO_{17} block polymers required in producing 1kg of the Pluronic 123 product. 122

Figure 5.11: Environmental impact predictions for 1kg of Pluronic 123 produced by the traditional three-stage method and hypothetical two stage method. 124

Figure 5.12: Impact predictions for 1 kg of silica powder produced according to various synthesis methods. 126

Figure 6.1: Schematic workflow of methods used to investigate the environmental impact of silane coupling agents.....136

Figure 6.2: Schematic representation of optimization algorithm used during process design optimization. 141

Figure 6.3: Overview of process models used to estimate mass and energy use of producing 3-aminopropyltriethoxysilane via formation of 3-chloropropyltrichlorosilane (top), 3-chloropropyltriethoxysilame (middle), and amino-propyltriethoxysilane (bottom). 142

Figure 6.4: Overview of process models used to estimate mass and energy use of producing octyltrichlorosilane (OTCS, top), octyltrimethoxysilane (OTMS, bottom). 144

Figure 6.5: Illustration of system boundaries associated with life cycle inventory models reported on the production of trichlorosilane as a main product of a direct chlorination method (top), and as a co-product of silicon metal manufacture according to the Siemens process (bottom). 146

Figure 6.6: Scope of foreground and background life cycle activity included in life cycle inventory models cycle assessment of 3-aminopropyltriethoxysilane products including production of 3-chloropropytrichlorosilane (CPTCS, top), 3-chloropropyltriethoxysilane (CPTES, middle), and 3-aminopropyltriethoxysilane (APTES, bottom) 149

Figure 6.7: Scope of foreground and background life cycle activity included in life cycle inventory models cycle assessment of octyltrimethoxysilane product including production of octyltrichlorosilane (OCTS, top) and production of octyltrimethoxysilane (OTMS, bottom). 150

Figure 6.8: Change of maximum profit observed as a function of iteration made by the TCS production process optimizer. Inset: data viewed with a logarithmic scale. 152

Figure 6.9: Box plot of profit of successful designs identified in each generation (top) and designs accepted into the differential population (bottom). Boxes display interquartile range and median based on inclusive method. The black line inside each box plot represents the mean profit of designs within a given generation. 154

Figure 6.10: Environmental impact predictions for 1kg of trichlorosilane produced by the Siemens and Direct Chlorination processes.....156

Figure 6.11: Contribution of major activity categories to the overall impact of trichlorosilane produced via siemens process (left) and direct chlorination (right). GWP: Global Warming Potential, FDP: Fossil Depletion Potential, TAP: Terrestrial Acidification Potential, WDP: water depletion potential. 157

Figure 6.12: Environmental impact predictions for 1kg of 3-aminopropyltriethoxysilane (APTES) and the associated amount of 3-chloropropyl triethoxysilane (CPTES) and 3-chloropropyl trichlorosilane (CPTCS) used during the APTES production. 158

Figure 6.13: Environmental impact predictions for 1kg of octyltrimethoxysilane (OTMS) and the associated amount of technical grade trichlorosilane (TCS) produced during the OTMS product life cycle. 161

Figure 6.14: Environmental impact predictions for all organosilane products considered on a per mole of product basis. 162

Figure 6.15: The effect of allocation philosophy on the environmental impact of trichlorosilane produced according to Siemens and Direct Chlorination processes. 165

Figure 7.1: Schematic workflow of methods used to investigate the environmental impact of using silica-based adsorbent materials for recovery of vegetable oils. 170

Figure 7.2: Illustrations of surface chemistry associated with each of the three adsorbent powders considered, having silanol (a), amine (b), and butyl (c) surface chemistry. 171

Figure 7.3: Method of image analysis used to determine particle size distribution of adsorbent powders. 171

Figure 7.4: Method of immersion and filtration used to measure the adsorption capacity. 174

Figure 7.5: Relationship of UV absorbance at 270 nm with concentration of sunflower oil in ethanol. 175

Figure 7.6: Illustration of method used for investigating reusability of adsorbent powders. 176

Figure 7.7: Scope of activity included in life cycle assessment of recovering fat, oil and grease-type pollution using silica based adsorbent materials. 178

Figure 7.8: Representative images of adsorbent powder with (a) silanol, (b) butyl, and (c) amine powders taken via optical microscopy. 182

Figure 7.9: Nitrogen adsorption isotherms associated with silica gels with silanol, butyl, and amine surface chemistry. Error bars represent standard deviation based on analysis of a total of three repeats per sample. 183

Figure 7.10: Relationship of pore size and effective pore blockage associated with adsorbent powders modified with (a) amine and (b) butyl surface chemistries 185

Figure 7.11: Adsorption capacity of various vegetable oils during first-time use of adsorbent according to gravimetric methods post-filtration. 188

Figure 7.12: Schematic representation of key phenomena in adsorption of vegetable oil in adsorbent pores including (a) physical filling based on monolayer adsorption, transition to multilayer adsorption, and subsequent pore filling with a bulk liquid phase, and b) difference in bonding possible between adsorbents with silanol, amine and butyl surface chemistry and their effect on orientation of the monolayer structure, where dashed lines between hydrogen and oxygen groups indicate the presence of hydrogen bonding. 189

Figure 7.13: Effect of solvent use ratio on the concentration of sunflower oil present in the extraction solvent (a), implied total amount of oil extracted (b), and extraction efficiency (c). Markers with a white fill represent observations associated with a saturated oil-in-ethanol solution. 191

Figure 7.14: Adsorption capacity of adsorbents with silanol and butyl surface chemistry before and after re-use. 192

Figure 7.15: Environmental impact predictions for the recovery of sunflower oil using adsorption-solvent extraction process (top) and associated contributions based on activity category (bottom). Results are based on impact assessment assuming one time use of adsorbent. 193

Figure 8.1: Addressing key questions in understanding across the life cycle of silica-based adsorbent materials. 199

Figure B.1: Process flow diagram of Aspen Plus model approximating the production of cetyldimethylamine from cetyl alcohol. 237

Figure B.2: Process flow diagram for model approximating the production of cetrimmonium chloride (CTAC). Dotted lines represent transitions in conceptual processing stage within the same single batch process equipment. 238

Figure B.3: Process flow diagram of Aspen Plus model approximating the production cetrimmonium chloride. 239

Figure C.1: Process flow diagram of Aspen Plus model approximating the production of poly(propylene oxide)$_{17}$. 242

Figure C.2: Process flow diagram of Aspen Plus model approximating the production of poly(propylene oxide)$_{70}$. 244

Figure C.3: Process flow diagram for model approximating the production of Pluronic 123. Bold arrows represent transitions in processing stage occurring within the same process vessel. 246

Figure C.4: Process flow diagram of Aspen Plus model approximating the production of Pluronic 123. 247

Figure F.1: Process flow diagram of the process used to model the production of octyltrichlorosilane in the Aspen V11 software. TCS: trichlorosilane 265

Figure F.2: Process flow diagram of the process modelled for octyltrimethoxysilane production. OTCS: octyl trichlorosilane, OTMS: octyltrimethoxysilane, HCl: hydrogen chloride. 267

Table of Tables

Table 1.1: Justification of relation of the work to UN sustainable Development Goals 33

Table 2.1: Topics and motivations of information covered in the literature review. 34

Table 2.2: Chemical composition of free fatty acids present in common vegetable derived foodstuffs. 42

Table 2.3: Chemical composition of free fatty acids present in common animal-derived foodstuffs. 42

Table 2.4: Chemical composition of free fatty acids in used cooking oil. 43

Table 2.5: Chemical composition of free fatty acids in materials found in physical separators. NDF: not defined. 43

Table 2.6: Mass efficiency and by-products associated with traditional precursors of silica production. 62

Table 4.1: Material and energy flow inventory for producing 1kg of precipitated and pyrogenic silica product. 86

Table 4.2: Inventory models used to account for background life cycle activity linked to the production of commercial silica substrates based on the EcoInvent v3.10 database. 87

Table 4.3: Mid-point metrics considered in life cycle impact assessment of commercial silica and use justifications. 87

Table 4.4: Contribution of the silicon tetrachloride reagent life cycle to the predicted impact of pyrogenic silica. 92

Table 4.5: Contribution of the sodium silicate reagent life cycle to the predicted impact of precipitated silica 92

Table 4.6: Contribution Mineral Feedstock to the impact of precipitated and pyrogenic silica products. 94

Table 5.1: Life cycle inventory data for cetyldimethylamine (CDMA) and cetrimmonium Chloride (CTAC). 109

Table 5.2: Life cycle inventory data for poly(propylene oxide)$_{17}$ (PPO_{17}), poly(propylene oxide)$_{70}$ (PPO_{70}), and Pluronic 123 (P_{123}). NC: not considered 110

Table 5.3: EcoInvent v3.10 database models used to account for background life cycle activity linked to the production of surfactant templates. 112

Table 5.4: Inventory models used to account for background life cycle activity linked to the production of emerging silica substrates based on the EcoInvent v3.10 database.....115

Table 5.5: Life Cycle Inventory data for silica produced according to the Stober, MCM, SBA, and Bio-inspired synthesis methods. 116

Table 5.6: Minimum mass of silica reagents required to produce 1 kilogram of silica product according to reaction stoichiometry. 116

Table 5.7: Impact factors considered during life cycle impact assessment of surfactant and silica products in this work.....117

Table 5.8: Impact predictions for cetrimmonium chloride (this work) and non-ionic surfactant products 119

Table 6.1: Sources of cost data used in calculation of capital costs when modelling the production of trichlorosilane 138

Table 6.2: Sources of cost data used in calculation of capital costs when modelling the production of trichlorosilane 139

Table 6.3: Life Cycle Inventory for producing 1 kg of trichlorosilane based on direct chlorination process.....146

Table 6.4: Inventory models used to account for background life cycle activity linked to the production of trichlorosilane by direct chlorination based on the EcoInvent v3.10 database. 147

Table 6.5: Life Cycle Inventory for producing 1 kg of trichlorosilane as a co-product of the Siemens process.....147

Table 6.6: Life Cycle inventory model for production of 3-aminopropyltriethoxysilane and its chemical intermediates.....148

Table 6.7: Life Cycle inventory model for production of cetyltrimethoxysilane and its chemical intermediates.....150

Table 6.8: Inventory models used to account for background life cycle activity linked to the production of silane coupling agents based on the EcoInvent v3.10 database. 151

Table 6.9: Impact factors considered during life cycle impact assessment of surfactant materials and silica produced occurring to emerging sol-gel methods.....151

Table 6.10: Design results of the optimized direct chlorination process.....153

Table 6.11: Mass and Energy flows associated with operation of the optimized process for producing trichlorosilane. 155

Table 6.12: Selling prices assumed for co-products of trichlorosilane manufacturing processes during economic allocation. 164

Table 7.1: Powder characteristics as reported by the silica powder manufacturer. 170

Table 7.2: Life cycle inventory data used to model activity associated with the production of butyl and amine functionalised silica powders. 177

Table 7.3: Inventory models used to account for background life cycle activity associated with products. 178

Table 7.4: Life cycle inventory information used in modelling the recovery of vegetable oil using adsorbents. 180

Table 7.5: Inventory models used to account for background life cycle activity associated with products. 180

Table 7.6: Summary of BET model parameters identified for adsorbent powder nitrogen adsorption isotherm. 183

Table A.1: Data quality score card for Silicon Tetrachloride. Model: Silicon Tetrachloride - GLO 223

Table A.2: Data quality score card for hydrogen. Model: market for hydrogen, liquid - RER 224

Table A.3: Data quality score card for electricity. Model: market group for heat, district or industrial, natural gas - RER 224

Table A.4: Data quality score card for hazardous waste. Model: market for hazardous waste, for incineration - Europe without Switzerland. 225

Table A.5: Data quality score card for landfill. Model: process-specific burdens, sanitary landfill, (product flow). 225

Table A.6: Data quality score card for carbon dioxide. Model: carbon dioxide, fossil. 226

Table A.7: Data quality score card for chlorine. Model: emission to air 226

Table A.8: Data quality score card for hydrogen chloride. Model: emission to air 227

Table A.9: Data quality score card for nitrogen oxides. Model: emission to air 227

Table A.10: Data quality score card for particulates. Model: emission to air 228

Table A.11: Data quality score card for Volatile organic carbons. Model: emission to air 228

Table A.12: Data quality score card for Sodium Silicate. Model: market for sodium silicate, without water, in 37% solution state - RER 229

Table A.13: Data quality score card for electricity. Model: market group for heat, district or industrial, natural gas - RER 229

Table A.14: Data quality score card for Sulfuric Acid. Model: market for sulfuric acid - RER 230

Table A.15: Data quality score card for Deionised Water. Model: market for water, deionised - Europe without Switzerland.....230

Table A.16: Data quality score card for non-hazardous waste. Model: process-specific burdens, sanitary landfill, (product flow). 231

Table A.17: Data quality score card for wastewater. Model: wastewater, average. 231

Table A.18: Data quality score card for carbon monoxide. Model: emission to air.....232

Table A.19: Data quality score card for chemical oxygen demand (COD). Model: emission to water 232

Table A.20: Data quality score card for dissolved solids. Model: emission to water.....233

Table A.21: Data quality score card for nitrogen oxides. Model: emission to air 233

Table A.22: Data quality score card for particulates. Model: emission to air 234

Table A.23: Data quality score card for sulfate. Model: emission to water 234

Table B.1: Predicted energy flows for equipment used in the production of 1 kg of cetyldimethylamine (CDMA).....236

Table B.2: Predicted energy flows for equipment used in the production of 1kg of cetrimmonium chloride (CTAC).....238

Table C.1: Predicted energy flows for equipment used in the production of 1kg of poly(propylene oxide)$_{17}$. 241

Table C.2: Predicted energy flows for equipment used in the production of 1kg of poly(propylene oxide)$_{70}$. 245

Table C.3: Predicted energy flows for equipment used in the production of 1kg of Pluronic 123. 248

Table D.1: Predicted energy flows for equipment used in the production of 1kg of trichlorosilane. 253

Table D.2: Parameters for calculating utility costs using the cost correlations of Ulrich and Vasudevan [172].....255

Table D.3: Parameters used in calculating purchase costs of equipment using the cost correlations of Sinnott and Towler [168] 255

Table D.4: Parameters used for calculating the bare module cost of individual equipment according to Guthrie's method [204]. Values taken from those listed by van Amsterdam [170]. 256

Table E.1: Predicted energy flows for equipment used in the production of 1kg of 3-chloropropyltrichlorosilane.....261

Table E.2: Predicted energy flows for equipment used in the production of 1kg of 3-chloropropyltriethoxysilane. 262

Table E.3: Predicted energy flows for equipment used in the production of 1kg of 3-aminopropyltriethoxysilane. 264

Table F.1: Binary interaction parameters used for modelling liquid equilibria via the NRTL method while modelling the production of octyltrichlorosilane.....266

Table F.2: Predicted energy flows for equipment used in the production of 1kg of octyltrichlorosilane. 266

Table F.3: Predicted energy flows for equipment used in the production of 1kg of octyltrimethoxysilane. 268

Abbreviations

Abbreviation	Definition
APTES	3-aminopropyltriethoxysilane
BBO	Black Box Optimization
BI	Bio-inspired
CPTCS	3-chloropropyltrichlorosilane
CPTES	3-chloropropyltriethoxysilane
CTAC	Cetrimmonium Chloride
EI	Environmental Impact
EWP	Emerging Wastewater Pollutant
FDP	Fossil Depletion Potential
FOG	Fat, Oil and Grease
GWP	Global Warming Potential
LCA	Life Cycle Assessment
LCI	Life Cycle Inventory
LCIA	Life Cycle Impact Assessment
MCM	Mobil Composition of Matter
OTCS	Octyltrichlorosilane
OTMS	Octyltrimethoxysilane
P_{123}	Pluronic 123
PEHA	Pentaethylenehexamine
QAS	Quaternary Ammonium Salt
SBA	Santa Barbara Amorphous
SBAM	Silica Based Adsorbent Material
SSO	Sewer System Overflow
UCO	Used Cooking Oil
WDP	Water Depletion Potential

1. Introduction

1.1. Research Motivations

1.1.1. Upward Trends in Pollution to Natural Waters: Globally and in the UK

Increases in population, production and consumption are exacerbating pollution worldwide and increasing the risk of catastrophic environmental system change [1]. However, while recent events have driven an agenda particularly on climate action, there exists a range of wider factors that must be addressed if we are to ensure sustainable development in the future. Included in this, is the need for a more sustainable relationship with water.

At present, around 50% of wastewater produced globally is released to the environment without adequate treatment [2]. Though industrial polluters are partly to blame, this problem includes significant contributions from non-industrial sources. For instance, 70% of pollution affecting natural water sources in China has been attributed to residential sewage [3]. Similar issues are also present in the United Kingdom, where the quality of natural waters has been identified as a growing public health concern [4].

One major source of decreasing water quality in the UK is an increase in the frequency of combined sewer overflows (CSOs) – which have more than doubled in frequency from 2022 to 2023 [5]. CSOs are the purposeful release of diluted sewage to inland waters and the sea to avoid urban flooding (i.e. sewage backup [6]). Increases in the frequency of these events are associated with increases in rainfall [7][8] due to climate change [9] as well as increasing base loads placed on sewer systems due to population growth. These factors have the effect of lowering the bar for the extent of rainfall required to trigger sewer system overflows (SSOs) [10]. Unfortunately, the frequency of SSOs is expected to increase in the short term, given expected increases global warming and in municipal sewer loading (e.g. 50% increase by 2050 [2]) and urban population densification [11].

1.1.2. Fat, Oil and Grease as a Catalyst for Urban Sewer Overflows

One major contributing factor to CSOs in urban areas is the improper disposal of fat, oil and grease (FOG). This is responsible for more than 50% of all SSOs which occur in the UK and USA

per year [12, 13]. This is due to its tendency of FOG to accumulate as large solid deposits on sewer walls, obstructing sewage flow. In some cases, these deposits may be as large as 180 tonnes [14] before being addressed. Unsurprisingly, a large amount control of FOG control is reactionary in nature, with control costing as much as £50 million in the UK annually [13]. A strong incentive therefore exists for developing new, cost-effective approaches that minimise the need for reactive control of FOG pollution.

1.1.3. Adsorbent Materials as Treatments for Emerging Pollutant Chemicals

One major issue leading current water pollution issues is the imbalance in demand and available capacity for wastewater treatment [2]. This has led to hurried development of a great deal of approaches by which individual contaminants may potentially be treated. Among these, the adsorption-based approach has been particularly attractive due to benefits including cost-efficiency, ease of use, and versatility in addressing several types of contaminants [15]. For example, this is reflected in the widespread use of activated carbons to treat conventional water contaminants. However, following the rise of EWPs, a significant amount of effort has been placed into developing new adsorbent materials with advanced adsorption performance.

Recent trends in adsorbent design have focussed on two major features affecting adsorbent performance: pore geometry, and surface chemistry. As shown in Figure 1.1, this has enabled the production of adsorbent materials with pore geometry and surface chemistry that are customised to suit the adsorption of specific emerging pollutants based on a combination of pollutant size and pollutant chemistry. These factors are important in exploiting the relationship of pore and pollutant size on capillary condensation phenomenon within pores and chemical affinity of pollutant-adsorbent surface interactions respectively.

1.1.1. Use of Silica in the Design of Novel Adsorbent Materials

Among new adsorbent materials being developed to treat EWPs, silica-based adsorbent materials (SBAMs) have received a significant amount of interest. This due to several practical benefits of using silica as an adsorbent substrate, including the abundance and low price of associated raw materials (e.g. quartz sand); the chemical inertness of silica, contributing to an increased adsorbent lifetime and ability for SBAMs to be used in harsh chemical conditions;

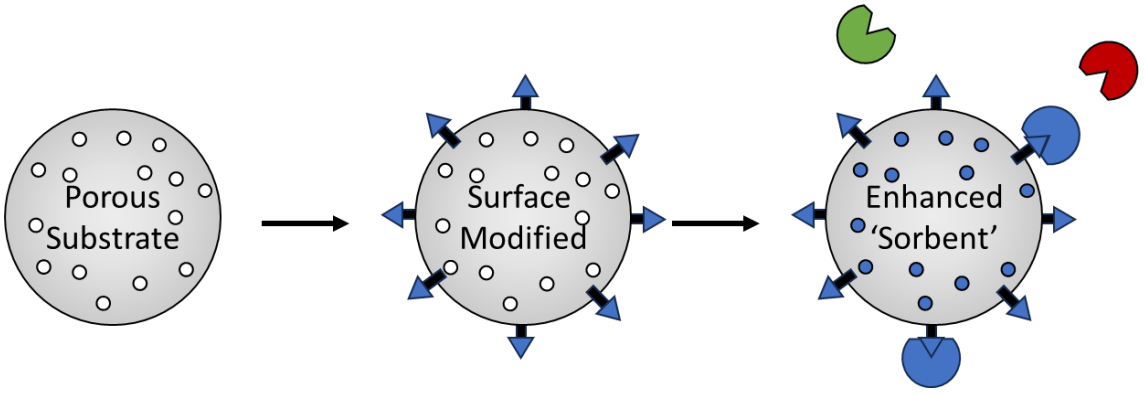


Figure 1.1: Optimized adsorbent design focussed on mesoporous adsorbents with surface chemistry modification.

and the low toxicity of silica, which makes it safer to handle. This is reflected in traditional use of SBAMs, which has involved chemical catalysts [16], chromatographic column fillings, and desiccants (i.e. water vapor adsorbents) in consumer products and industry.

In addition to the general properties of silica, SBAMs are of particular interest in treating EWPs due to the synergy that silica provides with the pore size and surface chemistry paradigms present in contemporary adsorbent design. For example, many methods for producing silica products (e.g. silica gel and zeolites) are now commercialised and technologically mature; this includes a range of methods by which silica-based adsorbent substrate may be produced with porosity of a well-controlled size and geometry (e.g. [17]). Additionally, though generally unreactive, silica-based materials are beneficial in being able to have their surface chemistries modified by a range of well-understood processes (e.g. [18]) – enabling the manufacture of SBAMs with surfaces that have strong chemical affinity with many types of EWPs. Consequently, SBAMs provide a strong foundation from which new adsorbent material innovations may be developed.

Interestingly, silica-based adsorbents also have the possibility for used in shaped adsorbent designs. Shaped designs are designs in which adsorbent materials are used to form coatings that cover other materials. These are often desirable in combining the benefits of silica adsorbent design with other beneficial properties of the underlying material that the silica is bonded to. This includes underlying materials with pore characteristics that cannot be achieved by the desired SBAM manufacturing methods, or materials with other desirable material properties. For example, materials coated in adsorbent nanoparticles [19], or coated

sponges with micron-sized porosity capable of undergoing mechanical compression have been reported in the wider literature [20].

1.1.2. Silica-Based Adsorbent Materials for Fat, Oil and Grease Pollution

One area in which SBAMs may be particularly useful is as treatments for FOG-type EWPs [21]. For example, silica nanoparticles with surface chemistry modifications have been recently employed within the research group of Dr. Jerry Heng as part of treating oily wastewater [19]. Similarly, SBAMs have been used to adsorb lipidic materials in a range of wider use cases including in vegetable oil bleaching processes [22], and as part of biodiesel manufacturing operations involving waste cooking oil (a common FOG contaminant in wastewater) [23].

For SBAMs to be used optimally to treat FOG pollution in wastewater, a consideration must be made for the relationship between their place of application within the wastewater network in addition to their traditional adsorbent design (i.e. pore characteristics and surface chemistry). Optimized SBAMs could be deployed in multiple ways across the wastewater/sewer system to address FOG pollution.

As shown in Figure 1.2, this includes in surface coatings acting to protect surfaces in high-risk sewerage applications, insert-style products that can be placed and removed for ease of use and maintenance, loose powders that could be introduced to streams and later recovered (e.g. by filtration), and packed/trickling-beds (e.g. similar to those used in wider wastewater treatment). In practice, selecting desired application will require consideration of a broad range of wider factors; for instance, this may include consideration for the user (e.g. residential polluter or municipal wastewater controller) and the region of application – though many other practical factors may also be present.

1.1.3. Environmental Impact of Nanofabricated Silica-Based Adsorbent Materials

While much work has demonstrated the ability of nanofabricated SBAMs to have improved adsorbent properties, little work is available covering the EI associated with their production. This is despite questions have therefore been raised regarding the environmental sustainability of approaches compared to more traditional methods [24-26]. For example, new methods often in include the use of organic surfactants as additives to create mesoporous

silicas. Similarly, surface chemistry modification requires the use of additional modifying reagents, known as silane coupling agents [27].

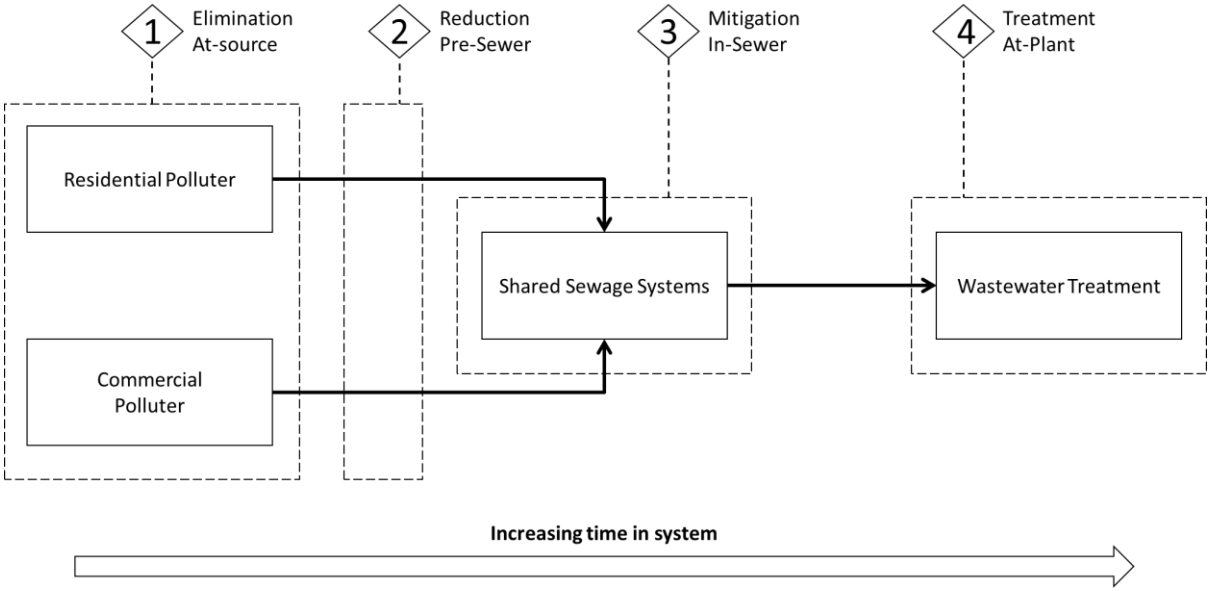


Figure 1.2: Applications of silica-based adsorbent materials (SBAMs) in addressing fat, oil and grease pollution in traditional municipal wastewater settings. Note: reduction pre-sewer includes consideration for application of SBAMs at sewage pumping stations which act to collect to sewage before entering a combined municipal sewer system.

Despite this, very little understanding is currently available within the literature with regards to the explicit amount of material use and energy use associated with the nanofabrication methods – see Figure 1.3. In many cases, this includes a lack of understanding even for the EI of intermediate materials (e.g. surfactants) being used in the manufacturing process. The result is that experimental research has progressed significantly without an equivalent expansion in understanding for the EI of the methods being used.

For novel silica-based adsorbents to be truly optimal, they must be produced in a way that maximises their benefit to society [28]. Doing so involves not only adsorbent performance, but also balancing chemical safety and EI of the entire SBAM life cycle. New information must therefore be generated to map the impact of SBAM products across their lifecycle.

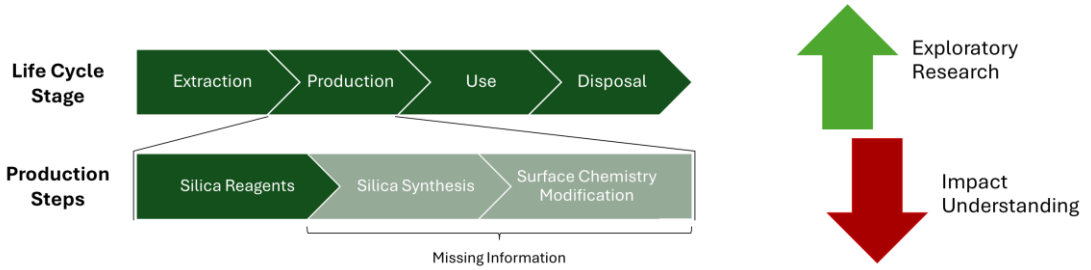


Figure 1.3: Understanding for the impact of silica based adsorbent materials is lacking due to missing information in the stages of silica synthesis and surface chemistry modification.

1.2. Research Aims

1.2.1. Overview

Research carried out in this work aims to address gaps in the literature for the EI of SBAMs. This is to be achieved by developing more transparent understanding for material use and energy use associated with producing SBAMs as well as key intermediates and products required for SBAM manufacture. As shown in Figure 1.4 this is done with the hope that it will enable future research to make informed decisions regarding the sustainable design of SBAMs for use in a range of end-use cases.

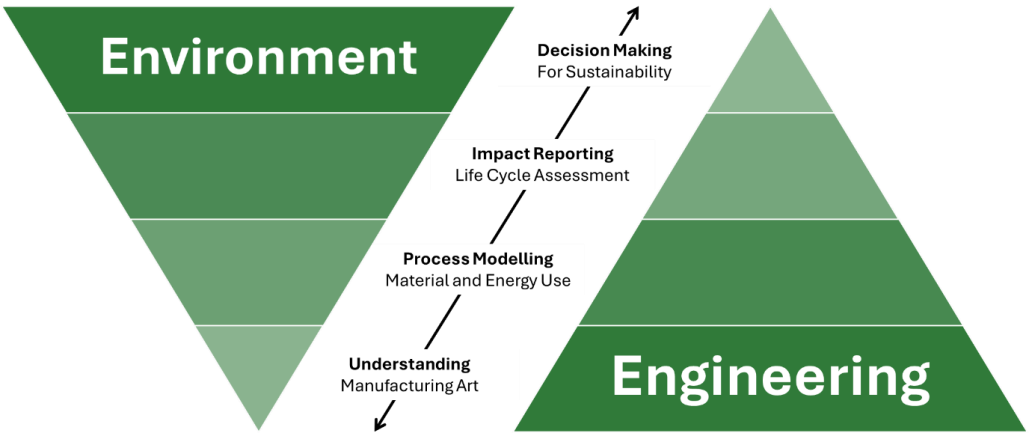


Figure 1.4: A framework for sustainable decision making through manufacturing understanding, process modelling, and impact reporting.

Given the scale of lack of information available (discussed later in Chapter 2) this has been done in a way that provides case-studies for all materials and intermediates in the typical life cycle of a typical silica-based adsorbent material. As illustrated in Figure 1.5, this includes: 1) synthesis of silica substrates, 2) synthesis of silane coupling agents, 3) modification of silica surface chemistry, and 4) application to the adsorption of FOG material.

1.2.2. Relation to Sustainable Development Goals

Implications of this work may be associated with addressing 8 of the 17 Sustainable Development Goals laid out by the United Nations for 2030. These are summarised in Figure 1.6; further information on each relation is provided in Table 1.1.

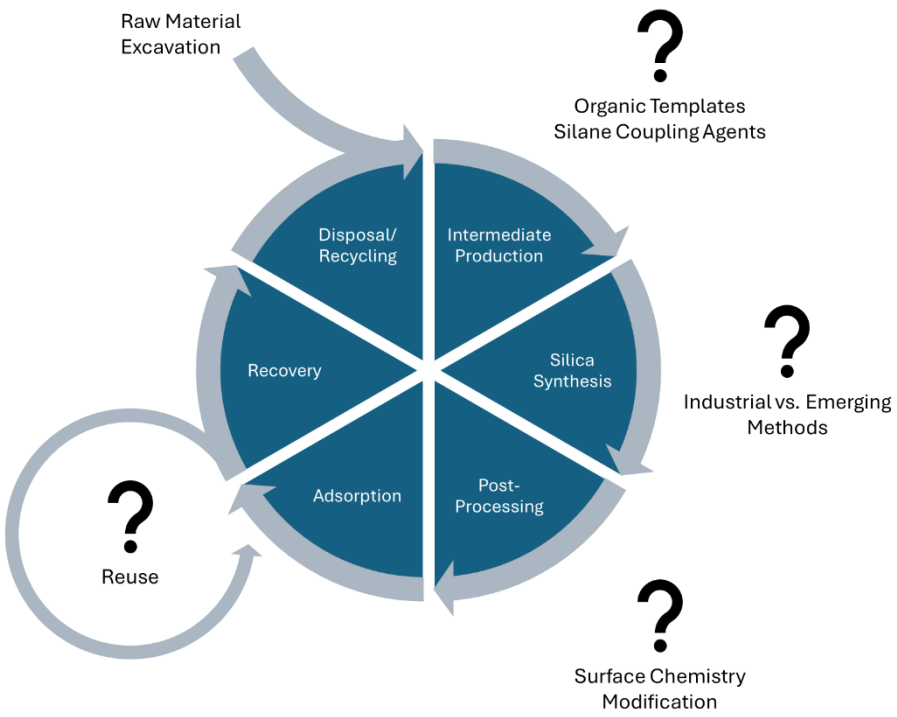


Figure 1.5: Illustration of major questions surrounding understanding the environmental impact of silica-based adsorbent material life cycles.



Figure 1.6: Relation of proposed research to 8 of the 17 UN Sustainable Development Goals for 2030.

Table 1.1: Justification of relation of the work to UN sustainable Development Goals

Goal	Name	Relevant Targets
6	Clean Water and Sanitation	Focus of work on application of SBAMs in wastewater treatment
8	Decent Work and Economic Growth	Implications of work on potential FOG circularity, improving resource efficiency in consumption and production. Implication of work on promoting sustainable economic growth
9	Industry, innovation and infrastructure	Promotion of sustainable industry and innovation directly through impact assessment of products still in development.
11	Sustainable Cities and Communities	Focus of work on addressing FOG pollution, which is particularly problematic in urban areas Interest in development of sustainable treatment approaches for communities effected by FOG pollution
13	Climate Action	Relation of environmental impact assessment to decision making that may minimise the contribution of SBAM manufacture to global climate change Additional possibility of SBAM materials being used as adsorbents for pollutants driving climate change
14	Life Below Water	Focus of work on adsorbent manufacture, including environmental impact metrics relevant to aquatic life Focus of work on application of SBAMs to wastewater pollution
15	Life on Land	Focus of work on adsorbent manufacture, including environmental impact metrics relevant to life on land

1.3. Thesis Structure

The remainer of this work is split into a further 7 chapters. Chapter 2 establishes further understanding required to understand the perspectives from which research has been carried out. Having established necessary understanding, Chapter 3 then outlines the high-level approach to Life Cycle Assessment and Process modelling taken by research in the work. Chapters 4, 5, and 6 the tackle the development of life cycle understanding relevant for intermediate chemical products used in the manufacture of silica adsorbents. Particularly, this includes silica substrates produced by commercial methods (Chapter 4), by emerging sol-gel technologies for mesoporous silicas (Chapter 5), and organosilane surface modifying reagents (Chapter 6). Chapter 7 then provides a final case study relating the performance of three silica-based adsorbent materials in the application of adsorbing vegetable oil materials. Wider implications are discussed and concluded in Chapter 8.

2. Literature Review

2.1. Introduction

Chapter 1 has established the need to better understand the environmental impacts of SBAMs if they are to be used as pollution abatement products. This includes for the treatment of emerging wastewater pollutants - including Fat, Oil and Grease (FOG). However, this requires an appreciation for the assessment methods by which environmental impacts may be measured (life cycle assessment) as well as ways by which production activities may be estimated (process modelling)

This chapter provides a summary of information necessary to understand current state of the art relevant to assessing the environmental impact of SBAMs, and their application to FOG pollution abatement. It includes a total of 6 sections.

First, an understanding of FOG pollution is wastewater is reviewed in Section 2.2; second, the methods of process modelling, and life cycle assessment used to model life cycle impact in this work are introduced in Sections 2.3 and 2.4; third, information for the major paradigms in SBAM manufacture, and supporting additive materials are reviewed in Section 2.5, 2.6 and 2.7. A larger summary is provided in Table 2.1.

Table 2.1: Topics and motivations of information covered in the literature review.

Section	Topic	Relevance
2.1	Introduction (*this section)*	Initial context for the rest of the chapter
2.2	Fat, Oil and Grease	Understanding for social dimensions of FOG pollution, material properties, and formation of blockages in sewer networks
2.3	Life Cycle Assessment	Modelling framework used in environmental impact assessment of chemical products
2.4	Process Modelling	Modelling framework used to estimate missing life cycle inventory information
2.5	Silica as an Adsorbent	Principles of manufacturing silica materials for adsorbent applications
2.6	Organic Templating Agents	Principles of manufacturing organic templates used to produce mesoporous silica products
2.7	Silane Coupling Agents	Principles of manufacturing silane coupling agents and their use in SBAM surface chemistry modification

2.2. Fat, Oil and Grease as a Wastewater Pollutant

2.2.1. Overview

Fat, oil, and grease (FOG) is a broad category of organic material originating from dietary lipids, such as vegetable oils and animal fats [29]. Owing to their chemical complexity, FOG material may be described in multiple ways. One common definition involves linkage to food stock sources - where fats are lipidic materials that are solid at room temperature, oils are lipidic material that are liquid at room temperature, and greases are solid or viscoelastic materials at room temperature that are derived from complex arrangements of materials deriving from fats and oils (see Figure 2.1).

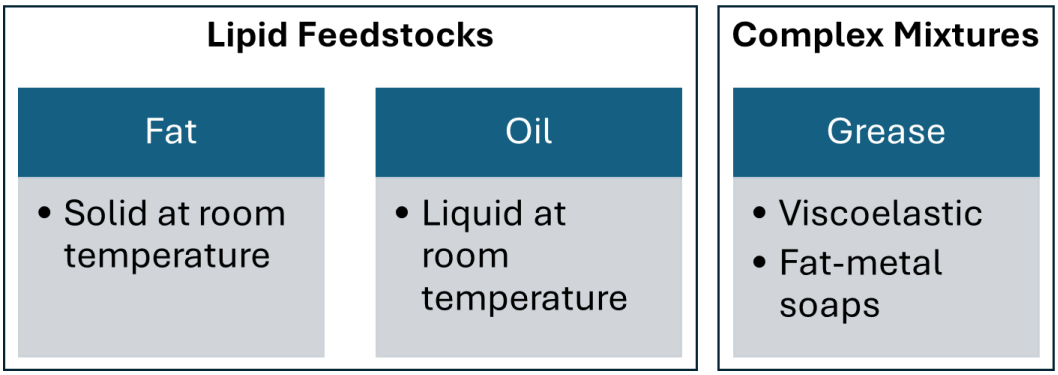


Figure 2.1: General characteristics distinguishing fat, oil and grease materials.

Nonetheless, it is also common for FOG materials to be classified according to other practical bases included chemical composition and properties. This includes categorisation based on pollution source [30], physical properties [31], and underlying chemistry (see Section 2.2.2).

Drivers of FOG Pollution Issues

Pollution of FOG in sewers is ultimately a problem driven by societal misuse of sewer systems. However, stopping this misuse is difficult due to the decentralised nature of sewer networks. Until this issue is addressed, an appreciation for societal drivers behind FOG pollution is therefore helpful.

Societal trends of population growth, urbanisation, and diet change are leading drivers of FOG pollution. This is due to increased base-loading of sewers associated with the former, and tendency for fat consumption to increase with urbanisation - as shown in Figure 2.2.

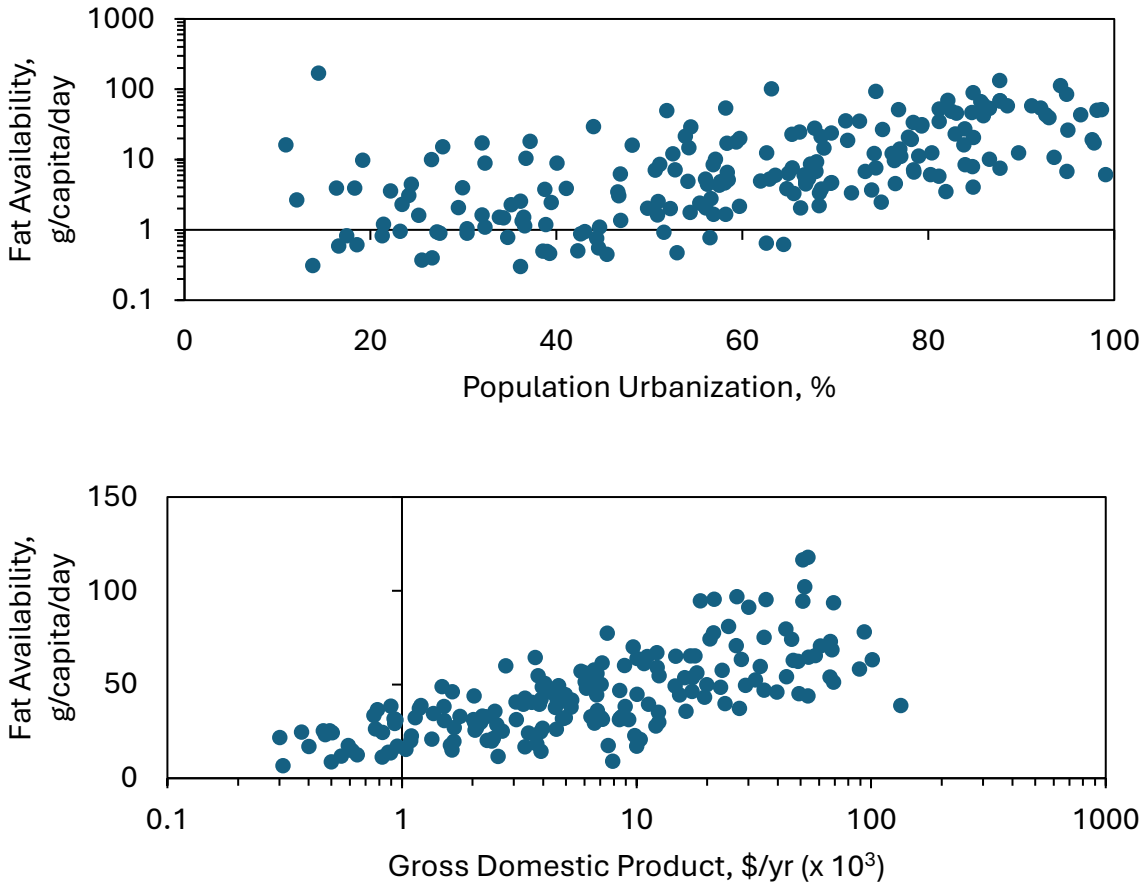


Figure 2.2: Correlation of fat availability with degree of urbanization (top), and gross domestic product with(bottom). Based on data from [32].

Climate change is also having indirect effect on FOG-related issues. This includes two factors - increasing rainfall attributed to climate change [33], which is increasing the frequency of SSOs and rising sweater levels. Higher rainfall frequency acts to increase the likelihood of SSO by increasing the likelihood of partially blocked sewers with FOG deposits experiencing intolerable loading. Conversely, rising sea levels can lead to the ingress and infiltration of sea water into coastal sewer networks; these waters may rapidly increase the degradation of concrete-based sewer walls by enhancing the process of microbe induced concrete corrosion (MICC, see also Section 2.2.3), increasing FOG deposit deposition. Similar issues exist with rising groundwater levels.

Finally, understanding of FOG deposit formation mechanisms indicate that the state of health of sewerage systems may have adverse effects on the rate of FOG deposit formation. This is linked to the effect that sewer wall degradation can have on accelerating the rate at which FOG pollution deposits to form solid blockages - see Section 2.2.3.

Emission Sources

Sources of FOG pollution in municipal sewers are typically split across industrial, commercial (e.g. Food Service Establishments, FSEs), and residential actors [34, 35]. Urban centres and residential areas are the most greatly affected by FOG deposition [36]. Conversely, industrial buildings are often the least significant source of FOG emission in municipal wastewater.

The low contribution of industrial sources likely reflect achievements of regulatory constraints, which has led to at-source pollution treatment becoming an industrial paradigm [29]. Conversely, water companies do not have any legal right to access and assess the state of pollution from individual FSEs in the UK [37].

Residential buildings are believed to be the largest contributors to total FOG pollution, accounting for as much as 55 % of FOG which enters sewers in Scotland [34]. On the other hand, commercial buildings - such as restaurants and other food service establishments (FSEs) - often appear to be the most concentrated, localised sources of FOG emission. This is due to three confounding factors: 1) the high concentration of FOG typically present in their wastewater effluent [38], 2) the tendency for FSEs to exist in close-vicinity of one-another in urban centres, and 3) the volume of activity associated with food production and sale. For example, FSEs have been recorded as present in the vicinity of 80% of sewer blockages in a recent study [34]. This is also reflected in the output of a single FSE being roughly equivalent to that of a 7-floor high-rise residential building in the USA [39].

Existing Treatment Methods

Existing treatments for FOG pollution typically utilise a physical, biological, or chemical approach [40]. As shown in Figure 2.3, these approaches can vary in the point of application and whether they are destructive of non-destructive in nature.

Physical Methods

Physical methods typically involve the use of grease traps, grease separators, or grease removal units [37]. These are non-destructive methods which operate based on separation of oil and/or grease from water, and sedimentation of food particles.

Typically, equipment relying on physical separation are installed at-source to separate FOG while at its highest concentration – i.e. before being passed into the wider wastewater system. For example, this includes in food service establishments.

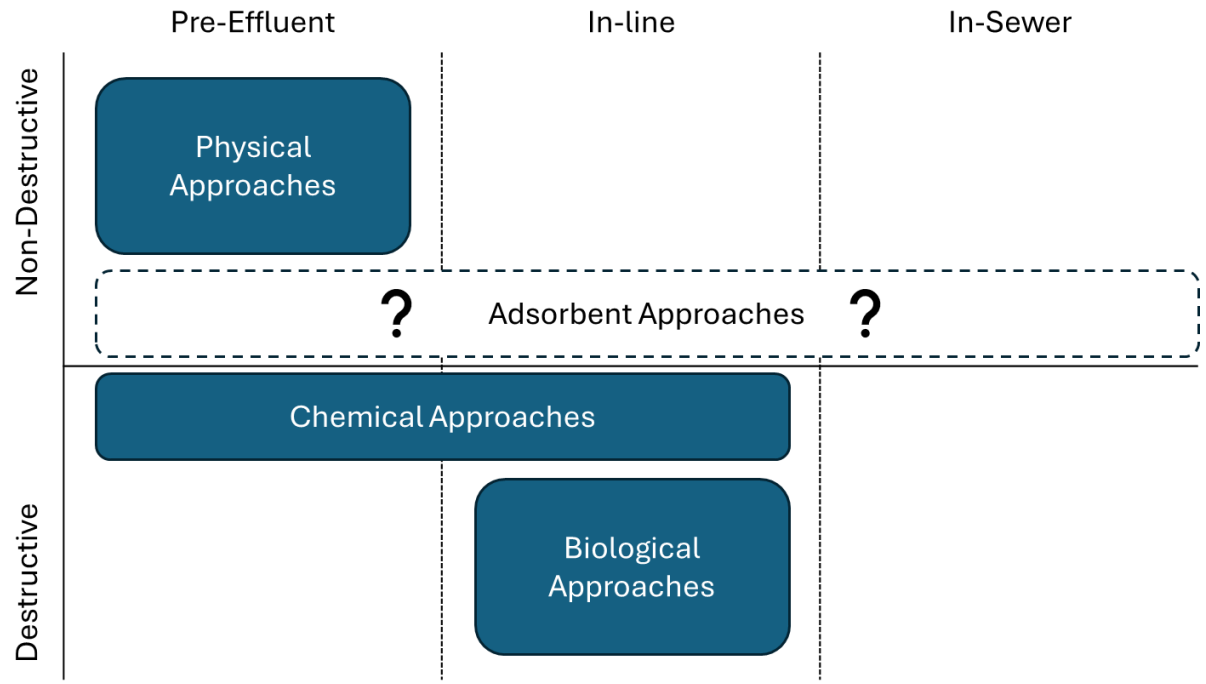


Figure 2.3: Overview of common approaches for FOG pollution treatment, the nature of their treatment of their approach, typical point of application, and potential for use of adsorbent materials. Pre-effluent relates to applications of treatments to wastewater prior to its introduction into a wastewater management system. In-line refers to any treatments applied to wastewater within lines carrying wastewater from the initial point of disposal to the sewer system (e.g. within wastewater pipes or within pumping stations where relevant). In-sewer represents all treatments applying to directly to wastewater present within sewer systems.

A major challenge with physical methods arises from their tendency to be poorly implemented in practice. This arises from the installation of incorrectly sized equipment as well as the tendency for inadequate maintenance after installation [13]. Both factors may lead to a failure of equipment to capture FOG waste effectively, leading to continued sewer system pollution.

Biological Methods

Biological dosing systems use biological processes to break down FOG material. Because of their reliance on biological breakdown methods, they are typically done without need for harsh conditions, under relatively benign processing conditions (e.g. 37 C and atmospheric pressure).

Conversely, the use of living organisms poses challenges for adequate operation including rate of treatment and influent control.

Firstly, regarding rate of treatment, the rate of breakdown is typically relatively low, meaning larger equipment sizes are required. This can be problematic in practice given space and hygiene constraints present in residential buildings and FSE settings.

Secondly, regarding influent control, the performance of biological treatment can be heavily affected by variations in material supplied to them. Under poor management, this can lead to failure of the biotreatment process – for example, arising from shock loading of FOG, and subsequent death in microbial community present in the bioprocess. For this reason, bioprocess are typically recommended as a secondary treatment measure following primary treatment according to physical methods [37] – where the composition of FOG influent is comparatively better controlled.

Finally, biological processes present issues for FOG circularity. This is because of the destructive nature of the biological approaches, which means that the residual materials left over are of a different chemical nature. This reduces the potential for recovering FOG [37], though does open other avenues for resource circularity. For example, anaerobic digestion typically leads to the production of biogas (an energy vector) and nutrient-rich residual organic material that can be reused in a circular manner (e.g. for crop spreading).

Chemical Methods

Chemical methods include methods such as electrocoagulation or surfactant additives [41] and rely on the introduction of additional chemicals to separate and recover FOG from wastewater. As shown in Figure 2.3, they can be applied in purpose-built vessels before FOG is disposed of as an effluent, or through chemical dosing approaches of chemicals in-line.

A significant downside of chemical processes is their reliance on the introduction of additional chemicals into wastewater system. This is undesirable from an environmental perspective due to the risk of introducing more chemicals into the wider wastewater network as well potential the need for additional specialised equipment at the pollution source. Additionally, this introduces an additional cost basis associated with treatment, which is also undesirable.

The potential for circularity when using chemical approaches will differ significantly dependent on whether the approach is destructive (i.e. it changes FOG chemically) or not, and whether it is employed in a way which enables the recovery of treated material. If the method

is non-destructive and enables FOG recovery, then a potential may exist for re-use of the FOG as a resource in a circular manner. Other opportunities may arise for destructive methods which recover breakdown products. These are not considered further within the scope of this work.

Adsorption Methods

Adsorption methods are those methods which rely on the use of adsorbent materials to separate and recover FOG from wastewater.

Comparatively little use of adsorbent materials is present for FOG treatment currently. This is despite the use of adsorbent materials in treating lipidic/FOG-like material in a wide range of other applications (e.g. vegetable oil purification [22] and biodiesel production [23]). As a treatment approach, the use of adsorbents may be considered as non-destructive, falling between a mixture of physical and chemical methods. That is, physical in the use of physical adsorption and capillary condensation as methods for driving adsorbent performance, but chemical in the use of chemical affinity of the adsorbent and adsorbate to enhance adsorbent performance.

As shown in Figure 2.3, adsorption methods have the potential to be used across much of the wastewater lifecycle. For example, adsorbent products may be used pre-effluent in in-sewer through use of 'inserts' of packed adsorbent beds into existing infrastructure, in-line through the introduction of packed beds of adsorbents into pipelines. This reflects the flexibility of use case of adsorbent materials and their design.

As adsorbent materials are non-destructive, they provide an opportunity resource circularity through the direct recovery and reuse of FOG material. However, dependent on adsorbent design, this may introduce a practical drawback in requiring an additional processing stage to recover adsorbent material. For example, this may include, chemical methods such as solvent washing, or physical methods such mechanical compression [20].

Circularity Opportunities

Differences in the methods available for FOG treatment create significant differences in the opportunities for resource circularity associated with each method. This may in turn drive interest in the treatments used based on their financial incentive for resource recovery.

Generally, FOG treatments based on non-destructive methods may have the potential for use in the production of biodiesel products – thus providing an avenue for resource circularity. However, this relies on the fact that a significant fraction of FOG being fatty acids in nature (see Section 2.2.2).

By contrast, FOG treatments based on destructive measures convert FOG to other chemicals, potentially removing the opportunity for FOG circularity (e.g. FOG-derived biodiesels and specialty chemicals). Despite this, the methods may open other avenues for resource circularity. That is, the materials produced because of breakdown may be products or intermediates for other processes biogas. For example, consider the case of biogas (a natural gas derivative) and nutrient rich residual material discussed for anaerobic digestion (see Biological Methods section above).

For optimal circularity of FOG waste treatment, a comprehensive assessment is required accounting for cost, practicality (i.e. ease of implementation and maintenance), and environmental factors in overall decision-making process. Despite this, rule of thumbs exist for the order in which methods should be selected for implementing resource circularity. For example, the EU The Waste Framework Directive of 2008 identifies an approach prioritising reuse > recycling > energy recovery, with disposal being a last resort.

Cost

As mentioned in Chapter 1, the cost of reactive measures for removing FOG deposits is values at roughly £100 million per year in [42] – up from an estimated £15 to £50 million a decade prior [13]. A major factor in determining optimal treatment will be cost-adjusted benefit of individual treatment strategies. This cost may vary significantly depending on the strategy employed given differences in the capital and operational expenditure associated with the methods used as well as their effectiveness.

In addition to financial cost, existing reactive measures for addressing FOG blockages incur costs to health and safety. This is because reactive measures often include the removal of FOG by jetting or manual removal [13], typically requiring exposure of human operators to the sewer system and FOG deposits. Minimizing the need for reactive measures – especially those involving sewer exposure - is therefore desirable.

Finally, FOG carries with it environmental cost associated with the adverse environmental outcomes of poor FOG pollution management. FOG pollution has been attributed to as much as 50 % of sewer blockages in Ireland [43], 55% in Scotland [34], 60% in the UK [13], and 70% in Malaysia [44]. It therefore follows that contribution of FOG to environmental damage associated with sewer system overflow is likely very high too.

2.2.2. Chemical Composition

As outlined in Section 2.2, FOG materials originate largely from lipidic material present in dietary fats. These lipid materials are present as triglycerides molecules – which are large molecules based on the transesterification of free fatty acids (FFAs), with glycerol [44]. As a result, the chemical composition of FOG material is commonly discussed in terms of FFA content within literature. Major constituents often include palmitic, oleic, and linoleic acids – which represent saturated fatty acid (SFA), mono-unsaturated Fatty Acid (MUFA) and poly-unsaturated Fatty Acid (PUFA) chemistries respectively [13, 45, 46]. Example FFA content of dietary foodstuff and wastewater influents are provided in the following subsections.

Dietary Foodstuffs

Table 2.2 and Table 2.3 provide a summary of FFA breakdown in major dietary fat sources based on primary saturated, monounsaturated, and polyunsaturated chemistries.

Table 2.2: Chemical composition of free fatty acids present in common vegetable derived foodstuffs.

Source	Main Component			Component Content, wt%			Ref
	SFA	MUFA	PUFA	Palmitic	Oleic	Linoleic	
Rapeseed	Palmitic	Oleic	Linoleic	7.3	62.9	30.5	[47]
Corn	Palmitic	Oleic	Linoleic	13.6	25.6	60.8	[47]
Olive	Palmitic	Oleic	Linoleic	12.1	80.9	7.0	[47]
Plan	Palmitic	Oleic	Linoleic	49.4	39.5	11.1	[47]
Peanut	Palmitic	Oleic	Linoleic	19.4	48.5	32.0	[47]
Soybean	Palmitic	Oleic	Linoleic	15.4	23.3	61.3	[47]

Table 2.3: Chemical composition of free fatty acids present in common animal-derived foodstuffs.

Source	Main Component			Component Content, wt%			Ref
	SFA	MUFA	PUFA	Palmitic	Oleic	Linoleic	
Chicken Fat	Palmitic	Oleic	Linoleic	33.0	45.2	21.4	[47]
Lard	Palmitic	Oleic	Linoleic	41.8	47.9	9.9	[47]
Tallow	Palmitic	Oleic	Linoleic	47.9	47.4	3.3	[47]

Wastewater Influent

Information on typical composition of used cooking oil and materials common in physical separators are shown in Table 2.4 and

Table 2.5.

Table 2.4: Chemical composition of free fatty acids in used cooking oil.

Source	Main Component			Component Content, wt%			Ref
	SFA	MUFA	PUFA	Palmitic	Oleic	Linoleic	
UCO	Palmitic	Oleic	Linoleic	60.6	25.0	43.0	[48]
UCO	Palmitic	Oleic	Linoleic	26.3	59.4	14.3	[49]
UCO	Palmitic	Oleic	Linoleic	14.8	50.7	13.6	[50]
UCO	Palmitic	Oleic	Linoleic	8.0	61.4	26.1	[51]
UCO	Palmitic	Oleic	Linoleic	11.6	21.1	61.1	[52]
UCO	Palmitic	Oleic	Linoleic	5.7	46.6	47.5	[53]

Table 2.5: Chemical composition of free fatty acids in materials found in physical separators. NDF: not defined.

Source	Main Component			Component Content, wt%			Ref
	SFA	MUFA	PUFA	Palmitic	Oleic	Linoleic	
GTW Effluent	Palmitic	Oleic	Linoleic	57.8	9.8	1.4	[54]
Yellow Grease	Palmitic	Oleic	Linoleic	38.6	48.1	7.7	[55]
Brown Grease	Palmitic	Oleic	Linoleic	37.0	45.5	12.9	[55]
Soapstock	Palmitic	Oleic	Linoleic	21.6	15.7	62.7	[55]
NDF	Palmitic	Oleic	Linoleic	37.6	39.8	20.1	[56]
NDF	Palmitic	Oleic	Linoleic	46.5	36.1	15.3	[57]

2.2.3. Deposit Formation and Characteristics

Relatively few reports are currently published discussing major chemical and physical aspects of FOG deposits retrieved from sewers [13, 44, 58-63]. Additionally, the majority of reports may be considered to report relatively small sample sizes (i.e. mostly less than 10 individual deposits per author), [13, 35, 58-60, 62], coming largely from sewers in the USA [58-61]. Nonetheless, findings are in significant consensus that deposits are based by a majority weight on FFAs (i.e. >50 wt%), with lesser extents of general debris, calcium mineral ions and metallic elements also being present [13, 58]. Additionally, deposits have also been reported to have relatively low (10 to 24%) porosity and highly variable moisture contents (10 to 60%) [53]. It is therefore clear that FOG deposits must incorporate FFAs into their structure selectively. Several reports have found that SFFAs compose most of the FOG fraction followed by MUFAs

[13, 58, 59, 61, 62]. In almost all cases, palmitic acid appears to represent the primary saturated chemistry [13, 58, 63] (though stearic acid has also been reported by Keener *et al.* in 1 of 6 samples [58]); similarly, oleic acid appears to be the primary MUFA in almost all cases (though palmitoleic acid has been noted in 2 of 3 cases by Williams *et al.* [13]) [58, 62, 63]. Contrarily, linoleic acid has been reported consistently as the primary PUFA present [13, 58, 62, 63] in all samples. Interestingly, Williams *et al*. have also noted that changes in relative SFA, MUFA and PUFA composition occur as a function of distance down-stream of emission source [13]; however, further work is required to substantiate this further. When comparing deposit and dietary lipid compositions, several authors have noticed a seemingly disproportionate amount of saturated FFAs into deposit structures. Though the reason for this is not fully understood, it has been suggested that this may be due to the hydrogenation of MUFAs and PUFAs during processes such as during cooking (as demonstrated by Williams *et al*. with tallow and palm oil [13]), or microbial activity occurring within grease trap interceptors and sewers [44].

The lack of correlation between water hardness and calcium concentration (of deposits) has also caused a significant proportion of literature to investigate the extent to which FFAs undergo saponification [13, 60, 64]. This is believed to be associated with the leaching of calcium which occurs naturally in sewers due to biological processes such as microbially Induced Concrete Corrosion (MICC) [60]. From this, it has been suggested that the adhesion of deposits may be aided by the concentration of calcium (local to corrosion sites) which is as much as 10,000 times that in water [65]. Del Mundo *et al*. have also demonstrated a sensitivity of deposits to calcium source based on changes in colour of deposits grown in-vitro [66]. It is suggested that this may be an actor in the wider discontinuous layering reported previously by Keener *et al*. [58]. However, given lack of comprehensive understanding for the timescales over which FOG deposits form, more work is required to develop mechanisms by which sources of calcium in sewer change to such an extent as to validate this hypothesis. A summary of major formation mechanisms present in FOG deposition is shown in Figure 2.4.

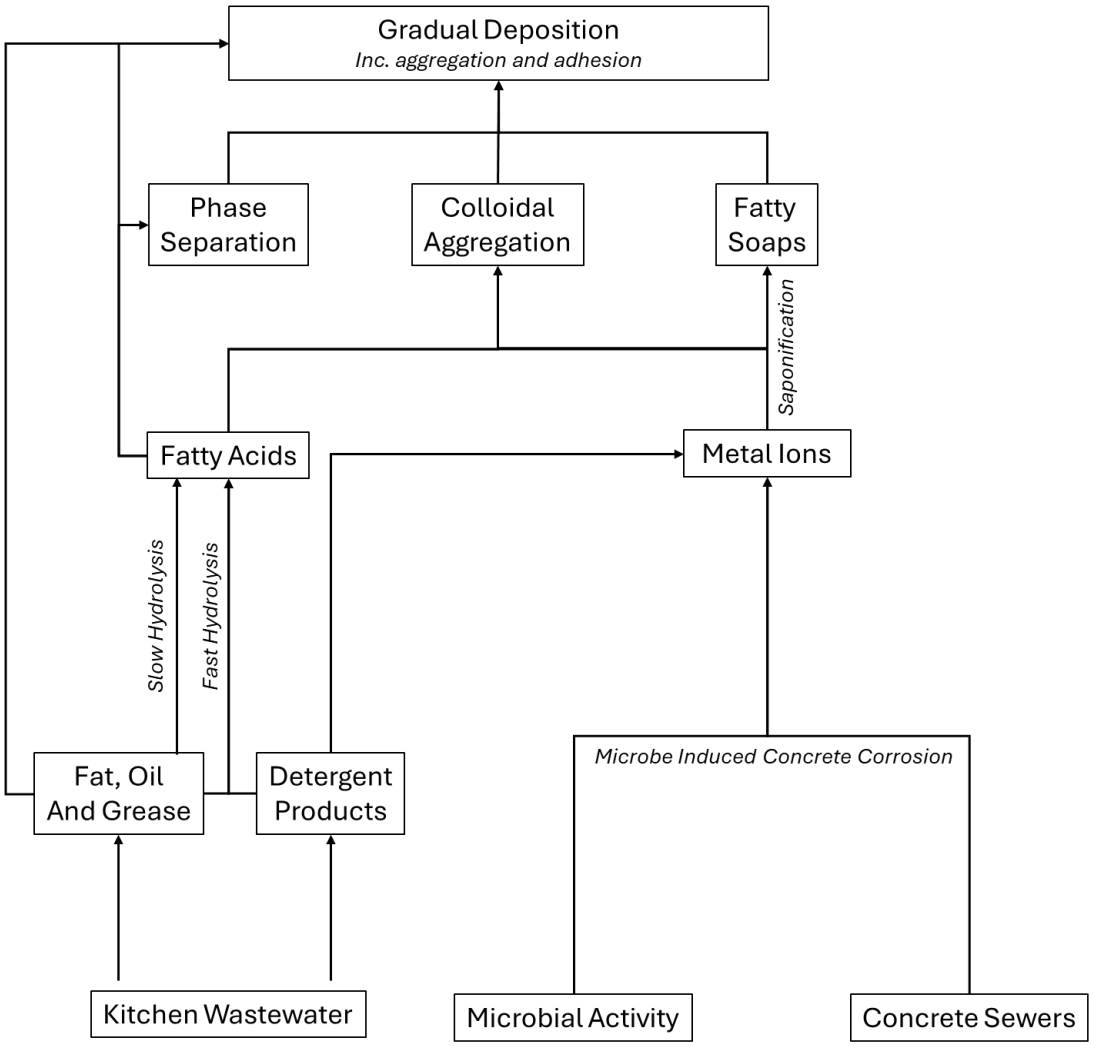


Figure 2.4: Relation of FOG deposit formation to interaction between metals, FOG-derived pollutants, and their relation to pollution source.

2.3. Life Cycle Assessment as an Impact Assessment Method

2.3.1. Overview

Life cycle assessment (LCA) provides an approach for assessing the impact of products based on the sum of activities associated with their production, use, and disposal. It is used extensively in industry as a tool for evaluating the impact associated with product life cycle and to make informed decisions about life cycle activity. Developed originally in the 1970s [67], LCA is now a widely adopted method through which the life cycle of a product may be systematically appraised. This includes existing international standards, which have been developed and refined since the early 1990s [67, 68].

2.3.2. Assessment Framework

A common reference for use of the of methods are the international standard organisation (ISO) documents – the most recent of which are ISO 14040:2006 and ISO 14044:2006 [69, 70]. In this framework, LCA is split into a total of four conceptual stages [69]: goal and scope definition, life cycle inventory modelling, impact assessment, and interpretation. This is illustrated in Figure 2.5.

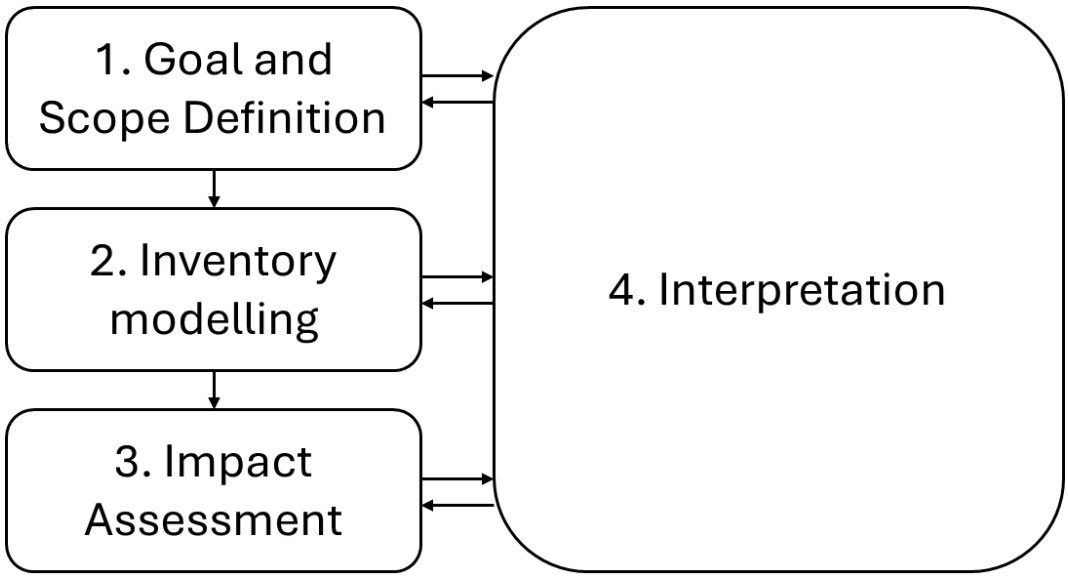


Figure 2.5: Relationship of major stages in the Life Cycle Assessment Framework according to ISO 14040 [69].

In the first stage (goal and scope definition), boundaries are set out regarding the level of detail to be expected of the LCA being reported. This includes information such as the functional unit by which impact will be assessed, boundaries for what life cycle aspects will be

included and excluded in modelling, impact categories to be considered, and allocation procedures by which impact will be attributed to products.

In the second stage, inventory modelling focusses on aggregating information for activity occurring within the life cycle, and flow of material and energy associated with this. This is commonly referred to as quantifying the activity present in the Technosphere associated with the system boundary defined for the LCA. Data can come from multiple sources, and the extent of data aggregated is directly subject to the scope of the LCA.

In the third stage, impact assessment then focusses on quantifying the overall impact associated across the life cycle. This is achieved by using impact characterisation factors, which act to take a quantitative amount of activity present in the Technosphere model (see above) and convert it into equivalent impacts based on impact categories outlined for consideration during goal and scope definition.

The generation of characterisation factors used in impact assessment includes a complex and varying field that varies dependent on the type of impact being quantified. It requires both identifying relevant cause-impact pathways for the system of interest (e.g. environmental system models, biological systems models), and finding quantifiable units of activity that link the cause-impact pathway to Technosphere activity. This has led to the establishment of a small number of impact characterisation methods in the literature that most LCA studies rely upon. These methods are commonly subdivided based on whether they provide impact estimates associated with outcomes somewhere within or at the end of the cause-impact pathway; these are referred to as mid-point and end-point methods respectively [71].

2.3.3. Use in Chemical Product Design

The chemical industry has a major effect on the extent to which global sustainability can be achieved. It is therefore imperative that decisions are made to change ways in which current chemical industry operates to achieve a future industrial system that can grow within sustainable limits. However, doing so requires understanding of the impact of activity in the chemical industry contributes to, or detracts from, the ability to achieve sustainable development targets. LCA provides a standardised approach by which this may be achieved.

The applicability of LCA as a tool for impact assessment has become widespread in chemical industry. Importantly, reviews in literature suggest that many studies currently being reported

are comparative in nature, focussing on the effect of different production pathways on product impact [72]. Whereas this is likely accurate for research literature, other impact assessment may also be established more widely as part of meeting regulatory requirements or voluntary information including wider marketing activities and environmental product declarations.

Contrasting the LCA of existing products, additional difficulties often arise when considering application of LCA to emerging products with lower technological readiness level (TRL). This is because of the lack of information existing for material and energy use present for low-TRL processes – which arises from the tendency of laboratory results to have significantly lower energy than methods used in industrial process implementations, and lack of pre-process and post-processing information [73]. For some authors, this has led to the suggestion of relying on more qualitative approaches such as green chemistry during the earliest of stages [73]. Contrarily, the suggestion has been made that such cases can be bridged through appropriate application of process simulation methods in combination with expert judgement surrounding process design. This is especially so in the case of estimating energy use.

Issues of the low-TRL methods are challenging as they create greater uncertainty in the reliability of comparison made between emerging technologies, and existing manufacturing technologies [74]. In attempting to shed light on this issue, authors have suggested several terminologies such as “ex-ante LCA” [75], “anticipatory” [74], and “prospective LCA” [74]. Though discussion exists, there still appears to be no consensus approach by which LCA should be conducted in such cases [74]. Thus, until rigorous agreement is provided, ensuring transparency in modelling approach, and limitation is perhaps the more responsible approach that can be taken to ensure the future utility of research findings.

2.4. Process Modelling for Estimating Mass and Energy Use

2.4.1. Overview

Discussion in Section 2.3.3 mentions process modelling as a tool for estimating missing information during LCA of chemical products (including SBAMs). While the field of process modelling is well established, it requires a foundation in engineering principles that acts as barrier to use for many. Thus, key concepts in the use of process modelling for engineering design are outline here.

2.4.2. Use in Process Design

Process design involves addressing major conceptual stages of 1) process system synthesis, and 2) process unit modelling.

Process Systems Synthesis

Process system synthesis involves the description of overall processing system required to achieve manufacture of a desired product or products. This requires description of a network of processing stages in which individual physical, chemical, or energetic transformations may take place as part of producing the desired product(s). This results in identification of general processing unit technologies required for manufacturing in addition to key performance descriptions of equipment. For example, this may include specifications to desired operating conditions, or otherwise to achieved extents of performance that indirectly lead to constrain of operating conditions. An illustrative case of decision making inherent to process systems synthesis is shown in Figure 2.6.

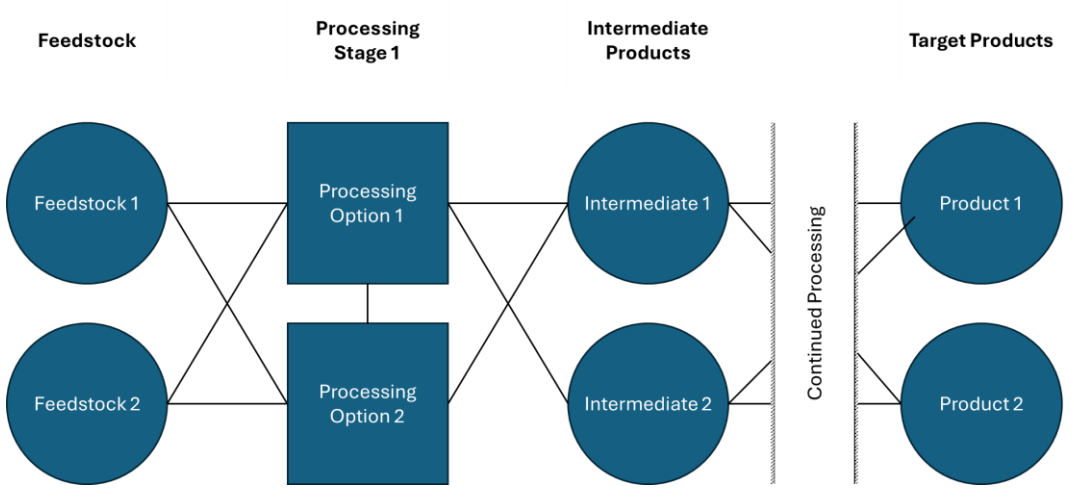


Figure 2.6: Illustrative example of decision making for equipment networks present in process systems modelling.

Process Unit Modelling

Process unit modelling involves establishing fundamental relationships by which individual processing equipment achieve the chemical, physical and energetic changes desired within a hypothesised process system network. This relies on a greater level of detail surrounding physical and energetic aspects of the equipment, and practicality of unit operation.

Fortunately, the maturity of engineering literature means that rigorous models exist which describe most processing equipment. For those models that are computationally expensive, simplified "shortcut" methods often exit. For example, this includes models for reaction chemistry based on reaction stoichiometry alone, or shortcut methods for distillation processes that use empirical models to estimate optimal design conditions. The Fenske-Underwood-Gillian-Kirkbride (FUGK) distillation shortcut method [76] (used in this work) is a classic example of this.

2.4.3. Use of Process Optimization

The need for price competitiveness typical of the chemical industry creates a demand for identifying process designs that can operate at or near economically optimal conditions. This has led to the generation of a vast field of research into the use of mathematical optimization methods that can be implemented to explore process design to identify. As shown in Figure 2.7, this may include consideration for varying levels of design complexity including both process systems specification, and process-unit level modelling. Owing to the iterative nature of design space exploration, and availability of modelling software, this is usually performed using computerised approaches. Due to the variability and complexity of many real-world models, and limits imposed by use of existing software, this has led to a large focus on the use of black-box optimization (BBO) paradigm in practical applications.

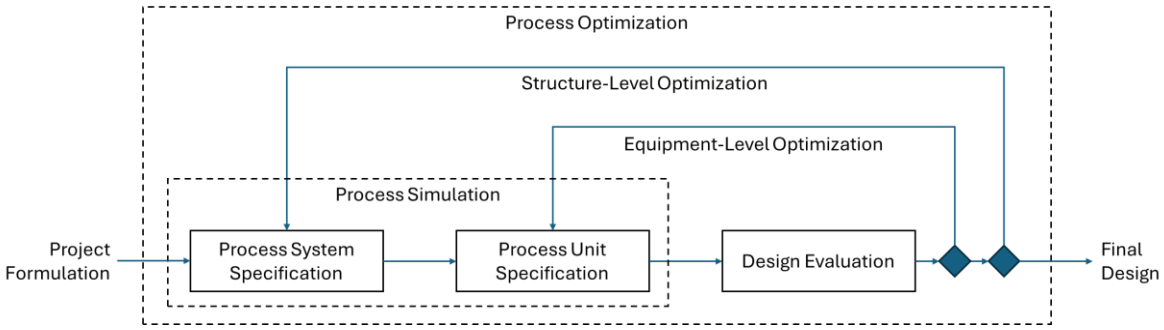


Figure 2.7: Relationship between process system specification and process unit specification in a typical process design optimization problem.

The nature of all but the simplest of process arrangements leads to mathematical models that are hard to solve analytically. This often includes process models with non-linear process behaviours with the presence of more than one local optimal design condition. As a result, approaches to optimization have become heavily focussed on the use of computer aided optimization approaches to rapidly searching for and identify desirable process design conditions. Particularly, availability and limitations of existing software, this has led to the development of approaches that avoid optimization reliant on gradient-derived directions of steepest ascent/descent. These methods are often referred to as black box methods.

Typical black box optimization problem can be considered as following a framework consisting of three main stages: 1) formulation, 2) implementation, and 3) execution.

In the formulation stage, an explicit definition of the metric form optimization (objective function) is defined alongside limitations to design consideration such as practical design constraints. In the implementation stage, a policy is defined by which exploration of the design space specified during formulation will occur.

The execution stage then focusses on creation and use of practical computer-read code by which computerised optimization occurs. This relies far more on practical aspects of code implementation and optimization typical of computer science field.

Optimization Approaches

The black box approach to optimization relies on developing methods that do not rely on explicit definition of analytical form of objective function gradient. This enables them to address a broad range of mathematical models in a modular, more generalised way. They are also practical in the way that they relate to calculation process as a clearly distinguishable add-on programmatic solution, which enables their applicability to a wide range of problems.

Typical approaches to black box optimization include three high-level approaches: 1) derivative approximation, 2) stochastic searching, and 3) model-based methods.

Derivative approximation methods attempt to estimate the gradient of the objective function. This requires an iterative approach in which the gradient is calculated for an individual point in the search space by first sampling several points in the vicinity, and fitting models to observed changes in the objective function.

Stochastic methods rely on use of exploration policies that incorporate random sampling methods. They typically require more computational iterations but have the benefit of being able to sample across the entire sampling space.

Surrogate-based methods rely on developing approximate models for the objective function surface for use as the basis of optimization search policy [77]. From this, the surrogate model is then used as the basis of decision-making policy for further exploration and exploitation of the design space.

Choosing the "best" method

The diversity and complexity of objective functions arising in process design mean that there is no generalisable single "best" optimisation algorithm – an issue commonly referred to as the "no free lunch" (NFL) principle [78]. The NFL principle also applies to data-driven search algorithms used in BBO [79]. Unfortunately, this includes many approaches typically employed in black-box optimization, and therefore real computer-aided design problems.

Nature-Inspired algorithms

Nature-inspired algorithms are a subset of heuristic methods commonly employed in optimization. They are typically stochastic in nature and rely on generation of samples according to methods that have been inspired by features in wider nature. This includes a number of algorithms inspired by the process of evolution of species – i.e. evolutionary algorithms.

Many evolutionary algorithms are common within the space of chemical process design engineering due to their ease of use and their ability to search spaces highly non-leaner, multimodal design spaces. However, the stochastic nature of the method typically leads to a greater number of searches to be used when compared to deterministic methods.

2.4.4. Use in Life Cycle Assessment

As established in Section 2.3.3, use of process modelling can be of great support to LCA through enabling the establishment of estimates for material and energy use associated with activity in the production stage of a product life cycle.

Use of process modelling provides opportunities for more transparent overview of sensitivity of technical factors to overall environmental performance. This can be instrumental to understanding natural limitations of processing approaches, therefore contributing to further improvement of technological approaches [80].

Consequently, though the use of process modelling is in no doubt a positive tool for life cycle understanding, great care must be taken in its use as a tool for approximating life cycle inventories.

2.5. Silica as an Adsorbent Substrate

2.5.1. Overview

Previous discussion has highlighted the reasons driving interest in using SBAMs as a solution for pollution abatement. This section expands on this by providing information necessary to understand how the chemistry of silica ultimately enables the production of SBAMs and summarising the typical methods by which SBAM substrates are typically manufactured. This is concluded with a discussion on these topics from a life cycle perspective

2.5.2. Chemistry

Solid-State Structure

Solid state silica is composed of close packed repeating units of silicon-oxygen bonds. Owing to the valency of silicon, structures are built based on the repetition of tetrahedral structure of the $[SiO_4]^{4-}$ silicate anion structure (see Figure 2.8).

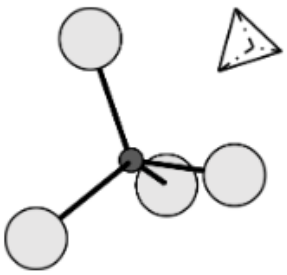


Figure 2.8: Tetrahedral structure of the silicate anion.

Surface Chemistry

The formation of surfaces leads to a natural break in the tetrahedral structure that solid state silica seeks to form. Consequently, those structures present at the surface seek to establish valence stability by forming alternative bonds. Under standard conditions, this leads to the formation of surface hydroxyl groups termed silanol structures (see Figure 2.9a-c) and siloxane bridges (Figure 2.9d). Dependent on orientation relative to the surface, the silicate anion can be theoretically terminated with as many as three hydroxyls. However, in practice, only one-site and two-site terminations are observed experimentally. Groups with these environments are termed geminal and vicinal silanol groups respectively (see Figure 2.9). The relative proportion of geminal and vicinal silanol groups is affected by temperature due to the tendency of silanol to undergo condensation reaction to form siloxane bridges at temperature

above 150 C [81]. This affects the behaviour of silica surfaces due to associated change from hydrophilic silanol chemistry to the relatively hydrophobic siloxane bond chemistry.

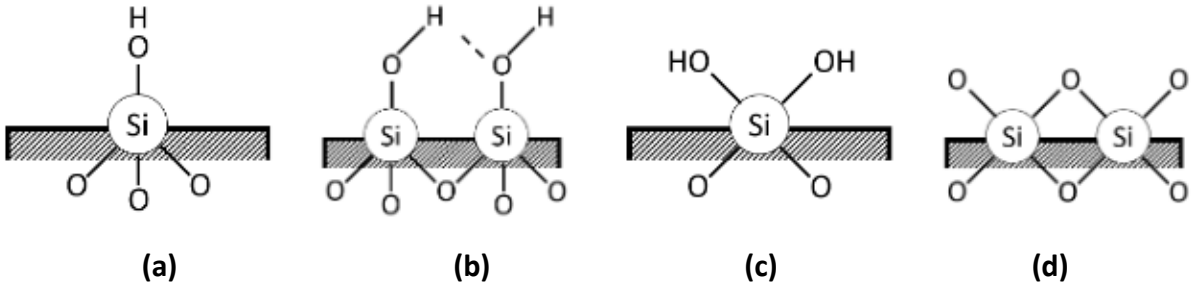


Figure 2.9: Surface chemistry of unmodified silica surfaces including silanol (a-c) and siloxane (d) functional groups.

Reactivity

Much of the behaviour of silicon dioxide is relatable to the chemistry of the silicon atom. As a group 14 element, silicon acts similarly to that of carbon. However, its larger atomic number causes the bonds formed by silicon to be weaker than carbon analogues. This makes it more reactive – a feature commonly exploited in silica synthesis and surface chemistry modification (see Section 2.7.3)

One major difference rising from the size of the silicon atom (compared to carbon) is the effect on the chemical structure of silicon dioxide. While carbon dioxide can form a simple molecular structure stabilised by C=O double bonds, silicon dioxide forms a geo-polymer structure based stabilised by Si-O single bonds. This is due to the atomic size of silicon being too large to produce an Si-O double bond that is energetically favourable. This difference is the fundamental property that gives rise to production of silica (silicon dioxide) as a solid substrate.

Reactivity of the silanol surface chemistry is another feature for silica substrates. It is important in enabling chemical substitution reactions - where different chemistries become covalently bonded to the substrate. This is discussed further with regards to its application in reaction with silane coupling agents in Section 2.7.

2.5.3. Manufacture

Several manufacturing methods exist for producing silica-based adsorbent substrates. Many of these materials appear as fluffy, white powders. However, the processing history and resulting properties can vary significantly. At present, there exist two major methods for production of silica powder at commercial scale. Conversely, multiple methods exist for

producing silica according to emerging technological paradigms – of which self-sharpening (i.e. Stöber synthesis), templated synthesis, and bio-inspired (BI) methods are particularly prevalent. Further information of each approach is provided in the following subsections.

Commercial Methods

Pyrogenic Silica

Manufacture of silica according to pyrogenic method relies on the pyrolysis of gaseous silicon reagents in the presence of hydrogen (see Equation 2.1). This involves use of chlorosilane products as the primary reagent – particularly silicon tetrachloride, $SiCl_4$ is used extensively in industry.

$$SiCl_4 + O_2 + 2H_2 \rightarrow SiO_2 + 4HCl \tag{2.1}$$

Hundreds of kilotons of pyrogenic silica are produced annually [82]. Products are typically of a purity equal to or greater than 99.8 wt% SiO_2 [82], and are non-porous on a primary particle level. Post-processing of pyrogenic silica is typically limited to collection and storage [82].

Precipitated Silica

Manufacture of silica according to precipitated method relies on a sol-gel approach in which a silicate reagent is treated with acids, casing silica particles to precipitate out of solution. This occurs using sodium silicate as a reagent product, which undergoes hydrolysis and subsequent condensation reactions to form silica as shown in Equations 2.2 and 2.3.

$$\equiv SiO - R_1 + H_2O \rightarrow \equiv SiO - H + HO - R_1 \tag{2.2}$$

$$\equiv SiO - R_2 + HO - Si \equiv \rightarrow (\equiv Si)_2O + HO - R_2 \tag{2.3}$$

The post processing of precipitated silica produced by commercial sol-gel method is dependent on the intended product use case. This may include filtration, drying, milling, granulation, and storage [82]. Products produced by this method may be either sol, powder, or gel product form. Importantly, powder and gel structures are capable of exhibiting porous primary particle structures [82]. Their use in traditional adsorption applications is therefore well established.

Emerging Methods

Several emerging methods based on sol-gel synthesis approach are considered within the literature. They are differentiated from the commercial sol-gel approach through their

inclusion of additional materials during synthesis that act to provide greater control over either the synthesis chemistry (i.e. hydrolysis and condensation), or solution structuring. Typically, this is achieved using organic chemistries to manipulate the mechanisms by which precipitation occurs within aqueous media. Of these, the self-sharpening and surfactant templating approaches are perhaps the most common. Further information on principles of each approach is provided in the following.

These methods rely on the same reaction chemistry as outlined for commercial precipitation methods outlined above. However, they incorporate use of organic functionalities either within reagent choice, or additive choice, which acts to provide further control over which the mechanisms of precipitation occur.

Stöber Silica

The ionic nature of metal-silicate silica reagent used in commercial sol-gel silica leads to fast hydrolysis in aqueous environments, which is a critical factor in producing the multi-modal particle size distributions typical of commercial precipitated silicas. Self-sharpening methods address this problem using silicate reagents that act to reduce the kinetic rate of hydrolysis, causing particles of narrow particle size distribution to form.

Reduction in hydrolysis kinetics is practically achieved using alkoxy-silicate reagents, which reduce the rate of hydrolysis via steric hinderance of the alkoxy groups. First published in 1968 by Stöber, Fink and Bohn [83], this has been popularised as the “Stöber” method. This follows equivalent stoichiometry to traditional hydrolysis and condensation reactions (Equations 2.4 and 2.5) but leads to the condensation of an alcohol product. Increasing alcohol group size is associated with greater reduction in hydrolysis kinetics [84].

Therefore, in practice, methoxy and ethoxy terminated silicates are usually used. Owing to the hydrophobic nature of the alkoxy-silicate groups, this method is associated with additional organic solvent use – typically including alcohols [84].

$$\mathrm{Si(OR)_4 + H_2O \rightarrow Si(OR)_3OH + ROH} \tag{2.4}$$

$$\mathrm{Si(OR)_3OH + Si(OR)_3OH \rightarrow O[Si(OR)_3]_2 + H_2O} \tag{2.5}$$

The methods can generally be used to produce particles in the size range of 50 to 2000 nm [85].

Mesoporous Silica

Templated synthesis approaches rely on the use of surfactant molecules to create molecular-scale structures which constrain the geometry in which silica precipitates are formed [86]. This includes creation of silica product with disorder, or order across one-dimensional, two-dimensional, and 3-dimensional scales [87].

As shown in Figure 2.10 the surfactant templating processes can be split into three chronological stages - template formation, solid precipitation, and template removal.

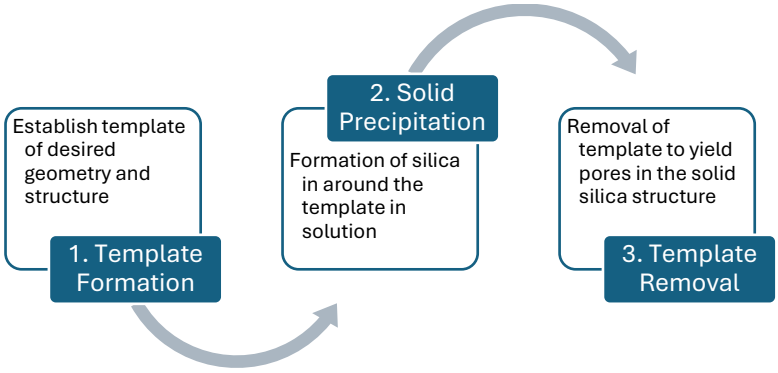


Figure 2.10: A summary of main conceptual stages in the synthesis of silica substrates according to surfactant templating approaches.

In the template formation stage, an appropriate solution environment is typically created in the absence of silica feedstocks to produce a desired structure of silica product. Both the surfactant choice and solution conditions play a large role in determining the outcome of surfactant templating. This is because of the effect of both on the type of self-assemblies and aggregate structures that a surfactant may form – for example, spheres, rods, tubules, lamellae, and vesicles. By changing the size of the aggregate structure produced it is possible to control the pore size of the silica material produced; typically, surfactants with larger chain lengths will form larger aggregates and therefore produce large pore sizes. Organic solvents may be used to cause surfactant assemblies to swell – increasing pore size in the resulting silica structure [88]. The use of cosolvents, cosurfactants, or various salts is also common within these methods [89]

In the solid precipitation stage, a silica precursor is added to the solution to initiate the beginning of solid formation. The silica precursor used is typically an alkoxysilane, though sodium silicate can also be used.

Finally, in the template removal stage, post-synthesis processing is carried out to remove surfactant template from synthesised particles, revealing a pore network. This is typically achieved by solvent washing followed by drying and calcination. Calcination is extremely prevalent due to the hydrophobic nature of the surfactant template and potential issues with pore penetration when solvent washing alone.

Templating approaches are traditionally classified into families of approaches within the literature. Each family relate to a collection of methods that typically rely on templating using a certain kind of template material. The most common of these materials include the use of cationic and non-ionic species. Particularly, this includes the use of cationic quaternary ammonium salts (QASs), and linear triblock copolymers (LTCs) (see Section 2.6). The use of these materials is typically associated with individual families – of which the Mobil Composition of Matter (MCM), and Santa Babara Amorphous (SBA) are the most common.

This includes, for example, MCM-41, MCM-48, MCM-50, SBA-1, SBA-2, and SBA-3 Products [90]. MCM-41 and MCM-48 products can have surface areas in the range of 1000-1500 m^2/g [91]; crystallinity, thermal stability and high specific surface area make them useful in a range of catalytic, adsorption and separation-based applications [91]

Bio-inspired Silica

BI synthesis methods refer to an approach in additives used are based on their ability to mimic process of biomineral formation [86]. Though many additives are being considered (e.g. polypeptides, polysaccharides, synthetic polymers, proteins and enzymes) [92], amine based chemical species are particularly well investigated owing to the effect that the amine chemistry plays on facilitating hydrolysis and condensation of silica precursors [87].

Bio-inspired approaches are desirable due to the relatively mild processing conditions in comparison to other methods of advance geometric control (e.g. Stöber, MCM, SBA) [86] – typically involving atmospheric pressure and room temperature. Bio-inspired methods also use organic solvents less often by avoiding the restrictions associated with use of alkoxide precursors [86], and may involve relatively low amount of surfactant use – see, for example

Brambila *et al*. [93]. The BI method may also include some beneficial approach with regards to minimising impact of post-processing of silica products owing to the aqueous solution-based washing and cleaning of particles post-synthesis (as opposed to standard calcination methods, for example).

Finally, production of bio-inspired silica is already being pushed toward the industrial scale. Particularly, works have been reported by Patwardhan and their co-authors on feasibility studies [94] and patents [95]. Several other relevant patents are also summarised elsewhere [86].

Recent research has identified as a molecule providing best control off silica synthesis products [86] that use of pentaethylenehexamine (PEHA) as an additive of choice citing high reaction yields, and material properties of silica products obtained [86, 94].

2.5.4. Life Cycle Perspective

Information above provides a clear outline of approaches to manufacturing by which solid silica substrates may be manufactured. Despite this understanding for manufacturing methods, varying levels of information exist on LCA of these products.

In the case of commercial methods, Roes *et al*. have reported predictions for the environmental impact of silica sols, silica gels, precipitated silica, and pyrogenic silica products [96]. The predictions are based on reported averages for material and energy use within EU-15 industry [82]. However, the impacts reported are limited to global warming potential and non-renewable energy use of each product only. This work is unique in the use of industrial scale data to inform LCA. Despite this, the consideration of only one environmental impact (GWP) prevents the reader from forming a holistic perspective on the environmental impact of each product. Thus, more work is required to consider environmental consequence of commercial manufacturing methods according to other impact categories.

Notably, there are also LCA works on the topic of titanium dioxide – a similar product manufactured by similar methods – that can be used as cross references for life cycle understanding (e.g. [97, 98]).

In the case of emerging methods, LCA understanding is significantly less developed. This is reflected in the lack of appropriate LCI models available for reagents used in emerging

methods [99], the level of sophistication of life cycle inventories used in recent publications, and works focused on metrics that are easier to calculate (e.g. green chemistry metrics and E-Factors) [93].

While differences in the level of development of LCA models for commercial and emerging methods may be expected, the absolute state of art associated with both methods are relatively lacking. This is especially so given the scale of manufacture associated with commercial methods, and the thousands of publications currently reported in literature regarding the emerging sol-gel methods (see Chapter 4).

Given the availability of information on process design in patent and academic literature, it seems as though the opportunity exists to provide a more comprehensive investigation and comparison of impacts associated with the production of all common manufacturing methods – including silica produced by pyrogenic, precipitated, MCM, SBA, and BI processing methods. Owing to the availability of data, many of these methods have enough information available directly in literature not to require more explicit approaches such as process modelling at the silica-manufacturing stage. Nonetheless, the lack of LCA information for all methods lead to a range of questions still existing regarding potential sustainable development of the materials.

This includes questions to impact of existing methods, and relative increase in impact associated with additional auxiliary material use arising from the emerging sol-gel methods, which have arisen previously in literature through discussion of materials on qualitative green-chemistry bases.

Importantly, it appears that many of these factors may link back to a wider question of silica reagent choice. This is done through first considering challenges associated with the implications of reagent choice on immediate synthesis stage. Further discussion around auxiliary material usage, and their co-dependence somewhat on reagent choice is then discussed. Finally, reagent choice must be seen as a key factor through the effects that it has on use of all other auxiliary materials discussed in the following subsections.

Relation to Reagent Choice

A great deal of discussion around silica materials has focused on assessment from a green chemistry perspective – owing to the more qualitative, approachable nature associated. This has led to a significant amount of discussion particularly on the importance of reagent

choice/silica source as a key factor in responsible design of silica. Direction of discussion in this area can be seen as relating to one of three interlinking issues:

1) Safety of chemistry required in reagent production,
2) Inherent limitations of reagents on process mass efficiency
3) Effect of reagent chemistry on wider processing conditions required for effective synthesis.

Limitations to mass efficiency can commonly discussed by way of reagent atom economy (see Table 2.6**)**.

Table 2.6: Mass efficiency and by-products associated with traditional precursors of silica production.

Species	Molar Mass, g/mol	Atom Economy, %	Silica Synthesis By-product	Common Use
Silica	60	-	-	-
Sodium Silicate	*122	49	Sodium Hydroxide	Precipitated sols and gels
Potassium Silicate	154	39	Potassium hydroxide	Electronics
Silicon Tetrachloride	170	35	Hydrogen chloride	Pyrogenic silica
Tetramethyl Orthosilicate	152	39	Methanol	MCM, SBA, Stöber
Tetraethyl Orthosilicate	208	29	Ethanol	MCM, SBA, Stöber

* The molar mass of water glass is dependent on sodium hydroxide molar ratio present. For more information, see discussion of the author in Errington *et al*. [100].

A focus on chemical safety can sometimes lead to over-emphasis of certain impact factors. For example, the presence of chlorine chemistry, though undesirable, is likely to appear significantly more important than potential issues associated with harsh basic chemicals and associated metal depletion associated with production of sodium and potassium silicates.

An additional challenge exists in that focus on such qualitative factors provides difficulty in understanding holistic impact of reagent choice. For instance, by comparison atom economy and chemistry of potassium silicate and tetramethyl orthosilicate, quite different life cycle impacts may arise from differences in processing despite equivalent atom economy of both products.

In the case of MCM materials, the most used silica source reagents are believed to be methoxy and ethoxy alkoxy silicates [91].

Auxiliary Substance Use

In many cases, auxiliary substance use (e.g. solvents, catalysts, templates) forms a large part of differentiating the properties of silica sold substrate produced by different processing methods. Ideally, the materials used should be innocuous [101]. However, in many cases for emerging sol-gel technologies this is simply not true.

Major areas for concern arising from production are split across solvent, catalyst and template use associated with production of silica products. Likely the most important of these factors in general is solvent use, which is heavily interlinked to several aspects of wider decision being made in the way that silica products are currently synthesised.

Surfactant Use

A key issue in the current processes in the mass inefficiency associated with use of both QAS and LTC surfactant templates. This is present both with regards to mass efficiency of surfactants used to achieve porosity, and lack of methods for the recovery of surfactant material for re-use.

The extent to which surfactant use can be minimised is not well discussed within the literature. Moreover, given lack of existing life cycle assessment information, it is unclear the extent to which this affects the impact of producing silica products.

Regarding recovery of surfactant material: Tendency to remove a significant fraction via calcination leads to inability for this material to be recovered as a co-product or recycled to achieve material circularity. There are undoubtedly issues with the potential of this being done – particularly in sensitivity of product synthesis to impurities and need for refinement of recovered solutions as a result. Given the lack of existing life cycle impact information, little understanding is currently available for the extent of benefit that such methods could create.

Solvent Use

Perhaps, the most immediate threat, organic solvent use. A major factor not considered appears to be the amount of solvent used additionally in the washing of silica products post-synthesis product purification. In many cases, this can be attributed to likely irresponsible solvent wash mass ratios used during purification [25]. From a practical perspective, these

methods can be to some extent discounted as they are unlikely to be economically viable, and therefore overall impact will be limited due to lack of production scaling.

In the case of organic alkoxy-silicate reagent use, a challenge arises from poor miscibility of the apolar organic precursor and polar water (required for hydrolysis). This causes anhydrous reaction mechanisms to become impractical and leads to the use of organic cosolvents.

Contrarily, in the case of large organic surfactant template use, thermodynamic and kinetics limits lead to the requirement of minimum amount of solvent in all practical use cases. Thermodynamically, this arises from limits to solubility of the surfactant templates and their aggregate structures within solution. Additionally, solvent use is dictated through the effect of solvation on the rate and extent to which solvent washes can effectively penetrate and clear porous networks. Some respite may arise here in advanced methods with multi-model pore network structures – originally created to address issues of pore diffusion limitation during sorption – however, not enough information is available in the literature generally yet to discuss this topic in extreme detail.

Use of structuring in the production of templated silicas is important due to the additional material use and associated life cycle processing that their incur. Use of QASs in silicas produced according to the M41S family are particular interest given their natural toxicity (associated with antibacterial properties).

Additional material use associated from structuring behaviour raise additional potential challenges. This includes cosolvent, cosurfactant, and varying salt use [89] – all of which act to increase the size of the life cycle associated with silica substrate product.

Processing Conditions

Most methods for producing silica products occurs under relatively mild conditions when compared within the context of general chemical process engineering industry. However, differences do occur in conditions achievable by different sol-gel processing methods. Most notably, the use of PPAs reported by Patwardhan *et al.* demonstrate ability for synthesis at standard conditions [86, 87]. This can be attributed to the catalytic nature of the PAA additives being used. Given difference of the product to traditional hydrolysis catalysts, it would be interesting to understand if such methods could gain benefit from recovery and reuse of products. Despite this, emerging processes in general appear to overly rely on linear resource

consumption models, without considering potential for circularity through material recycling and re-use.

Functional Unit

The processing history of silica products lead to silica products with significantly different material properties [82]. Despite this, many of the substrates are considered for design of adsorption-based separation technologies based on relationships with economic and technological performance. This is challenging from a life cycle perspective, as it creates difficulty in selecting a functional unit for comparison of products in the form they exist at-gate. Nonetheless, the current lack of life cycle understanding for impacts associated with each product and risks inherent in their life cycles lead to the conclusion that development of information at-gate is a beneficial approach to developing life cycle understanding in a way that is most generalisable (and thus transferable) to the broad research landscape in which such silica products are being researched and used. Given this, it is suggested that use of a physical basis for comparison may be desirable starting point – as keeping in line with ISO standards [69].

Scope of System Boundary

The manufacturability and customisability of SBAMs make them capable of being designed to meet a range of different product forms and pollution-centric use cases. This is likely to significantly affect the ways in which any SBAM product is used within the use-phase of the lifecycle – directly effecting information required when carrying out LCA of any SBAM product which includes the use phase. Given the range of use cases that may be considered for SBAMs, it is hard to provide an exhaustive account of areas of variability as observed within the LCI associated with the life cycle of any individual SBAM product. Nonetheless, differences may arise from the use phase in whether adsorbents are reused, techniques used to recover adsorbent pollution (e.g. solvent extraction, thermal treatments, electrochemical approaches) from the adsorbents, techniques used to regenerate adsorbents (e.g. thermal and solvent treatments), and the handling of adsorbents at the end of their use phase.

Issues with variability of product-specific life cycles arising from the use phase are avoided when considering only impacts associated with production within the scope of cradle-to-gate. This is beneficial in providing a significant reduction in the amount of life cycles that may be associated with SBAM production within this system scope. The cradle-to-gate is also a bottle

neck of information, which is required if LCAs including the use phase of an SBAM are to be considered. Given this, and lack of information present currently for impact of the production stage of SBAMs, a focus on developing LCA information for the cradle-to-gate scope of a range of SBAMs is likely to provide a significant contribution to existing literature.

2.6. Organic Surfactants as Additives for Substrate Synthesis

2.6.1. Overview

The discussion of surfactant templating approaches in Section 2.5.3 highlights the use of organic surfactants as additives to modify properties of silica substrates produced. This includes use of QASs, LTCs, and PAAs in the case of MCM, SBA and BI silica methods respectively.

The organic surfactants used in emerging methods have their own processing history that must be considered to understand full implications. Despite this, in many cases, very little life cycle understanding is present, and no comprehensive life cycle assessments have been reported.

The following subsections provide further information necessary for understanding how three types of surfactant molecules used in silica substrate synthesis are produced – these are: QASs (common to MCM-type silica products), LTCs (common to SBA-type silica products), and PAAs common to BI-type silica products.

2.6.2. Quaternary Ammonium Salts

Quaternary ammonium salts are a broad group of chemicals commonly used for their antiseptic properties. Nonethless, trimethylammonium halides are often used as liquid crystal templates for producing mesoporous silicas [102]. Choice of alkyl chain length can be used to dictate the size of pores within the silica structure – through the effect of chain length on the size of surfactant aggregates, which form pore space. Of these, alkyl trimethylammonium halides are often selected, with cetrimmonium chloride (CTAC) and cetrimmonium bromide (CTAB) being common [102]. Use of QASs is particularly prevalent in the production of Mobil Composition of Matter (MCM) family of silica substrates [102]. Further information on industrially relevant methods by which QAS are produced is provided in the following subsection.

Manufacture

The production of alkyl trimethylammonium halides may occur according to multiple different approaches. Most common approaches include derivation from alpha-linear molecules with carboxylic acid, alcohol, or alkene group chemistry. The methods of processing typically

include amination, and subsequent alkylation – though this is feedstock reagent dependent. The choice of reagent is somewhat governed by desired alkyl chain length.

2.6.3. Linear Triblock Copolymers

Overview

Linear triblock copolymers are a broad group of chemical species used for their temperature-dependent thermo-reversible gelling properties in water. This includes the branded group of Pluronic products, which are produced by BASF [103].

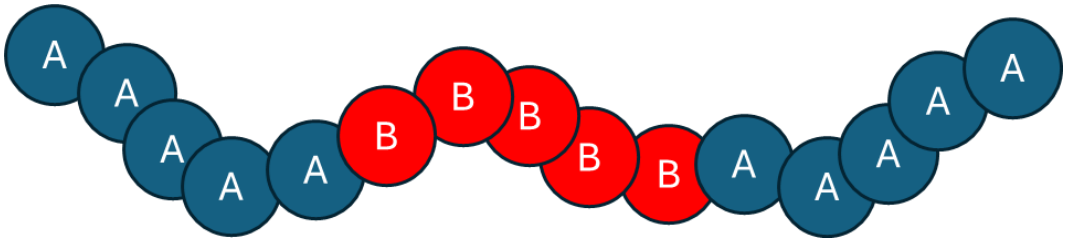


Figure 2.11: Schematic representation of an ABA triblock copolymer formed by a sequence three distinct polymer 'block' sections.

Poloxamer LTCs are typically used in the production of silica according to multiple approaches, most notably of which includes Santa Barabara Amorphous (SBA) family (see Section 2.5.3). The most well-known of these is the use of P_{123} in producing Santa Barbara Amorphous method [104].

Nonetheless, the use of these LTC products have become particularly attractive due to being nontoxic, biodegradable, inexpensive and easily separated from the silica product [89]. SBA-15 products typically have thicker pore walls than MCM products derived using Quaternary ammonium halide salts [105] – which can mean greater hydrothermal stability [105]

Manufacture

Several sources in literature a report that poloxamer LTCs are produced according to catalysis with metal hydroxide compounds [103, 106]. This is typically applied in less than stoichiometric amounts [107].

Nonetheless, use of metal hydroxide catalysis is limited to the production of LTC blocks with low molecular weight. This is due to issues associated with hydroxides catalysing the unwanted formation of alkene chemistry [108], which acts as a product impurity as the molecular weight of the poloxamer LTC increases [109]. Consequently, products with molecular weight above 1000 g/mol (including many major poloxamer materials used in silica

synthesis) are instead often produced using double metal cyanide catalysis (DMC) catalysts [107].

Despite this, it is still common for metal hydroxide catalysis to as the initial stage in the production of LTCs. This is because, while producing pure poloxamer blocks [107], DMC tend to become deactivated by presence of monomeric start materials used to produce poloxamer LTCs (such as ethylene oxide and propylene oxide). This leads to production of poloxamer LTCs according to a multi-stage manufacturing process. In the case of Pluronic 123, this may involve initial production of a sub-1000 g/mol poly(propylene oxide) (PPO) the production of LTCs according to multi-stage methods in which metal catalysis (e.g. the KOH method) are used to produce starting blocks of low molecular weight (i.e. < 1,000 g/mol) material that can be grown into pure poloxamer blocks according to a DMC catalysis approach.

To produce P_{123}, a total of three production stages are required. These are: 1) production of a low molecular weight PPO material via metal oxide catalysis, 2) growth of the PPO material to the desired PPO_{70} material, and 3) addition of terminal poly(ethylene oxide)$_{20}$ groups. In practice, the short molecular size of PEO_{20} enables the final stage to occur according to a metal oxide-based addition method.

2.6.4. Poly(alkylamines)

Overview

Poly(alkylamine)s are a group of polymeric compounds capable of simultaneously acting as structure directing agents, hydrolysis catalysts and inter-particle bridging agents [87]. The degree of their functionality is dependent on the specific molecule considered. Choice and use of PAA is therefore application dependent, and several poly(alkylamine) chemicals have been reported to be used to synthesise silica according to BI methods. Of these, Pentaetylenehexamine (PEHA) has been repeatedly investigated by Parthadwan *et al*. – e.g. [87, 94] – owing to high reaction yields, and material properties of silica products obtained [94]. It is, however, also corrosive and toxic to aquatic wildlife [110].

Manufacture

Production of PAA materials may occur according to polymerisation approaches derived from one of multiple pathways. Most commercial methods appear to involve reaction according to the ethylene dichloride process (other process being available, though used less) [111]. In this

process, ethylene dichloride is reacted with ammonia at high pressure 13 to 140 bar and moderate temperatures of 100 to 400 C [112]. This leads to the production of a crude PAA mixture containing distinct PAA products of varying chain length and hydrochloride salt by-products [113]. These products are typically separated according to initial salt separation followed by of the PAA mixture. All PAA oligomers have high (i.e. >200 C) boiling points, and thus vacuum distillation may be required; oligomers larger than tetraethylenepentamine (TEPA) are typically considered to be 'higher molecular weight' poly(ethyleneamine) chemicals [113].

A major factor in the production of PAAs is distinguishing between branched and linear PAA products, and avoiding formation of cycling piperazine molecules [114]. Typically, catalyst selection is done to ensure that adequate selectivity for the linear product is made.

2.6.5. Life Cycle Perspective

Information in this section provides a clear outline of approaches to manufacturing by which major surfactants used on the production of silica are used. Yet, despite this understanding for manufacturing methods, little information exists regarding LCA of these products. This is reflected in in the low level of sophistication involved in modelling impacts associated in QASs, LTCs, and PAAs. For instance, several recent publications have approximated impact of surfactant life cycles based on stoichiometric ratios of immediate reaction materials alone without consideration for auxiliary substance and energy use; this includes for QAS methods [115], and LTC methods [116]. No life cycle assessment information was found for PAAs.

The presence of large gaps in information regarding the amount of energy and material used in the production of each stage, stemming from a number of compounding factors including: 1) complexity of methods by which several of the surfactants may be produced (e.g. Quaternary Ammonium salts), 2) variation in production techniques and material sources available for manufacturing products, 3) lack of transparent studies provided in literature about industrial scale production and 4) relatively niche nature of several of the products.

Despite existing gaps in literature, a lack of methods developed for accurately assessing the environmental impact associated with these surfactant products is necessary for LCA of any products that they are involved in the production - including SBAMs produced using substrates from the MCM, SBA and BI methods (see Section 2.5.3). Consequently, work must be

developed to provide better understanding for material and energy use involved in typical commercial product manufacture.

Given the availability of information on process design in patent literature, and availability of life cycle inventory models for substances involved in the manufacture of all surfactant types (e.g. [93]), it appears as though this could be achieved in part by use of process modelling methods, which may provide first estimates for immediate reactant, auxiliary substance and energy use with key processing stages across QAS, LTC, and PAA life cycles. In doing so, this would enable beginning to ask additional wider questions regarding hotspots of impact deriving from life cycle activity involving each surfactant product type. This includes, for example: how important is petrochemical product use, how important is energy use, and does the nature of current production methods leave any simple cases by which impact reductions can be made? More immediately relevant to the SBAMs considered in this work, assessing the total impact associated with each surfactant product will also provide greater ability for the contribution of surfactant use to SBAM manufacturing by different methods – through which more robust conclusions can be made as to major impact hotspots associated with silica manufacture, and potentially outlining fundamental “problem” surfactants associated with certain forms of silica manufacture (e.g. MCM, SBA and BI silica).

2.7. Silane Coupling Agents as Surface Chemistry Modifiers

2.7.1. Overview

Silane coupling agents (SCAs) are a group of chemical products used in the modification of surface chemistry. They encompass a range of specialised chemical compounds including chlorosilane, organosilane, and silane functionalities. Their utility comes from their ability to act as adhesion promoters, which can be exploited in a number of use cases ranging from adhesion promotion for fillers in rubber materials (e.g. tyres [117]) to superhydrophobic coatings used for self-cleaning surfaces. Owing to their broad range of manufacturable chemical functionalities and their ability to undergo covalent bonding with several surfaces, SCAs now also find widespread use as surface chemistry modifiers in adsorbent material design.

The conceptual definition of SCA products is typically done by categorising their functional group chemistry as functional and non-functional chemistries. Non-functional groups are those groups designed to readily undergo covalent bonding with target surfaces. Their design is therefore selected dependent on the silanization reaction pathway, and typically includes chlorosilane or alkoxysilane chemistry. Of the alkoxyl group chemistries, only methoxy and ethoxy groups are typically considered due to issues with hydrolysing large alkoxide groups during the silanization reaction.

Functional groups are intended to reside on the surface after surface modification, and as such are selected from a much broader range of chemistries dependent on intended surface properties required.

2.7.2. Commercial Production

The commercial production of organosilane reagents used in surface modification relies heavily on exploiting differences in the silyl (Si-H) and chlorosilyl (Si-Cl) chemistry of chlorosilanes. These intermediates are commonly further processed to introduce desired organic and functional group properties. The major methods involved in these stages are hydroxylation (for organic group addition) and alkoxylation (for functional group customisation). This leads to a few possible production pathways depending on the desired organosilane product as shown in Figure 2.12. Further information on the individual stages is provided below.

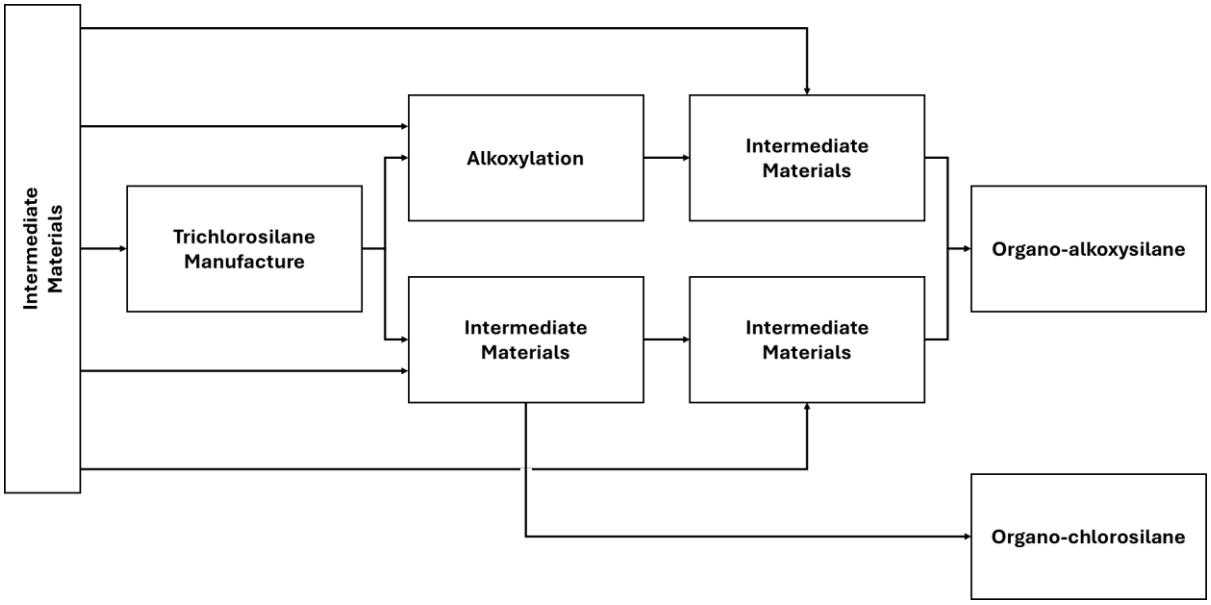


Figure 2.12: Major synthesis pathways for producing organosilane coupling agents depending on desired product chemistry.

Chlorosilane Feedstock

Commercial production of chlorosilanes is carried out by the chlorination of silicon metal. This reaction leads to the production of several chlorosilane species including monochlorosilane (SiH_3Cl), dichlorosilane (SiH_2Cl_2), trichlorosilane (TCS, $SiHCl_3$), and tetrachlorosilane ($SiCl_4$) as well as some amount of oligomeric chlorosilane species (e.g. monochlorodisilane and dichlorodisilane).

Typically, the chlorination process is done by the reaction of metallurgical grade purity (~98 wt%) silicon with hydrogen chloride gas under preferable conditions. The temperature and pressure of reaction is dependent on the desired products of interest due to implications that they have on equilibrium yield [118]. Nonethless, temperatures around 260 C are typically used to target TCS production [118] and pressures up to 5 bar are used to increase TCS yield [118].

Of chlorosilanes available, TCS is by far the most common used to produce SCAs. This due to the improved hydrolysis resistance that tri-functional organosilane coatings provide to chemically-modified SBAM surfaces – owing to the formation of multiple covalent bonds.

The production of trichlorosilane is linked heavily between markets for SCA, and high-purity silicon metals. Around 60% of the TCS market is linked to silane coupling agents [119], the remainder being largely attributable to silicon metals.

Coincidentally, the production of trichlorosilane is also heavily linked to production of high-purity silicon metals. Particularly, trichlorosilane is produced as a co-product of the Siemens process for high purity silicon production [120]. Trichlorosilane produced in this way is typically of a reagent-grade (~98wt%) purity or higher. Consequently, its use in production of silane coupling agents is often economically incentivised [121]. In fact, in some cases, the use of high-purity TCS has been remarked as being "essential for […] success" in achieving high conversions associated with producing silane coupling agent products [122].

Substitution of Functional Groups

The substitution of functional group chemistry typically occurs via alkoxylation reaction. In alkoxylation, alcohols react with chlorosilane chemistry to form alkoxy-silane groups and a hydrogen chloride by-product as shown in Equation 2.6.

$$\mathrm{nROH} + \mathrm{Cl_nSiH_{4-n}} \rightarrow \mathrm{(RO)_nSiH_{4-n}} + \mathrm{nHCl} \tag{2.6}$$

Alkoxylation can occur as the first or second stage of chlorosilane processing (see in Figure 2.12). It may involve gas, gas-liquid, or liquid based reaction phases dependent on reagent use.

Preferable industrial production of alkoxylation occurs via a gas phase reaction within a column at temperatures near the boiling point of the alcohol being used [123]. This process typically involves use of a dedicated reactor followed by reactive distillation sequence focussed on minimising residual chlorine content of products [124, 125]. Under these conditions, it is possible to produce alkoxylated silane products surpassing reagent grade purity without need for further purification [124]. This has been done traditionally only using alcohols of small molecular. This is because of organosilanes with large alkoxy functionalities typically having the drawbacks of low reaction kinetics, selectivity, and efficiency [126] (e.g. see Figure 2.13), - causing a need for large alcohol excess during reaction [125]. Nonethless, recent developments have overcome limitations to some extent through appropriate column design [125].

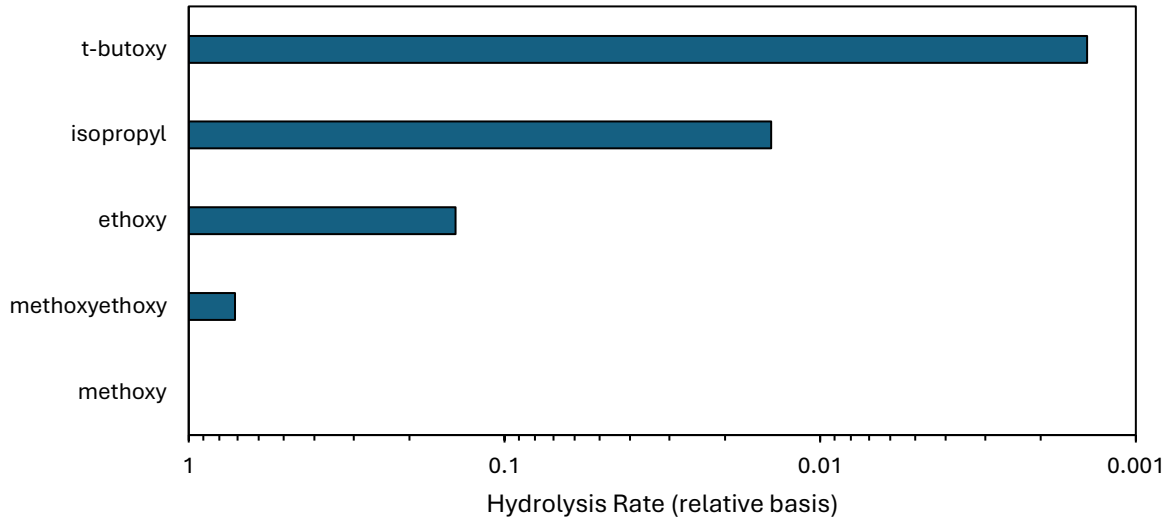


Figure 2.13: Effect of functional group chemistry on hydrolysis rate. All rates displayed relative to methoxy only functional group chemistry. Adapted from [127].

The alkoxylation of a trichlorosilane is desirable in producing alkoxysilanes intermediates that are amenable to production of a broad range of organo-alkoxysilane products. The elimination of hydrogen chloride earlier in the life cycle is often also desirable as part of chlorine recycling approaches [123].

Liquid-phase methods for alkoxylation also exist within patent literature and may be considered in cases where approach can make use of either in liquid or multi-phase conditions (see above) are not desirable [128, 129].

Addition of Non-Functional Groups

The addition of non-functional, organic group chemistry typically occurs via a hydrosilylation reaction. In hydrosilylation, alkenes are reacted with silyl (Si-H) bonds as part of an addition reaction. This is done in the liquid phase in the presence of platinum-based catalysts [123] as shown in Equation 2.7.

$$\mathrm{SiX_3H + CH = R \rightarrow SiX_3(CH_2R)} \tag{2.7}$$

Where X is the functional group capable of undergoing silanization and R represents an organic group associated with the alkene reagent. The extent of material use of platinum catalyst associated with hydrosilylation is relatively low – typically being present in concentrations of hundreds of ppm [129]. Consequently, commercial applications do not typically bother with recovery of the catalyst as part of optimal economic operation [130].

Hydrosilylation can occur as either the first or second stage in production of an organo-alkoxysilane from a chlorosilane [131]. This involves either: 1) hydrosilylation of a chlorosilane to form an organo-chlorosilane, or 2) hydrosilylation of an alkoxysilane to form an organo-alkoxysilane.

The hydrosilylation of a chlorosilane (approach 1) occurs in cases where either an alkoxylated product is not desired, or when production of the hydrosilylated chlorosilane product does not provide further challenges to downstream processing. It can be desirable due to the benefit of greater reactivity of chlorosilanes when compared to their alkoxysilane homologues [123].

The hydrosilylation of an alkoxysilane (approach 2) typically occurs in cases when protective groups are required to avoid undesired reaction of chlorosilanes during hydrosilylation. Dependent on the molecular size of the alkoxysilane, the approach can make use of either in liquid or multi-phase conditions - see, for example [128, 129].

Production scales associated with the hydrosilylation of trichlorosilane have previously been reported as being preferably of the scale of 10 to 1000 kg/hr [129].

The commercial hydrosilylation of allyl chloride has been carried out for more than 40 years [126]. Consequently, a great wealth of patent art focus on production of this method specifically [132], and other small organic groups [133]. Higher alkyl group chemistry may differ significantly from that of allyl chloride, thereby affecting reliability of patent art.

For production involving bulky alkyl groups (e.g. higher alkenes and cyclic chemicals), reaction conditions may be done involving a liquid phase wherein the hydrosilylation itself acts as the solvent solution [134].

Enthalpy of reaction of hydrosilylation is often in the range of 100 to 180 kJ/mol [135]. Catalyst recycling is not always carried out [136].

2.7.3. Use in Surface Chemistry Modification

Silane coupling agents can be used to introduce new functional groups to select solid surfaces. This occurs via the process of silanization, in which the agent undergoes a condensation

reaction that leaves it covalently bonded to the surface. Eligible surfaces include polymers, metal oxides. This includes silica products bearing silanol surface chemistry**.**

Use of SCAs in producing SBAMs with surface chemistry modification can occur according to either on-pot or post-synthesis modification methods. In one-pot methods, the SCA agent is included silica reagents used during synthesis. In post-synthesis methods, powders already produced according to silica synthesis methods are then silanized in a dedicated processing stage.

Anhydrous liquid phase deposition is often preferred when modifying small particles and nano-featured substrates [127]. However, this method is too costly for economic commercial operation [137]**.** Consequently, most processes reported in literature are based on reaction in aqueous or mixed aqueous environments.

A common practise in modification is the use of solvent washing stage as part of product purification. This may involve polar and/or nonpolar solvents. The amount of solvent use is somewhat dependent on the SCA chemistry being parted – owing to solubility of unreacted chemicals affecting efficiency of solvent wash procedure. However, overall solvent use usage amounts are often high.

Alternatively, in some cases, methods have been reported where reaction solution is sufficiently dilute as not to require additional drying stage [138]. This approach is not the standard at least in research literature. Moreover, effectiveness may vary depending on silica porosity solution environment, and silane coupling agent under consideration.

After washing, powders are typically dried to low (10-20 wt% [82]) moisture content. This may occur according to many standard approaches including spray drying [138] and fluidized beds [139].

Beyond immediate impact of producing SCAs, typical methods for their use in surface chemistry modification of solid surfaces may also be significantly impactful. This can be seen to arise from significant amount of solvent use associated with satisfying the silanization reaction, as well as washing procedures commonly carried out in post-processing of silanized products.

2.7.4. Life Cycle Understanding

Information in Sections 2.7.2 provide a clear outline of approaches to manufacturing by which major SCAs may be produced. SCAs are important to assessing the impact of SBAMs because of their use in surface chemistry modification procedures. Yet, despite this importance, and understanding for manufacturing methods, very little information exists regarding LCA of these products. This is reflected in the low level of sophistication involved in modelling the environmental impacts associated with major SCAs as considered in existing academic literature. For instance, this includes modelling impact based on material use derived from the reaction stoichiometry associated with APTES (the largest single SCA product manufactured) [140].

The reliance of many products on underlying chlorine chemistry raises large questions from the perspective of chemical safety and green chemistry.

The presence of large gaps in information regarding the amount of energy and material used in the production of each stage, stemming from multiple compounding factors including: 1) complexity of methods by which several of the SCAs may be produced, 2) variation in production techniques and material sources available for manufacturing products, and 3) the niche nature of associated industry (low volume and specialty). Further questions then arise in the amount of material and energy use associated with the use of SCAs in producing SBAMs with surface chemistry modifications.

3. Research Approach

3.1. Introduction

Chapter 1 has laid out a high-level approach to developing greater understanding for the sustainability of methods being used to develop silica based adsorbent materials. It has been demonstrated that this first requires a more thorough understanding for how these materials (and their intermediates) are made.

In beginning to address this, Chapter 2 has provided as review of current understanding for the methods by which silica-based adsorbent materials are produced. Nonetheless, it has also identified significant gaps in practical understanding for the impact of these methods in doing so. These gaps derive from missing information on associated material use and energy use associated with manufacturing. Consequently, an approach has been developed in this thesis to provide understanding for both materials use and energy use associated with manufacture and inform environmental impact predictions of SBAMs.

This chapter further explains how a combination of process modelling and life cycle assessment methods have been developed in in this work as part of a wider approach focussed on impact modelling of SBAMs. Further information on each modelling approach is provided in Sections 3.2 and 3.3, alongside a description of use of the python programming language in Section 3.4. Whereas further information on how they have been compared with the python language in Section 3.5. A final note on interpretation of the work is then provided in Section 3.6.

3.2. Understanding Life Cycles using Prior Art

Accurate impact assessment requires the generation of life cycle inventories that reflect real conditions under which product manufacture occurs. This often requires significantly greater level of understanding for engineering process design than is provided in dedicated experimental literature. Consequently, a great extent of effort has been provided in utilising information available in prior patent art in generating process understanding. This is reflected in the preference for use of patent-derived information in modelling of life cycle activity throughout the case-studies provided in this work.

3.3. Process Modelling using the Aspen Plus Software

When process understanding is available, estimates for mass and energy use can be made using process engineering modelling software. Such results can provide a primary tool to expanding discussion of the impact of silica based adsorbent materials (substrates, SCAs and surface-modified adsorbents).

The modelling of process level systems carried out in this work has been done using the Aspen Plus (V11) software. Owing to a lack of existing information, this has been carried out for several products and intermediate materials relevant to the production of surfactants used in emerging silica synthesis methods (Chapter 5) and nearly all materials considered in the silane coupling agents (Chapter 6). Further detail will be introduced in the respective chapters.

3.3.1. Property Estimation

Notably, modelling of many of the processes considered in this work is challenging owing to the non-petrochemical nature of chemicals used – making thermodynamic data availability low. Thankfully, a range of methods now exist for the prediction of thermodynamic properties. As a result, several simulations rely on estimated properties to approximate the material and energy use in. Further information on methods used and property estimates is provided in relevant sections of later chapters provided in this work.

3.3.2. Use of Shortcut Methods

The nature of equipment considered during process modelling in this work often involves complex, non-linear relationships, making finding the “optimal” design conditions hard. However, these conditions often effect the material and energy efficiency of a process. Consequently, market competition often dictates that real commercial processes operate under design conditions that are at- or near-optimal regarding process profitability.

For some processing stage, such as distillation, shortcut methods exist which act to drastically reduce the computation challenge associated with optimal design. These are typically achieved through simplification of real governing equations of the process, and use of empirical correlations based on existing designs reported in literature. Owing to the current state of literature, the choice has been made to use shortcut methods during process modelling at some points in this work. This has been done to provide to provide balance

between providing reasonable first estimates. Further information on when these have been used is provided in relevant sections of chapters later in this work.

3.4. Life Cycle Assessment using the openLCA Software

As outlined in Chapter 2, the execution of life cycle assessment requires handling of information from Technosphere and Biosphere for potentially large life cycle activity networks. Given the existing availability of databases with predefined data structures, this makes the use of dedicated LCA software an attractive tool when carrying out LCAs.

The modelling of life cycle inventories and calculation of associated environmental impacts has been carried out using the openLCA software in this work. This software is due to being readily available, open-source, and easily integrable via python integration (see Section 3.5).

3.5. Advanced Modelling using Python Integration

Throughout execution of research, it has been observed that modelling software used (Aspen Plus and OpenLCA) have associated limitations within which they can be used. However, for both software, there exists a possibility to further customize modelling capabilities through linking with external coding software. In doing so, it becomes possible to further expand the ways in which modelling software is handled using computer algorithms built in-house.

Advanced modelling capabilities have developed in this work to model beyond limitations of software used by the development of in-house code following the python computer language. In all cases, this code has been developed in a way where a python interpreter acts as a thinking 'head' from which decisions are made, and the simulation runs are executed. This is illustrated in Figure 3.1. Further information on capabilities developed throughout this work are discussed in the following subsections.

3.5.1. Process Design Optimization

While shortcut methods (see Section 3.2) are used extensively in this work, an opportunity arises in Chapter 6 for more rigorous process design optimization to be carried out. In this case, python-based modes have been used specifically to execute decision making and execution of process modelling simulations associated with an in-house stochastic optimization solution algorithm. Further information on this is provided in Section 6.1.

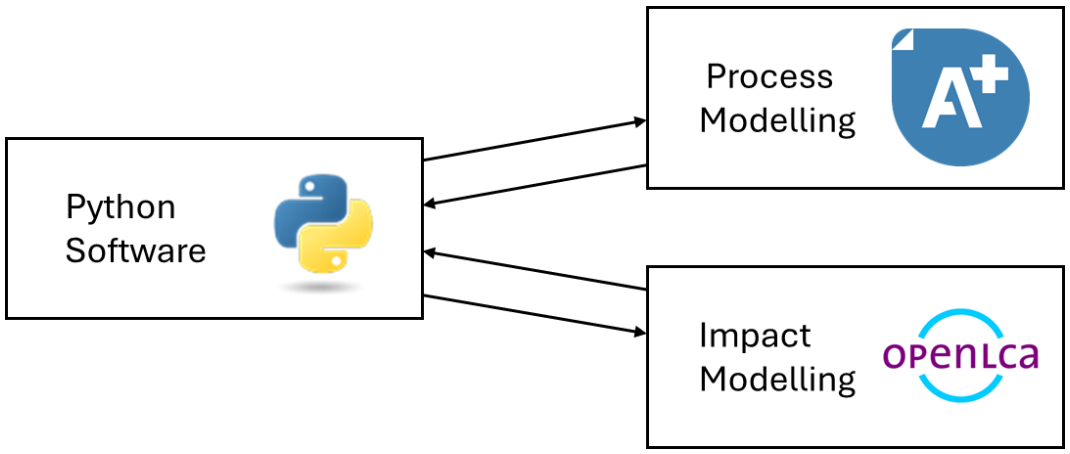


Figure 3.1: Use of computer algorithms scripted in the python language to call the execution of individual software simulations (Aspen Plus and OpenLCA) as part of investigations in computational experiments.

3.5.2. Monte-Carlo Modelling of Impact Uncertainty

Acknowledging uncertainty of impact assessments is critical to ensuring reliable decision making. A common method in which this is often done using Monte-Carlo modelling to numerically approximate how uncertainty in life cycle activities through to associated impact of a product life cycle. As life cycle complexity increases, such methods require an increasing number of estimations to ensure robust uncertainty estimates. Despite this, the openLCA software has systemic limitations to the number of estimates that can be evaluated within the GUI-based version of the software. Thus, python scripts have been used to surpass the limit of evaluations available to Monte-Carlo simulation using openLCA.

3.6. A Note on Interpretation

Owing to the broad range of SBAMs that could be manufactured, this thesis has been limited to SBAMs manufactured in a powder form. Other forms of silica adsorbent (e.g. shaped adsorbents and coatings) are not considered to ensure a manageable number of case-studies.

As a result of limited focus to powders, the results of this work should not be considered transferrable to other forms of SBAM < based product. This arises from potential differences in life cycle activities which may arise for SBAMs produced in ways different. This includes with regards to differences in energy use, materials use, and the number of materials required during production, use and disposal/re-use stage of the SBAM life cycle (which must be considered on a case-by-case basis for fully transparent environmental impact assessment of unique products). Readers must keep this in mind when interpreting results for the rest of this thesis.

4. Industrial Silica Products

4.1. Introduction

4.1.1. Background

To assess the environmental impact of SBAMs, information is first required regarding the impact associated with producing the solid silica substrates that they are built from. When interpreting impact results, it is often useful to establish benchmark cases to which impacts predictions of SBAMs may be compared. Given the low technological readiness level of many SBAM materials, establishing benchmarks based on silica substrates produced at the commercial scale may be especially helpful.

Commercial silicas are produced using either gas or liquid phase reaction. These approaches are commonly referred to as 'dry' (i.e. gas phase) or 'wet' (i.e. liquid phase) respectively [82].

Silica production according to liquid-phase reactions are referred to as "wet" methods and rely on precipitation of silica out of solution arising during the hydrolysis of sodium silicate solutions. This is done in acid-catalysed conditions and follows the reaction stoichiometry shown in Equation 4.1. Silica produced according to these forms may be either dispersed sols, or gels and are typically referred to as precipitated silicas [82].

$$Na_2O \cdot SiO_2 + H_2SO_4 \rightarrow SiO_2 + Na_2SO_4 + H_2O \quad (4.1)$$

Silica production according to gas-phase reactions are referred to as "dry" methods and follow a reaction pathway reliant on the pyrolysis of silicon tetrachloride at high temperature in an inert atmosphere as shown in Equation 4.2. This leads to production of very small aggregates composed of nano-scale silica particles that have come into contact during reaction. Silica produced by this method is typically referred to as pyrogenic silica [82].

$$SiCl_4 + 2H_2O \rightarrow SiO_2 + 4HCl \quad (4.2)$$

Despite having been established for many decades, little information is available on the environmental impact associated with pyrogenic and precipitated products [24, 100]. This creates ambiguity in the environmental impacts associated with each method. For example, the dry method involves the use of chlorine chemistry (silicon tetrachloride) and production

at high (1100 C) temperatures, while wet methods use harsh aqueous environments and require additional solid-liquid processing steps.

4.1.2. Aims and Objectives

This chapter aims to address research gaps associated with understanding the environmental impact associated with producing precipitated and pyrogenic silica products via commercial manufacturing methods. This is done with the main objectives of:

1. Establishing life cycle inventories for commercial methods of producing pyrogenic and precipitated silica.
2. Estimating the environmental impacts associated with each method.
3. Identifying major activities contributing to the impact of each product.
4. Assessing certainty in the impact of pyrogenic and precipitated silica products.

4.2. Methods

This work combines aspects of life cycle inventory modelling, life cycle impact assessment, and statistical modelling to develop understanding regarding the impact of pyrogenic and precipitated silica. This includes reporting on impact with regards to standard single-point impact estimates as well as data quality uncertainty. As shown in Figure 4.1, the approach is split into two sections regarding life cycle assessment and uncertainty assessment.

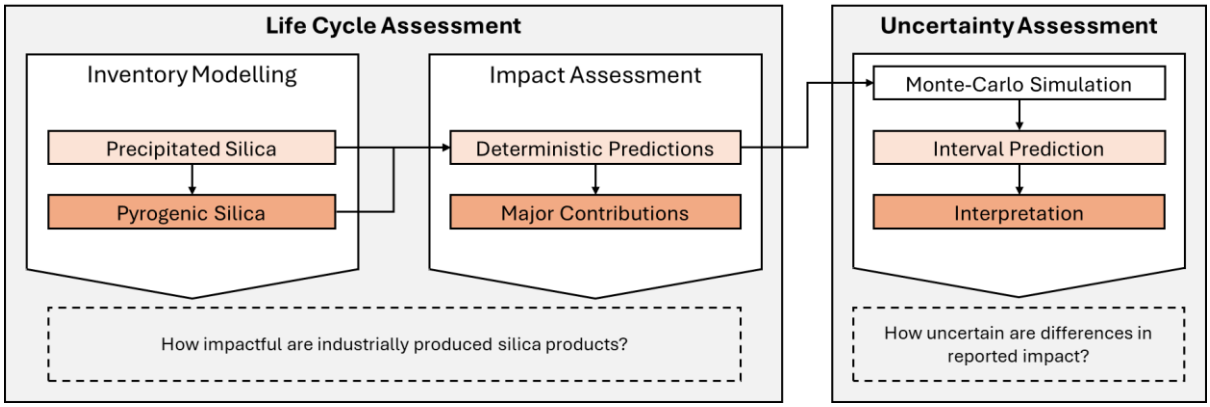


Figure 4.1: Schematic workflow of methods used to investigate the environmental impact of producing silica substrates according to commercial synthesis methods.

4.2.1. Inventory Modelling of Commercial Silica Substrates

Goal and Scope Definition

Two models have been developed to characterise EI associated with the production of precipitated silica and pyrogenic silica according to commercial methods (see Figure 4.2**)**. This has been done using an attributional LCA approach and a functional unit of 1 kg of dried product as an assessment basis. All products have been assessed using a Cradle-to-Gate scope.

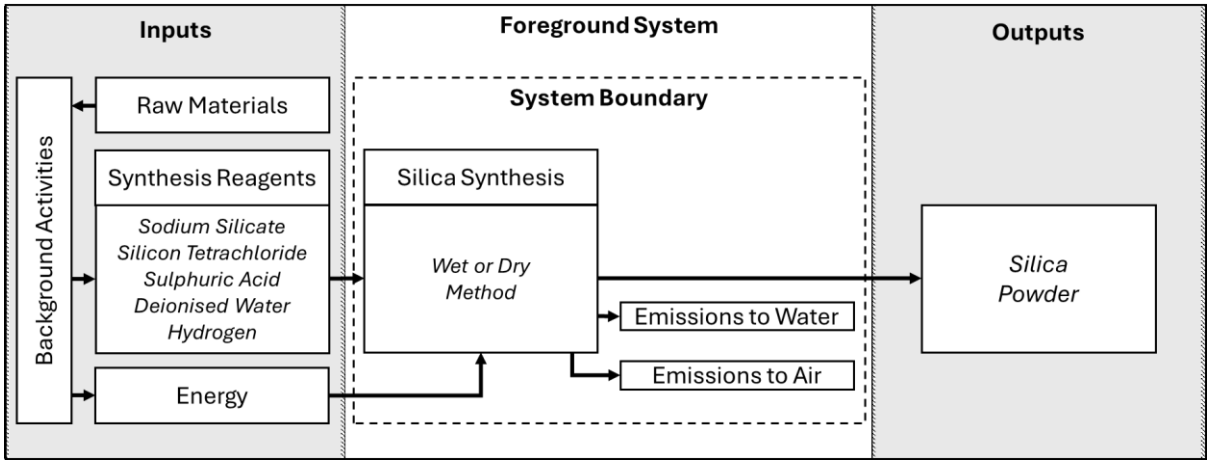


Figure 4.2: Scope associated with the production of precipitated and pyrogenic silica according to commercial methods.

Life Cycle Inventory Modelling

Life cycle inventory models used for precipitated and pyrogenic silica products are shown in Table 4.1. This information is based on industrial averages of material use, energy use and material emissions reported within a "best available techniques" document currently adopted in the European Union [82]. The data covers a total of 18 plants operating production capacities between 12 and 100 kt/year – an amount representing roughly 30% of global manufacturing capacity at the time of reporting [82]. Given the maturity of the industry, these values are expected to reasonably reflect material and energy amounts still in use to date.

It has been assumed that all energy demand is supplied by natural gas; this is due to lack of further distinction in energy use based on electricity and heat in the source document [82], and given that an significant portion of energy use is attributed to heat-based drying [82]. A summary of inventory models used to represent background life cycle activities is provided in Table 4.2. For further information on these models see Errington *et al*. [100].

Data Validation Approach

Additional data validation has focussed on ensuring consistency of material amounts reported with minimum mass balances for underlying reactions of each manufacturing process (see Equations 4.1 and 4.2 and Table 2.6). Where a range of values is provided, the midpoint has been taken, and cases where values are reported as less than a minimum detection limit, the detection limit has been taken to consider the effect that emissions near the detection limit may have. Consideration for data quality is described further in Section 4.2.3.

4.2.2. Environmental Impact Assessment

Environmental impact estimates were made using the ReCiPe 2016 Hierarchical mid-point characterisation method [71]. A summary of metrics selected is given in Table 4.3.

Table 4.1: Material and energy flow inventory for producing 1kg of precipitated and pyrogenic silica product.

Flow Type	Flow	Amount		Unit
		Precipitated Silica	Pyrogenic Silica	
Reagent	Sulfuric Acid	0.63	-	kg
	Sodium Silicate	3.90	-	kg
	Water	42.52	-	kg
	Silicon Tetrachloride[a]	-	[a]2.70	kg
	Hydrogen	-	82.00	g
Energy	Heat (Natural Gas) [a]	19.50	16.50	MJ
Air Emissions	Carbon Monoxide	[c]825.00	-	mg
	Carbon Dioxide	-	[b] 0.64	mg
	Nitrogen Oxides	[c]0.72	[b] 0.10	g
	Chlorine	-	[b] 0.05	g
	Hydrogen Chloride		[b] 0.10	g
	Volatile Organic Compounds	-	[b] 0.30	g
	Particulate Matter	[d]1.30	[b]0.30	mg
Water Emissions	Sulphate	0.59	-	kg
	Chemical Oxygen Demand	12.00	-	g
	Dissolved Solids	6.60	-	g
	Wastewater	[c]35.00	-	g
Waste	Non-hazardous waste	29.00	10.00	g
	Hazardous waste	-	2.00	g
Product	Silica	1.00	1.00	kg

[a] Value taken based on midpoint of range reported in the source text, [b] value taken as maximum value of inequality (<) reported in the source text [82], [c] based on average value reported in source document [82], [d] based on average dust emissions reported in the source text [82].

Table 4.2: Inventory models used to account for background life cycle activity linked to the production of commercial silica substrates based on the EcoInvent v3.10 database.

Inventory Item	Model	Region
Sulphuric Acid	Market for sulfuric acid	RER
Sodium Silicate	Market for sodium silicate, furnace method	RER
Water	Market for water, deionised	EU exc. CH
Silicon Tetrachloride	Market for Silicon Tetrachloride	GLO
Hydrogen	market for hydrogen, liquid	RER
Heat (natural gas)	Market group for natural gas	RER
Carbon Monoxide	Emission to air, unspecified	N/a
Carbon Dioxide	Emission to air, unspecified	N/a
Nitrogen Oxides	Emission to air, unspecified	N/a
Chlorine	Emission to air, unspecified	N/a
Hydrogen Chloride	Emission to air, unspecified	N/a
Volatile Organic Compounds	Emission to air, unspecified	N/a
Particulate Matter	Emission to air, unspecified	N/a
Sulphate	Emission to water, unspecified	N/a
Chemical Oxygen Demand	Emission to water, unspecified	N/a
Dissolved Solids	Emission to water, ground water	N/a
Wastewater	market for wastewater, average	EU exc. CH
Hazardous Waste	market for hazardous waste, for incineration	EU exc. CH

Table 4.3: Mid-point metrics considered in life cycle impact assessment of commercial silica and use justifications.

Impact Metric*	Abbreviation	Justification
Global Warming Potential (100 years), kg CO_2-eq	GWP	Global-scale climate change implications
Land Use, m^2 crop-eq	LUP	Relevance of land use to mining operations
Mineral resource scarcity, kg Cu-eq	MRS	Use of quartz mineral feedstock
Marine Eutrophication, kg N-eq	MEP	Relevance to wet processing
Stratospheric Ozone Depletion, kg CFC-eq	ODP	Global-scale climate change implications
Terrestrial Acidification, kg SO_2-eq	TAP	Trans-boundary pollution issue
Terrestrial Ecotoxicity, kg 1,4-DCB-eq	TEP	General significance
Water Depletion, m^3	WDP	General significance, relevance to wet processing

* eq. stands for “equivalent”

4.2.3. Uncertainty Assessment

The uncertainty associated with life cycle impact measurements has been calculated based on an uncertainty propagation method. This has been done by considering uncertainty in models present in the life cycle inventory model only. More specifically, uncertainty in the exact amount of material and energy use associated with each material inventory has been modelled of probability distributions intended to reflect uncertainty arising from associated data quality of life cycle inventories.

Life Cycle Inventory Uncertainty

Uncertainty in material and energy amounts in the life cycle inventory stage have been represented mathematically using probability distribution functions. This has been done using lognormal probability distributions with location and variance defined according to the data quality pedigree method of Frischknecht and their co-authors [141]. The basis of definition is shown in Equations 4.6 and 4.7. Further information on the data quality scoring used to define uncertainty distributions is provided in Appendix A.

$$F \quad = \text{lognormal}\left(\mu^* , {\sigma^*}^2\right) \tag{4.6}$$

$${\sigma^*}^2 = \sum_{i=1}^{5} \ln\left(\sigma_i^*\right) \tag{4.7}$$

Life Cycle Impact Assessment Uncertainty

Uncertainty in environmental impact assessment has been calculated based on a Monte-Carlo based error propagation method. Specifically, impact assessment was carried out a total of 150,000 times for life cycle inventories produced based on random resampling of inventory amounts according to probability distributions described in above. Handling of resampling of inventory amounts was done using methods within the version 2 of the openLCA software.

Interpretation of Uncertainty

Interpretation of results has been done by the method of pairwise comparison of product impact of pyrogenic and precipitated silicas. This has been done using the absolute difference of product impacts as a performance metric – as shown in Equation 4.8

$$\Delta_{kpi} = EI_{kpi}^{precipitated} - EI_{kpi}^{pyrogenic} \tag{4.8}$$

Where $\Delta_{kpi}$is the difference in impact between precipitated and pyrogenic for impact category, kpi (units vary with kpi, see Table 4.3).

The concept of prediction intervals to reflect the reflect the spread of uncertainty in impact estimates. Prediction intervals were defined on a two-tailed basis to reflect an agnostic position on the impact of any process being better than another.

4.3. Results and Discussion

4.3.1. Environmental Impact Predictions

Impact predictions for precipitated and pyrogenic silica products are shown in Figure 4.3, activities contributing to the overall impact are then shown in Figure 4.4. Results in Figure 4.43 show precipitated silica to have a lower environmental impact in 3 of 8 the categories considered, those being: GWP, ODP, and WDP. On the contrary, pyrogenic silica has a lower impact in 5 of the 8 categories, those being: LU, MU, MRS, TAP, and TEP.

For both products, results in Figure 4.4, indicate that environmental impact is heavily driven by reagent use. This is most so the case of pyrogenic silica, where reagent use accounts for more than 90% of total product impact in 7 of 8 cases (GWP being the exception at 79%). Nonetheless, it is also significant for precipitated silica, where it contributes 69% or more in 6 of 7 impact categories (MUP being the exception with a contribution of only 21%).

After reagents, energy use is the second most consistent contributor to impact. This is so particularly for GWP, ODP and TAP for both precipitated and pyrogenic silica products, which show contributions consistently lower than 30%, including contributions less than or equal to 1% for the remaining impact factors.

Given the higher energy requirement of the wet process, it would seem logical that energy provides greater contributions to the impacts of the wet method, which is observed. Moreover, the fact that energy contributions also occur in categories such as GWP, ODP and TAP is also intuitive because these categories are strongly associated with the utilisation of fossil-fuel energy.

Nonetheless, energy use in general is found to be of lower importance when compared to reagent use. This is important as the findings demonstrate that process energy use cannot be used alone as a good gauge for process impact or process comparison; this is in agreement

with findings for the dry and wet methods of titanium dioxide and zirconium dioxide reported previously [98].

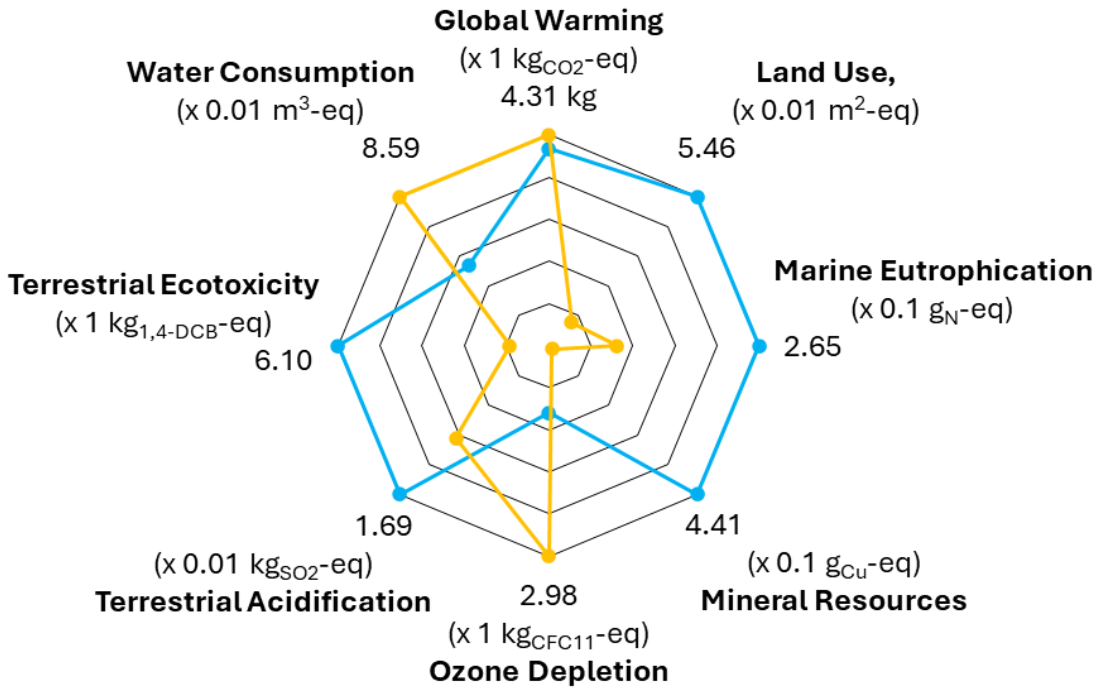


Figure 4.3: Environmental impact predictions for producing 1 kilogramme of precipitated and pyrogenic silica products according to commercial methods.

Finally, the negative contribution of waste to the WDP of precipitated silica stands out as a unique feature Figure 4.4. This contribution is associated with the inclusion of wastewater treatment in the life cycle, providing a reduction of 68% of the reported impact. Future work may benefit from refinement of the wastewater process model used to ensure that impact predictions accurately reflect the real wastewater treatment process used in industry.

Important of Precursor Choice

Results in Figures Figure 4.3 and Figure 4.4 show the impacts of precipitated and pyrogenic silica are largely attributed to reagent use. They do not, however, provide understanding for what causes the impact of reagents to be so large (in comparison to other foreground activities). In fact, the magnitude of reagent contributions is heavily governed by each process' silica precursor – sodium silicate (Sod. Sil.) and silicon tetrachloride (SiCl4). This is explored in further detail now.

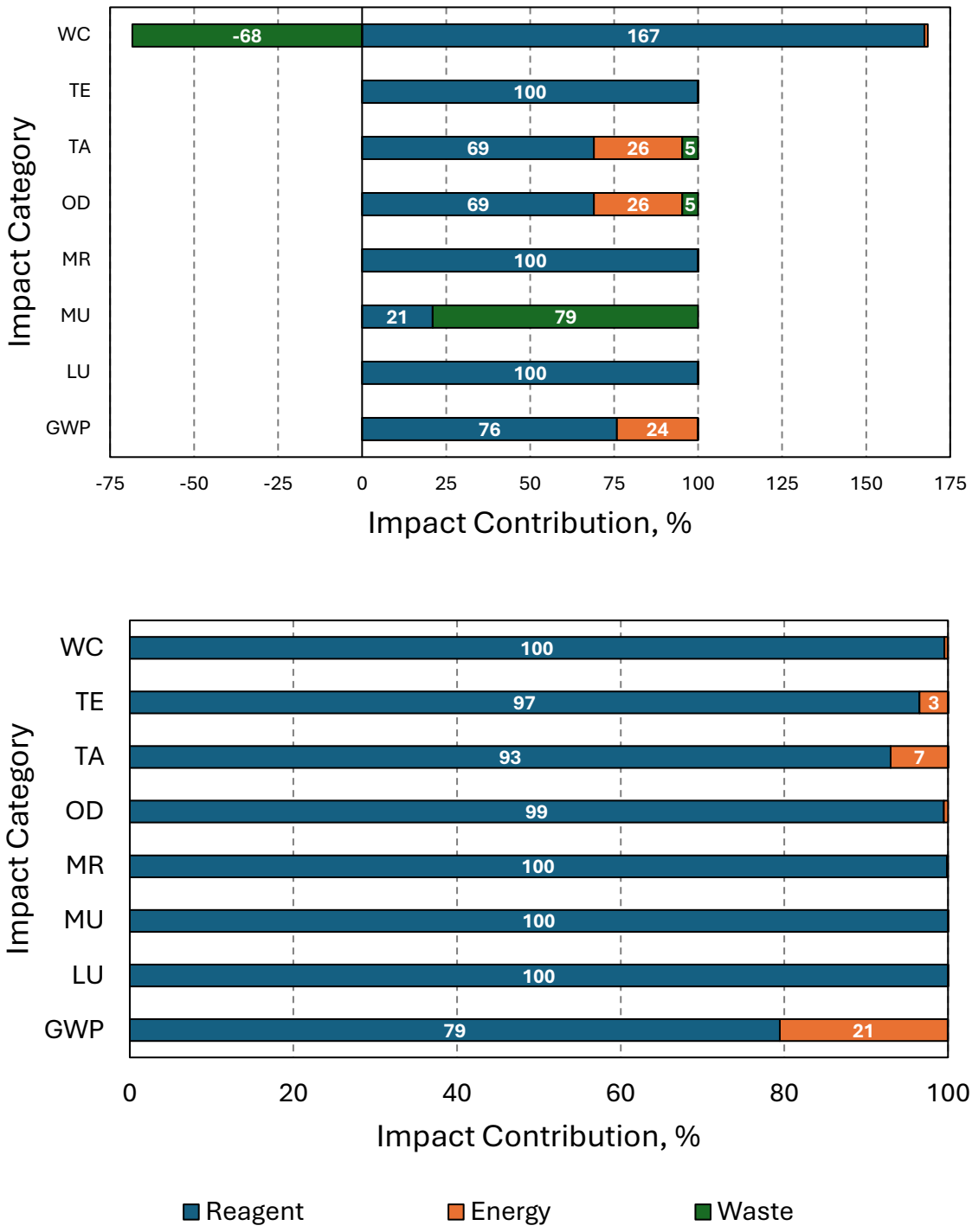


Figure 4.4: Contributions of foreground activities to environmental impact of producing 1 kilogramme of precipitated (top) and pyrogenic (bottom) silica products according to commercial methods.

Results in Table 4.4 and Table 4.5 summarise impact contributions associated with each silica precursor for precipitated and pyrogenic silica respectively.

Table 4.4: Contribution of the silicon tetrachloride reagent life cycle to the predicted impact of pyrogenic silica

Impact Factor	Impact Contribution, %		
	Silicon Tetrachloride [a]	Chlorine [b]	Carbon Black [b]
GWP	69.8	43.6	15.1
LUP	100.0	-18.7	-0.2
MEP	98.5	93.2	0.6
MRS	25.6	23.7	0.0
ODP	92.1	71.9	16.0
TAP	93.8	57.5	28.8
TEP	1.1	1.0	0.1
WDP	96.2	65.1	0.4

[a] used to manufacture pyrogenic silica, [b] used to manufacture silicon tetrachloride.

Table 4.5: Contribution of the sodium silicate reagent life cycle to the predicted impact of precipitated silica

Impact Factor	Impact Contribution, %		
	Sodium Silicate [a]	Energy [b,c]	Soda Ash [c]
GWP	74.9	32.2	12.0
LUP	100.0	31.6	17.5
MEP	20.8	5.7	14.2
MRS	100.0	16.3	83.5
ODP	67.4	39.3	11.2
TAP	66.4	26.9	29.5
TEP	72.2	49.2	12.5
WDP	75.5	14.3	50.8

[a] used to manufacture precipitated silica, [b] used to manufacture sodium silicate, [c] combined heat and electricity.

Results in Table 4.3 show that, for pyrogenic silica, the contribution of silicon tetrachloride to the total process impact is governed by two main factors – chlorine and carbon black. On one hand, chlorine, which is required for the tetrachloride (i.e. Cl_4) chemistry, is derived from the electrolysis of basic chemicals in wet environments. Consequently, it contributes significantly across all impacts largely due to its energy use as well as due to the aquatic impact of the basic chemicals used (i.e. for MEP). On the other hand, carbon black is derived from petrochemical sources [142], which causes it to provide significant contributions to impacts on land and in air, such as GWP, ODP and TAP.

Similarly, for precipitated silica, results in Figure 4.4 show that the contribution of sodium silicate is also explained by two main factors – energy use and soda ash. Energy (split across electricity, heat from natural gas and heat from other sources) – is required for the furnace process used in sodium silicate production. Consequently, it contributes 32% to the GWP, 39% to the ODP and 49% to the TEP of precipitated silica. Soda ash, which acts as a source of sodium for sodium silicate, accounts for 30% TAP, 51% of the WDP, and 83.5% of the MRS of

precipitated silica. This is because soda ash is modelling as being recovered from lime rock via the Solvay process, which is both energy intensive and requires aqueous alkaline solutions – linking it to aquatic impact indicators.

Finally, a note should be made for cases where the silica precursor is not a dominating contributor. In these cases, important contribution typically arises from sulfuric acid use for precipitated silica, whereas hydrogen use contributes significantly to the case of pyrogenic silica.

Importance of Precursor Material Use Efficiency

Differences in the magnitude of contribution of each silica precursor to overall impact can also be partly understood in terms of the material efficiency of each process. Particularly, the atom economy of silicon tetrachloride use in the dry process (29%) is lower than that of the sodium silicate wet process (42–59%). Given the similar conversion efficiencies of each process, this increases the amount of silicon tetrachloride required per functional unit of SAS produced when compared to sodium silicate. Consequently, the absolute impact associated with use of silicon tetrachloride is amplified by the inefficiency of the chemistry on which the process relies (silicon tetrachloride, $SiCl_4$). This agrees with findings for equivalent methods of manufacturing (i.e. the dry and wet methods) used to produce titanium dioxide and zirconium dioxide [97].

Finally, the dominance of silicon tetrachloride in the impact of dry SAS (also recently noted by Resalati et al. [143]) also has wider implications on the environmental impact that can be expected for SAS produced using alkoxy-silicate precursors; this includes silica substrates produced by emerging methods (see also Chapter 5), which is common in academia currently. This is because alkoxysilane precursors are derived from silicon tetrachloride [24]. This is investigated further in Chapter 5.

Importance of Mineral Feedstock

Results in previous sections detail the importance of reagent use and factors governing this finding. However, they fail to provide understanding for the contribution of the source of silica used on the overall impact of the synthetic silica products. This is particularly interesting given a broad spectrum of research going into alternative silica feedstocks – including from biomass

resources. Consequently, the importance of silica feedstock used to produce precipitated and pyrogenic silica products is considered further here.

Results in Table 4.6 outline contribution of silica sand – the geologically derived silica feedstock used for commercial manufacturing – to the overall impact of precipitated and pyrogenic silica. Results show that the use silica sand is not a major contributor to the environmental impact of either product; that is, except for land use, which is intuitive given its derivation from mining operations, which are typically land use intensive. Consequently, these findings create a strong case that the impact of both products comes significantly from the intermediate processing of silica sand into a silica precursor, rather than from feedstock generation. This finding is crucial in suggesting benefits of silica derived from alternate feedstocks are likely to be minimal unless they provide intermediate processing routes that act as lower impact alternatives when compared to current commercial methods for manufacturing silica precursors (sodium silicate and silicon tetrachloride). This idea is explored further and consolidated outside of this thesis in research previously published by the author on the case of generating silica precursors (and commercial silica products) from rice husk [100].

Table 4.6: Contribution Mineral Feedstock to the impact of precipitated and pyrogenic silica products.

Impact Factor	Impact Contribution, %	
	Precipitated	Pyrogenic
GWP	2.7	1.1
LUP	49.1	141.2
MEP	0.3	0.2
MRS	0.1	<0.1
ODP	2.7	0.3
TAP	3.2	2.1
TEP	1.6	2.8
WDP	2.0	0.4

4.3.2. Product Impact Comparisons

Figure 4.5 visualises uncertainty in the absolute difference of a precipitated and pyrogenic silica products ($EI_{kpi}^{precipitated} - EI_{kpi}^{pyrogenic}$). This is done based on visualisation of the range covered by predictions intervals covering the central 10, 50, 95 and 99% of probability density associated with the uncertainty distributions produced by Monte-Carlo simulation; centralised (i.e. two-tailed) intervals are used to reflect the assumption of no prior information

regarding the performance of one process relative to the other. The overlap of a prediction interval with the zero line indicates lack of discernability (i.e. lack of certainty) in the difference in impact of products to the associated level of confidence of the prediction interval (e.g. 10, 50, 95, or 99%). Diamond markers are placed to indicate the position of impact prediction taken from deterministic predictions discussed in Section 4.3.1. Owing to differences in scale, and the use of lognormal uncertainty distributions in the foreground model, results are shown on a logarithmic axis.

Figure 4.5 show that the difference in impact between precipitated and pyrogenic products is discernible to some level across impact categories for the prediction intervals considered. Most notably, land use, mineral resources, and terrestrial ecotoxicity show discernability at the 99% prediction interval; ozone depletion is discernible at the 95% level. Difference in impact of the remaining impact categories is discernible only at levels below the 95% prediction interval; given analogy with hypothesis testing, this is taken to reflect results for which current LCA models are unable of providing strong evidence for difference in impact, given limitations of uncertainty associated with the models – i.e. those categories do not suggest significance difference in impact.

Findings thereby demonstrate the importance of accounting for uncertainty when making pairwise comparisons. This is because results indicate only 3 of the 8 impact categories considered in Section 4.3.1 may be interpreted to reflect a reliable difference in impact of the precipitated and pyrogenic silica products based on LCA data. Results therefore demonstrate the importance of considering uncertainty when making comparisons of environmental impact predictions. Consequently, results in this work must be considered in this context when if they are to be used in decision making process.

4.3.3. Shortcomings of Inventory Models

The results shown in this work represent a significant expansion in understanding for environmental impacts associated with the production of silica substrates according to commercial methods. Nonetheless, life cycle inventory models used as part of impact prediction feature shortcomings which much be considered within the interpretation of results. These are discussed in further detail below.

Firstly, the use of average industrial data as a basis for life cycle assessments acts to obscure differences in impact associated with different production plant, which may arise in many ways.

Secondly, the averaging of data based on EU-based plants may not accurately account for differences associated with the geography of manufacture – for example, in the US and Asia. This may lead to difference in technological implementations, difference in regulatory constraints on pollution, and differences in fuel blends associated with energy use. This applies for both for the immediate foreground model, and regional supply chains used to model background life cycle activity.

Thirdly, further limitations are also present in the modelling of energy present within life cycle inventories. Particularly, this arises from the level of granularity of data available within the source document used [82] – which is a single aggregated value. This has led models in this work to model all energy use based on the impact of heat from natural gas – on the basis that a significant proportion of energy may be associated with drying products and for the generation of heat in other process areas (natural gas being a common low-cost energy source for industrial heat generation applications. This falls short of providing a holistic interpretation of all energy used on site, and completely neglects impacts associated with energy use for both products. Consequently, some inaccuracy in predictions must be expected on this part.

Fourthly, the life cycles represent a mixed interpretation when regarding consideration for emissions associated production. In general, emissions to air and water have been based on average values reported within the source document. Nonetheless, in some cases of molecular emissions to air (NO_x, Cl_2, etc.) have been modelled more cynically because their amounts are reported as inequalities (i.e. “<”) in the source document. The treatment of emissions within the inventory models must therefore be considered only as an average, with variability arising for individual process implementations – as per further discussion within the source text [82].

Impact predictions could therefore be improved in future work by refining the source and granularity of information present within future life cycle inventory models.

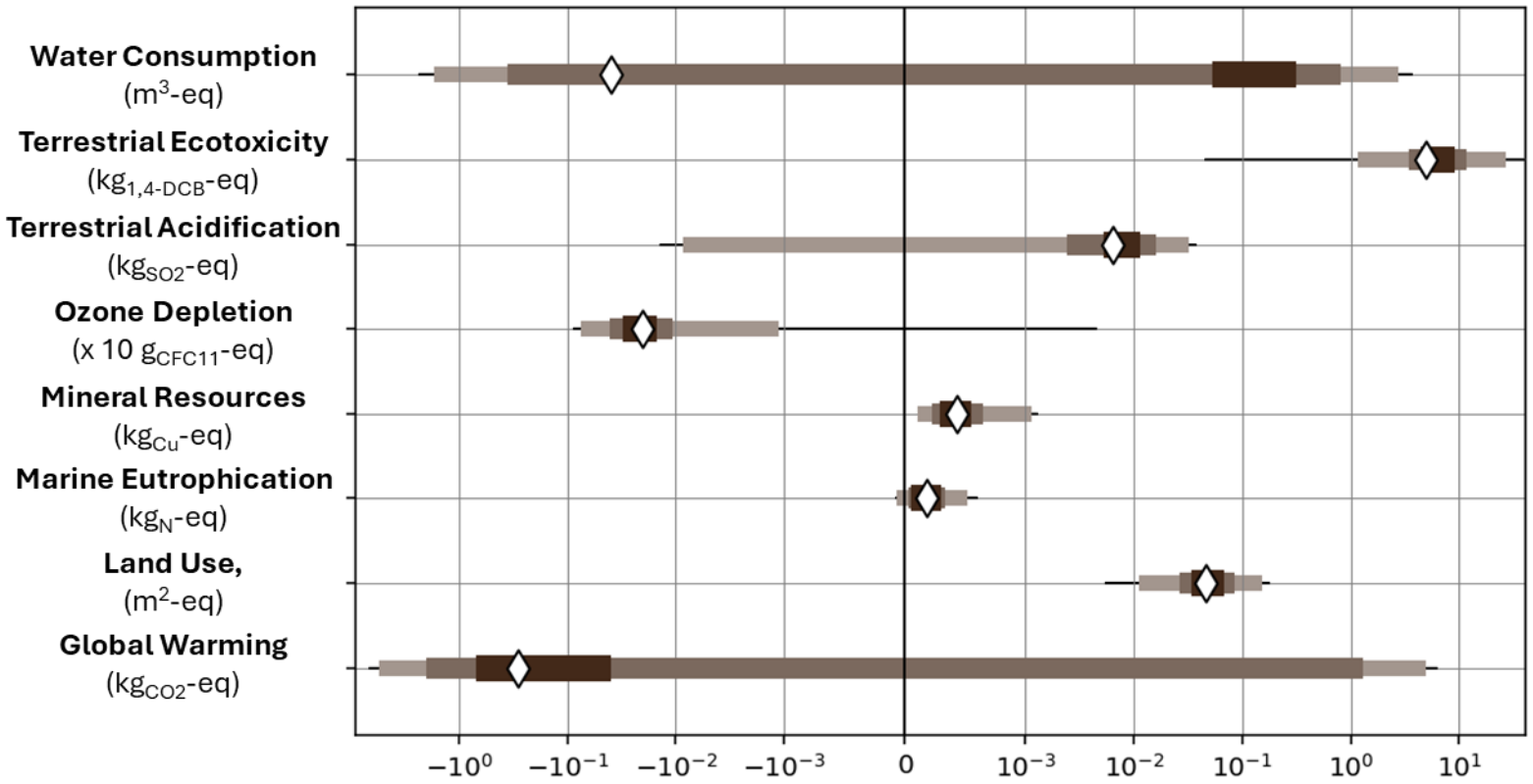


Figure 4.5: Uncertainty in the impact of individual silica products relative to one-another based on pairwise comparison. Bars represent the 10, 50, 95, and 99 % prediction intervals in order of increasing bar width, diamond markers represent the position of impact predictions made without consideration of uncertainty (i.e. Section 4.3.1). The positive portion of the x axis reflect probability space where the impact of precipitated silica is larger than pyrogenic silica, the negative portion reflects the opposite.

Conclusions

Research in this chapter has aimed to develop an understanding for the environmental impact of producing silica substrates according to industrial pyrogenic and precipitated methods. This has been done in two stages: (1) improvement of existing SAS-LCA models to evaluate the environmental footprint of existing commercial production, and (2) consideration for the effect of uncertainty on the discernability of the environmental impacts of pyrogenic and precipitated silicas.

Findings of the work reaffirm previous literature suggesting the importance of silica precursor (silicon tetrachloride and sodium silicate) on the impact of each product. This is followed by energy use, which typically ranks as the second most significant impact contributor after reagent use.

Crucially, further analysis also shows that the footprint of silica precursors is unavoidable due to the processing demands (energy demand, material chemistry and atom economy) associated with achieving their chemistries, rather than the derivation of either silica precursor from a specific feedstock (mineral or biomass). This is important in suggesting that the benefits of silica precursors derived from alternate feedstocks are unlikely to significantly affect the impact of commercial silica products unless they provide the opportunity of alternate intermediate processing routes that avoid impacts associated with traditions silica precursor manufacture. Consequently, it is recommended that life cycle assessment should be used to assess the benefit of a range of feedstock alternatives currently being considered within wider literature (e.g. biomass materials such as rice husk, rice straw, and other agricultural stubbles).

This work therefore highlights three key points to consider within the future sustainable development of silica products:

1) Impact associated with silica precursor are chemistry-linked, and therefore difficult to improve without disruptive process innovations.
2) Choice of silica feedstock source (e.g. quartz sand) is unlikely to improve impact unless enabling co-product production that reduces impact allocated to silica.

Findings of this work are novel given the lack of information currently available on the environmental impacts of commercially produced silica. Implications of precipitated silica are of particular importance owing to the production by a simple sol-gel method – from which emerging methods for mesoporous silica have been developed.

Observations are built on in subsequent chapters by using impact prediction as benchmarks when assessing emerging silica products in Chapter 5, and in assessment of surface modified SBAMs in Chapter 7.

5. Emerging Sol-Gel Silica Products

5.1. Introduction

5.1.1. Background

Research in Chapter 4 has established new benchmarks for the impact of silica substrates produced via commercial manufacturing methods. This has led to the finding that silica precursor use contributes significantly to the impact of both commercial silica products.

Nonetheless, the results in Chapter 4 fall short of providing a comparison between the impact of commercial silica products and those produced according to emerging sol-gel methods. This is important as: 1) some emerging methods may use alkoxysilanes as silica precursors (which are derived from the precursor used to produce pyrogenic silica), and 2) the emerging methods use extra solvents and additives not included in common commercial manufacturing. Consequently, it is uncertain whether the impacts of emerging sol-gel substrates are comparable with that of substrates produced commercially.

Currently, the Stöber, Mobil Composition of Matter (MCM), Santa Barbara Amorphous (SBA), and bio-inspired (BI) methods represent a significant portion of emerging substrates being reported in academic literature - accounting for thousands of publications per year (see Figure 5.1).

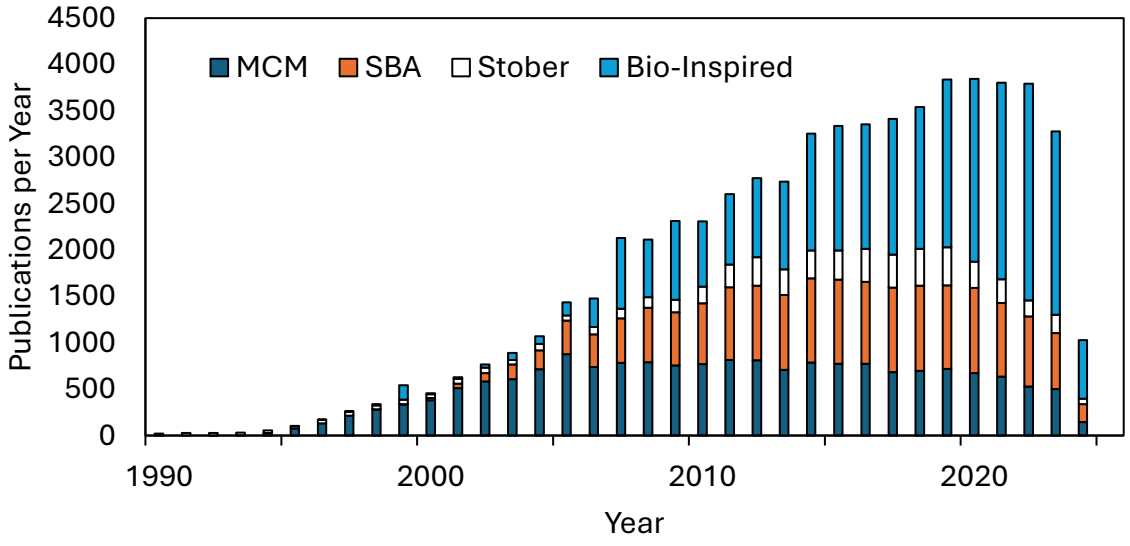


Figure 5.1: Total annual publications discussing the production of silica substrates according to the Stöber, MCM, SBA and bio-inspired silica synthesis methods. Results are based on search data from the Web of Science search engine (June 20th, 2024), using the following search terms: "MCM-41 OR MCM-48", "Stöber", "SBA-15", and "bio-inspired silica".

At present, very little is known about the true impact of silica substrates produced according to the Stöber, MCM, SBA, and BI methods. This is due to many reasons including 1) the low technological readiness associated with many of the method implementations reported, and 2) the lack of adequate LCA information on materials involved in their manufacture. For example, there is currently no LCA model for tetramethyl orthosilicate (a common silica precursor used in Stober, SBA, MCM methods) in the EcoInvent database. Similarly LCA models for surfactant templates used by the MCM, SBA and BI methods are also missing - as acknowledged recently by Benitez *et* al. for surfactants used in production according the SBA method [144].

Significant improvements in life cycle understanding are therefore required to enable accurate impact assessment of silica substrates manufactured according to emerging synthesis methods. This includes the need for improved life cycle understanding regarding both: 1) the emerging silica synthesis methods, and 2) the production of surfactants used as part of the emerging methods.

5.1.2. Aims and Objectives

This chapter aims to address gaps in understanding for the environmental impact associated with silica substrates produced according to emerging sol-gel methods. This is done by developing new understanding for mass and energy use associated with each method, with the intention of establishing environmental impact predictions via LCA. Owing to their prevalence in academic literature, this is done with a focus on emerging substrates produced according to the Stöber, MCM, SBA, and BI synthesis methods. The objectives of the work are:

1. To estimate missing information for mass and energy use associated with surfactant templates used by the emerging silica synthesis methods.
2. To create life cycle inventories modelling the production of silica according to emerging methods.
3. To predict the environmental impact of silica products produced by each emerging synthesis method.
4. To identify the main sources of impact associated with silica substrates produced by each method.

5. To assess the importance of silica precursor choice on the impact of silica substrates produced by each method.
6. To compare the impact of silica substrates produced by emerging sol-gel products with the benchmarks for commercial products established in Chapter 4.

5.2. Methods

Multiple modelling methods have been used in this chapter as part of assessing the environmental impacts of emerging sol-gel silica products. As shown in Figure 5.2, the approach is split into three phases reflecting: 1) process modelling, 2) inventory modelling, and 3) impact assessment. Further information on the approaches taken in each stage is provided in the following subsections.

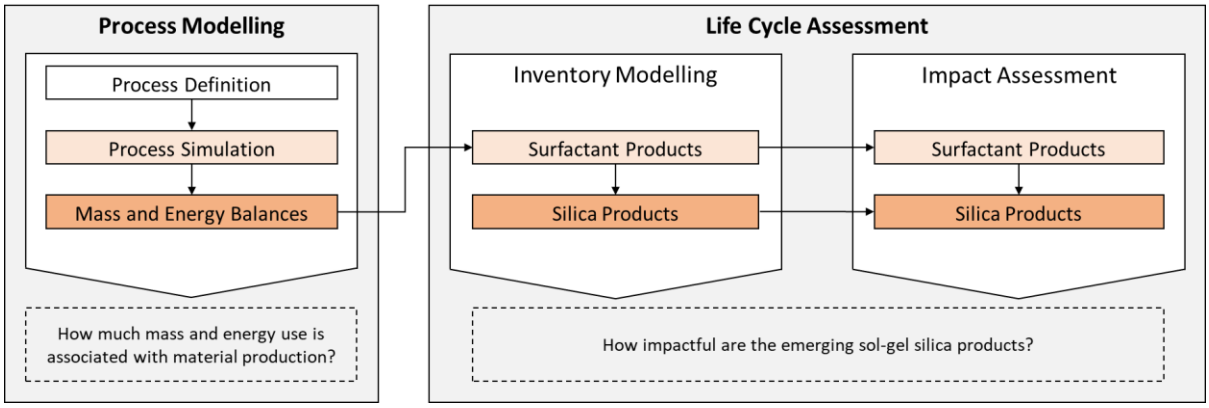


Figure 5.2: Schematic workflow of methods used to investigate the environmental impact of silica substrates produced according to emerging synthesis methods.

5.2.1. Process Modelling

Process modelling has been used to estimate material and energy use associated with producing cetrimmonium chloride (CTAC) and Pluronic 123 (P_{123}). These are organic surfactant templates related to the production of silica by the MCM and SBA methods respectively. In all cases, this was done using the Aspen Plus V11 software for process simulation. Operating conditions used in process modelling were validated using values reported in patent literature to ensure realistic processing conditions. In all cases, thermodynamic modelling of vapor and liquid equilibria has been done using the NRTL-RK method. All starting materials were assumed to enter the process at 25 C and 1 bar pressure; reagent inputs to each process were also assumed to be completely pure.

Process optimization has not been considered due to the extent of information on processing conditions provided within patent literature. Further information on the modelling of each process is provided in the following subsections.

Cetrimmonium Chloride (CTAC)

Process Description

CTAC production has been modelled according to the commercial method of reacting cetyl alcohol (CA) with dimethyl amine (DMA) (stage 1) [145], followed by the commercial method of reductive alkylation of cetyldimethylamine (CDMA) with methyl chloride (stage 2) [146]. A schematic representation of flow diagrams for both processes is shown Figure 5.3.

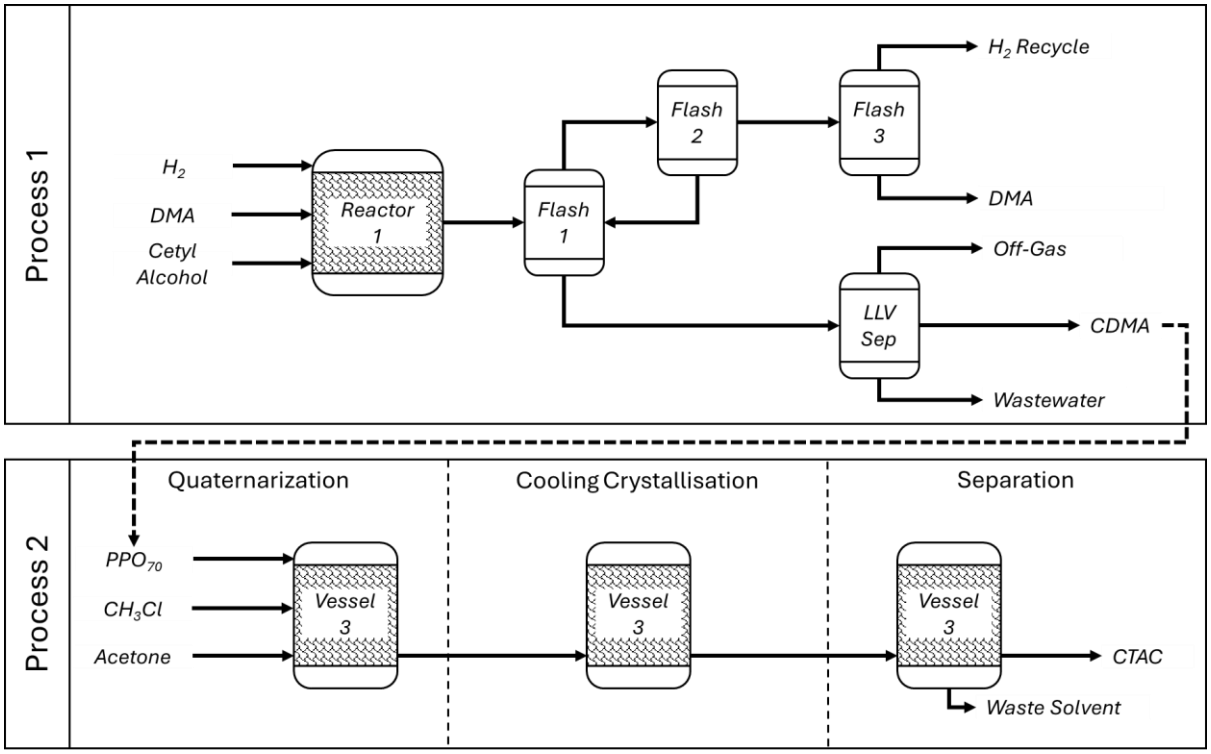


Figure 5.3: Process flow diagram of processes modelled to estimate material and energy use associated with the production of cetyldimethylamine (CDMA, top) and cetrimmonium chloride (CTAC, bottom).

Production of cetyldimethylamine, CDMA

The production of CDMA was modelled according to the continuous process design reported in patent [147]. Reaction conditions and feed ratios were taken from patent [145]. Chemical reactions producing CDMA (Equation 5.1), and the by-products dicetyl methylamine and trimethylamine (Equation 5.2) were considered to occur - based on the work of Abe et al. [148]. Overall reagent conversion and reaction selectivity was modelled based on [149] and [150, 151] respectively.

$$\mathrm{ROH} + \mathrm{NH(CH_3)_2} \rightarrow \mathrm{RN(CH_3)_2} + \mathrm{H_2O} \quad (5.1)$$

$$2\mathrm{RCH_3OH} + \mathrm{DMA} \rightarrow (R)_2N(\mathrm{CH_3}) + TMA \quad (5.2)$$

Where R represents the organic cetyl alkyl group, DMA represents dimethylamine, and TMA represents trimethylamine.

Temperatures and pressures associated with the operation of flash condensers were taken from [145] and conditions of the final liquid-liquid-vapour product separation were taken from [152].

Further information on all conditions associated with production are available in Appendix B.

Production of Cetrimmonium Chloride, CTAC

The production of CTAC was modelled according to the batch processing approach and associated conditions reported in [146]. Only the reaction producing the desired product (Equation 5.3) was considered. The cooling crystallisation stage was modelled based on performance reported in patent literature [153]

$$\mathrm{RN(CH_3)_2} + \mathrm{CH_3Cl} \rightarrow \mathrm{R[(CH_3)_3N]^+Cl^-} \quad (5.3)$$

Where $\mathrm{R[(CH_3)_3N]^+Cl^-}$ represents cetrimmonium chloride.

Further information on all conditions associated with production are available in Appendix B.

Pluronic 123 (P_{123})

Pluronic 123 production was modelled based on the commercially practiced three-stage polymerisation route involving stepwise synthesis of PPO_{17}, PPO_{70}, and P_{123}. This is shown in Figure 5.4.

Production of poly(propylene oxide)$_{17}$, PPO_{17}

The production of PPO_{17} was modelled according to a KOH-catalysed, batch-wise processing approach (see Chapter 2, Section 6.1) using propylene glycol as a starter – as reported in patent literature [107]. This includes polymerisation to form PPO_{17} at 115 C and 3.5 bar [107] (see Equation 5.4), followed by neutralisation of KOH using phosphoric acid [154] (see Equation 5.5), and polymer separation via filtration. A PPO_{17} product was targeted to reflect

1000 g/mol limit typical of the KOH method (see Section 2.6.3). Filtration was assumed to recover 100% of the PPO_{17} product.

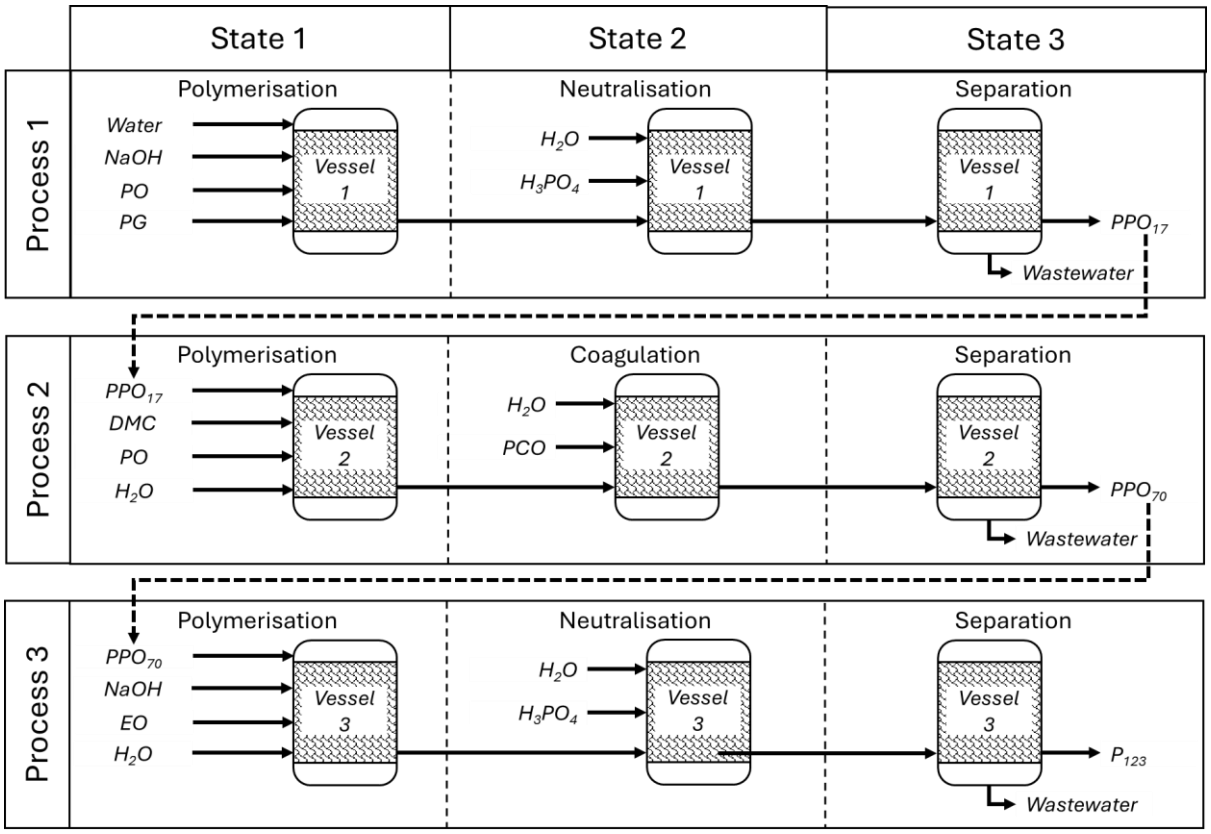


Figure 5.4: Major stages modelled in the production of Pluronic 123 according to the manufacture of PPO_{17} (top), PPO_{70} (middle), and Pluronic 123 (P_{123}, bottom). Each process is based on a one-pot synthesis approach, with three processing states. NaOH: sodium hydroxide, PO: propylene oxide, EO: ethylene oxide, H_3PO_4: Phosphoric acid, DMC: Double metal cyanide catalyst, PCO: polycarboxylate.

$$\mathrm{PG} + 16\mathrm{PO} \rightarrow \mathrm{PPO}_{17} \tag{5.4}$$

$$\mathrm{H_3PO} + \mathrm{KOH} \rightarrow \mathrm{KH_2PO} + \mathrm{H_2O} \tag{5.5}$$

For further information relating to modelling assumptions see Appendix C.

Production of poly(propylene oxide)$_{70}$, PPO_{70}

The production of PPO_{70} was modelled according to a continuous, DMC catalysed process patent reported previously by BASF [155]. This includes polymerisation (see Equation 5.6), coagulation using polycarboxylate additive, and product separation by filtration. Information on the polymerisation and coagulation conditions were taken from patents [155] and [156] respectively. Filtration was assumed to recovery 100% of the desired product. PPO_{17} was assumed to be used as a polymerisation starter.

$$PPO_{17} + 53PO \rightarrow PPO_{70} \quad (5.6)$$

For further information relating to modelling assumptions see Appendix C.

Production of Pluronic 123, P_{123}

The production of Pluronic 123 was modelled according to a KOH-catalysed, batch-wise production process – as reported in [154]. This includes polymerisation (Equation 5.7) according to conditions reported in patent [154], followed by neutralisation of KOH using phosphoric acid [154], and separation of the Pluronic 123 product by filtration. It was assumed to recovery 100% of the desired product. PPO_{70} was assumed to be used as a polymerisation starter.

$$PPO_{70} + 40EO \rightarrow PEO_{20}PPO_{70}PEO_{20} \quad (5.7)$$

Further information on all conditions associated with production are available in Appendix C:.

5.2.2. Inventory Modelling of Surfactant Products

Goal and Scope Definition

The goal of the LCA reported in this section is to estimate the environmental impact associated with producing CTAC, P_{123}, and PEHA surfactant products. This has been done using an attributional LCA approach using a functional unit of 1 kg of dried product and a Cradle-to-Gate model scope. For transparency, the impact of intermediates present in the production of CTAC (i.e. CDMA), and P_{123} (i.e. PPO_{17}, PPO_{70}) has also been included when reporting results. Further information on product-specific system boundaries follows below.

Inventory Modelling

Cetrimmonium Chloride

Life cycle inventory models for CDMA and CTAC are based on material and energy estimates taken from process modelling described in Section 5.2.1. Background activity associated with material and energy supply chains has been modelled using existing models available in the EcoInvent v3.10 database [157]. Materials recovered in reagent grade purity during processing have been assumed to be recycled to offset material use associated with each inventory where possible (see Table 5.1).

A summary of the life cycle inventory information associated with CDMA and CTAC is provided in Table 5.1. An illustration of system boundaries for the production of CDMA and CTAC is provided in Figure 5.5. For further information on background activity models see

Table 5.3.

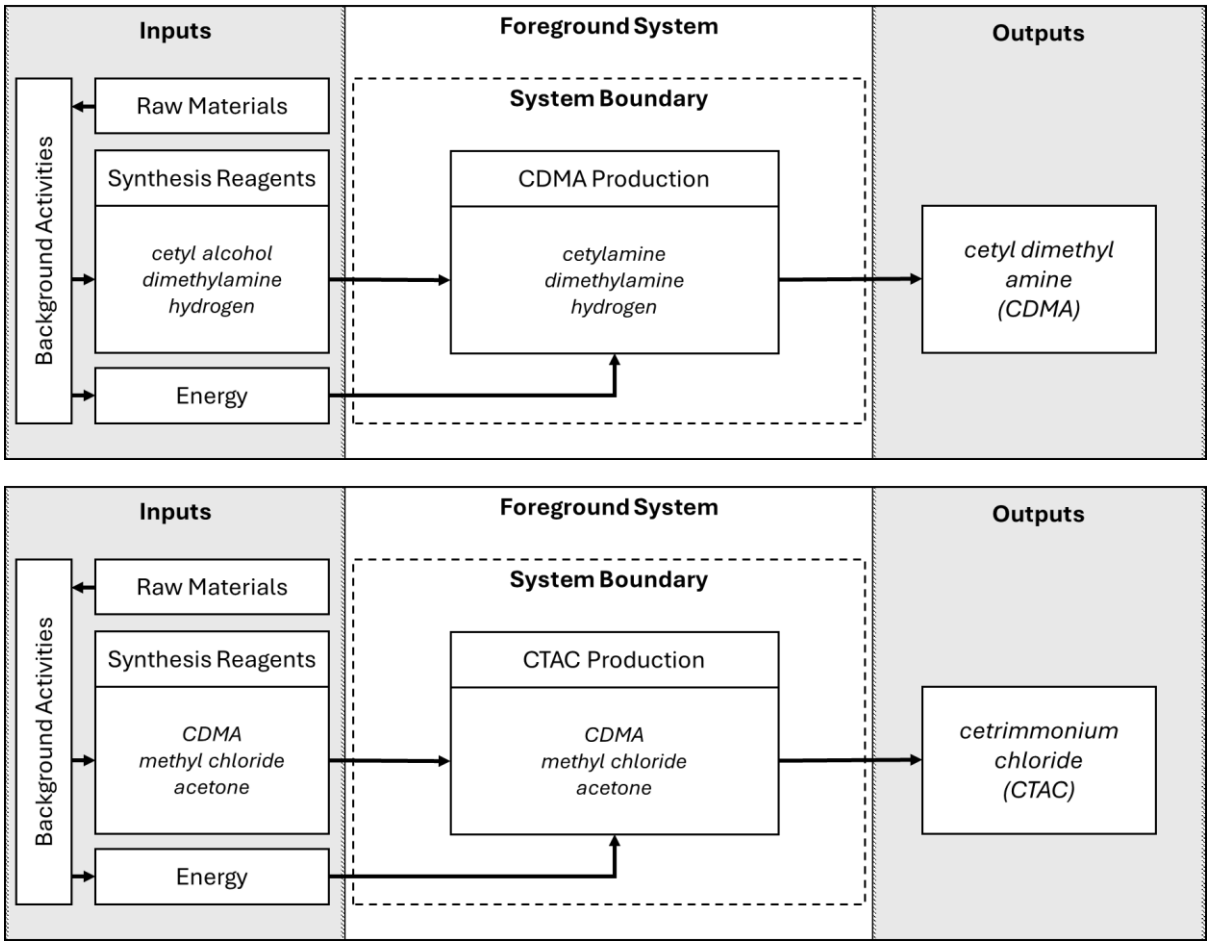


Figure 5.5: Illustration of system boundaries associated with life cycle inventory models reported on the production of cetyldimethlyamine (CDMA, top) and cetrimmonium chloride (bottom).

Pluronic 123

Life cycle inventory models for PPO_{17}, PPO_{70}, and Pluronic 123 are based on material and energy estimates taken from process modelling described in Section 5.2.1. Background activity associated with material and energy supply chains has been modelled using existing models available in the EcoInvent v3.10 database [157].

Materials recovered in reagent grade purity during processing have been assumed to be recycled to offset material use associated with each inventory where possible.

In all cases, wastewater treatment operations associated with production assumed to occur on-site but are not considered explicitly within the scope of the LCA due to lack of available information.

Table 5.1: Life cycle inventory data for cetyldimethylamine (CDMA) and cetrimmonium Chloride (CTAC).

Type	Flow	Amount		Unit
		CDMA	CTAC	
Materials	Cetyl Alcohol	0.93	-	kg
	Cetyldimethylamine	-	0.89	kg
	Dimethylamine	0.24	-	kg
	Hydrogen	[a]<0.01	-	kg
	Methyl Chloride	-	0.19	kg
	Water	0.28	0.11	kg
	Isopropyl alcohol	-	1.33	kg
Energy	Electricity, medium Voltage	0.119	0.149	kg
	Steam	0.238	-	kg
Output	Cetyldimethylamine	1.0	-	kg
	Cetrimmonium Chloride	-	1.0	kg
	Wastewater	[b]0.00	-	kg

[a] Value includes substitution occurring due to material recycle, [b] results from process modelling suggest production of no wastewater, though potential for production was included; a value of 0.00 is included to reflect this reality.

An illustration of system boundaries associated with the production of PPO_{17}, PPO_{70}, and Pluronic 123 is provided in Figure 5.6. A summary of the life cycle inventory information is provided in Table 5.2**.** Further information on background activity models is provided later in

Table 5.3.

Table 5.2: Life cycle inventory data for poly(propylene oxide)$_{17}$ (PPO_{17}), poly(propylene oxide)$_{70}$ (PPO_{70}), and Pluronic 123 (P_{123}). NC: not considered

Type	Flow	Amount			Unit
		PPO_{17}	**PPO_{70}**	**P_{123}**	
Input	Propylene Glycol	0.08	-	-	kg
	PPO_{17}	-	0.253	-	kg
	PPO_{70}	-	-	0.731	kg
	Propylene Oxide	1.162	0.759	-	kg
	Ethylene Oxide	-	-	0.318	kg
	Water	1.809	0.675	0.007	kg
	Potassium Hydroxide	0.065	-	0.011	kg
	DMC Catalyst	-	N.C.	-	kg
	Phosphoric Acid	0.019	-	0.019	kg
	Polycarboxylate	0.005	-	-	kg
	Electricity	<0.001	<0.001	0.009	kWh
	Heat, from Steam	0.912	0.132	0.013	kWh
Output	PPO_{17}	1.000	-	-	kg
	PPO_{70}	-	1.000	-	kg
	Pluronic 123	-	-	1.000	kg

Background Life Cycle Models

A summary of inventory models used to model backgrounds life cycle activity of surfactant templates is provided in

Table 5.3.

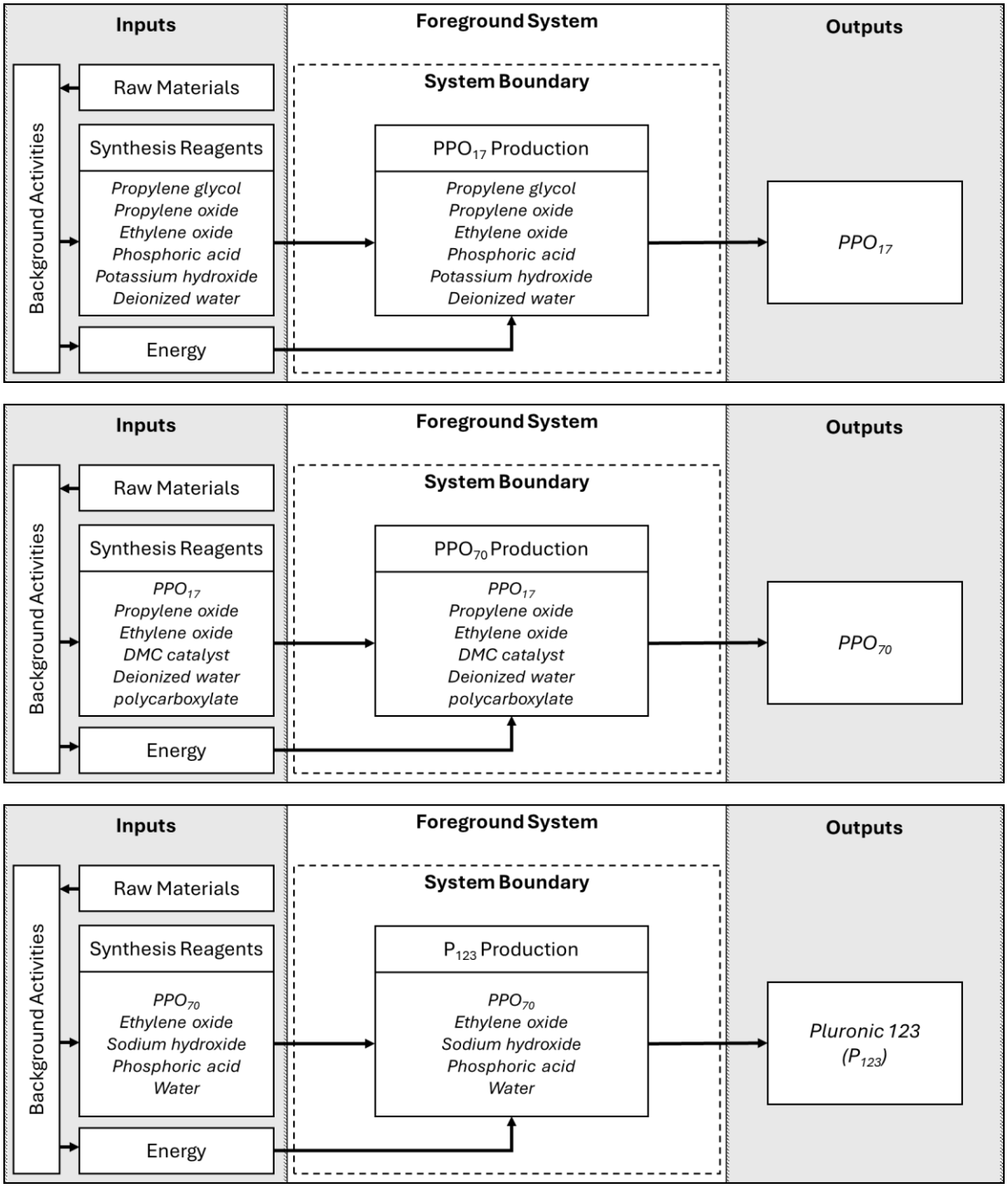


Figure 5.6: Illustration of system boundaries associated with life cycle inventories modelling the production poly(propylene oxide)$_{17}$ (PPO_{17}, top), poly(propylene oxide)$_{70}$ (PPO_{70}, middle), and Pluronic 123 (bottom).

Table 5.3: EcoInvent v3.10 database models used to account for background life cycle activity linked to the production of surfactant templates.

Inventory Item	Model	Region
Cetyl Alcohol	market for fatty alcohol	RER
Dimethylamine	*market for dimethylamine*	RER
Hydrogen	market for hydrogen, liquid	RER
Methyl Chloride	market for methylchloride	RER
Water	market for water, deionised	EU w/o CH
Isopropyl alcohol	market for isopropanol	RER
Propylene Glycol	market for propylene glycol, liquid	RER
Propylene Oxide	market for propylene oxide, liquid	RER
Ethylene Oxide	market for ethylene oxide	RER
Potassium Hydroxide	potassium hydroxide production	RER
DMC Catalyst	Not considered	N/a
Phosphoric Acid	purification of wet-process phosphoric acid to industrial grade, product in 85% solution state	RER
Polycarboxylate	Not considered	N/a
Electricity	market group for electricity, medium voltage	RER
Heat, from Steam	market for heat, from steam, in chemical industry	RER
Methanol	market for methanol	GLO
Ethyl Acetate	*market for ethyl acetate*	GLO
Ethanol	market for ethanol, without water, in 99.7% solution state, from ethylene	RER
Biomethanol	market for methanol, from biomass	CH
Bioethanol	market for ethanol, without water, in 99.7% solution state, from fermentation	GLO

5.2.3. Inventory Modelling of Emerging Silica Substrates

Goal and Scope Definition

The goal of the LCA reported in this work is to provide estimations for the environmental impact associated silica substrates produced according to the Stöber, MCM, SBA and BI synthesis methods. This has been done using an attributional LCA approach according to a functional unit of 1 kg of dried product as an assessment basis. As shown in Figure 5.7, assessment of all products has been set to consider a Cradle-to-Gate scope. For fair comparison, the system boundary of all products considered has been set to include the stages of silica synthesis, product washing, and post-treatment by drying.

Inventory Modelling

Life cycle inventories have been produced by aggregating material and energy use information available within a mixture of patent literature and academic publications. In all cases, information for solvent use for product washing and wastewater (including waste solvents)

produced has not been included. This was done to avoid skewing impact predictions with extremely high (and unrealistic) amount of material use typically reported within academic literature – reflecting the low technological readiness level of many methods being employed, rather than representing reliable estimates for a commercially feasible process. Conversely, inventory information relating to powder drying has been considered constant across all methods – to provide consistent basis for impact comparison. Further information on silica produced according to individual synthesis methods is provided in the subsections following below.

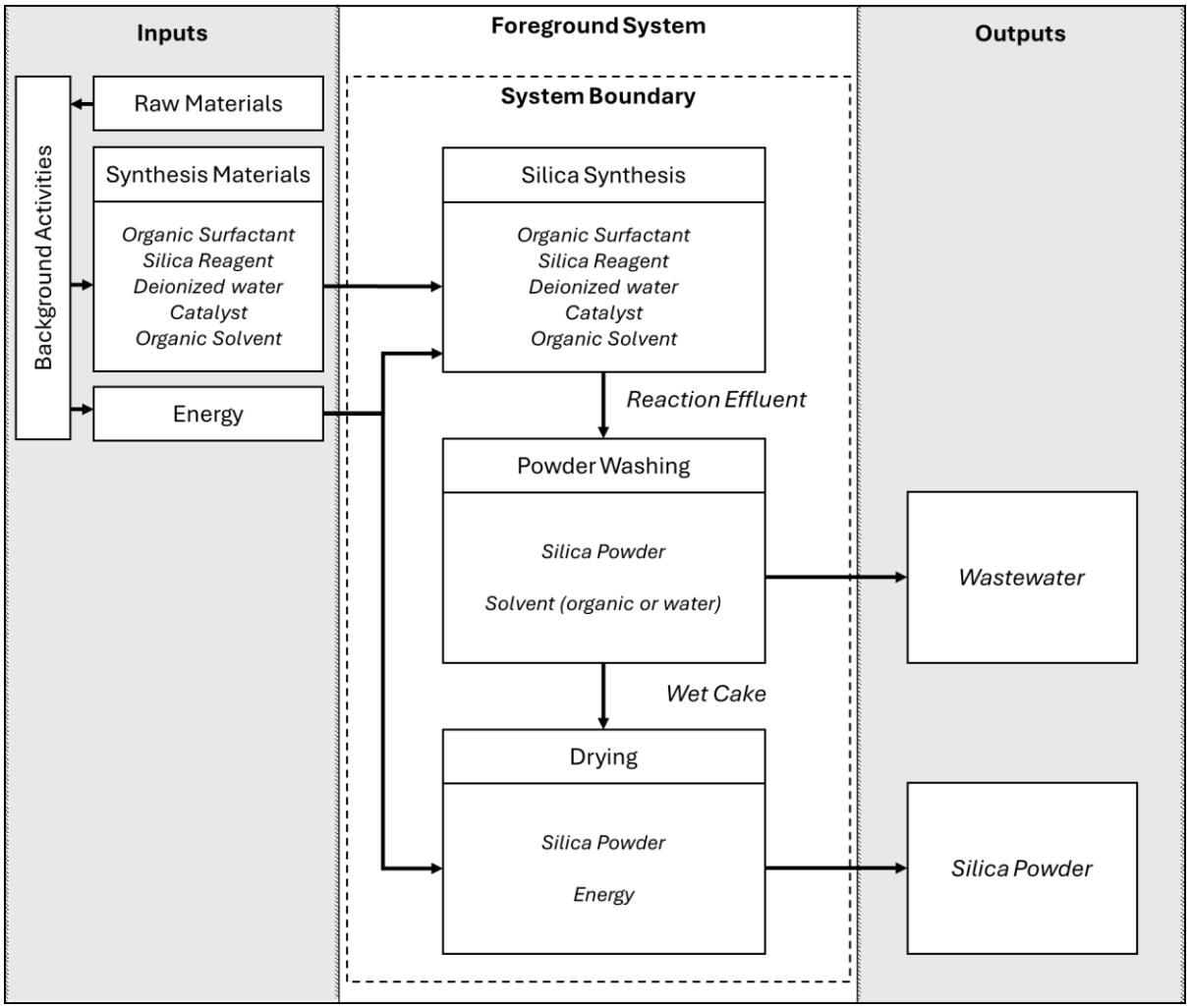


Figure 5.7: Illustration of system boundaries associated with life cycle inventories modelling the production of silica powder according to the Stöber, MCM, SBA, and BI synthesis methods.

Table 5.4 shows a summary of EcoInvent database life cycle models used for each inventory. Table 5.5 shows a summary of life cycle inventories for all products modelled.

Powder Drying

Powder drying has been assumed to incur an energy use amounting to 19.5 MJ/kg for all products. This is based on values for powder drying reported for precipitate silica in EU-15 industry [82] (see also Chapter 4).

Synthesis via the Stöber Method

Material and energy use associated with the production of Stöber silica has been taken from values reported by Brambila *et al*. [93]; these values summarise production method originally reported by Stöber, Fink and Bohn [83]. This information reflects synthesis done under experimental conditions.

Synthesis via the Santa Barbara Amorphous Method

Two separate inventories have been created for modelling the impact of SBA silica. These are based on material and energy use associated for processes using TEOS (as reported by Brambila *et al*. [93]), and sodium silicate (as reported by Choi *et al*.) to produce SBA-15. Both inventories reflect synthesis under experimental conditions and both inventories include the use of Pluronic 123 as a surfactant template. Life cycle activity associated with Pluronic 123 use was modelled using life cycle inventories reported earlier in Section 5.2.1).

Synthesis via the MCM Method

Two separate inventories have been created for modelling the impact of MCM silica. These are based on material and energy use associated for a process using TEOS to produce MCM-48 (as reported by Brambila *et al*. [93]), and a process using sodium silicate to produce MCM-41 (as reported by Wang *et al*. [158]). Both sources reflect synthesis under experimental conditions and both inventories include the use of CTAC as a surfactant template. Life cycle activity associated with CTAC use was modelled using life cycle inventories reported earlier in Section 5.2.1).

Synthesis via the Bio-inspired Method

Material and energy use associated with the production of Stöber silica has been taken from values reported by Brambila *et al*. [93]. This source reflects synthesis under experimental conditions and assumes use of PEHA as a surfactant template.

Table 5.4: Inventory models used to account for background life cycle activity linked to the production of emerging silica substrates based on the EcoInvent v3.10 database.

Inventory Item	Model	Region
Sodium Silicate	Market for sodium silicate, furnace method	RER
Tetraethyl orthosilicate	Market for tetraethyl orthosilicate	GLO
Tetramethyl orthosilicate	*Adapted from Market for tetraethyl orthosilicate (GLO)*	GLO
Water	Market for water, deionised	EU exc. CH
Sodium Hydroxide	Market for Sodium hydroxide, 50% solution state	RER
Hydrochloric Acid	Market for hydrochloric acid	
Ethanol	Market for ethanol from ethylene, 99.97wt%	RER
Cetrimmonium Chloride	*See Section 2.2 of this work*	*This work*
Pluronic 123	*See Section 2.2 of this work*	*This work*
Pentaethylenehexamine	*See Section 2.2 of this work*	*This work*
Heat (natural gas)	Market group for natural gas	RER

5.2.4. Environmental Impact Assessment

Environmental impacts have been calculated using version 2 of the openLCA software in combination with the impact characterisation factors of the ReCiPe Hierarchical 2016 method [71]. All calculations include a 0.1% cut-off method. A summary of impact factors considered, and justifications is provided in Table 5.7**.**

Table 5.5: Life Cycle Inventory data for silica produced according to the Stober, MCM, SBA, and Bio-inspired synthesis methods.

Type	Flow	Amount						Unit
		Stöber	MCM-41	MCM-48	SBA-15 1	SBA-15 2	Bio-Inspired	
Material	Sodium Silicate	-	-	2.03	-	2.03	2.18	kg
	Tetramethyl orthosilicate	-	-	-	-	-	-	kg
	Tetraethyl orthosilicate	4.07	3.54	-	3.54	-	-	kg
	Water	8.65	16.84	36.00	12.51	1.02	27.03	kg
	Ammonia	1.69	-	-	-	-	-	kg
	Sodium Hydroxide	-	0.32	-	-	-	-	kg
	Hydrochloric Acid	-	-	-	3.63	0.21	4.86	kg
	Sulphuric Acid	-	-	0.46			-	kg
	Ethanol	59.77	-	-	-	-	-	kg
	Methanol	-	-	-	-	-	-	kg
	Cetrimmonium Chloride	-	2.61	1.07	-	-	-	kg
	Pluronic 123	-	-	-	1.67	0.16	-	kg
	Pentaethylenehexamine	-	-	-	-	-	0.05	kg
Energy	Heat (natural gas)	19.50	19.50	19.50	19.50	19.50	19.50	MJ
Output	Silica Powder	1.00	1.00	1.00	1.00	1.00	1.00	kg
	Yield	85	98	100	98	100	93	%

Table 5.6: Minimum mass of silica reagents required to produce 1 kilogram of silica product according to reaction stoichiometry.

Species	Minimum Amount, kg/kg_{SiO2}
Tetraethyl orthosilicate	3.47
Tetramethyl orthosilicate	2.54
Silicon tetrachloride	2.81
Sodium silicate	2.03

Table 5.7: Impact factors considered during life cycle impact assessment of surfactant and silica products in this work.

Impact Factor	Justification
Global Warming Potential	Global climate change driver
Fossil Fuel Depletion	Indicator of reliance on non-renewable resources
Terrestrial Acidification	Historical transboundary pollution problem
Water Depletion	Relevance to water scarcity issues

5.3. Results

5.3.1. Environmental Impacts of Surfactant Products

Cetyltrimethylammonium Surfactants

Figure 5.8 shows impact predictions for producing CTAC and CDMA.

Results in Figure 5.8 show environmental impact predictions of 5.25 kg CO_2-eq, 2.86 kg oil-eq, 0.21 m^3 H^2O-eq, and 21.1 mg SO_2-eq per kilogram of CTAC produced and impacts of 2.33 kg CO_2-eq, 1.00 kg oil-eq, 0.21 m^3H_2O-eq, and 10.4 mg SO_2-eq per kilogram of CDMA.

Differences in the impact of CTAC and CDMA reflect a strong tendency of CDMA to contribute to the impact of CTAC significantly across all impact factors. This is especially so in the case of the water consumption impact metric, where CDMA use dominates the impact of the CTAC product. In all cases, this may be somewhat reflective of the relatively mild operating conditions associated with producing CTAC, including:

1) the lack of use of aqueous solutions due to poor solubility of CDMA reagent,
2) mild conditions of the CTAC synthesis reaction (75C and atmospheric pressure),
3) the endothermic nature of the Menshutkin reaction – meaning heating, rather than cooling is required.

Further assessment indicates that fatty reagent use (i.e. cetyl alcohol use) is also a significant contributor to the impact associated with the CDMA product. This is interesting given that the production pathway of cetyl associated with vegetable/bio-oil sources, which may lead one to initially expect low impact contribution. Nonetheless, these products require a significant amount of energy use, which likely provides a significant contribution to their overall impact profile. Unfortunately, no alternative life cycle model was available within the EcoInvent database for further comparison of impacts based on derivation from other sources.

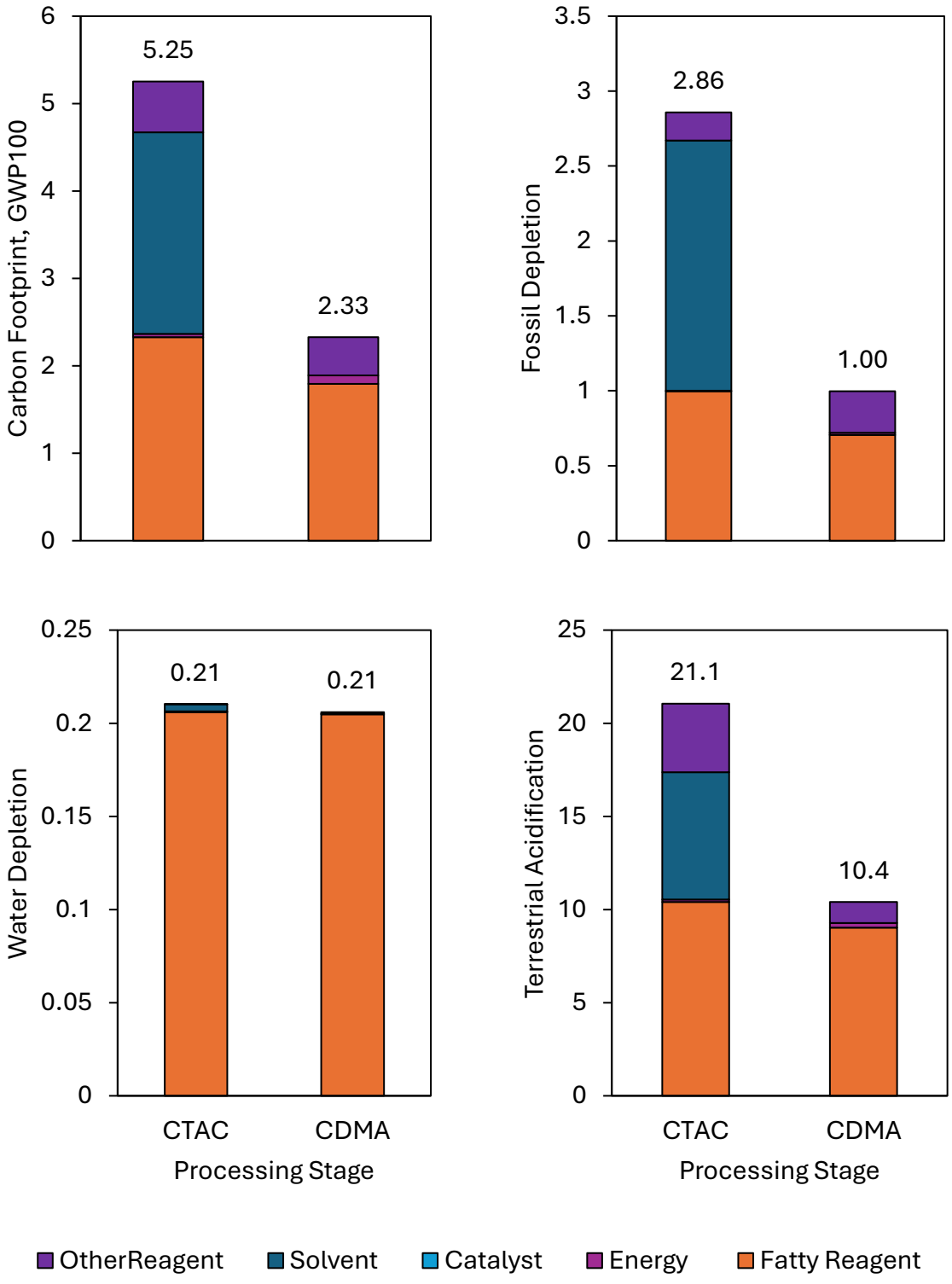


Figure 5.8: Environmental impact predictions for 1kg of Cetrimmonium Chloride (CTAC) and the associated amount of cetyldimethylamine (CDMA) produced during the CTAC product life cycle.

Following fatty reagent contributions, solvent use appears to be the next large contributor of impact for CTAC across all impact factors considered. This is intuitive given the relatively large amount of isopropyl alcohol used in producing CTAC when compared to amount of other reagent required for production (see process modelling information in Section 5.2.1).

On the contrary, reagents form the major contribution to impact associated with the CDMA products. This is also intuitive given the lack of organic solvent used in the production of CDMA, the ability to recycle the majority of hydrogen involved in the production process and the relatively low amount of energy use associated with the product (see Table 5.1).

Comparison with Surfactant Products Available in the EcoInvent Database

Notably, impact predictions are also of similar values to those reported for non-ionic surfactant production based on models already existing within the EcoInvent database. This is illustrated based on assessment of preexisting non-ionic surfactant production model available within the EcoInvent data base in Table 5.8. It must be stressed that similarity between the two product types should also not be taken as certain. Therefore, whereas the comparison should only be taken as not providing alarm as opposed to suggesting reliability of the life cycle inventory and/or impact assessment reported in this work. Further analysis and discussion of divergences between these datasets where out-of-scope for this work.

Table 5.8: Impact predictions for cetrimmonium chloride (this work) and non-ionic surfactant products

Impact Factor	Cetrimmonium Chloride	Non-ionic Surfactant*	
		Ethylene Oxide Route	Fatty Acid Route
Carbon Footprint, kg CO_2-eq	5.25	2.51	4.25
Fossil Depletion, kg oil-eq	2.86	1.25	0.65
Water Depletion, m^3 H_2O-eq	0.21	0.30	0.05
Terrestrial Acidification, kg SO_2-eq	0.02	0.01	0.01

* Taken from existing models for production (RER region) in the EcoInvent v3.10 database

Importance of Solvent Choice in the Quaternization Stage

Results for the effect of organic solvent choice on impact of CTAC relative to that produced using IPA is shown in Figure 5.9**.**

Results in Figure 5.9 show that the choice of solvent used in can lead to improvement of worsening of product impact. The extent of this change (improvement or worsening) is varying between -50 to 90% or approximately 20% on average (arithmetic mean).

Importantly, the choice of alcohol as organic solvent seems to provide the most consistent expected improvement in impact of CTAC product. Improvement appears to me most pronounced for biomass derived methanol followed by methanol, then ethanol and

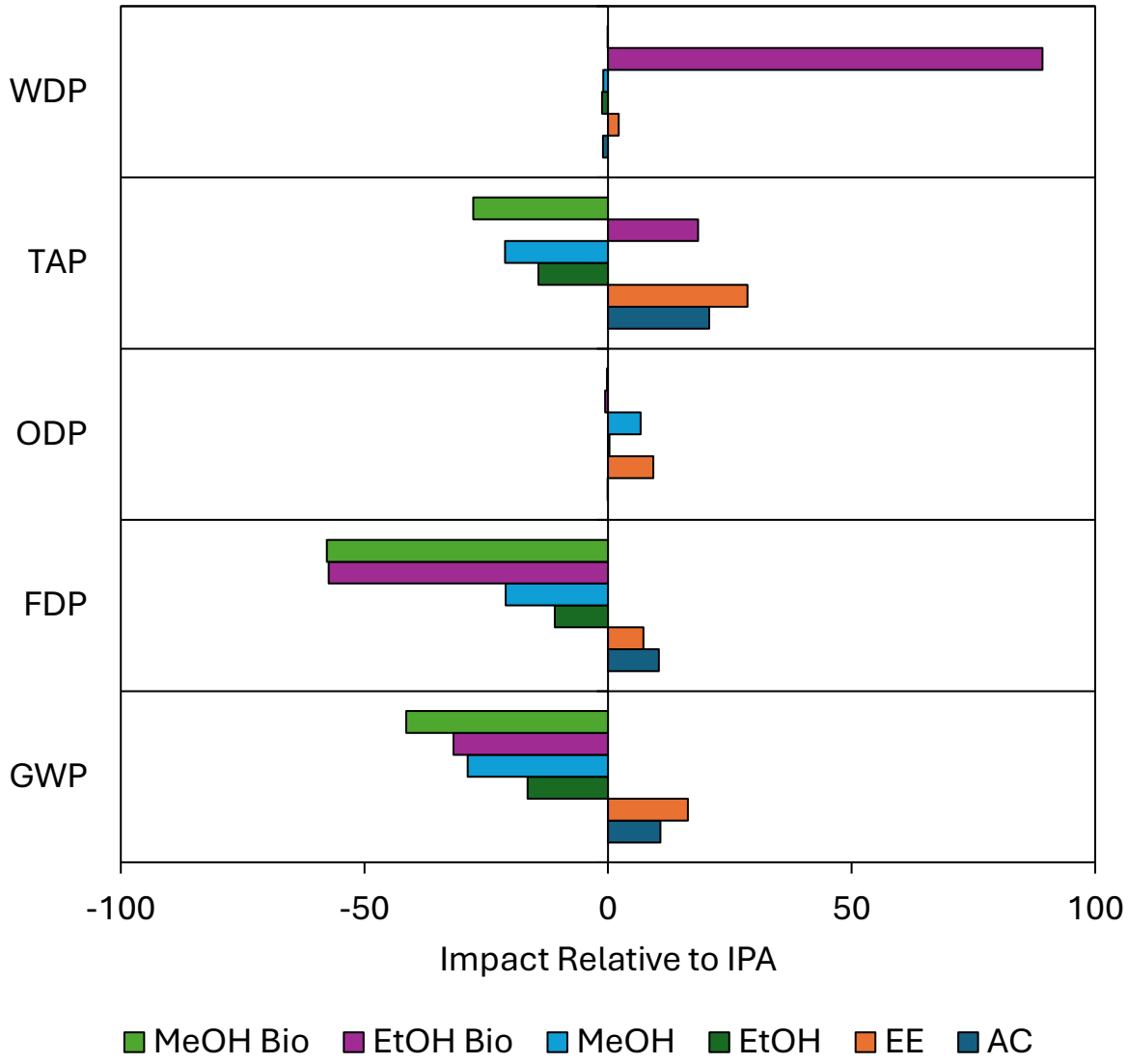


Figure 5.9: Effect of quaternization solvent choice on the impact prediction of 1 kilogramme of cetrimmonium chloride.

bioethanol when considering all five impact categories. Notably, the choice of bioethanol and methanol are problematic regarding water and ozone depletion respectively though. These exceptions to the general trend can be understood based on technological differences in production. Particularly increase water use of bioethanol is attributable to use water use associated fermentation methodology while ozone depletion of methanol can be attributed to derivation from coal. Notably, the production of bio-methanol occurs via a gasification technology, which is why it does not show similar issues for water depletion.

Finally, it must be noted that results of comparison should be used only as an indication for the sensitivity of CTAC impact to solvent choice, rather than an indication of best solvent choice. This is due to lack of consideration captured in Figure 5.9 for the effect of differences

in solvent choice on nuances of the quaternarization of CDM. This includes effects on limitations to reagent solubility, differences in reactivity, and issues with product separation that may be associated with solvent choice. Nonetheless, results in Figure 5.9 tend to indicate that solvent choice is likely to be important. Thus, more rigorous future life cycle assessments based on inventories with optimized solvent use would be desirable.

Pluronic 123

Predicted impacts associated with production of are shown as a function of life cycle stage in Figure 5.10**.** The contribution of DMC catalyst use is not included due to the lack of publicly available LCI information online. However, it is notable that LCIs reported based on proprietary LCIs for DMC production subprocess tend to suggest that contribution of the catalyst may be low in the case of carbon footprint [159]. Other impact factors, especially metal use, may vary. The full extent of this is not clear due to lack of direct reporting of contributions from DMC catalyst alone – see von der Assen and Bardow [159].

The importance of contribution of starter and monomer materials to fossil depletion are unsurprising given their petrochemical derivation. The same can be said for energy use.

Interestingly, results across all impact factors seem to suggest that the production of PPO_{70} contributes more significantly to the impact profile of Pluronic 123 than the production of PPO_{17}. This may reflect differences in processing approach involved in this stage. That is, the use of DMC based catalysis method to produce PPO_{70} when compared to a KOH method.

The importance of impact contributions identified for the PPO_{70} manufacturing stage is also interesting considering 'favourable' processing factors that it includes when compared to the "better performing" P_{123} and PPO_{17} production stages. Particularly, the PPO_{70} demonstrates a higher impact despite being modelled to have a higher reaction efficiency, a lower reaction pressure and ignoring impact from catalyst contribution.

The unexpectedly large contribution associated with manufacturing PPO_{70} likely reflects the use of PPO_{17} as a polymerisation starter. This may be explained considering the stoichiometric limitations present in the need for 53 propylene oxide monomer units to produce a PPO_{70} polymer block when starting from the PPO_{17} precursor. In contrast, only 40 moles of ethylene oxide are required to produce the final P_{123} product (from PPO_{70}), and only 16 moles of propylene oxide are required to produce the initial PPO_{17} polymer block from the associated

propylene glycol starter. This interpretation is directly reflected in the fact that contributions for the impact of the PPO_{70} are almost entirely associated with the monomer unit; especially so, given that both PPO_{70} and PPO_{17} are produced using the same monomer (propylene oxide).

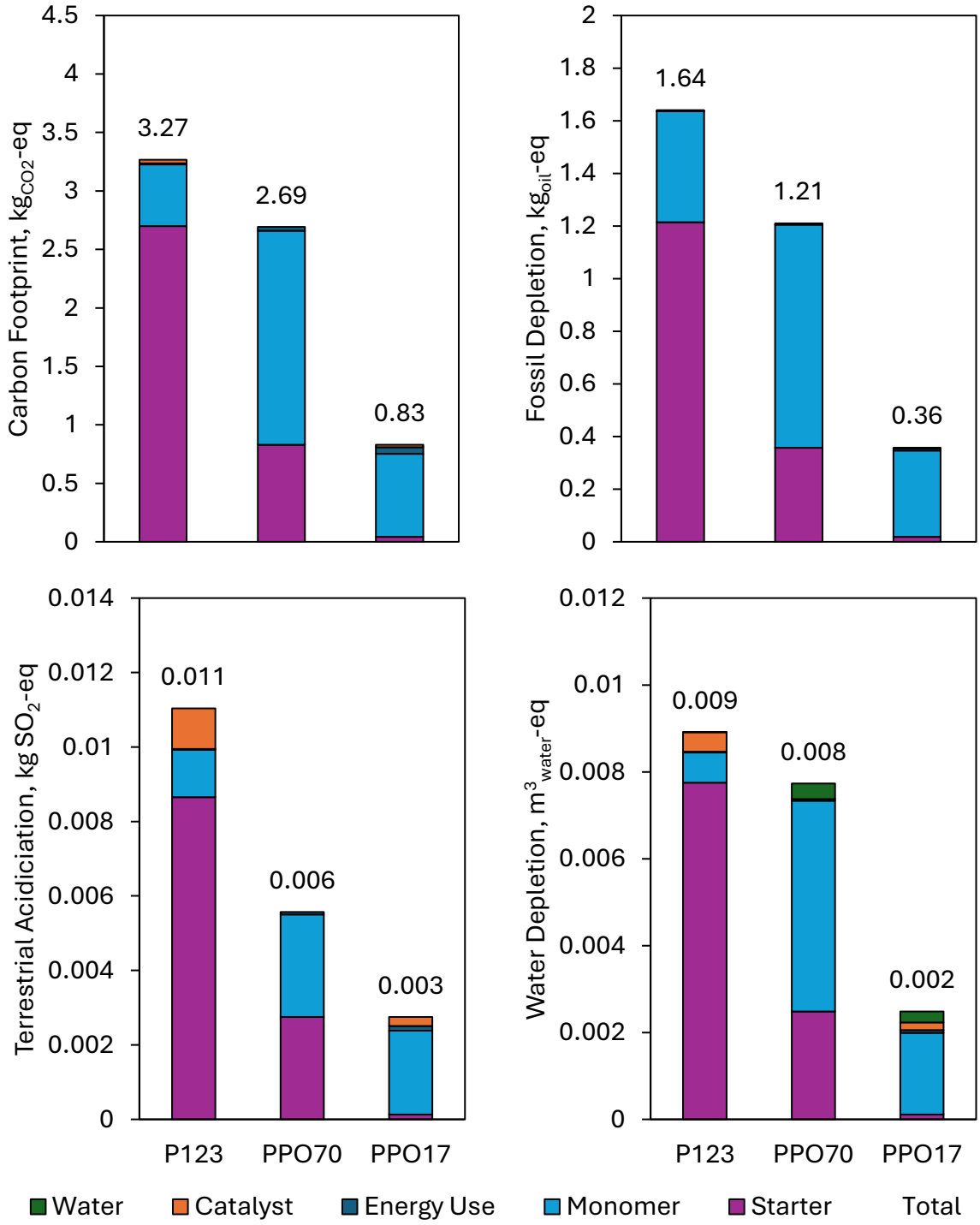


Figure 5.10: Environmental impact predictions for 1kg of Pluronic 123 (P123) and associated amount of PPO_{70} and PPO_{17} block polymers required in producing 1kg of the Pluronic 123 product.

Consequently, the observed importance of monomer use in PPO_{70} production, and the relatively larger contribution of PPO_{70} processing to P_{123} should not be considered as

conclusive evidence of harm associated with the DMC process generally. This is because the amount of monomer use associated in the PPO_{70} stage is itself dependent on the molecular weight of the PPO_{17} starter produced in the first stage.

In fact, having accounted for dependence (of the DMC processing stage impact) on polymerisation starter size this suggests that the impact associated with PPO_{70} production is itself somewhat dependent on the decision of the size of PPO product to use as a starter.

Further discussion of the practical upper limit of PPO block polymer production associated with KOH are considered outside the scope of this work. However, it is worth noting that there is practical limitation to size of block that may be produced by in the initial stage – as well as limitations of minimum starter size.

Importance of DMC vs KOH catalysis stage

Results in Figure 5.11 illustrate impact predictions associated with producing P_{123} according to three-step (KOH-DMC-KOH) and two-step (KOH-KOH) catalysis pathways. This is provided based on general scientific interest, and likelihood of production by the two-stage method should be considered given practical challenges associated with allyl group formation (KOH method), and catalyst deactivation with small molecule starts (DMC method).

Results in Figure 5.11 demonstrate a consistently higher impact prediction of the two-stage method for the impact factors considered. This is most pronounced in the case of terrestrial acidification – where impact of the two-stage method is roughly 33% larger than the three-stage method. For other impact factors, differences are markedly lower, averaging a difference of less the 10%.

Differences in impact of both methods must originate from differences in process of producing PPO_{70} block polymer modelled within respective life cycle inventory. This amounts to differences in assumed mass efficiency of polymerisation (95% yield for two-stage, 100% for DMC), and differences in scope of catalysis use (DMC catalyst not accounted for within the three-stage process).

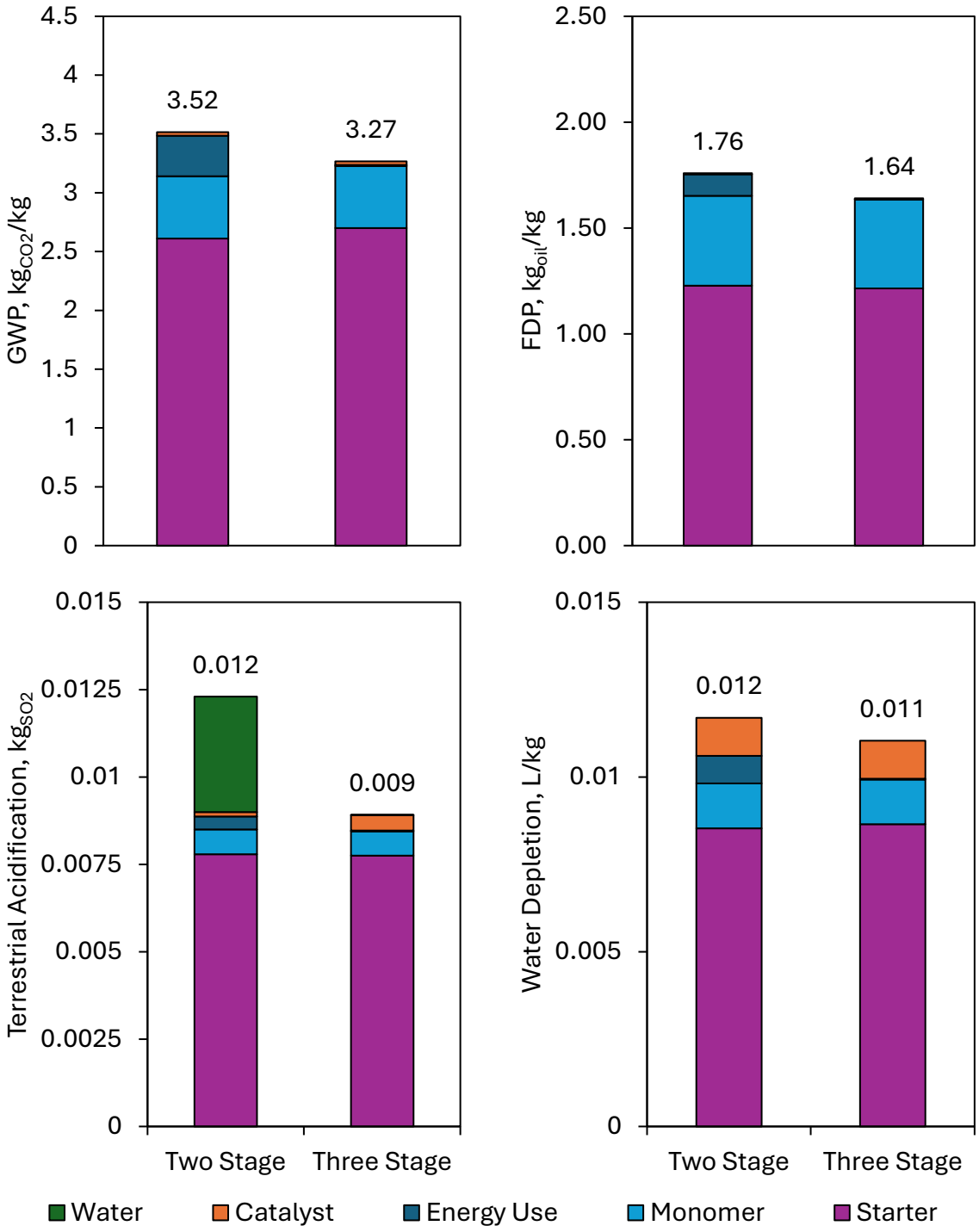


Figure 5.11: Environmental impact predictions for 1kg of Pluronic 123 produced by the traditional three-stage method and hypothetical two stage method.

Importantly, the similarity in impacts reported reflect the importance of reagent life cycle on overall impact of the P_{123} products. This can be interpreted as suggesting the strong governance of reagent use (starter and monomer materials) in the overall impact of P_{123} - agreeing with general trends discussed above.

Nonetheless, the similarity of impact predictions reported in Figure 5.11 likely mean that a discernible significant difference cannot be drawn between the two methods. This is due to relatively high uncertainty typically associated with life cycle inventory modelling in general – and especially so given the approximate nature of methods used to generate life cycle inventories in the case of this work. The most plausible major conclusion to be drawn from the results is therefore that the impact predictions appear to suggest that us of the three-stage cycle does not carry with it significantly larger impacts than could be achieved by two-stage methods after discounting for practical limitations for the latter) - at least with regards to impact factors considered. This must be qualified as a preliminary observation, which may also not carry well to extrapolation for other impact factors – for example, metal depletion.

Finally, it must be noted that the most rigorous life cycle model (KOH-DMC-KOH method) reported in this work is itself still a simplification compared to the real-life cycle associated with true commercial production of Pluronic 123. This is because of the relatively restrictive scope considered in generating mass and energy balances for a life cycle based on chemical engineering process simulation alone. Additionally, the model predictions also include additional sources of uncertainty associated with broad contextual factors such as variability in technologies used and location-specific differences.

Future work could benefit on further refinement of mass and energy balances associated with real-world production of Pluronic 123. Ideally, this should include uncertainties surrounding technological improvements, operational (i.e. beyond chemical process) efficiencies, and the geography of production. For true accuracy, this would require information provided by product manufacturers (e.g. BASF), none of which were contacted directly for comment and/or collaboration during this work.

5.3.2. Environmental Impact of Emerging Sol-Gel Silica Products

Results in Figure 5.12 show impact predictions associated with the production of 1 kilogram of commercially produced precipitated silica and silica produced by bioinspired, SBA, MCM and Stöber methods. Results illustrate a remarkably consistent relationship between processing method and magnitude of impact prediction. Specifically, impacts tend to follow the general rank of precipitated < bioinspired < SBA < MCM < Stöber.

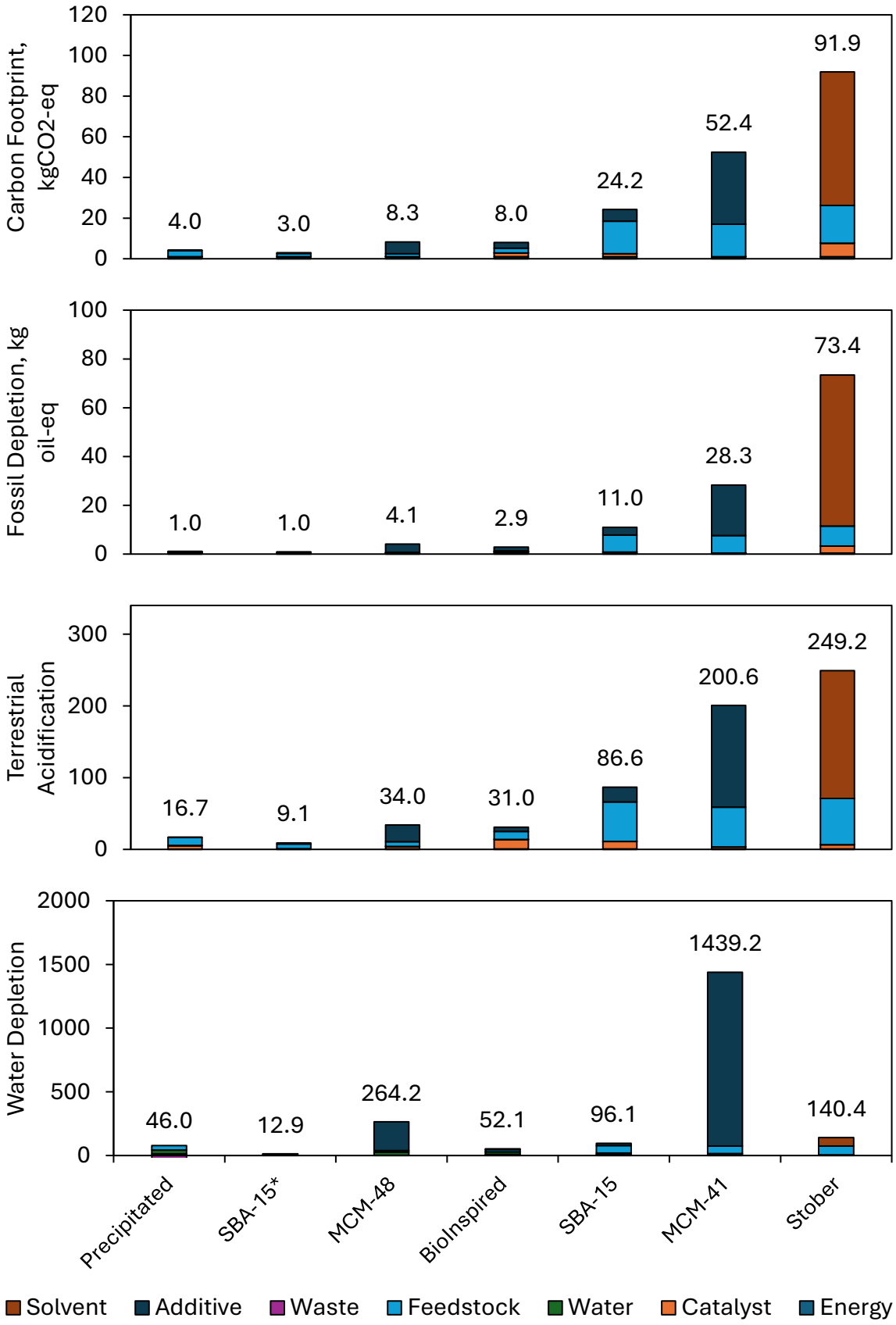


Figure 5.12: Impact predictions for 1 kg of silica powder produced according to various synthesis methods.

Transferability of Findings

Findings for environmental impact associated with each method must not be used to produce sweeping generalisations regarding wet processing methods. This is particularly so for generalised comparison the ordered mesoporous silica synthesis methods (e.g. SBA and MCM) due to variability arising from inclusion of additional chemicals and varying solvent use. For example, use of organic solvents as swelling agents is common, but not considered explicitly within impact predictions. This demonstrates a need for more research into specific implementations of order mesoporous silica synthesis methods in the future – particularly for consideration of reduced additive and solvent use when producing silica substrates according to the emerging methods.

5.4. Discussion

5.4.1. Silica Reagent Choice

Findings for silica produced using sodium silicate and alkoxy silicates shows a consistent trend of increased impact of methods using alkoxysilanes (specifically TEOS) as a silica reagent instead of sodium silicate. In the case of the SBA-15 methods, this corresponds to a reduction in carbon footprint of 88%, whereas a reduction of 84% is observed when comparing the MCM-48 (sodium silicate derived) and MCM-41 (TEOS derived) products.

In the case of SBA-15 products, an interesting feature is that in both cases, reductions in overall impact come not only from direct impact reductions associated with the silica reagent alone, but also from the amount of additive used too. Specifically, the carbon footprint contribution of Pluronic 123 when using for sodium silicate as a silica precursor is only 0.45 kg_{CO2} equivalent, compared to 5.8 kg_{CO2}-eq in the product produced using TEOS.

A similar correlation of silica reagent choice and additive impact contribution is also visible when comparing the MCM products. Particularly, a carbon footprint contribution of 35.4 kg_{CO2} equivalent is observed for the TEOS-derived MCM-41 product while a contribution of only 5.8 kg_{CO2} is found for the sodium silicate-derived MCM-48 product.

Given the limited scope of inventories considered in this work, it is hard to determine whether these differences reflect an inherent causal relationship or not. For example, observed differences may simply represent reliance on life cycle inventories for an implementation

which featured excessive use of templating. Further research of a broad range of implementations of products derived by the SBA and MCM methods using both alkoxy silicate and sodium silicate precursors is therefore required before making stronger conclusions.

5.4.2. Energy use

A decision was made during life cycle inventory modelling to assume a consistent energy use of 19.5 MJ/kg associated with the drying of each product. This is taken from energy use reported based on an average of silica produced by sol-gel processing in the EU-15 industrial region [82]. Whereas this provides a reasonable estimate given lacking information, potential sources of accuracy inevitably arise from its use.

Firstly, differences in pore size may cause differences in energy use required for drying. For example, larger pores can facilitate lower resistance to the drying process by providing less resistance to the transport of liquid from within pores to external surfaces. Conversely, the presence of smaller pore sizes may lead to increased resistance to evaporation due to contribution of capillary forces.

Secondly, differences in solvent use may cause the energy estimate used (i.e. 19.5 kJ/kg) to be larger than required. This is because the amount used is based on the drying of commercial silicas produced in aqueous solution – and therefore the drying of water-wet silica. This is important as the heat of vaporisation of water (2140 kJ/kg), is around double the values typical for nonpolar organic solvents – such as those typically used in emerging methods, including in solvent washing.

Despite the factors considered above, it appears as a consistent trend across all impact factors that contributions of energy use assumed in this work are relatively insignificant. This is also consistent with trends found in Chapter 4, which suggested that energy use was of secondary importance in governing the impact of commercial silicas when compared to silica precursor choice. Consequently, though it is right to consider and refine modelling of energy use across the emerging processes from the perspective of data quality, findings suggest that the sensitivity of reports to further refined values are likely to be of low significance.

5.4.3. Additive Choice

Having highlighted issues in reagent choice and relative low importance of energy use, a further question stands regarding the importance of additive choice. This is a more difficult

area to consider given the effect of additive choice on mechanisms underlying porosity control when using the merging methods. Nonetheless, comparison of additives used is important given inherent differences in the consequence of producing and using each additive (e.g. refer to discussion of previously discussed in Chapter 2, Section 6).

Regarding water depletion, it appears additive choice may have a particularly significant effect through the large contributions that quaternary ammonium salts provide to MCM products considered - a feature which is consistent irrespective of silica reagent choice. This must link to inherent impact associated with the CTAC product, as well as trends in the amount of CTAC used by the MCM methods.

5.4.4. Functional Unit

A major challenge in the environmental impact assessment of mesoporous silica particles considered at this stage is differences in the true functional unit associated with their use as a product. This can be demonstrated even for products within the same methodological family (e.g. SBA or MCM), which can exhibit varying pore structures-based solution conditions despite using the same surfactant template. A more use-case specific functional unit is therefore really required to enable comparing the environmental impact of each product in a fair way. This is extremely challenging given the near infinite scope of use-cases in which the silica substrates considered could be applied. Consequently, comparison on this basis is considered outside of the scope of this current work. Nonetheless, results presented provide clear foundation from which future authors may begin to assess the performance of their novel silica substrate processing approach through the lens of life cycle impacts.

5.4.5. Waste Production

Waste production has not been considered explicitly in any of the models. The extent to which this affects accuracy of impact predictions is hard to quantify. Lack of consideration for wastewater treatment may cause water depletion to be artificially higher.

Given the aqueous basis of sol-gel processing, a major area of concern for waste generation is particularly relating to wastewater. It is likely, given trends in precipitated commercial silica production, that additional material use for pH modification of water is also required [82].

Methods for the treatment of wastewater associated with differing methods require further consideration that are considered outside of the scope of this work given lack of existing

environmental impact assessment information in the literature. Nonetheless, methods for treatment may vary dependent on processes.

Issues with the handling of additives and their fate in wastewater are also of particular interest. For example, it is known that quaternary ammonium salts (used in MCM methods) may be incompletely treated by wastewater methods, leading to their persistence and sedimentation in natural waters [160].

For MCM methods, the QACs used are water soluble. Thus, it is likely that commercial processes may favour water solvent use over organic solvent during washing to minimize problems for handling, processing and toxicity [82].

For SBA methods, poloxamer products used (e.g. P_{123}) are typically water insoluble.

5.4.6. Shortcomings of Inventory Models

It must be reiterated that decisions made during LCI modelling lead to the need for significant caveats to surrounding the interpretation of LCIA results. This includes the use of process-simulation as a source for material inventory, as well as decisions made in excluding the post-synthesis solvent washing stage associated with production of silica products.

The use of process simulation as a source of material and energy use estimates undoubtedly leads to inaccuracies in LCI models compared to true process implementations. This comes from multiple factors, including 1) the simplification of reactions and impurities present in the model (when compared to real-world processes), and 2) the lack of consideration for energy of filtration in relevant processes.

The decision to exclude post-synthesis washing from life cycle inventory models also cannot be understated. Having failed to consider the contribution of this stage may significantly affect the extent to which reported environmental impact correlate with the true impact of a dry silica product produced by each method. Nonetheless, exclusion of the section has been seen as necessary in the case of this work particularly due to the variability of washing method reported throughout literature as well as excessive use.

The potential for the solvent washing stage to skew results derives from the excessive solvent use associated with nanoparticle synthesis research. It is not uncommon for research to report solvent washing ratios on the scale of use of litters of solvent per gram of powder [161]. This

has led as much as a 400-fold increases in the E-Factor (waste to product mass ratio) for solvent washing of metal oxide nanoparticles as reported in literature [24]. Moreover, choice of solvent varies widely across research from use of aqueous and/or organic systems.

While including solvent washing in the LCI scope may make the results of this work appear more comprehensive, it may significantly affect the true reliability of findings given the relatively low sample size considered of process embodiments considered.

Consequently, it is believed that results shown represent the most appropriate development in understanding that could be presented to develop a better understanding for the general issues associated with production of silica by any of the emerging sol-gel methods considered. This is especially so considered within the context of current understanding for life cycle inventory modelling of the emerging sol-gel methods for silica synthesis.

5.4.7. Uncertainty Modelling

Section 5.4.6 highlights several sources of uncertainty in the inaccuracy of environmental impact predictions relative to the true the environmental impact of the products being considered. This leads naturally to the potential to further model the uncertainty associated with impact predictions – for example, as has been done in Chapter 4. Indeed, doing so would be valuable in attaining better understanding for the extent to which impacts predicted for individual products can be considered significantly different from one another (e.g. as previously done for commercial products in Chapter 4). Despite this, uncertainty modelling is not considered in this section; this is done for the following reasons.

Firstly, as outlined in Section 5.4.6, multiple aspects of material and energy use have been omitted from current LCIs. As discussed in Section 5.4.6, this is because information available within literature reflects unrealistic amounts of material use, low Technological Readiness Level of emerging methods being considered in this chapter, which may act to seriously bias the reported impact of products if included.

By not accounting for material use it becomes difficult to apply modern methods of LCA uncertainty modelling (e.g. data quality pedigree matrix method, see Chapter 4). This is because uncertainty is modelled by proxy through the definition of uncertainty in amount of substance use associated with each activity within a life cycle inventory. Moreover, methods for defining uncertainty associated with the require a reasonable estimate for

Consequently, reporting of uncertainty associated with models as they currently stand could be misleading to the reader.

For uncertainty to be included in future work, it is suggested that additional understanding is required for realistic information on the amount of material used for missing materials within LCIs. For these to be reasonable, the amount must reflect values that are both technologically possible (e.g. solvent use capable of adequate solvation) and economically feasible (e.g. capable of producing a competitive market product at profit). This also requires consideration for information that is currently missing from inventories by choice – e.g. regarding solvent use during powder washing.

Secondly, the computational resource required to investigate the products (and their pair wise comparisons) is likely to be significant. For example, modelling of uncertainty reported in Chapter 4 typically took computational times on the order of days per dataset (for 150,000 Monte Carlo samples per dataset). Given shortcomings of uncertainty methods available, this significantly reduces the reasonableness, and value of carrying out uncertainty modelling on datasets reported in this work.

Conclusions

Research in this chapter has aimed to develop a better understanding for the environmental impact of producing silica substrates according to emerging sol-gel methods. This has been done in three stages: 1) estimation of mass and energy use associated with additives used in emerging methods, 2) life cycle assessment of additives, and 3) life cycle assessment of silica produced according to emerging sol-gel methods.

Owing to the scale of information missing on life cycle, this included the following main objectives:

1. To develop life cycle inventory models for materials used in advanced synthesis that are currently missing.
2. To provide environmental impact estimates for the advanced methods.
3. To assess the extent of environmental impact associated between choice in use of traditional water glass vs. common alkoxide methods.
4. To compare impact to commercial methods.

Results of the work have led to multiple important findings.

Firstly, results indicate an importance of silica precursor choice on the impact of products across methods – indicating agreement with observations made previously for substrates produced according to commercial methods (see Chapter 4). This is despite additional material use associated with organic additives in these methods, further demonstrating the importance of precursor choice.

Secondly, results also suggest precursor choice may also increase impact through necessitating the use of additional auxiliary materials (e.g. solvent and organic templates). Nonetheless, further work is required to provide conclusive evidence of this representing a causal link.

Thirdly, the impact of substrates produced according to the bio-inspired synthesis method is also found to inherit a distinct impact profile arising from a large amount of acid catalyst used. This is interesting in reiterating the importance of minimising the use of all materials associated with the production of silica substrates where possible.

Finally, the impact of silicas produced according to emerging methods using sodium silicate substrates are found to have environmental profiles like that of precipitated silica produced commercially for the impact categories considered. This is significant in suggesting the potential for using emerging methods to produce silica substrates having impacts that are competitive with those produced commercially – if designed under the right conditions. Nonetheless, further work is required to validate this.

Findings of this work are novel given the lack of information currently available on the environmental impacts of organic templates (CTAC and Pluronic 123) as well as silica produced from emerging sol-gel methods (e.g. MCM, SBA and BI-type silica). Information in the work may be of interest to practitioners in multiple fields where use of sustainably designed silica-based powders and/or adsorbent products is of interest.

6. Silane Coupling Agents

6.1. Introduction

6.1.1. Overview

Findings in Chapter 4 and 5 have highlighted the importance of reagent material choice in defining the environmental impact of silica substrates. This includes for substrates produced by both commercial and emerging methods. However, these results are for silica substrates without any surface chemistry modifications.

When designed for pollution abatement, many silica-based adsorbent materials (SBAM) include surface chemistry modifications to enhance their performance. Nonetheless, doing so requires the inclusion of an additional manufacturing stage within the SBAM product life cycle. Consequently, the impact of surface modification must also be included within the life cycle assessment to accurately predict the impact of many of the SBAMs being developed for real-world applications.

One way in which the surface chemistry of SBAMs is routinely modified is by silanization (see Chapter 2, Section 2.7). Silanization is a reaction-based processing method in which new surface chemistries are imparted by covalently bonding specialized chemicals to the SBAM surface. This is often achieved using a family of materials known as silane coupling agents (SCAs) as silanization reagents [137].

At present, very little is known about the true impact of SCAs, or the process of SBAM surface silanization. This is reflected in the simplicity of LCA models being used to approximate their life cycle in literature. For example, multiple authors have modelled the impact of 3-aminopropyltriethoxysilane (APTES) - the most common SCA product produced commercially [162] - based on reaction stoichiometries alone [140, 163]. Similarly, others have approximated the impact of APTES using alkoxy-silicate materials like tetraethyl orthosilicate as model proxies [144].

This is despite hundreds of distinct SCAs being produced commercially (for example, see [127]).

Three main reasons may explain why there is a lack of adequate impact prediction models for commercial SCA products.

Firstly, SCAs are relatively low volume, specialty chemicals – leading them to not yet be included in common LCA databases. Secondly, the chemical synthesis of many SCAs is relatively complex (see Chapter 2, Section 2.7), with a variety of chemical moieties being covered under the "SCA" umbrella term; this causes a large range of methods exist by which individual SCA products may be produced. Thirdly, there is also a lack of adequate LCA information for the materials used to produce SCAs; particularly, there is relatively little information on the LCA of trichlorosilane (TCS) - a platform chemical from which the majority of SCAs are currently produced.

In the case of TCS, a lack of adequate LCA models may be explained by the fact that TCS can be produced by multiple methods. This includes: 1) dedicated production of TCS via direct chlorination of silicon metal, and 2) production of TCS as a co-product of manufacturing high purity silicon metals via the Siemens process. This raises questions regarding the sensitivity of life cycle to the TCS manufacturing history/source.

Significant improvements to life cycle understanding are therefore required to enable accurate LCA of silanization-modified SBAMs. This includes the need, firstly, for improved life cycle understanding regarding: 1) the processes used to manufacture relevant SCAs used in silanization, and 2) the production of TCS used as a platform chemical for SCA manufacture.

6.1.2. Aims and Objectives

This chapter aims to address the current lack of understanding for the impact of producing SCA materials. This is done by investigating the production of two SCA products as a case-study: 3-aminopropyltrimethoxysilane (APTES), and octyl trimethoxysilane (OTMS). These products are considered due to their commercial scale production [162] and relevance to research ongoing within the Heng research group [164, 165] respectively; to the best of the authors knowledge, no rigorous summary of energy and material use has been reported for either product to date. Research is therefore carried out with the following objectives:

1. To estimate mass and energy use associated with producing the TCS, APTES and OTMS and their chemical intermediates.
2. To create life cycle inventory models for producing silane products.

3. To predict environmental impacts associated with producing each product.
4. To identify major factors contributing to the impact of the SCA products.
5. To compare the impacts of TCS and SCA products considered.

6.2. Methods

Multiple modelling methods have been used in this chapter as part of assessing the environmental impacts of the APTES and OTMS SCAs. As shown in Figure 6.1, the approach is split into three phases reflecting: 1) process modelling, 2) inventory modelling, and 3) impact assessment. Further information on the approaches taken in each stage is provided in the following subsections.

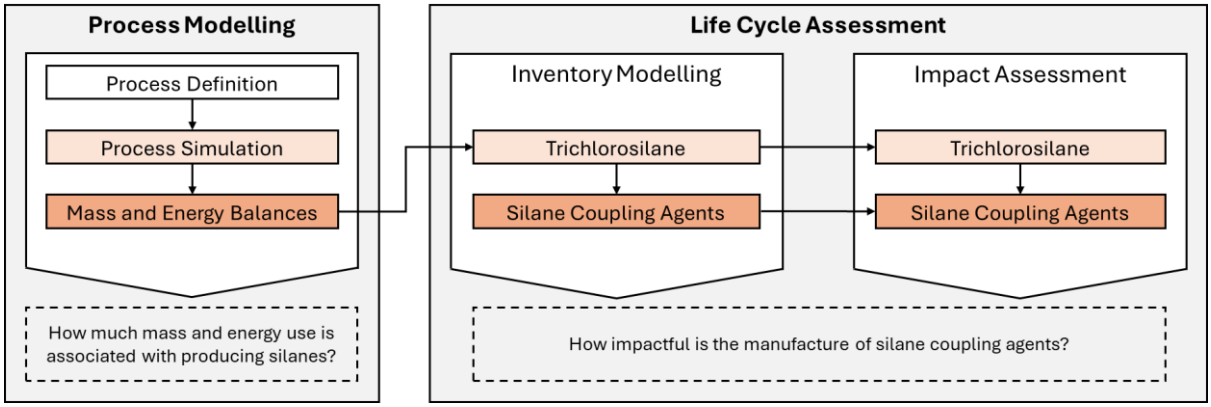


Figure 6.1: Schematic workflow of methods used to investigate the environmental impact of silane coupling agents.

6.2.1. Process Modelling

Process modelling has been used to estimate material and energy use associated with the manufacture of TCS, APTES, OTMS and their associated chemical intermediates. In all cases, this was done using the Aspen Plus V11 software to simulate processing network and equipment operating conditions based on art described within patent literature. In all cases, thermodynamic modelling of vapor and liquid equilibria has been done using the NRTL-RK method.

Process optimization was considered when modelling trichlorosilane, but not for APTES or OTMS – owing to the multi-stage processing that they require, and complexity that this entails. Further information on the modelling of each process is provided in the following subsections.

Trichlorosilane

Modelling Assumptions

Trichlorosilane production has been modelled according to the method of reacting silicon metal with hydrogen chloride gas (i.e. direct chlorination), followed by separation of chlorosilane products via distillation. This follows approaches equivalent to that reported in commercial Siemens process in patent literature [121].

Trichlorosilane, hydrogen and silicon tetrachloride (STC) are assumed to be produced according to reaction stoichiometry shown in Equation 6.1 and 6.2. Reaction conditions are taken as 260 C and 1.5 bar based on the recommendations of [166], based on interpretation of original results of the patent of Kotzsch *et al*. [167].

$$\mathrm{Si} + 3\mathrm{HCl} \rightarrow \mathrm{HSiCl_3} + \mathrm{H_2} \tag{6.1}$$

$$\mathrm{Si} + 4\mathrm{HCl} \rightarrow \mathrm{SiCl_4} + 2\mathrm{H_2} \tag{6.2}$$

Purification of the TCS and STC products has been assumed to occur by flash condensation of the reactor effluent (separating hydrogen chloride and hydrogen as gas), followed by distillation of the resulting chlorosilane mixture. Design of the flash separation and distillation equipment (including operating conditions) has been handled by process optimization; further information on optimization is provided below.

Further information on processing conditions and assumptions surrounding the process are shown in Appendix D:.

Process Costing

Costing calculations have been carried out to ensure process modelling results reflect economically feasible design and operating conditions. This includes consideration for capital and operational costs of the process. Further information on the calculation of each aspect is provided in the following subsections.

Capital Cost Calculations

Capital costing of process equipment was done using the method of Sinnott and Towler [168] for equipment purchase cost and converted to bare module costs via the method of Guthrie [169] using factors reported by van Amsterdam [170]. This is described mathematically as

shown in Equations 6.3 and 6.4. Further description of the equipment design and costing methods used are available in Appendix D.

$$CAPEX_{bm} = F_{bm} CAPEX_{purchase} \tag{6.3}$$

Where $CAPEX_{bm}$ is the capital cost associated for a unit of equipment on a bare module basis ($), $CAPEX_{purchase}$ is the capital cost of a unit on an as-purchased based ($), F_{bm} is a conversion factor used to account for costs associated with converting a purchased unit into a bare module unit (no units).

$$CAPEX_{purchase} = a + bS^n \tag{6.4}$$

Where a and b are cost correlation parameters taken from Sinnott and Towler [168] ($), S is the capacity of the unit under consideration (units vary depending on equipment), and n is an additional scaling factor parameter taken from Sinnott and Towler [168]. A summary of all data used for capital costing is provided in Table 6.1 Further information on values of cost parameters used is provided in Appendix D.

Table 6.1: Sources of cost data used in calculation of capital costs when modelling the production of trichlorosilane

Data Type	Calculation Method	Data Source	Ref
Purchase Cost	Cost Correlation	Sinnott and Towler	[168]
Bare Module Cost	Cost Scaling	van Amsterdam	[170]
Equipment Capacity, S	Engineering Design Calculations	Process simulation	N/a
CEPCI Index	N/a	Online repository	[171]

All costs were inflated to account for prices in the year 2022 based on the value of the CEPCI index [171] .

Operational Cost Calculations

Operational cost calculations were carried out using the method of Ulrich and Vasudevan [172] as shown in Equation 6.5.

$$OPEX_u = Q_u\left(aI_{CECPI} + bC_{sf}\right) \tag{6.5}$$

Where a and b are cost correlation factors specific to utility u as reported by Ulrich and Vasudevan [172] ($/amount, with amount units varying dependent on the utility considered), Q_u is the amount of utility required per year of operation (amount/year, with amount units

varying dependent on the utility considered) I_{CECPI} is the value of the CEPCI index for the year of interest, and C_{sf} is the cost of the source fuel being considered.

For simplicity, the value of C_{sf} was taken as the median electricity price for the IEA [173] ($/GJ). The value of I_{CECPI} was taken as 813 to reflect production in the year 2022. A summary of relevant values is provided in Table 6.2.

Table 6.2: Sources of cost data used in calculation of capital costs when modelling the production of trichlorosilane

Data Type	Value(s)	Calculation Method	Data Source	Ref
Utility OPEX, $OPEX_u$ ($/yr)	*See Appendix D*	Cost Correlation	Ulrich and Vasudevan Book	[172]
Amount of Utility, Q_u (amount/year)	Process-dependent	Thermodynamic Calculations	Process simulation	-
Electricity Source Cost, C_{sf} ($/kWh)	0.20	N/a	IEA Median Electricity Cost	[173]
CEPCI Index (-)	813	N/a	Online repository	[171]

Total operational time of the process was assumed to be 8000 hours per year – representing rough assumed downtime period of 1 month per year; this was decided based on reactor maintenance requirements described in patent [174].

Process Optimization

Optimization was carried out while modelling the production of trichlorosilane with the aim of finding conditions that maximise the total annualized profit associated with the entire modelled process – i.e. including net profit of the entire plant, including combined revenue of the trichlorosilane and silicon tetrachloride co-product (where relevant). This is defined based on total annualised profit, total annualized revenue, total annualized cost in Equations 6.6 and 6.7.

$$TAP = TAR - TAC \tag{6.6}$$

$$TAR = \sum_{p=1}^{n} \dot{m}_p c_p \tag{6.7}$$

Where TAP is the total annualized profit ($/yr), TAR is the total annualized revenue ($/yr), TAC is the total annualized cost ($/yr), $\dot{m}_p$ is the mass production quantity (kg/yr), and c_p is

the sale price ($/kg) of a product of product, p. The sale prices of TCS and STC were taken to be 2.00 and 0.98 $/kg respectively.

This was formulated subject to the production of TCS and STC at a purity of 99 wt% and considering a total of 7 operating conditions as decision variables. These were: 1) flash condenser temperature, 2) flash condenser pressure, 3) number of distillation stages, 4) distillation column feed stage position, 5) distillation column reflux ratio (mass basis), and 6) distillation column boil-to-feed ratio (mass basis). Additional equality constraints were included to enforce reasonable limitations to sensible operating ranges for individual equipment (see Equations 6.10 to 6.14). A summary of the objective formulation is provided in Equations 6.8 to 6.14.

$$(Max)TAP = f\left(T_F, P_F, RR, P_t, N_s, N_f\right) \tag{6.8}$$

$$s.t. \qquad y_{TCS}, y_{STC} = 99 \text{ wt\%} \tag{6.9}$$

$$-40 \leq T_F \leq 0 \tag{6.10}$$

$$1.1 \leq P_F \leq 4.5 \tag{6.11}$$

$$1.1 \leq P_t \leq 8 \tag{6.12}$$

$$3 \leq N_s \leq 100 \tag{6.13}$$

$$2 \leq N_f \leq N_s \tag{6.14}$$

Where T_F is temperature of the flash condenser (C), P_F is operating pressure of the flash condenser (bar), RR is the column reflux ratio (mass basis), P_t is the pressure at the top of the distillation column (bar), N_s is the number of stages in the column (no units), N_f is the distillation column feed stage (no units), and y_{TCS} and y_{STC} are the purity of TCS and STC (wt%). The final inequality constraint can be interpreted as enforcing the logical requirement of feed material entering the distillation column at a stage above the reboiler unit (which is represented as column stage 1 in the underlying distillation column model).

In all cases, the optimization is limited to consider costing based on the aggregation of individual units present within the simulation – i.e. consideration for process intensification/integration is not considered.

Optimization Algorithm

Solution of the optimization formulation was carried out using a hybrid algorithm developed in-house. The algorithm uses a bi-level optimization design to maximise the proportion of optimizer evaluation calls which resulted in feasible design simulation.

The upper level is designed to handle the selection of new trial conditions for the entire process (see Equation 6.8). A genetic algorithm (differential evolution) approach was chosen for its advantage of being able handle discontinuous, multi-modal problems [175], which may be expected in chemical process design optimization.

The lower level then refines trial conditions of the upper level to ensure satisfaction of product quality constraints specified in Equation 6.9. This is done by refining the values of column pressure, P_t, and reflux ratio, RR, based on a gradient based solver present within the Aspen Plus distillation column model.

The solver was set to run for a total of 25 generations (i.e. 5000 evaluations). Further information on the entire optimization algorithm is provided in Appendix D.

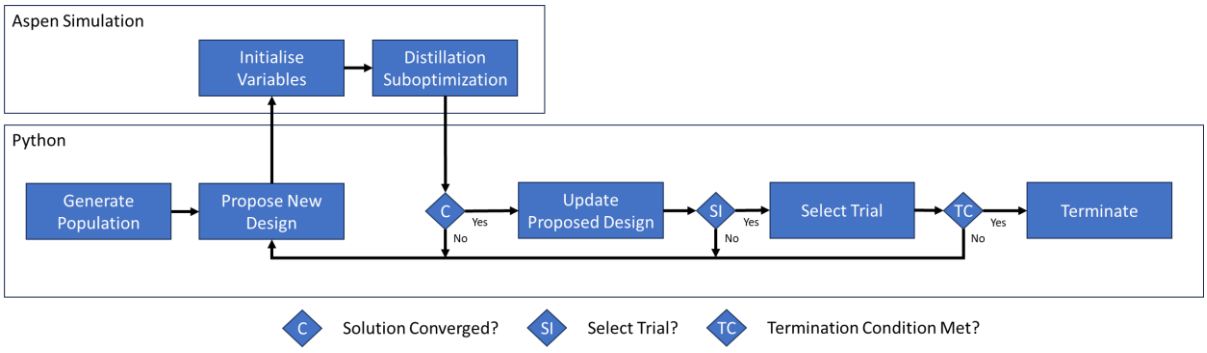


Figure 6.2: Schematic representation of optimization algorithm used during process design optimization.

Aminopropyltriethoxysilane

APTES production was modelled according to the commercial method of hydrosilylation of TCS with allylchloride (AC), followed by the ethoxylation 3-chloropropyltrichlorosilane (CPTCS), and ammoniation of 3-chloropropyltriethoxysilane (CPTES). These steps were assumed to represent three separate processing stages based on typical art reported in patent literature – e.g. [176-178]. A summary of process flow diagrams associated with each of the stages is shown in Figure 6.3. The modelling of each stage was considered independently.

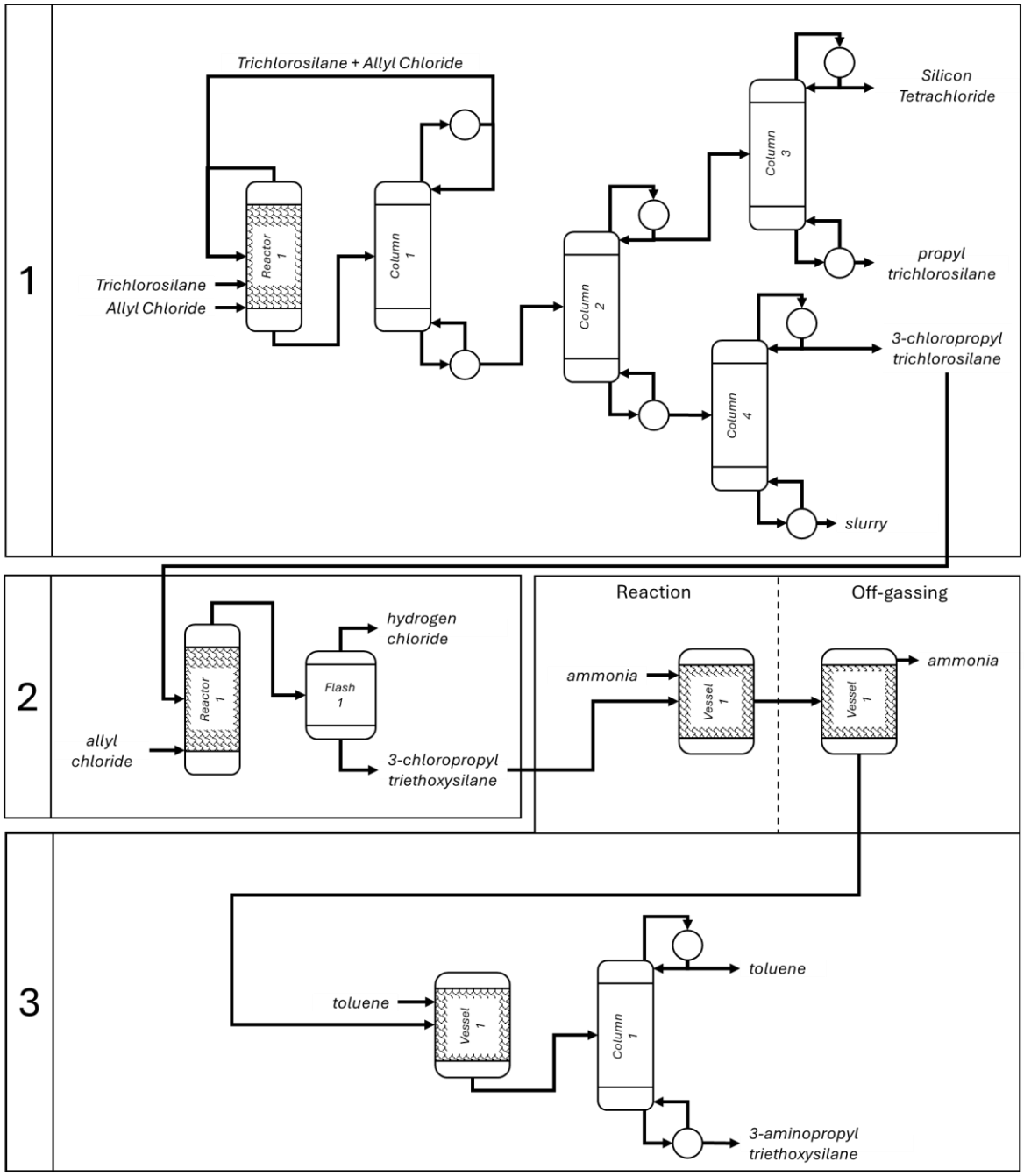


Figure 6.3: Overview of process models used to estimate mass and energy use of producing 3-aminopropyltriethoxysilane via formation of 3-chloropropyltrichlorosilane (top), 3-chloropropyltriethoxysilame (middle), and amino-propyltriethoxysilane (bottom).

Production of 3-chloropropyltrichlorosilane

The production of CPTCS has been modelled according to a continuous process of hydrosilylation of TCS with AC reported by a patent of Evonik Operations [176]. Reactions producing products and by-products were modelled according to the stoichiometries shown in Equation 6.15 and 6.16.

$$C_3H_5Cl + Cl_3SiH \rightarrow Cl_3Si(C_3H_6Cl) \quad (6.15)$$

$$C_3H_5Cl + Cl_3SiH \rightarrow Cl_3Si(C_3H_7) + SiCl_4 \quad (6.16)$$

Further information on all conditions associated with production are available in Appendix E.

Production of 3-chloropropyltriethoxysilane

The production of CPTES has been modelled according to a continuous process of CPTCS ethoxylation reported in a patent of Wacker Chemie [177]. This includes assumption of only the main product reaction occurring according to the reaction stoichiometry shown in Equation 6.17.

$$Cl_3Si(C_3H_6Cl) + 3C_2H_5OH \rightarrow (C_2C_5O)_3Si(C_3H_6Cl) + 3HCl \quad (6.17)$$

Further information on all conditions associated with production are available in Appendix E.

Production of 3-aminopropyltriethoxysilane

The production of APTES has been modelled according to the stepwise batch process described by a patent of Evonik Operations [178]. This involved ammoniation reaction forming APTES and ammonium chloride salt ($NH_4^+Cl^-$), as shown in Equation 6.18.

$$(C_2C_5O)_3Si(C_3H_6Cl) + 2NH_3 \rightarrow (C_2C_5O)_3Si(C_3H_6NH_2) + NH_4^+Cl^- \quad (6.18)$$

In all cases, reagent inputs to each process were assumed to be completely pure. Further information on all conditions associated with production are available in Appendix E.

Octyltrimethoxysilane

OTMS production was modelled according to the commercial method of hydrosilylation TCS with 1-octene to produce octyltrichlorosilane (OTCS), followed by methoxylation to produce octyltrimethoxysilane (OTMS) - as shown in Figure 6.4. These steps were assumed to represent three separate processing stages based on typical art reported in patent literature – e.g. [124] and [131]. A summary of process flow diagrams associated with each of the stages is shown in Figure 6.4. The modelling of each stage was considered independently.

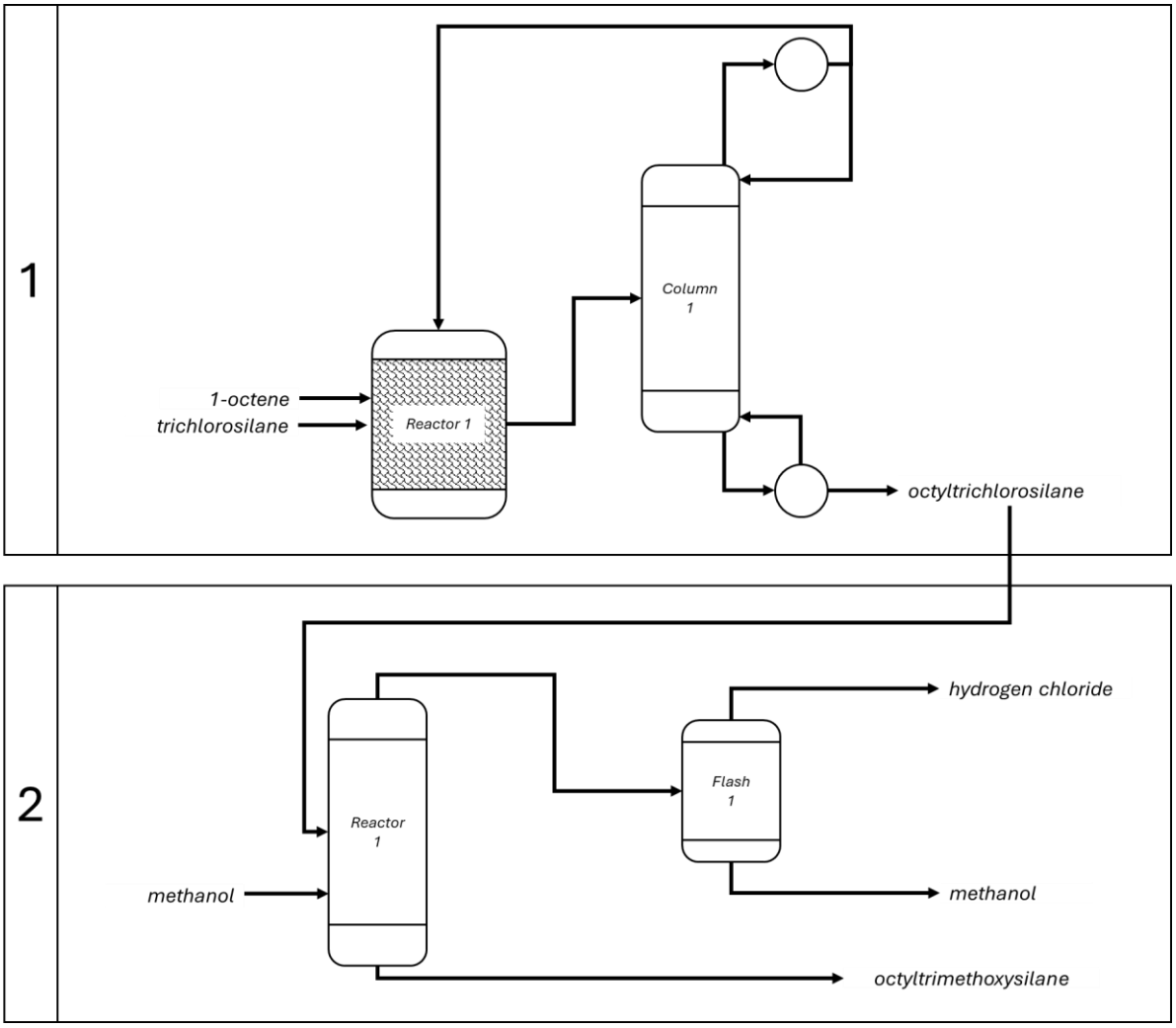


Figure 6.4: Overview of process models used to estimate mass and energy use of producing octyltrichlorosilane (OTCS, top), octyltrimethoxysilane (OTMS, bottom).

Production of octyltrichlorosilane

The production of OTCS has been modelled according to the continuous hydrosilylation method described by the patent of Tachikawa and Takei [131]. Only the reaction producing the OTCS product according to stoichiometry in Equation 6.19 was considered.

$$C_8H_{21} + Cl_3SiH \rightarrow Cl_3Si(C_8H_{21}) \quad (6.19)$$

The OTCS products was assumed to be separated via distillation and excess heat was used in process integration. Further information on all conditions associated with production are available in Appendix F.

Production of octyltrimethoxysilane

The production of OTCS has been modelled according to the continuous alkoxylation method described by in patent [124]. This includes assumption of only the main product reaction occurring according to the reaction stoichiometry shown in Equation 6.20.

$$Cl_3Si(C_8H_{21}) + 3CH_3OH \rightarrow (C_2C_5O)_3Si(C_8H_{21}) + 3HCl \quad (6.20)$$

Further information on all conditions associated with production are available in Appendix E.

6.2.2. Life Cycle Inventory Modelling of Trichlorosilane

Goal and Scope Definition

The goal of the LCA reported in this section is to provide estimations for the environmental impact associated with TCS. This has been done using an attributional LCA approach using a functional unit of 1 kg of product as an assessment basis. A total of two manufacturing routes are considered, these are: 1) the production of TCS by a direct chlorination process, and 2) the production of TCS as a co-product from the production of high purity silicon metal via the Siemens process.

Assessment of all products has been set to consider a Cradle-to-Gate scope including impacts associated with production of intermediate materials. Further information on specific system boundaries is provided for individual products is provided below.

Inventory Models

Main-product of Direct Chlorination Process

Life cycle inventory models for TCS produced as a main product of direct chlorination are based on material and energy estimates taken from process modelling described in Section 6.2.1. Background activity associated with material and energy supply chains has been modelled using existing models available in the EcoInvent v3.10 database [157].

Hydrogen and hydrogen chloride separated within the process (see Section 6.2.1) were assumed to be recovered (by further gas treatment processing) with mass efficiencies of 98wt%; this was based on values typical of the Siemens process [121]. Recovered hydrogen chloride was assumed to be recycled to offset reagent use. Recovered hydrogen was considered as a process co-product. TCS and STC present in the gas stream were assumed to be lost. No additional activities have been considered for the product process. The associated life cycle inventory is provided in Table 6.3.

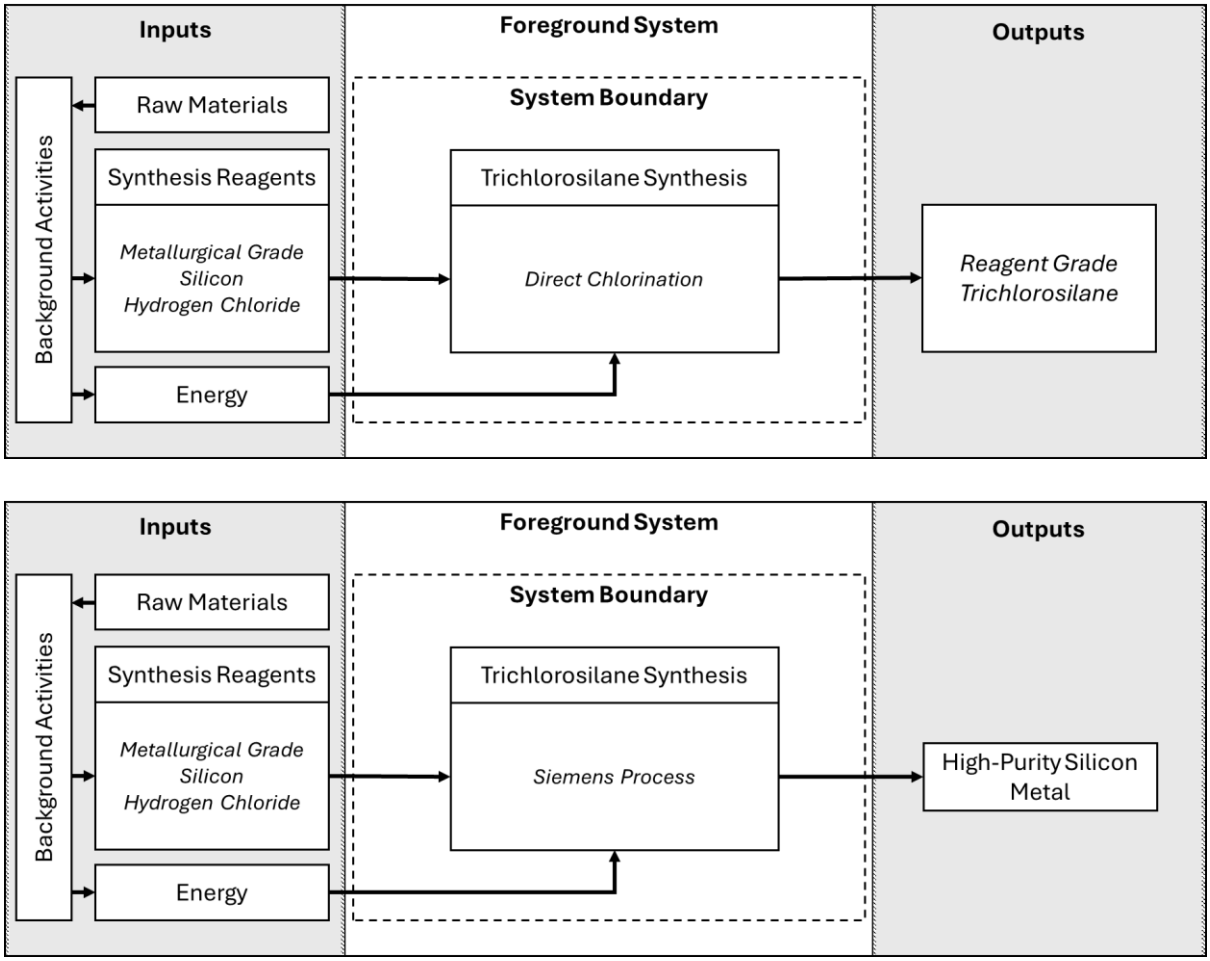


Figure 6.5: Illustration of system boundaries associated with life cycle inventory models reported on the production of trichlorosilane as a main product of a direct chlorination method (top), and as a co-product of silicon metal manufacture according to the Siemens process (bottom).

Table 6.3: Life Cycle Inventory for producing 1 kg of trichlorosilane based on direct chlorination process.

Type	Flow	Amount	Unit
Inputs	Metallurgical Grade Silicon	0.218	kg
	Hydrogen Chloride	0.870	kg
	Deionized Water (cooling)	<0.01	kg
Duty	HCl Compression	0.058	kWh
	HCl Heating	0.010	kWh
	Si Heating	0.005	kWh
	Reactor Cooling	0.473	kWh
	Flash Cooling	-0.158	kWh
	Reboiler Heating	0.109	kWh
	Condenser Cooling	0.090	kWh
	TCS Cooling	0.004	kWh
	STC Cooling	0.001	kWh
Outputs	Trichlorosilane	1.000	kg
	Silicon Tetrachloride	0.059	kg
	Hydrogen	0.016	kg

Table 6.4: Inventory models used to account for background life cycle activity linked to the production of trichlorosilane by direct chlorination based on the EcoInvent v3.10 database.

Inventory Item	Model	Region
Metallurgical Grade Silicon	silicon production, metallurgical grade	NO
Hydrogen Chloride	market for hydrochloric acid, without water, in 30% solution state	RER
Deionized Water (cooling)	market for water, deionised	EU w/o CH
Silicon, electronics-grade	silicon production, electronics grade	DE
Steam	steam production, as energy carrier, in chemical industry	RER
Electricity	market group for electricity, high voltage	RER

Co-product of Siemens Process

Life cycle inventory models for TCS produced as a co-product of the Siemens process are based an expansion of an existing model for production of electronics grade silicon according to the Siemens method in the version 3.10 of the EcoInvent Database [157]. Particularly, the EcoInvent database model (for solar-grade silicon produced in Germany has been scaled to account for production of reagent grade trichlorosilane as a co-product of the Siemens process. This was done assuming production of reagents grade and electronics grade trichlorosilane in a 1:4 [120], and production of 1 kg of electronic-grade silicon per 16 kg of electronic-grade TCS [166]. For completeness, silicon tetrachloride was also considered to be produced as a co-product in a mass ratio of 1:0.287 with respect to reagent grade trichlorosilane and silicon tetrachloride respectively [120]. The associated life cycle inventory is provided in Table 6.5.

Table 6.5: Life Cycle Inventory for producing 1 kg of trichlorosilane as a co-product of the Siemens process.

Type	Flow	Amount	Unit
Inputs	Silicon, electronics-grade	0.125	kg
Output	Trichlorosilane, reagent grade	1.000	kg
	Silicon Tetrachloride	0.287	kg
	Electronics Grade Silicon	0.250	kg

6.2.3. Life Cycle Inventory Modelling of Silane Coupling Agents

Goal and Scope Definition

The goal of the LCA reported in this section is to provide estimations for the environmental impact associated with APTES and OTMS products. This has been done using an attributional

LCA approach using a functional unit of 1 kg of product as an assessment basis. Further information on specific system boundaries is provided for individual products is provided during inventory modelling in the following subsections.

Inventory Models

3-aminopropyl triethoxysilane

Life cycle inventory models for CPTCS, CPTES, and APTES are based on material and energy estimates taken from process modelling described in Section 6.2.1. Background activity associated with material and energy supply chains has been modelled using existing models available in the EcoInvent v3.10 database [157].

A summary of the life cycle inventory information associated with CDMA and CTAC is provided in Table 6.6. An illustration of system boundaries associated with the production of CPTCS, CPTES, and APTES is provided in Figure 6.6. Further information on background activity models is provided later in Table 6.8.

Table 6.6: Life Cycle inventory model for production of 3-aminopropyltriethoxysilane and its chemical intermediates.

Type	Flow	Amount			Unit
		CPTCS	CPTES	APTES	
Materials	Trichlorosilane	0.472	-	-	kg
	Allyl chloride	0.852	-	-	kg
	1-dodecene	0.001	-	-	kg
	3-chloropropyltrichlorosilane	-	1.033	-	kg
	3-chloropropyltriethoxysilane	-	-	1.081	kg
	Ammonia	-	-	0.129	kg
	Ethanol	-	0.674	-	kg
	Water, deionised	0.271	0.229	0.624	kg
	Toluene	-	-	0.004	kg
Energy	Heat, from steam	0.397	0.343	0.155	kWh
	Electricity	-	-	0.155	MJ
Output	3-chloropropyltrichlorosilane	1.000	-	-	kg
	propyltrichlorosilane	0.169	-	-	kg
	Silicon tetrachloride	0.140	-	-	kg
	3-chloropropyltriethoxysilane	-	1.000	-	kg
	Hydrochloric acid	-	0.516	-	kg
	3-aminopropyltriethoxysilane	-	-	1.000	kg

Octyl trimethoxysilane

Life cycle inventory models for OTCS and OTMS are based on material and energy estimates taken from process modelling described in Section 6.2.1. Background activity associated with

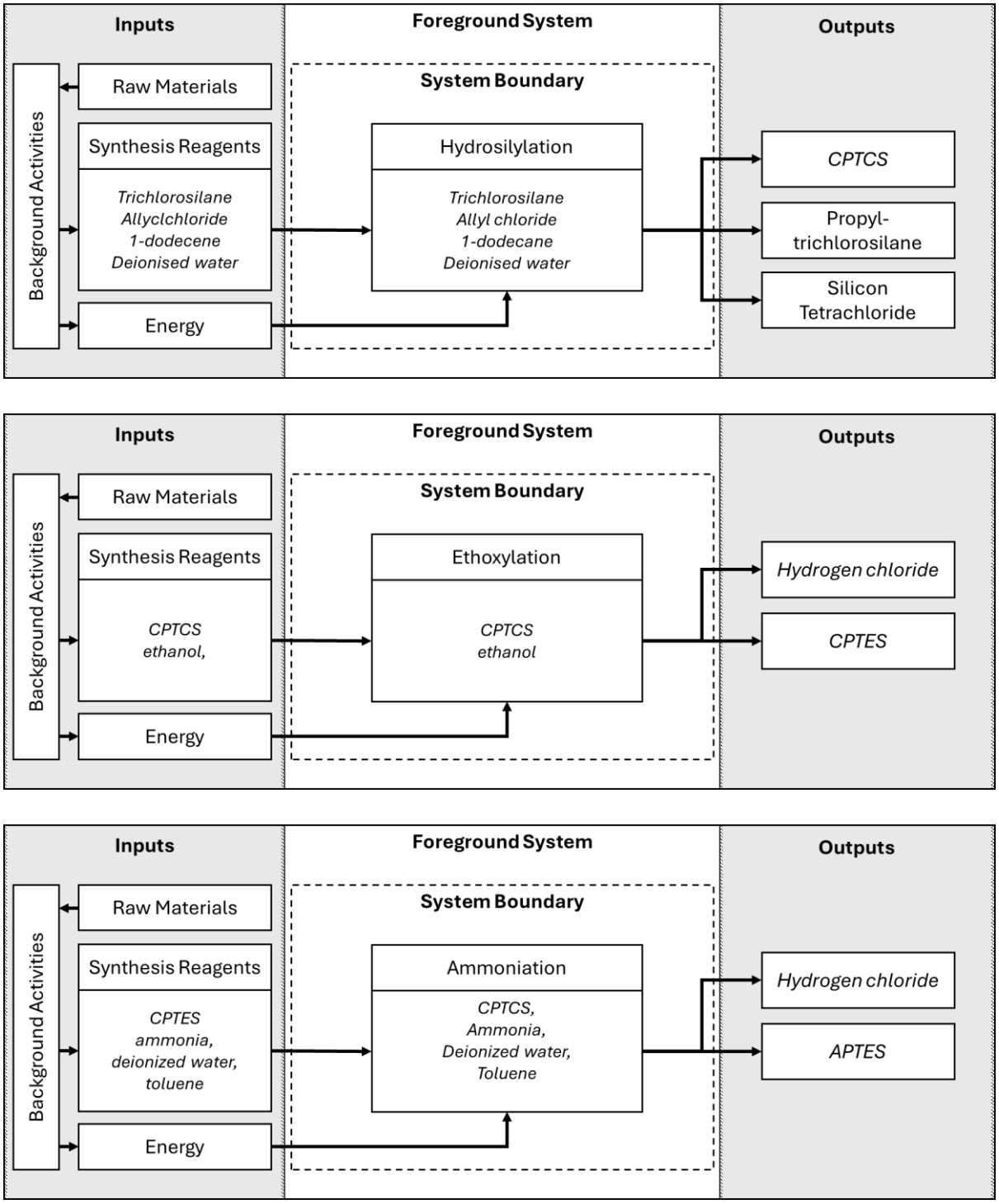


Figure 6.6: Scope of foreground and background life cycle activity included in life cycle inventory models cycle assessment of 3-aminopropyltriethoxysilane products including production of 3-chloropropytrichlorosilane (CPTCS, top), 3-chloropropyltriethoxysilane (CPTES, middle), and 3-aminopropyltriethoxysilane (APTES, bottom)

material and energy supply chains has been modelled using existing models available in the EcoInvent v3.10 database [157].

A summary of the life cycle inventory information associated with OTCS and OTMS is provided in Table 6.7. An illustration of system boundaries associated with the production of CPTCS, CPTES, and APTES is provided in Figure 6.7. Further information on background activity models is provided later in Table 6.8.

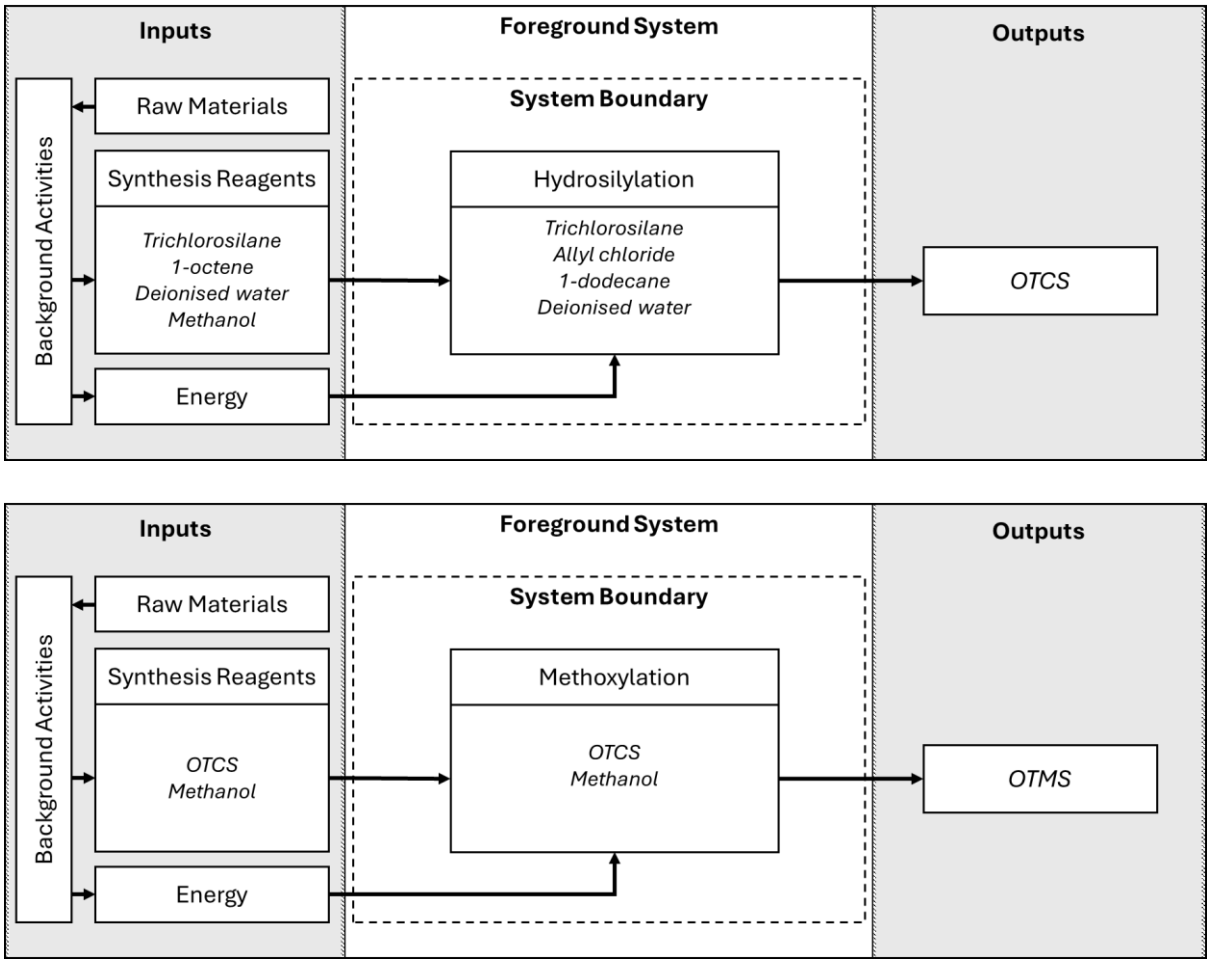


Figure 6.7: Scope of foreground and background life cycle activity included in life cycle inventory models cycle assessment of octyltrimethoxysilane product including production of octyltrichlorosilane (OCTS, top) and production of octyltrimethoxysilane (OTMS, bottom).

Table 6.7: Life Cycle inventory model for production of cetyltrimethoxysilane and its chemical intermediates.

Type	Flow	Amount		Unit
		OTCS	OTMS	
Materials	Trichlorosilane	0.510	-	kg
	1-octene	0.490	-	kg
	Octyltrichlorosilane	-	1.057	kg
	Water, deionised	0.173	0.410	kg
	Methanol	-	0.410	kg
Energy	Heat, from steam	0.415	0.173	kWh
Output	Octyltrichlorosilane	1.000	-	kg
	Octyltrimethoxysilane	-	1.000	kg

Background Life Cycle Models

A summary of inventory models used to model background life cycle activity of silane coupling agents is provided in Table 6.8.

Table 6.8: Inventory models used to account for background life cycle activity linked to the production of silane coupling agents based on the EcoInvent v3.10 database.

Inventory Item	Model	Region
Allyl chloride	*allyl chloride production, reaction of propylene and chlorine*	RER
1-dodecene	n-olefins production	RER
Ammonia	market for ammonia, anhydrous, liquid	RER
Ethanol	market for ethanol, without water, in 99.7% solution state, from ethylene	RER
Toluene	market for toluene, liquid	RER
Heat, from steam	market for heat, from steam, in chemical industry	RER
Electricity	market group for electricity, high voltage	RER
1-octene	n-olefins production	RER
Water, deionised	market for water, deionised	EU w/o CH
Methanol	market for methanol	GLO

6.2.4. Environmental Impact Assessment

Environmental impacts have been calculated using the openLCA v2 software in combination with impact characterisation factors of the ReCiPe Hierarchical 2016 method [71]. All calculations include a 0.1% cut-off. Impact allocation in co-product systems has been handled according to a mass allocation method to reflect the recommendations of ISO 14041. A summary of impact factors considered and justifications for their use is provided in Table 6.9.

Table 6.9: Impact factors considered during life cycle impact assessment of surfactant materials and silica produced occurring to emerging sol-gel methods.

Impact Factor	Justification
Global Warming Potential	Global climate change driver
Fossil Fuel Depletion	Indicator of reliance on non-renewable resources
Terrestrial Acidification	Historical transboundary pollution problem
Water Depletion	Relevance to water scarcity issues

6.3. Results

6.3.1. Process Optimization

Results in Figure 6.8 show observed change in the maximum profit design identified as a function of total number of iterations of the optimization algorithm.

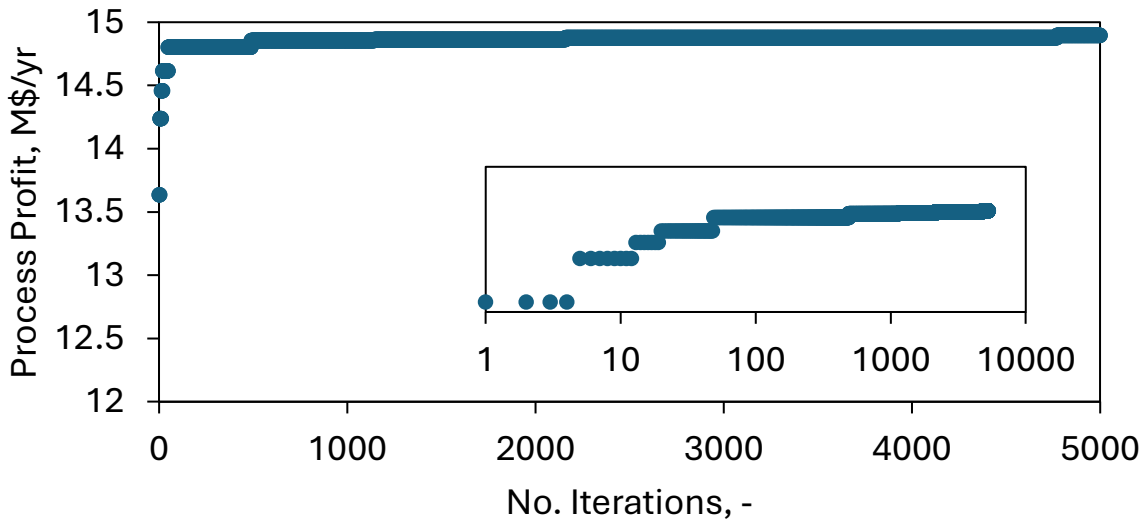


Figure 6.8: Change of maximum profit observed as a function of iteration made by the TCS production process optimizer. Inset: data viewed with a logarithmic scale.

Results in Figure 6.8 show a clear improvement in profitability of the identified optimal process design as the number of iterations increases. Particularly, this includes a sharp increase in performance identified within the first 200 iterations (13,636,391 to 14,802,027 $/yr), followed by a more gradual plateau toward a final maximum profit of 14,894700 $/yr at 5000 iterations.

This corresponds to improvement of 10 % relative to best case found within the first generation, or 99.1 % of the theoretical maximum revenue achievable based on theoretical sale of all TCS and STC present in the reactor effluent. This is considered a reasonable level of optimization and will be taken forward for estimating mass and energy use during life cycle assessment of trichlorosilane produced by the method.

A summary of design conditions, and mass and energy balances associated with the optimized process design is provided in Table 6.10.

Further information about the distribution of successful designs identified per each generation (200 iterations) are displayed as a box plot in Figure 6.9. Interestingly, results in Figure 6.9 (top) show a more consistent upward trend for results of successful designs when compared to that for designs accepted by the solver for consideration in future iterations Figure 6.9 (bottom). This reflects stochastic nature of the solver differential evolution algorithm used, which makes the decision to accept the current “child” design evaluation.

Table 6.10: Design results of the optimized direct chlorination process.

Stream Property	Reactor	Flash	Column
Inlet Flow, kg/hr	(MG-Si) 200.00 (HCl) 798.00	(H_2) 15.07 (HCl) 6.10 (STC) 60.49 (TCS) 916.34	(H_2) 0.00 (HCl) 2.22 (STC) 60.35 (TCS) 908.26
Stream Temp, C	MG-Si: 350, HCL: 100	347.42	-39.82
Output Flow, kg/hr	(H_2) 15.07 (HCl) 6.10 (STC) 60.49 (TCS) 916.34	Top: (H_2) 15.07 (HCl) 3.88 (STC) 0.14 (TCS) 8.08 Bottom: (H_2) 0.00 (HCl) 2.22 (STC) 60.35 (TCS) 908.26	Top: (H_2) 0.00 (HCl) 2.22 (TCS) 907.72 (STC) 6.95 Bottom: (H_2) 0.00 (HCl) 0.00 (TCS) 0.54 (STC) 53.40
Stream Temp, C	350	-39.82	Top: 25.21 Bottom: 140.88
Distillation Column Conditions			
Number of Stages			105
Feed Stage			61
Reflux Ratio			0.6505
Boil-to-Feed Ratio (m.b.)			0.055
Top Pressure, bar			1.87
Bottom Pressure, bar			3.97
Top Temperature, C			25.21
Bottom Temperature, C			140.88

based on if it outperforms a subset of “parent” individuals in the population that were used during generating the “child”. Consequently, the tendency of the distribution of accepted.

designs can be thought to reflect the failure of successful designs to outperform their “parents” (Figure 6.9 (top)), and therefore be accepted, despite those designs still providing potential improvements relative to other, worse performing designs within the current generation. This highlights natural challenges in the use of genetic algorithms – particularly regarding the potential for “losing” information by rejecting designs that could otherwise be used in other optimization algorithm frameworks. Nonetheless, despite the recognised shortcomings, the performance of the overall algorithm has been adequate for the intended application; moreover, it must not be forgotten that use of a genetic algorithm has provided

benefits in other areas – especially with regards to being able handle discontinuous, multi-modal problems [175], which is characteristic of the design optimization considered.

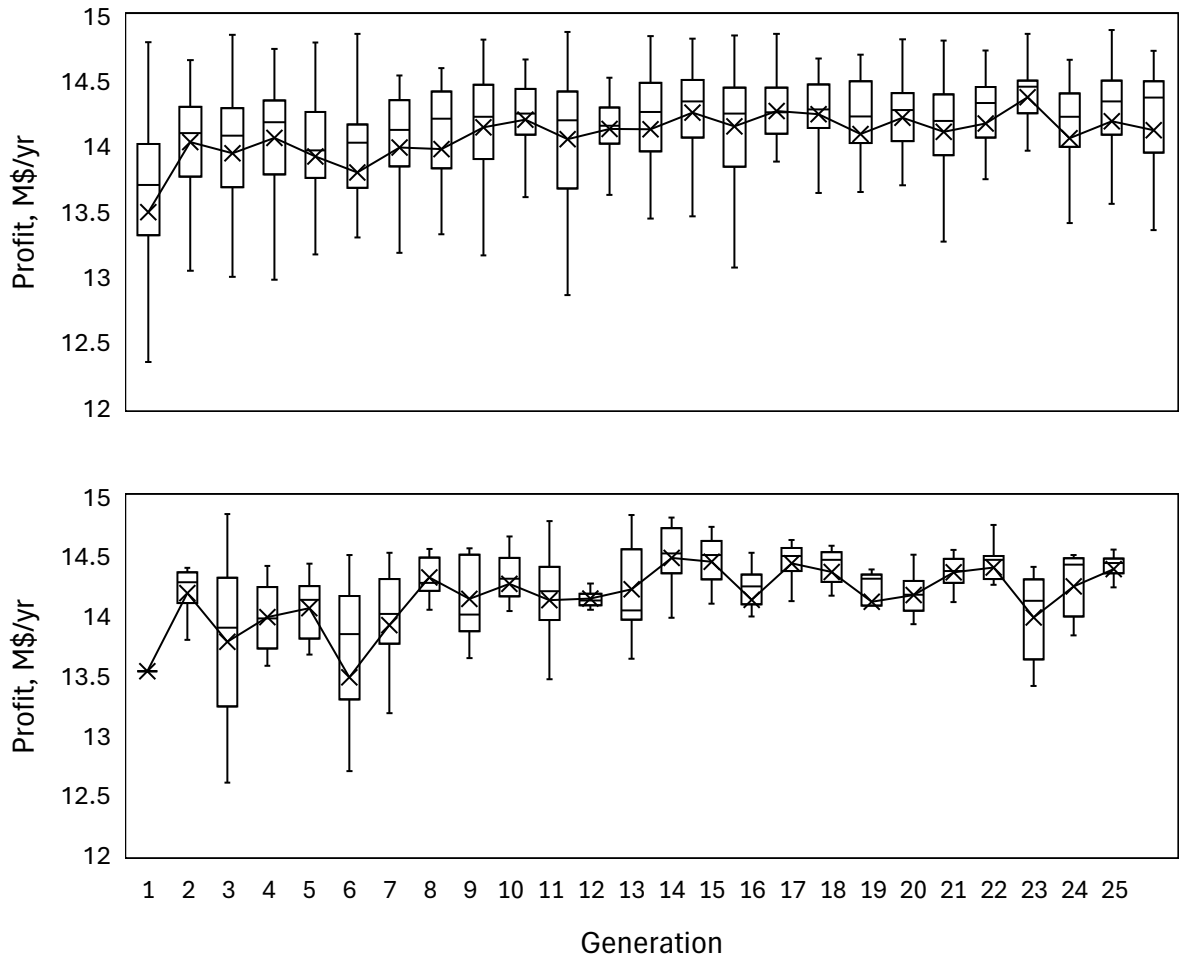


Figure 6.9: Box plot of profit of successful designs identified in each generation (top) and designs accepted into the differential population (bottom). Boxes display interquartile range and median based on inclusive method. The black line inside each box plot represents the mean profit of designs within a given generation.

6.3.2. Environmental Impact of Trichlorosilane

Impact predictions for TCS produced as a main product of direct chlorination and as a co-product of the Siemens process are shown in Figure 6.10. Impact contributions associated with each process are then shown in Figure 6.11.

Results show marked differences in the impact of trichlorosilane associated with direct chlorination process and Siemens process on a mass basis. For example, TCS produced by direct chlorination is predicted to have a carbon footprint and fossil depletion potential roughly 5 and 7 times smaller than that of TCS produced by the Siemens process.

Table 6.11: Mass and Energy flows associated with operation of the optimized process for producing trichlorosilane.

Process Stage	Flow	Amount	Unit	Utility Type
Input	Metallurgical Grade Silicon	200.00	kg	N/a
	Hydrogen Chloride	798.00	Kg	N/a
Output	Trichlorosilane	916.89	kg	N/a
	Silicon Tetrachloride	53.94	kg	N/a
	Off-gas	27.17	kg	N/a
Equipment Duty	HCl Compression	53.3	kWh	Electricity
	HCl Heating	8.9	kWh	Steam
	Si Heating	4.5	kWh	Nat. Gas
	Reactor Cooling	433.5	kWh	Steam
	Flash Cooling	-145.25	kWh	refrigerant
	Column Inlet Pump	<0.01	kWh	electricity
	Reboiler Heating	100.28	kWh	steam
	Condenser Cooling	82.58	kWh	refrigerant
	TCS Cooling	3.44	kWh	Cooling water
	STC Cooling	1.04	kWh	Cooling water

In most cases, the reason for large differences in the impact of TCS produced by each method can be attributed to energy use of the Siemens process. This is demonstrated by results in Figure 6.11, which suggest energy use contributes to more than 80% of the impact of the Siemens process with regards to WDP, FDP, and GWP.

The importance of energy contributions in governing the impact of TCS derived from the Siemens process is understandable given understanding surrounding the process. Particularly, the Siemens process is known to be an energy intensive manufacturing method; this characteristic arises from the ultrahigh purities of silicon metal that the process manufactures as well as thermodynamic limitations inherent in the distillation approach that the method is based on. Nonetheless, making direct causal links is difficult due to the complexity created by impact allocation across co-products in both processes.

Interestingly, in the case of terrestrial acidification, the siemens process does not contribute significantly to overall impact of TCS produced by the Siemens process. In this case, energy contributes only 7% of the impact, with silicon use reflecting the rest of the impact. On further inspection of the underlying EcoInvent database models, this appears to be associated with the reliance of the model on global metallurgical grade silicon supply chain – including higher impact electricity use present in the region of Asia and the Pacific. Thus, this result reflects the importance of global supply chain context on the footprint of TCS derived from the

Siemens process. This may be an assumption worth validating when developing LCA models for TCS-derived products in future work.

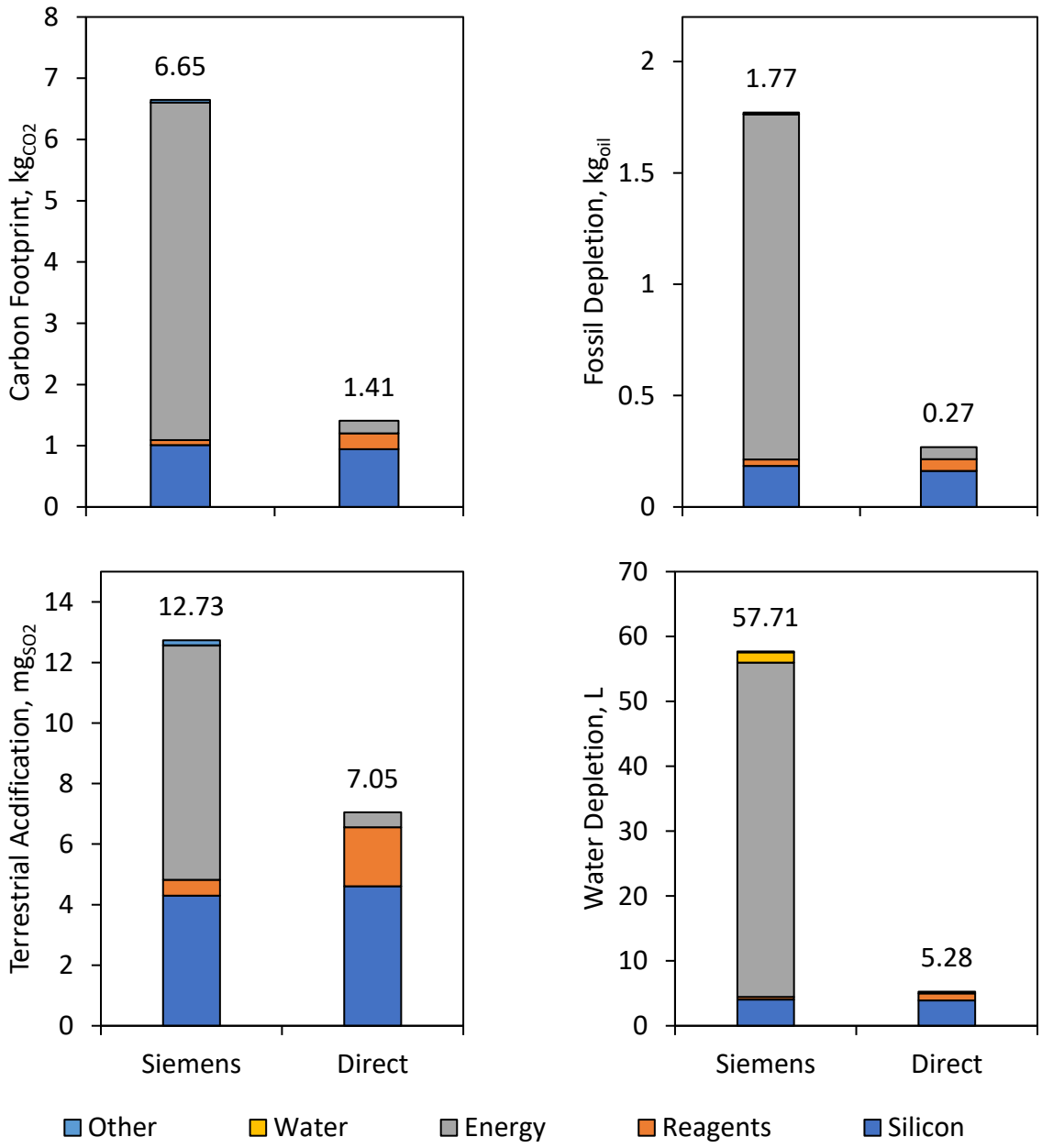


Figure 6.10: Environmental impact predictions for 1kg of trichlorosilane produced by the Siemens and Direct Chlorination processes.

Contrary to the results for Siemens process-derived TCS, results in Figure 6.11 indicate that the use of silicon metal is key in defining the impact of TCS derived by direct chlorination. They also highlight the relatively low importance of hydrochloric acid reagent use (as-per the "reagents" category) in all impact factors apart from terrestrial acidification. The relatively higher importance of hydrogen chloride in the case of terrestrial acidification appears intuitive, given that it is an acid gas. This is quite clearly different from the contribution of

impacts to trichlorosilane derived from the direct chlorination. On the other hand, the importance of silicon metal contribution comes again from the amount of energy use associated with the silicon metal feedstock's supply chain, and reliance on global manufacturing – particularly in Asia and the Pacific (see discussed above).

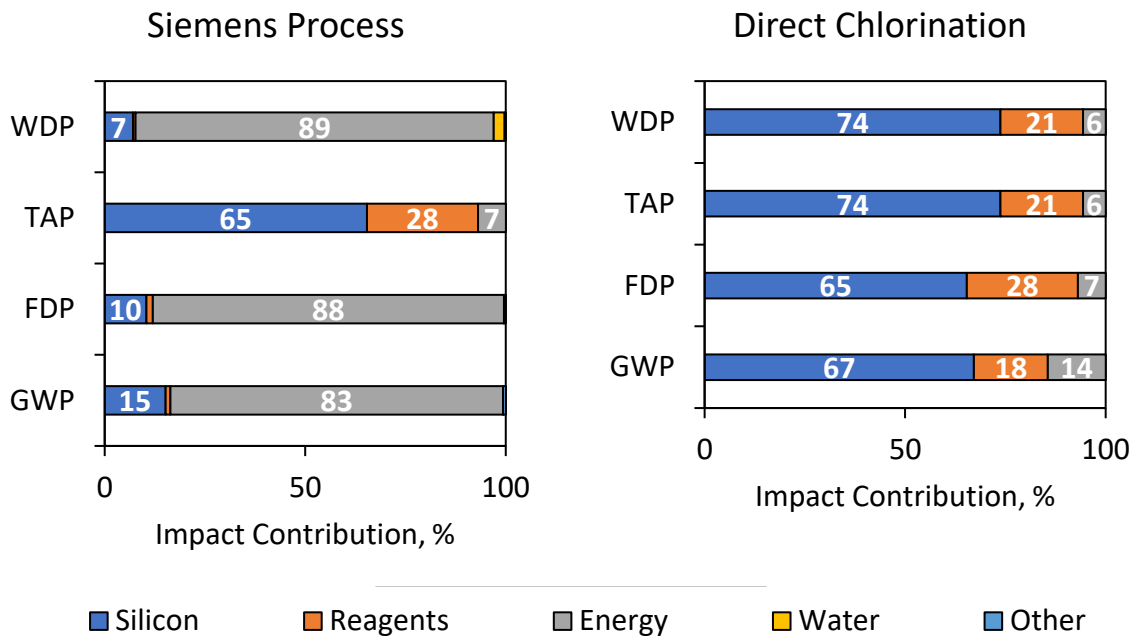


Figure 6.11: Contribution of major activity categories to the overall impact of trichlorosilane produced via siemens process (left) and direct chlorination (right). GWP: Global Warming Potential, FDP: Fossil Depletion Potential, TAP: Terrestrial Acidification Potential, WDP: water depletion potential.

6.3.3. Environmental Impact of Silane Coupling Agents

3-aminopropyltriethoxysilane

Impact predictions for producing 1 kilogram of APTES and associated CPTCS and CPTES intermediates are shown in Figure 6.12. All results assume use of TCS derived from as a co-product of the Siemens process.

Results in Figure 6.12 indicate the environmental impact of APTES to be 3.27 kg CO_2-eq, 1.35 kg oil-eq, 19.21 L H_2O-eq, and 7.01 mg SO_2-eq per kilogram TCS produced.

In all cases, the observed impact of SCAs appear to be driven from silane use, with contributions arising from TCS use being a significant impact driven in most cases. This highlights that impact of the product is heavily driven by impacts locked within the manufacture of TCS product used. The reason of this is already discussed as being associated.

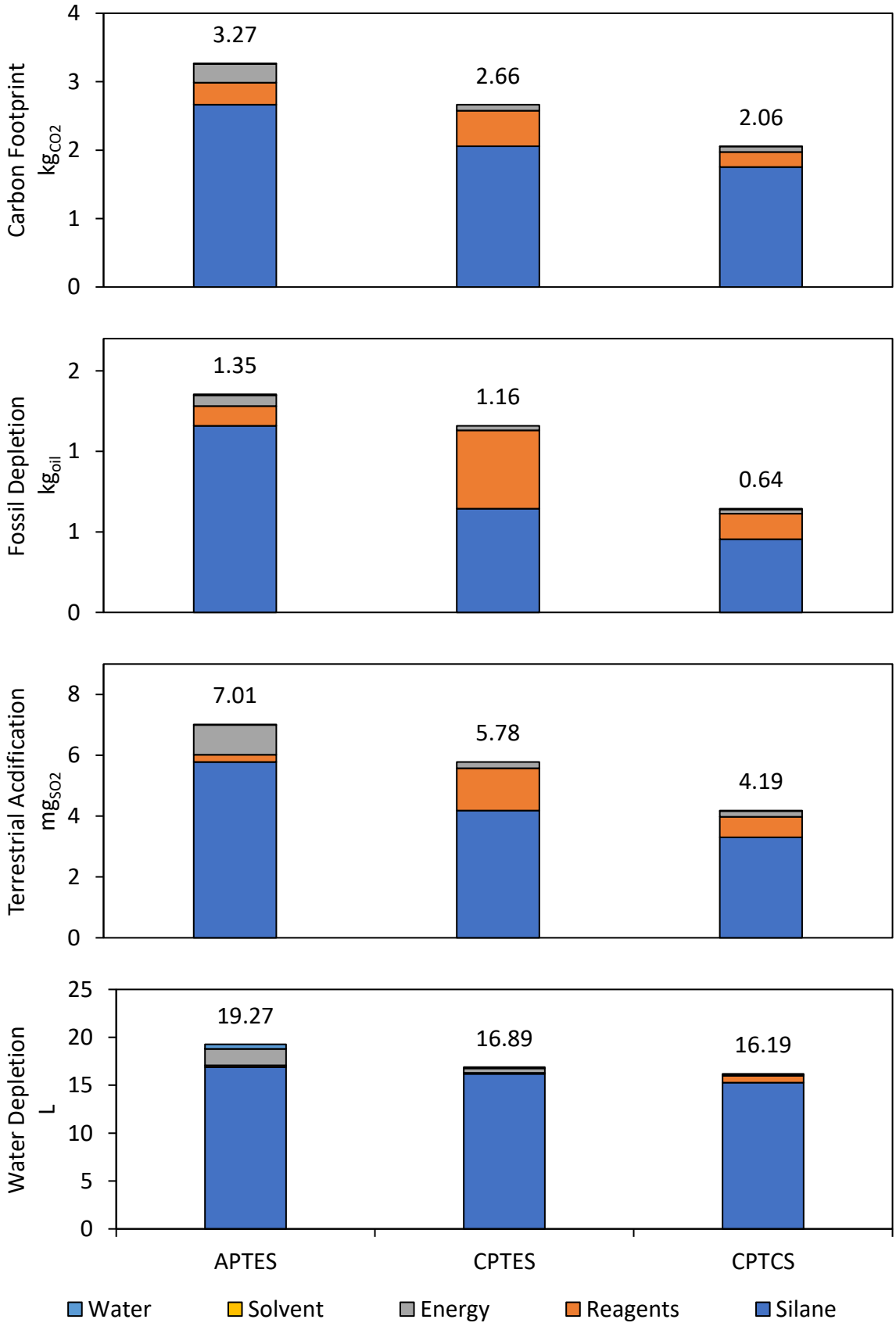


Figure 6.12: Environmental impact predictions for 1kg of 3-aminopropyltriethoxysilane (APTES) and the associated amount of 3-chloropropyl triethoxysilane (CPTES) and 3-chloropropyl trichlorosilane (CPTCS) used during the APTES production.

with the wider silicon metal supply chain linked to Siemens process-derived silica in Section 6.3.2.

The importance of TCS impact on the overall footprint of SCA products has important implications for the sustainable design of the SCA products considered. Particularly, the results suggest impact reductions through innovation in the manufacture of SCA products may be limited when compared to innovation within the TCS supply chain. For example, the governance of impact by silane derivatives suggests that alternative methods to produce APTES (e.g. via cyanoethylsilanes, or allylamine hydrosilylation) are unlikely to provide significant reductions relative to the allylchloride route considered in this work.

Regarding the importance of TCS contribution to overall impact, the results also suggest that major environmental impact associated with production could come through reduction of impact associated with the route by which TCS is produced. This could be achieved either through 1) improvement in the Siemens process (e.g. technological innovation), 2) transition to use of alternate processing methods to generate TCS, or 3) transition to use of alternative materials (instead of TCS) as platform chemicals for SCA production.

On one hand, the potential for reduction in impact through technological innovation in the Siemens process seems unlikely given that the industry is already mature and given thermodynamic limits of the processing method (see Section 6.3.2). Nonetheless, reductions may be possible through shifting reliance of the supply chain for metallurgical silicon metal used in the production of TCS via the Siemens process; this is due to the current associated with supply chains in the Asia-Pacific region (as discussed in Section 6.3.2).

On the other hand, the potential for reduction of impact through innovation in alternative manufacturing routes seems more plausible. For example, current research interest into the production of alkoxysilanes produced by direct alkoxylation of silicon metal – avoiding the need for chloro-silane chemistries may offer a valid alternative in the future. Nonetheless, this avenue will rely on the ability to produce platform chemicals for SCA manufacture in purities and at price points that are competitive with current industry. Moreover, transition to such chemicals may be hindered by economic reliance of some silicon manufacturing processes on the sale of TCS as a co-product as part of ensuring healthy process economics [121].

Octyl trimethoxysilane

Impact predictions for producing 1 kilogram of OTMS and the associated amount of OTCS intermediates are shown in Figure 6.13**.**

Results in Figure 6.13 indicate the environmental impact of OTMS is 3.29 kg CO_2-eq, 1.43 kg oil-eq, 22.25 L H_2O, and 6.87 mg SO_2-eq per kilogram produced.

In all cases, results for the OTMS and OTCS produces show similar trends with regards to the importance of silane feedstock in driving product impact. In fact, the contribution of silane reagents appears to be even larger for these products than those considered above for the PATES supply chain. The same points of discussion as provided above therefore apply.

Comparison of Impacts on a Molar Basis

Finally, a comparison is provided for the environmental impact of all products on a molar basis (i.e. 1 mole of product as a functional unit) in Figure 6.14.

The reason for considering impacts in this way is primarily because of the molar relationship inherent in the number of surface silanol groups present on an adsorbent surface (e.g. in mol/m^2), and the moles of required to change surface chemistry of the surface via silanization. As a result, understanding impact on a molar basis may give useful insight for practitioners of surface chemistry modification, who often think of material use in the molar basis. Similarly, thinking in this basis makes it possible to identify the minimum impact associated with silanization given a desired level of coverage of an adsorbent with a known number of surface silanol groups.

However, consideration of impact on a molar basis may also be of interest based on differences in molecular size of molecules. Particularly, because differences in molecular size suggest differences in molecular weight of coupling agents, which may skew results when compared on a molar basis, when compared to a mass basis.

This is done in to acknowledge to combining factors: 1) functionality of silane molecules come from adding individual molecules onto a surface, which could lead to interpretation on a mole basis of physicality, and 2) organosilane products can vary significantly in molecular size and weight, causing comparison on a kilogram basis to be potentially misleading.

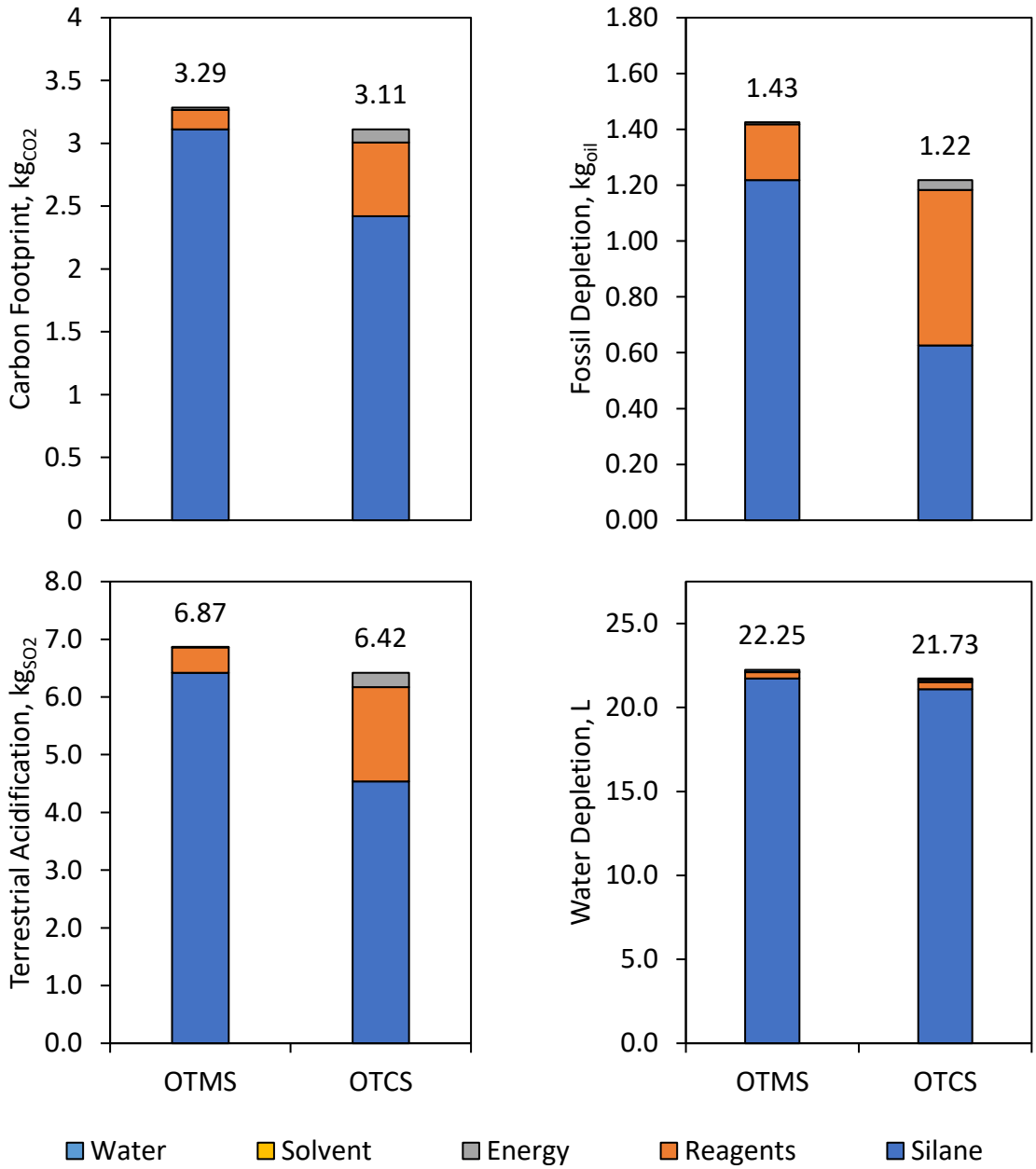


Figure 6.13: Environmental impact predictions for 1kg of octyltrimethoxysilane (OTMS) and the associated amount of technical grade trichlorosilane (TCS) produced during the OTMS product life cycle.

Results in Figure 6.14 show that there are significantly lower environmental impacts for all organosilane species compared to trichlorosilane when compared on a molar basis. This can be explained most simply based on relatively large contribution made by trichlorosilane to the impact of all precursors (see Figure 6.12 and Figure 6.13), and sizable differences in the molar mass of trichlorosilane (135 g/mol) when compared to the other agents (212 to 248 g/mol).

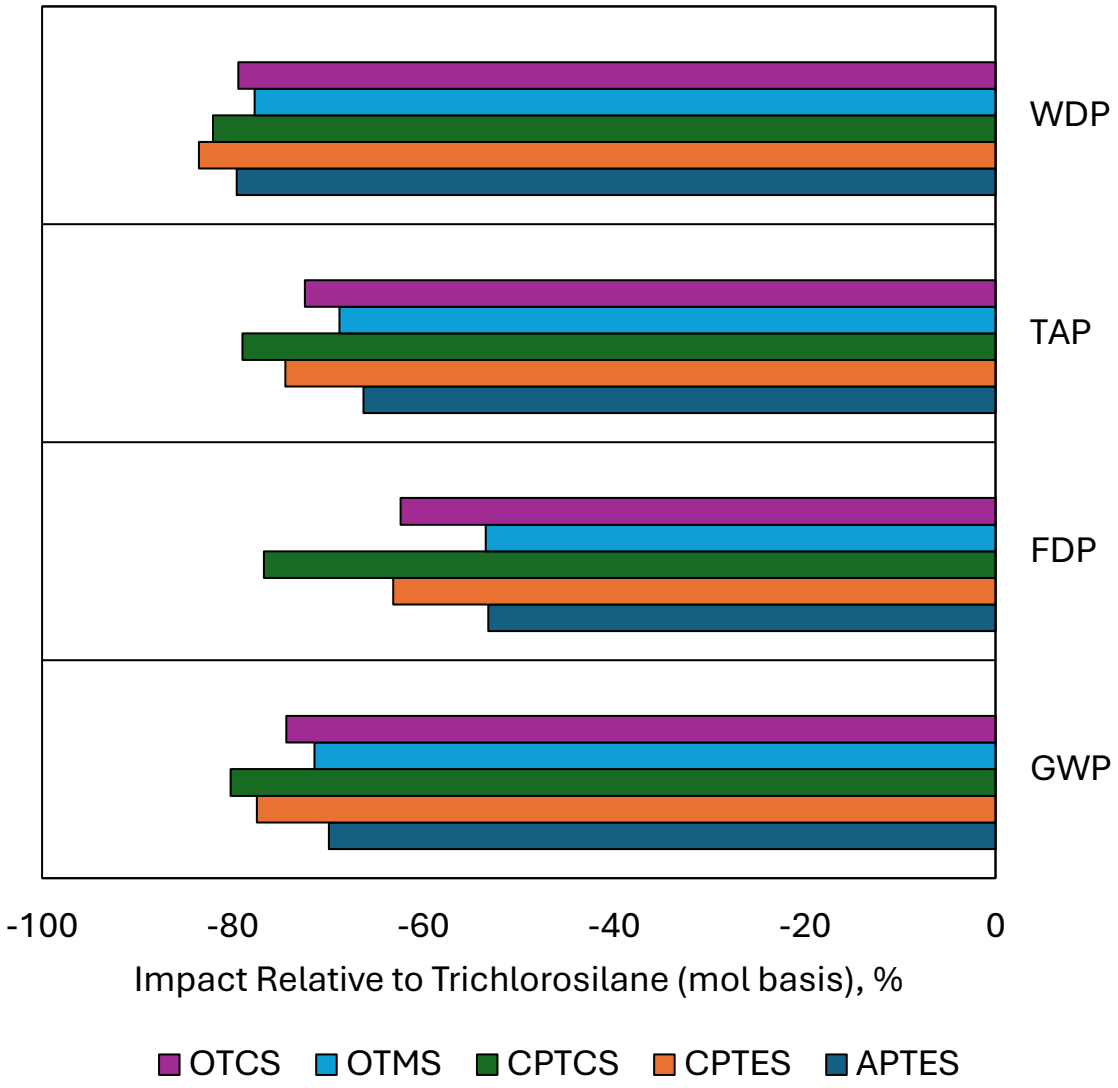


Figure 6.14: Environmental impact predictions for all organosilane products considered on a per mole of product basis.

6.4. Discussion

6.4.1. Process Modelling

Findings in Figure 6.9 illustrate a common issue associated with the use of stochastic solvers. That is, the perceived tendency for the differential solver used to discard "positive" design conditions dependent due to the parent-wise comparison method used to determine whether information is accepted or not. Whereas this is related to the evolutionary nature of the algorithm used, it raises questions about the extent to which the method allows data loss through not bothering to consideration information of rejected designs within further design space exploration. Moreover, a challenge may be raised as to the extent to which the selection procedure truly represents the phenomenon of *survival of the fittest*, given that "fitness" of new designs are compared to parent individuals alone. Both issues could be explored in

further depth in future work through development of different approaches within the evolutionary algorithm paradigm, as well as by increasing consideration for use of all information in a data-efficient optimization policy – e.g. using surrogate based approaches in place of evolutionary approaches.

Results of process optimization reported in this work provide initial estimates for mass and energy balances that have been used in life cycle assessment of trichlorosilane. Whereas results are deemed acceptable, it is noted that space exists for modelling to be further improved. Lack of consideration for treatment of gas separated by the flash condenser provides an oversight with regards to material and energy use of these subprocesses. Information is available for these processes, which appear to occur largely via wet scrubbing of hydrogen chloride in packed towers, followed by use of adsorbents to further purify the resulting hydrogen gas stream [121]. Accounting for this process incorporates additional number of design variables that would need to be considered if included in an entire process optimization. This may be considered in future work to provide more rigorous estimation.

6.4.2. Importance of Trichlorosilane Processing History

Not considered in this work is the increased conversion that may be achieved through use of high purity trichlorosilane produced as a co-product of the Siemens process. To fully unravel the extent of this dependence, more rigorous understanding of the relationship between trichlorosilane purity and material efficiency is required. Future work could therefore expand by establishing such relationships based on empirical evidence for differences in performance.

6.4.3. Importance of Desired Chemistry

Interestingly, findings suggest a relatively small effect of desired chemistry on the impacts of SCA products considered associated. More specifically, impacts of the APTES and OTMS products are similar despite having a significant difference in their functional chemistry - the amino group in APTES being polar and the octyl group in POTS being nonpolar. Nonetheless, it may seem surprising within the benefit of understanding developed in this chapter.

Despite this, results from this chapter cannot be used to suggest that the choice of desired chemistry will not affect the impact of silanization-modified SBAM products. This is because differing desired chemistries may affect the processing conditions required for SBAM silanization. For example, differences in polarity of the amino acid and octyl groups in APTES

and POTMS are likely to cause differences in solvents applicable for facilitating the silanization of silica substrates. This aspect of discussion is explored further in Chapter 7.

6.4.4. Importance of Allocation Factor

Findings in Section 6.3.2 outline the presence of a strong dependence of the impact of SCA products on contributions arising from TCS use. These results are based on impact assessment according to a physical (mass) allocation basis as per ISO 14041. Nonetheless, arguments may be made for using alternate allocation methods to assess impacts of TCS product. For example, this may include an argument for using an economic allocation based on revenue generated by each co-product. This may be made on the basis that there are multiple co-products to consider in the LCA models generated for TCS, including electronic-grade silicon metal, which has a significantly different economic value when compared to other co-products such as hydrogen or silicon tetrachloride (see Table 6.12). Consequently, a consideration has been made in this section for the sensitivity of results to choose of mass or economic basis of impact allocation at the trichlorosilane manufacturing stage. The case for main product is not considered as production ratios and prices are not likely to affect outcome significantly.

Table 6.12: Selling prices assumed for co-products of trichlorosilane manufacturing processes during economic allocation.

Material	Price, $/kg	Source
Trichlorosilane	2.00	[179]
Silicon Tetrachloride	0.98	[180]
Hydrogen	1.46	[181]
High Purity Silicon [a]	12.00	[118]

[a] based on the price of solar grade silicon reported by Jarkin *et al*. [118]

Results in Figure 6.15 show impact predictions for all silane products as a function of impact allocation factor for global warming potential.

Results in Figure 6.15 show that a change in allocation method does in fact effect the impact predicted for TCS. Moreover, the extent of change created by a change in allocation method varies between both processes significantly. Particularly, the impact prediction for Siemens process-derived TCS is reduced by 32%, whereas the impact of the direct chlorination-derived TCS is reduced by only 3%. This is an order of magnitude difference, which seems to validate the prior hypothesis that differences in production amounts and economic value of the co-products in the Siemens process introduce an additional subjectivity when considering the impact of TCS according to different methods. This finding is also applicable to SCA products

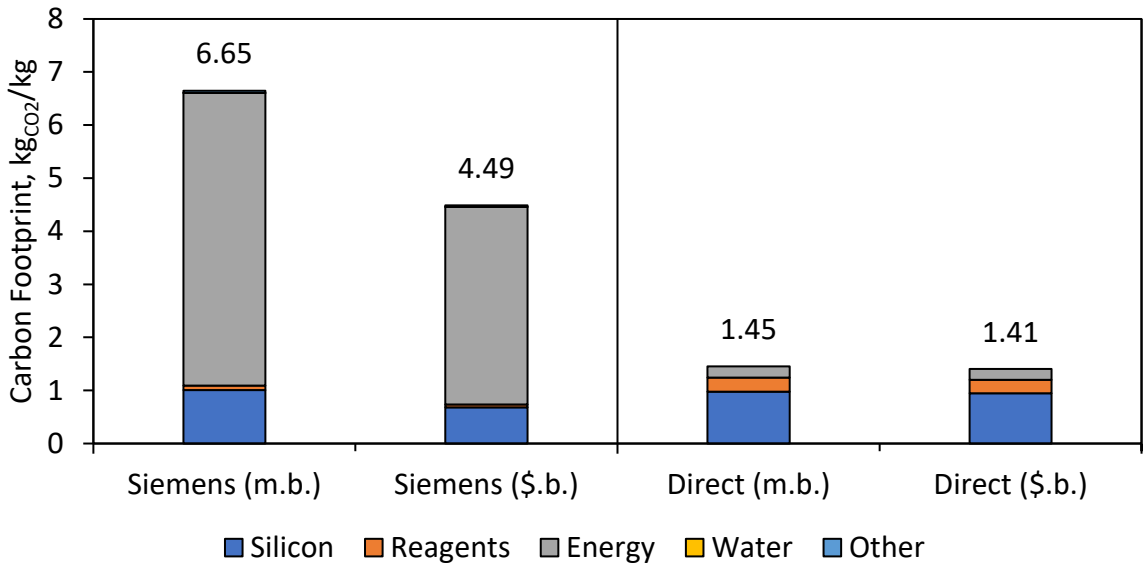


Figure 6.15: The effect of allocation philosophy on the environmental impact of trichlorosilane produced according to Siemens and Direct Chlorination processes.

produced using Siemens process-derived trichlorosilane due to the large impact contribution that trichlorosilane has been found to provide in those cases (see Section 6.2).

Finally, it must be stated that the overall ranking of impact of TCS process derived by each method does not appear to change as a function of allocation method.

6.4.5. Modelling Issues

Shortcomings of process modelling carried out are naturally also shortcomings of the life cycle assessment reported. Areas of uncertainty arising from process modelling include: 1) differences in system boundaries of trichlorosilane production processes considered, and 2) uncertainty in gas treatment of direct chlorination route for trichlorosilane production.

Regarding system boundaries, differences in data collection between the Siemens process and process modelling may lead to differences in effective scope of the models that have been compared. Specifically, data used for modelling the Siemens process come from treatment of aggregate data for the Gendorf facility in Germany, which is aggregated data based on the needs of an industrial complex including several different chemicals being produced. Differences in scope of life cycle inventories lead to increased uncertainty around the reliability of data. To address this, life cycle inventory models must be developed that use data aggregated from reasonably comparable data sources. The most transparent of these may include process modelling of the Siemens process – though doing so would not be trivial due to the additional process complexity of the Siemens process.

Conclusions

Research in this chapter has aimed to develop an understanding for the environmental impact of producing silane coupling agents commonly used in surface chemistry modification of silica and other metal oxides. Consideration has been made for two common products – 3-aminopropyl, triethoxysilane (APTES), and octyltrimethoxysilane (OTMS) – and their intermediates - trichlorosilane 3-chloropropyl-trichlorosilane (CPTCS), 3-chloropropyltriethoxysilane (CPTES), and octyl trichlorosilane (OTCS). This has been done in two stages: 1) estimation of material and energy use in during intermediate processing, and 2) life cycle assessment of TCS and associated SCA products.

Findings of the work highlight sensitivity of product impact to the processing history of the trichlorosilane product used as a chemical platform for SCA manufacture. This arises from the energy use associated with trichlorosilane when produced as a co-product of the Siemens process (for high purity silicon manufacture) as a main product of dedicated direct chlorination process. This equates to impact reduction of the TCS product of 80%. Likelihood of reducing impact of TCS co-produced by the Siemens process are low (saving from disruptive innovation) - owing to the technological maturity status of the Siemens process and inherent energetic limitations of its processing approach. Contrarily, economic factors likely to cause use of Siemens-derived TCS to be present in many products due to the scale at which it is manufactured, and benefits that the product typically provides for mass efficiency of subsequent processing of silane coupling agents.

Beyond trichlorosilane use, the next important source of impact for the SCA agents appears to arise from use of petrochemically derived material use – including alcohols used in alkoxylation and organic moieties intended to deliver desired surface modification to SBAMs. In the case of alcohol use, the impact of these contributions may be difficult to reduce given their inherent need to produce intended products; it appears however, that careful choice between methoxylation and ethoxylation (i.e. methanol or ethanol use respectively) may provide some basis for impact reduction when possible. Further research is required to investigate if the benefit of producing products by alternate processing routes.

Findings of this work are novel given the lack of information currently available on the environmental impacts of silane coupling agent products. Moreover, they provide a

foundation from which more realistic impact assessments can be made for products which involve use of SCAs in their manufacture – including many SBAMs with modified surface chemistry.

The results of this chapter are built upon in subsequent chapters by using inventory models during assessment of surface modified SBAMs in Chapter 7.

7. Environmental Cost of Silica-Based Oil Adsorbents

7.1. Introduction

7.1.1. Background

Food-derived fat, oil and grease (FOG) tends to form solid deposits when disposed of into municipal sewers. This can obstruct sewage flow, causing sewer system overflows and reductions in wastewater treatment efficiency. This is a growing problem particularly in urbanised areas, where high population densities and food service establishments create high FOG pollution loads.

Whereas the state of FOG pollution is a growing problem, it also presents a growing opportunity for resource circularity. This is because the organic chemistry of FOG, particularly free fatty acids (see Chapter 2, Section 2.2.2) has the opportunity for use in producing a number of specialty chemicals as well as being converted to biodiesel [182]. This, coupled with the volume at which FOG is produced and polluted, suggests a potential for recovery and valorisation of FOG waste subject to adequate chemical processing.

One way in which FOG waste could be recovered is using adsorbent-based approaches. This would involve introducing adsorbent materials to act as sacrificial surfaces on which FOG wastes preferentially deposit. Achieving this requires careful design of adsorbent material properties to ensure high chemical affinity, and selective recoveries of FOG pollution.

As previously outlined in Chapters 1 and 2, Silica based Adsorbent Materials (SBAMs) are one such adsorbent-based technology that could be used to treat FOG pollution [183, 184]. Research suggests that effective SBAM products are characterised as being optimized by some combination of control for adsorbent network geometry (e.g. pore size, size distributions, and void fraction) as well as surface chemistry.

However, producing such products also incurs some amount of environmental impact. As a result, and process utilising SBAM adsorbent material may be thought of as having an environmental abatement cost linked to combined technical efficiency and environmental cost of the SBAM treatment. Until recently, accurate understanding for these impacts has

been lacking due to unavailability of life cycle information associated with the emerging methods by which SBAMs area typically produced. Research in this thesis has provides the potential to assess the impact of SBAM materials more accurately, and therefore the abatement cost associated with use as adsorbent materials. It therefore follows that demonstration should be provided as to how models developed can be used in real-world assessment of abatement cost associated with SBAM pollution treatments – including treatments aimed at FOG pollution.

7.1.2. Aims and Objectives

This chapter aims to show how contributions of the entire thesis may be applied for the benefit of LCA of SBAMs, including as a tool for their sustainable development. In doing so, a focus is made on a demonstrative, 'toy' problem of performing on LCA for the use of SBAMs to recover vegetable oil (a contributor to FOG pollution in wastewater), assuming recovery of the oil according to a solvent-extraction based methods. As part of this, the chapter includes use of experimental methods to generate information required to establish reasonable estimates for material and energy use associated with using SBAMs under the described method. The purpose of the work - the experimental methods, and the LCA – are intended to be purely demonstrative, with experimental research serving solely as a basis for supporting generation of example LCIs required for LCA of the scenarios being considered. In this light, the objectives of the work are therefore:

1. Provide preliminary characterisation to account for changes in material structure likely occurring from factors of surface chemistry modification.
2. Demonstrate simple methods for quantifying sorption performance of each SBAM.
3. Use information generated from experimentation to establish reasonable estimates for material and energy use of a wider process involving solvent extraction of recovered adsorbate material (i.e. vegetable oil).
4. Report environmental impact cost associated with use of SBAM to recover FOG-like pollution.

7.2. Methods

A mixture of methods has been used in this chapter to assess the environmental impact associated with recovering FOG-like pollution using SBAMs. This includes use of experimental

methods to generate information regarding sorption performance of three types of SBAM products, which are used to generate life cycle inventory models for life cycle assessment. A summary of the workflow of research is shown in Figure 7.2.

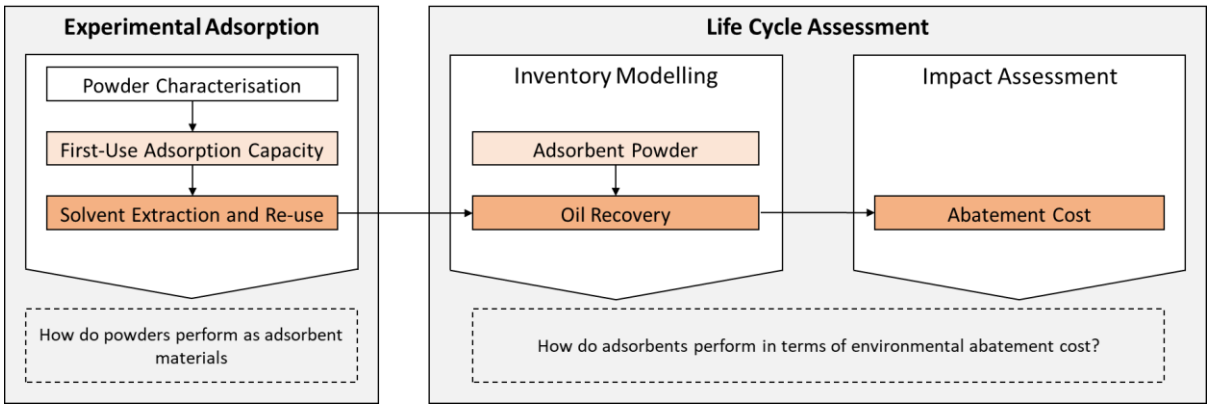


Figure 7.1: Schematic workflow of methods used to investigate the environmental impact of using silica-based adsorbent materials for recovery of vegetable oils.

7.2.1. Materials

Vegetable oils (olive, sunflower, and rapeseed) were purchased from a UK supermarket (Waitrose). Ethanol absolute (> 99.8 wt%) was used as purchased from VWR. De-ionised (DI) water was provided by a PURELAB Chorus 1 (ELGA LabWater) water purification system.

Silica powders with silanol (R100030B), butyl (R32030B), amine (R52030B) and surface chemistries (see Figure 7.2) were purchased from SiliCycle. Note that the butyl and amine powders are produced by modifying the surface chemistry of the silanol powder (R100030B). Therefore, all powders may be thought to be based on an the silanol powder (R100030B) as an underlying silica substrate – thereby sharing similar geometry and porosity properties. Nonetheless, some in-batch variation may exist due to lack of certainty that all powders were made from the exact same batch.

All powders were stored away from light at room temperature to emulate likely storage condition in real use. The properties of each powder (based on manufacturer reports) are summarised in Table 7.1.

Table 7.1: Powder characteristics as reported by the silica powder manufacturer.

Material	Silanol [a]	Butyl [b]	Amine [c]
Particle Size, um	**40 - 63**	**40 - 63**	**40 - 63**
Pore Size, nm	**6**	**6**	**6**
Silica Production Method*	**Precipitation**	**Precipitation**	**Precipitation**

* Confirmed by private communication.

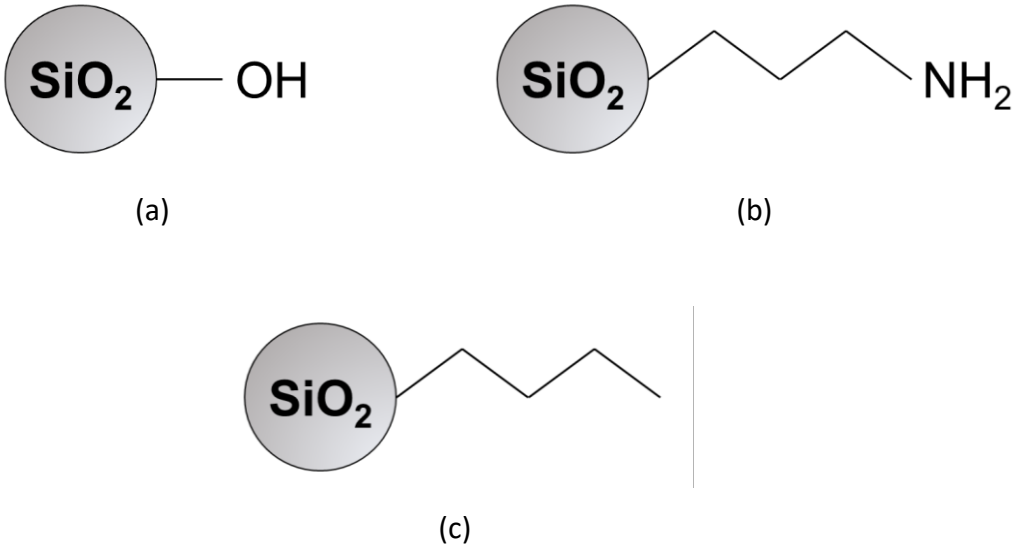


Figure 7.2: Illustrations of surface chemistry associated with each of the three adsorbent powders considered, having silanol (a), amine (b), and butyl (c) surface chemistry.

7.2.2. Adsorbent Characterisation

Particle Size Imaging

Analysis of particle size was taken based on visual assessment of images taken by light microscopy. Imaging was done using an Olympus CX41 optical microscope under an 50X magnification.

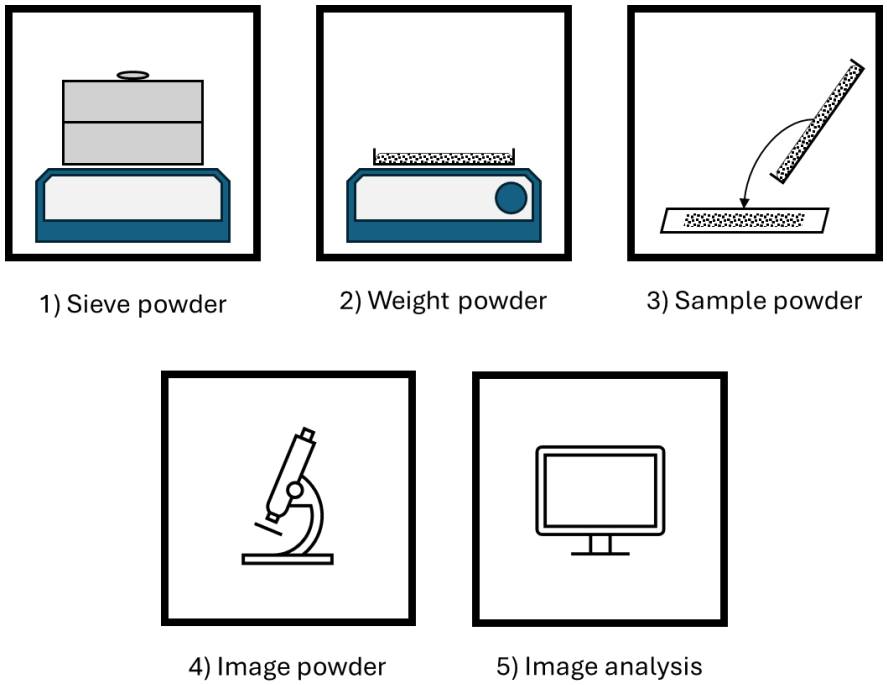


Figure 7.3: Method of image analysis used to determine particle size distribution of adsorbent powders.

Nitrogen Sorption Isotherms

Measurement of N_2 sorption isotherms was made using a Micromeritics TriStar 3000 Automated Gas Absorption Analyzer. Measurement was made for adsorption under relative vapor pressures in the range of 0.01 to 0.99 (based on atmospheric conditions). A static adsorption mode was used to ensure equilibration of adsorption at each relative pressure.

Prior to characterisation, samples were degassed overnight a temperature of 80C and near-vacuum pressure of 80 mbar. The temperature used, though low for traditional methods, was selected to avoid any change to the surface chemistry of SBAMs structure prior to collection of isotherms, based on consideration for robustness at this temperature in wider literature [185] and degassing methods typical within the Heng Research Group [186],[187].

Pore Geometry

Characterisation of pore geometry associated with adsorbents was carried out through combination of experimentally determined N_2 sorption isotherms and isotherm modelling. This was done to investigate both the specific surface area of the adsorbent as well as to provide understanding for pore size distribution.

Specific Surface Area

Estimates for specific surface area of powders was made by fitting sorption isotherm data to the BET adsorption model (see Equation 7.1) according to standard methods [185] using the implementation provided in the pyGAPS python package [188].

$$\frac{p/p_0}{n_{ads}(1-\frac{p}{p_0})} = \frac{1}{n_m C} + \frac{C-1}{n_m C}\frac{p}{p_0} \tag{7.1}$$

Where p is the measured pressure of the vapour (bar), p_0 is the saturation pressure of the vapour probe being used (bar), N_{ads} is the total amount of vapour probe molecules adsorbed (mol), n_m is the amount of material adsorbed in a statistical monolayer (mol/m^2), C is the BET constant (m^2/mol).

Pore Size Distribution

Estimates for pore size distribution of powders was made by fitting models to N_2 sorption isotherm data using the implementation provided in the pyGAPS python package [188]. The

micropore size distribution of adsorbent powders was calculated according to adsorption data from sorption of nitrogen vapor probes.

The BJH method was then used for pore size distribution measurement. the BJH model (see Equation 7.2) calculates effective pore size distribution of a powder sample (based on pore volume) by extension of Kelvin's equation for pore capillary condensation pressure of a vapor assuming a cylindrical pore geometry [185].

$$V_p = \left[\Delta V_n - \Delta t_n \sum_{i=1}^{n-1} \left(\frac{\bar{r}_{p,i} - t_n}{\bar{r}_{p,i}}\right) A_{p,i}\right] \left(\frac{\bar{r}_p}{\bar{r}_k + \Delta t_n}\right)^2 \quad (7.2)$$

Where V_p is the volume of pores (m^3) of size $\bar{r}_p$ (m), ΔV_n is the volume of gas adsorbed between two measurement points (m^3), Δt_n is the change in layer thickness between two measurement points (m), $\bar{r}_k$ is the average Kelvin radius between two measurement points (m and t_n is the layer thickness at point n (m).

Pore Blockage

Estimates for the extent of pore blockage present in functionalised (i.e. butyl and amine) powders were calculated based on the fraction of pore volume relative to the unfunctionalized (silanol) powder as shown in Equation 7.3

$$B_p = 100 \times \frac{V_{p,func}}{V_{p,ref}} \quad (7.3)$$

Where B_p is the blockage fraction of the functionalised powder (vol%), $V_{p,func}$ is the pore volume of the functionalised powder (m^3/kg), and $V_{p,ref}$ is the pore volume of the unfunctionalized powder used for reference (m^3/kg).

7.2.3. Adsorption Performance

Gravimetric Adsorption Capacity

The adsorption capacity of sorbents was carried out using a full immersion method. Therein, 0.5 g of adsorbent powder was mixed in 5 mL of vegetable oil, producing a solution with a solids content of 0.1 g/mL. The produced sample was then vortexer for a total of 5 minutes before being filtered through Whatmann (Type 1, < 11um pore size) filter paper under vacuum. A vacuum pump was used. This method is illustrated in Figure 7.4 below.

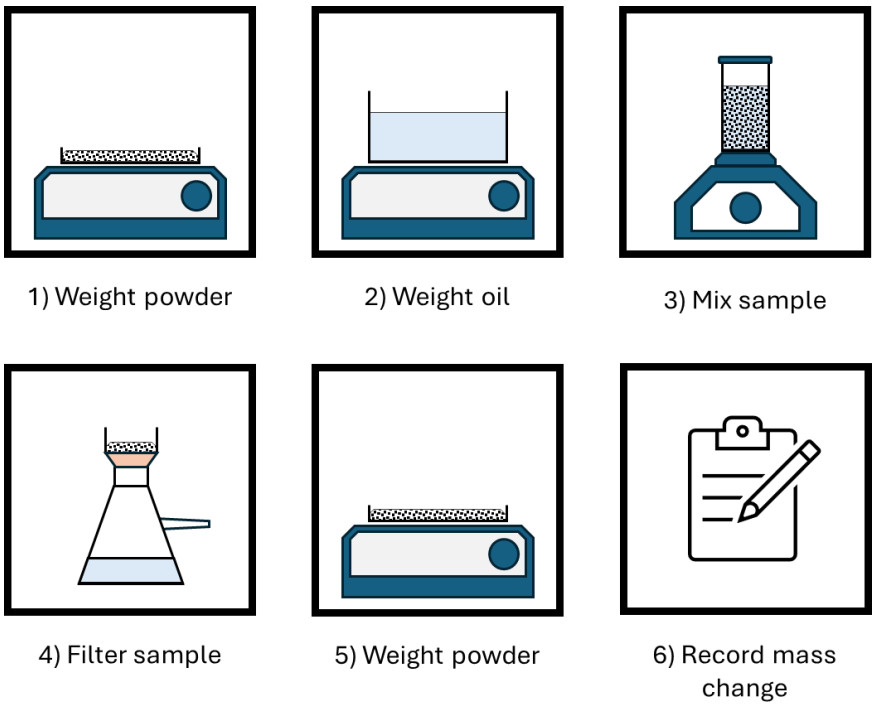


Figure 7.4: Method of immersion and filtration used to measure the adsorption capacity.

Oil Adsorption Capacity by UV-spectroscopy method

Sorption capacity of SBAM molecules were also measured according to spectroscopic methods. In this approach, the amount of oil adsorbed was inferred by calculating the amount of oil desorbed from powders in solvent solution. Information for absolute amount of oil desorbed was calculated based predetermined il-in-ethanol UV-vis absorption calibrations in the range of 0 to 5 wt% (experimentally observed saturation point) oil in ethanol.

Measurement of UV-vis absorbance of ethanol, and ethanol-vegetable oil solutions were carried out in-line using a Nanodrop apparatus. Measurement of UV-absorbance was selected at a wavelength of 270 nm. All measurements of absorbance are reported as an average based on a minimum of three readings.

A summary of the relationship of UV absorption (254 nm wavelength) with oil-in-ethanol concentration is shown in Figure 7.5 below. A quadratic calibration curve has been fit to approximate the absorbance-concentration relationship in the range of 0 to 5 wt% - representing the limit of solubility of the oil species.

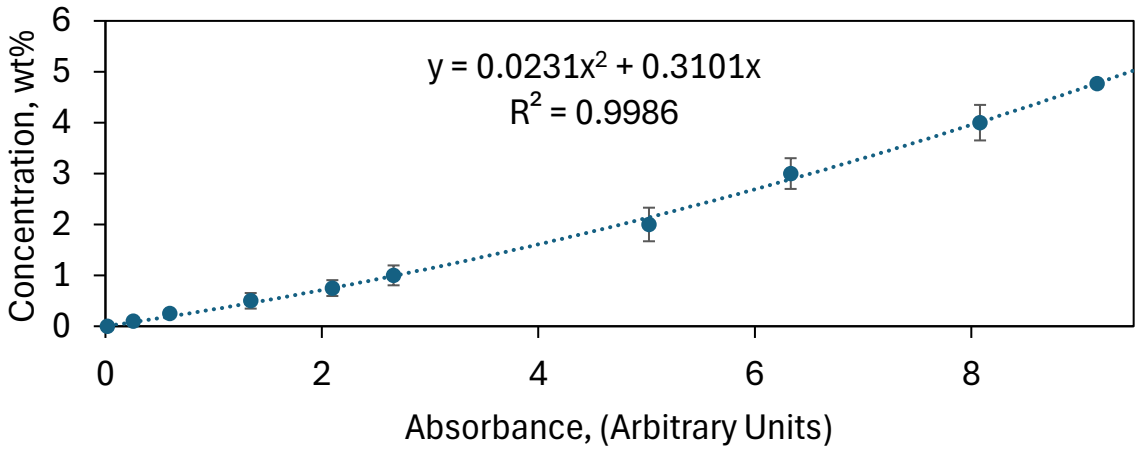


Figure 7.5: Relationship of UV absorbance at 270 nm with concentration of sunflower oil in ethanol.

Oil Recovery via Solvent Extraction

The potential for reuse of powders was investigated considering the use of solvent extraction to remove adsorbed material from used powders. To investigate the effect of solvent use on recovery efficiency, this involved iterative stages of powder dilution and mixing, solid-liquid separation, and solution concentration measurement via UV-vis spectrophotometry.

Extraction Solvent Choice

In all cases, ethanol was considered as the extraction solvent. The choice of an alcohol as the extraction solvent was made based on the potential for extraction solutions to be used directly in esterification of fatty acids to produce biodiesel. The use of ethanol specifically was decided based on the relatively low cost as an organic solvent, the use of alcohols within biodiesel synthesis [189], the lower toxicity compared to methanol, and the potential to produce ethanol from bio-derived sources (e.g. from sugars of crops or agricultural residues) to minimize food scarcity.

Sample Preparation

Preparation of samples was done by initially immersing used silica adsorbent in ethanol solution. Samples were vortexed to ensure mixing. Powder was then separated from the solution by centrifugation under 6000g force for 10 minutes. Solution samples of 5 µL were taken by pipetting. In all cases, the amount of powder and ethanol mixed was varied depending on practical experience to achieve extent of dilution that enabled sampling without

the entrainment of solid particles, or spinodal decomposition of solutions to form vegetable oil droplets dispersed within ethanol.

Powder Reusability

Measurements were taken for the adsorption of powder for a second and third use in adsorption to account for changes in the adsorption performance associated with reuse. This was done following method of adsorption and filtration, and liquid extraction discussed in Section 7.2.3. Solvent extraction was carried out in a single stage using a washing mass ratio of 50:1 with regards to solvent and adsorbed powder respectively. This value is certainly higher than the amount required but was used to ensure certainty in complete extraction of recoverable material after each run. An overview of the approach is shown in Figure 7.6.

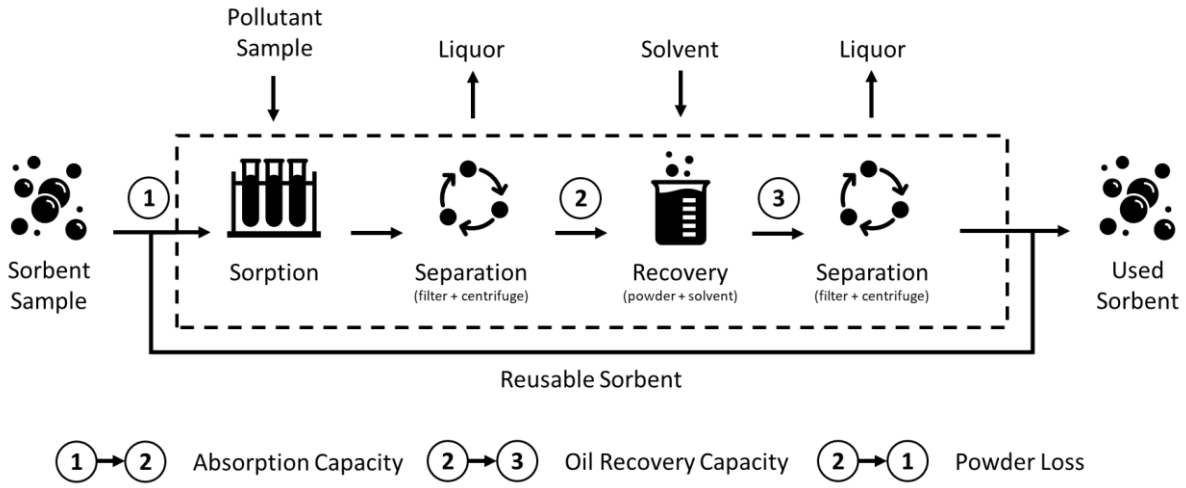


Figure 7.6: Illustration of method used for investigating reusability of adsorbent powders.

Calculation of the extraction efficiency associated with each solvent extraction procedure was calculated according to Equation 7.4.

$$E = 100 \times \frac{m_{des}}{m_{ads}} \tag{7.4}$$

Where E is the extraction efficiency (wt%), m_{ads} is the mass of material initially adsorbed (kg), and m_{des} is the mass of recovered following desorption (kg).

7.2.4. Life Cycle Inventory Modelling of Silanized Powders

Goal and Scope Definition

The goal of the LCA reported in this section is to provide estimations for the environmental impact associated with modification of surface chemistry of silica particles according to

standard post-synthesis silanization methods. This has been done focussing on the functional unit of producing one kilogram of functionalised powder.

Inventory Modelling

Inventory modelling of powder silanization has been carried out using a mixture of models developed within this thesis, and information from patent literature.

Life cycle activity associated with production of the silica substrate was modelled according to the model for precipitated silica reported previously in Chapter 4. Material use associated with SCA molecules in the have been taken based on values reported for functionalisation of colloidal silica with octyltrimethoxysilane in patent literature [138]; this includes material use associated with solvent washing associated with cleaning of functionalised powders. It has been assumed that functionalisation occurred using APTES and butyltrimethoxysilane as silanization agents for butyl and amine chemistries respectively. An energy use of 19.5 MJ./kg has been assumed to account for drying of powder after solvent washing; this value is taken based on amounts used for drying of water-wetted precipitated silica in EU industry [82]. Mass change associated with functionalisation of the powder has been assumed to be negligible. A powder loss of 1 wt% has been assumed to account for issues during purification and handling. Modelling of activity associated with the production of BTMS has been approximated using the model of OTMS.

A summary of the resulting inventories for amino and butyl functionalised silicas is shown in Table 7.2. Information on background process models is provided in

Table 7.3.

Table 7.2: Life cycle inventory data used to model activity associated with the production of butyl and amine functionalised silica powders.

Type	**Flow**	**Amount**		**Unit**
		Amine	**Butyl**	
Materials	Silica Powder	1.01	1.02	kg
	3-aminopropyltriethoxysilane (APTES)	70.70	-	mg
	Butyltrimethoxysilane (BTMS)	-	56.95	mg
	Water	1.68	1.68	kg
	Isopropyl alcohol	1.66	1.66	Kg
Output	Functionalized Silica	1.0	1.0	kg

Table 7.3: Inventory models used to account for background life cycle activity associated with products.

Inventory Item	Model	Region
Water	Market for water, deionised [a]	EU exc. CH
Isopropyl Alcohol	Market for Isopropyl Alcohol [a]	GLO
Silica Powder	Precipitated Silica [b]	RER
3-aminopropyl triethoxysilane	3-aminopropyl triethoxysilane [c]	RER
Butyltrimethoxysilane	Butyltrimethoxysilane [c]	RER

[a] Taken form the EcoInvent v3.10 database, [b] Taken from Chapter 4 of this work, [c] taken from Chapter 6 of this work.

7.2.5. Life Cycle Inventory Modelling of Recovered Oil

Goal and Scope Definition

The goal of the LCA reported in this section is to provide estimations for the environmental impact associated with recovering oil using a silica based adsorbent material and solvent extraction method. This has been done defining the functional unit as 1 kilogram of oil recovered, based on a combination of oil recovery observed experimentally. The scope of activity modelled during this approach includes all activities linked with the production of the SBAMs, vegetable oil recovery (via adsorption), solvent extraction of adsorbate (using ethanol), and adsorbent recovery. As the LCA is intended to be demonstrative in nature, it is assumed that the adsorbent is used only once, though recovery via solvent extraction and separation is included (see Figure 7.7).

All models were produced with consideration for the general European region to provide reasonable trade off in coverage and specificity.

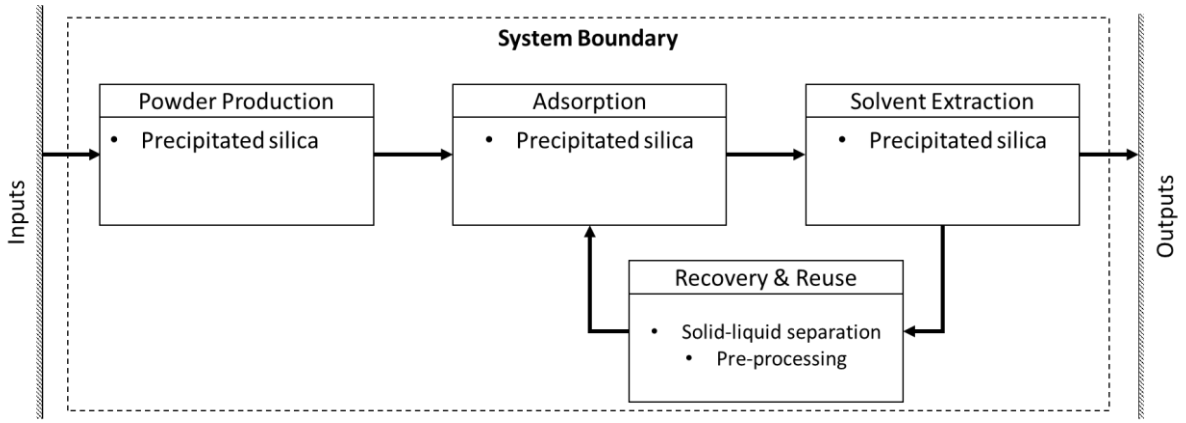


Figure 7.7: Scope of activity included in life cycle assessment of recovering fat, oil and grease-type pollution using silica based adsorbent materials.

Inventory Modelling

Inventories for material used are based on an aggregation of models already available within version 3.10 of the EcoInvent Database [157], models for silanized powders from this chapter (see Section 7.2.5), and additional estimates for material and energy use based on experimentation (this chapter) and expert judgement. A summary of data aggregation for each major activity is provided below.

SBAM Powder Production

Material and energy use associated with silica substrate synthesis was modelled using models for precipitated silica reported in Chapter 4 of this thesis. Activity associated with powder functionalisation was modelled according to inventories established in Section 7.2.4.

Adsorption and Solvent Extraction

Information on powder use and oil recovery amounts were taken directly from experimentation reported in in this chapter. Oil recovery was modelled based on experimentally determined re-use capacities. Assumptions therefore represent information taken at an experimental stage, the results of which are preliminary and may be subject to change relative to use on a larger scale.

Solvent Recovery

Given the demonstrative nature of the LCA, material and energy use associated with solvent recovery was assumed to occur via a solvent evaporation and distillation process. The extent of evaporation was assumed to target production of a residual oil-in-ethanol solution with mass ratio of 1:5 (oil:ethanol, i.e. 16 wt% oil) to reflect optimal ratio associated with the production of biodiesel [190].

Distillation was assumed to operate to produce a stream of pure ethanol. This is on the basis of large differences in the boiling point of ethanol (~78 C) and smoke and boiling points of sunflower oil (typically > 200 C [191]), which suggests ease of their separation.

Energy use associated with the distillation was estimated based on the heat of evaporation of pure ethanol. Recovered ethanol was assumed to be recycled, and therefore offset overall ethanol demand.

Assumptions therefore represent an estimate for solvent recovery performance based on theoretical grounds – likely better representing manufacturing scale estimates by excluding inefficiencies likely to occur at the experimental stage.

Powder Regeneration

Powder regeneration has been assumed to occur according to a thermal method in which residual solvent retained by the powder is removed by evaporation. For simplicity, estimates for energy use associated with this are assumed based on typical energy for drying of commercial silica powders in industry [82] (see also Chapter 4) – i.e. 19.5 MJ/kg. Assumptions therefore represent an estimate for drying performance based on large-scale engineering operations as opposed to lab-scale information.

A summary of life cycle inventory models associated with each inventory flow is provided in Table 7.5.

Table 7.4: Life cycle inventory information used in modelling the recovery of vegetable oil using adsorbents.

Stage	Flow	Amount			Unit
		Silanol	Butyl	Amine	
Input	Functionalized silica gel	2.04	-	-	kg
	Butyl functionalised silica gel	-	4.17	-	kg
	Amine functionalised Silica gel	-	-	3.03	Kg
	Ethanol	19.00	19.00	19.00	kg
Energy	Steam [a]	17.3	17.3	17.3	MJ
	Heat (Natural Gas) [b]	39.80	17.30	59.09	MJ
Output	Recovered Vegetable Oil	1.00	1.00	1.00	kg
	Recovered Ethanol [c]	18.80	18.80	18.80	kg

[a] assumed use for ethanol evaporation, [b] assumed use for powder drying, [c] assumed equivalent to input ethanol, and therefore interpreted as an offset during impact assessment.

Table 7.5: Inventory models used to account for background life cycle activity associated with products.

Material	EcoInvent Model	Region
Functionalized silica gel	Precipitated silica [b]	RER
Butyl functionalised silica gel	Butyl functionalised silica [c] (see *Section 2.4.2*)	RER
Amine functionalised Silica gel	Amine functionalised silica [c] (see *Section 2.4.2*)	RER
Ethanol	Ethanol, 99.97 wt%, from ethylene source [a]	RER
Steam	steam production, as energy carrier, in chemical industry [a]	RER

[a] Taken from the EcoInvent v3.10 database, [b] taken from Chapter 4 of this work, [c] taken from Section 7.2.4 of this chapter.

7.2.6. Environmental Impact Assessment

Life Cycle inventories were converted into environmental impact metrics using impact characterisation factors provided in the ReCiPe 2016 method [71]. Given that the LCA is based on preliminary laboratory work, and owing to the intended demonstrative nature of the LCA provided, only Global Warming Potential has been considered as an impact category.

7.3. Results

7.3.1. Experimental Results

Characterisation of Adsorbent Powders

Results from image analysis of powders are shown in Figure 7.8**.** This is in line with expectation, given that the powders are based on the same underlying silica gel. Overlapping particles through images were found not to be physically bound to each bound to each upon handling.

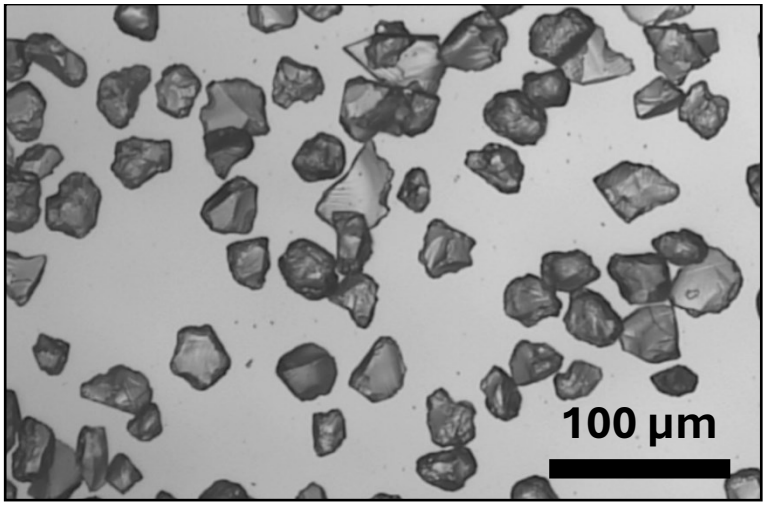
Adsorbent Pore Geometry

Nitrogen sorption isotherms associated with each of the four adsorbent powders considered are shown in Figure 7.9. Results associated with fitting of the BET adsorption model to data, and a summary of model fitting statistics are provided in Figure 7.9 and Table 7.6 respectively.

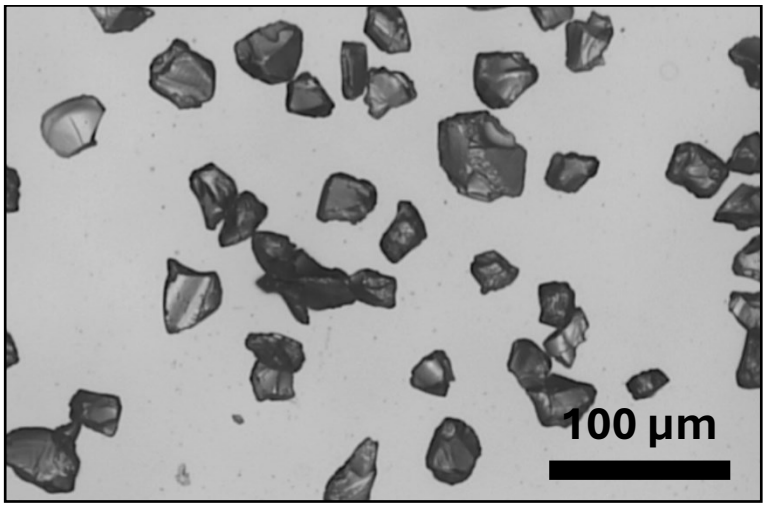
Results in Figure 7.9 reflect the nature of the IUPAC Type IV(a) isotherm, which is associated with mesoporous oxide gel adsorbents [10]. This is unsurprising given that silica (i.e. silicon dioxide) gel systems being considered in this work. The |type IV(a) isotherm is indicative of weak adsorbent-adsorbate interactions including capillary condensation within a mesoporous solid [8]. The nature of hysteresis of adsorption isotherms reported in Figure 7.9 appear to match that of the IUPAC Type H5 [10]. Type 5 hysteresis is commonly associated with porous solids that have a mixture of open and partially blocked pores [10].

No significant low-level hysteresis is observed at relative pressures below the boiling point of Nitrogen ($p/p_0 = 0.42$).

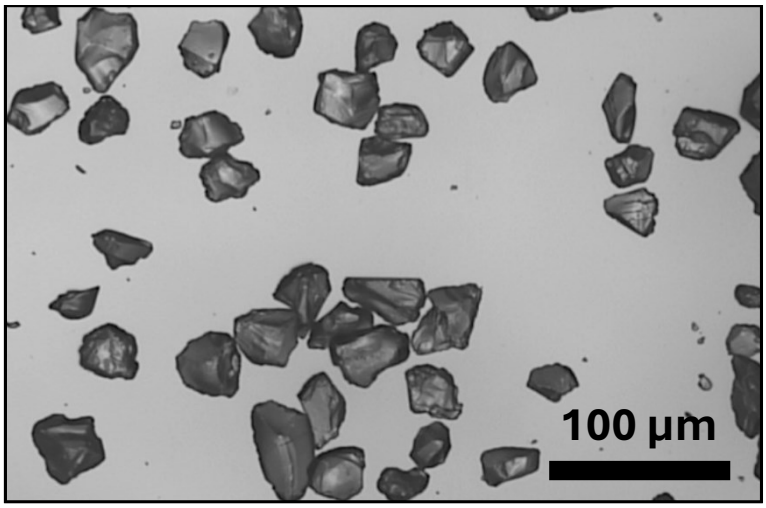
Importantly, onset of plateau near relative pressure of 1 (within measurement error) also suggests reliability of assuming that the powder is completely saturated prior to the onset of the desorption loop. This may suggest reliability of the observed desorption isotherm (Barrett *et al*., 1951).



(a)



(b)



(c)

Figure 7.8: Representative images of adsorbent powder with (a) silanol, (b) butyl, and (c) amine powders taken via optical microscopy.

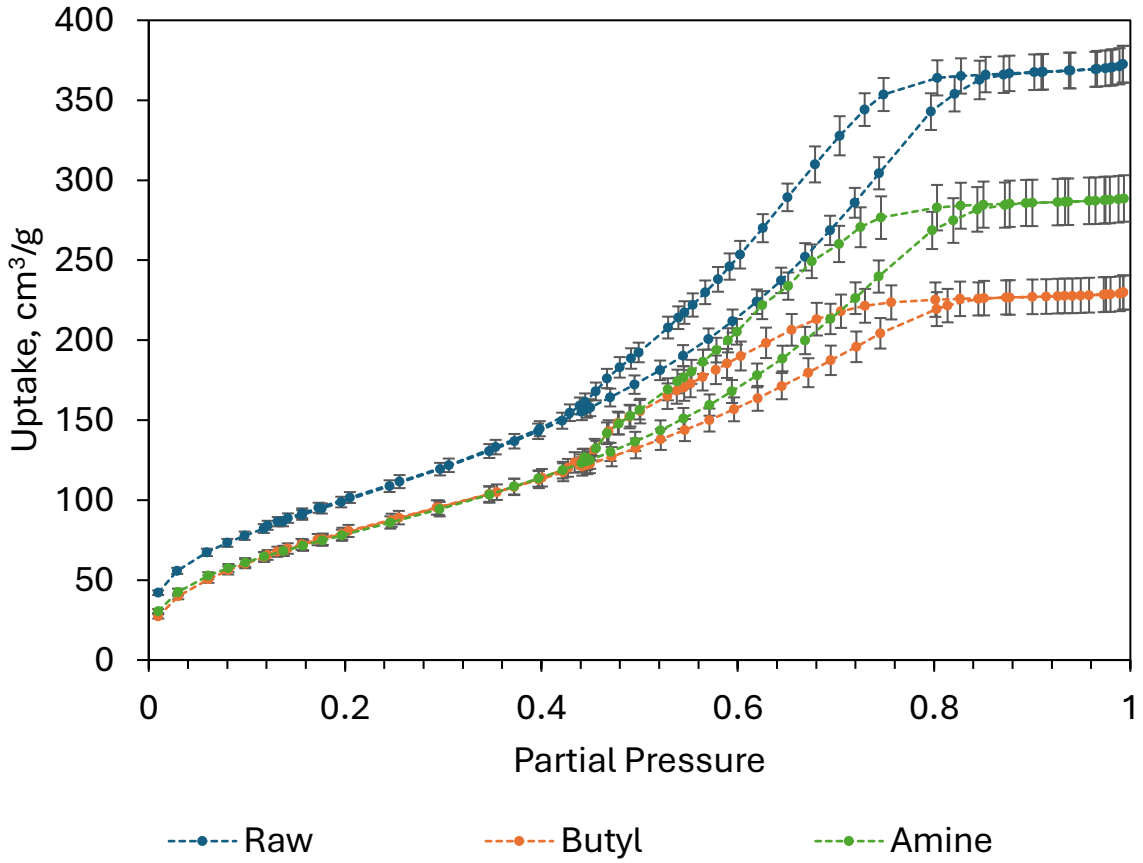


Figure 7.9: Nitrogen adsorption isotherms associated with silica gels with silanol, butyl, and amine surface chemistry. Error bars represent standard deviation based on analysis of a total of three repeats per sample.

Table 7.6: Summary of BET model parameters identified for adsorbent powder nitrogen adsorption isotherm.

Characteristic	Silanol	Butyl	Amine
BET Surface Area, A [m^2/g]	371.8 ± 0.2	306.7 ±0.3	296.0 ±0.1
BET Constant, C [kJ/mol]	46.7	33.1	42.2

Crucially, it may be observed that relatively similar adsorption isotherm occurs for both functionalised surface (butyl and amine) when compared to the silanol surface chemistry in the range of 0 to 0.45 partial pressure. This suggests fundamental changes in pore range for the functionalised SBAM powders. Given that powders are produced from a common silica gel substrate, this suggests potential pore blockage associated with the functionalisation of powders.

Specific Surface Area

Results of BET analysis indicate significant differences in the surface area of all three powders considered, in order of decreasing value silanol > butyl > amine. On the contrary, BET

constants associated with each surface also differ in. Importantly, absolute value of the BET fitting constant, *C*, are relatively low (i.e. C < ~50). This indicates that a significant overlap in pressures at which monolayer and multilayer coverage occur, which is not unexpected given previous works of surface modified mesoporous silica gels. In other words, this may suggest that extent of adsorbent-adsorbent interaction is not significantly different from adsorbate-adsorbate interactions [11]. For example, reductions in the value of *C* from ~ 120 to ~20 dependent on the extent of surface coverage considered [7]. However, it does mean that the assumption monolayer coverage present in BET model falls somewhat into question [8]. Consequently, specific surface areas reported in Table 7.6 should not be considered as 'real', but rather as a general metric for the level of activity of nitrogen on each surface [8].

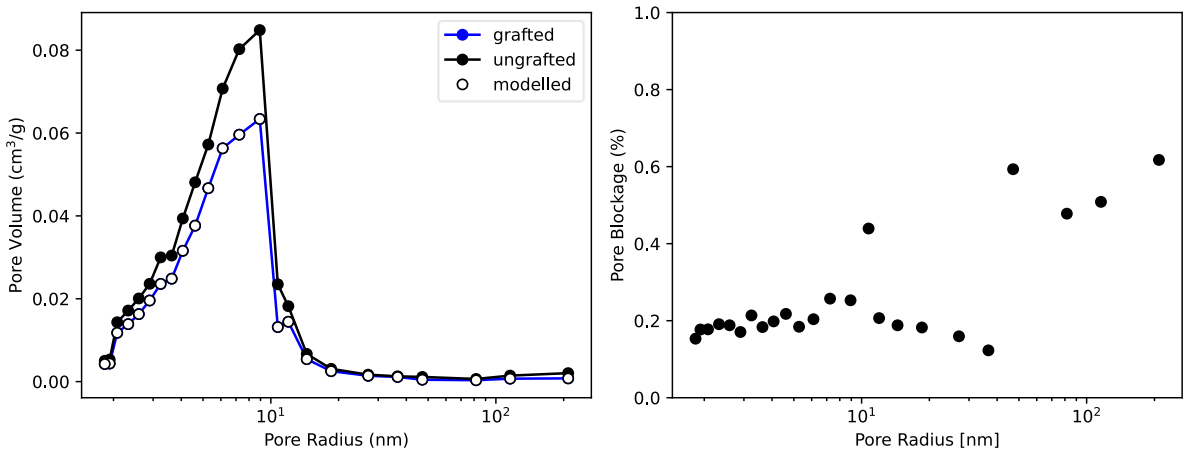
Nonetheless, it must be noted that regardless of the tendency for the BET to reduce with functionalisation, the initial BET constant for unfunctionalized silica (i.e. silanol chemistry) also corresponds to a C < 50.

Nature of Pore Blockage

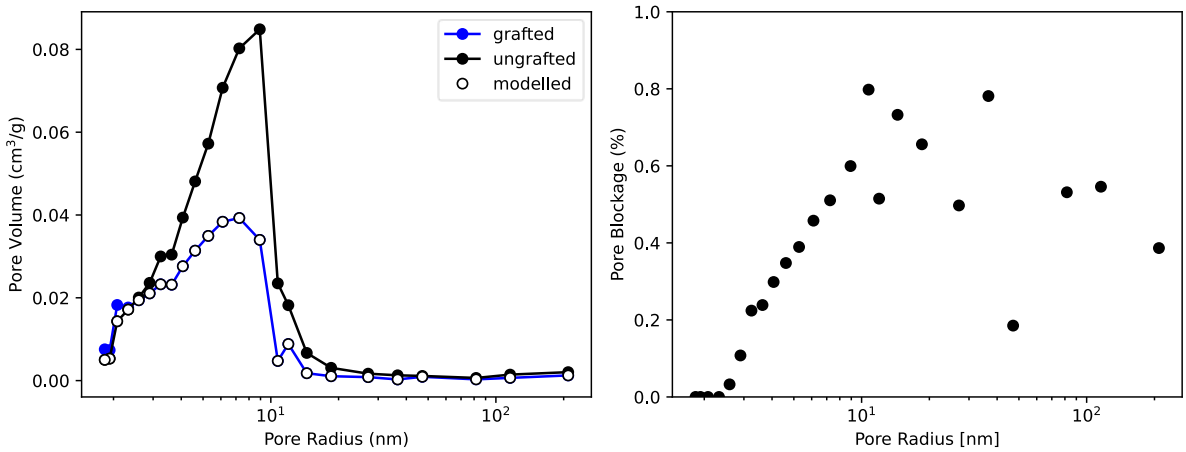
Observation of a Type 5 hysteresis loop, and reductions in available surface are of functionalised powders suggests the presence of blocked pores. Results in Figure 7.10 illustrate the extent of pore blockage implied for butyl and amine functionalised silica based observed pore volume relative to the unfunctionalized silanol powder both as aggregated functions, and as a function of pore size.

Results for show interesting differences in the relationship of pore size and pore blockage extent for adsorbent powders of differing surface chemistry. Particularly, it is observed that the extent of pore blockage of all powders increases with pore size over the size range considered (4 to 200 nm). Additionally, the maximum extent of pore blockage appears to remain roughly consistent at 80 vol% for all powder considered.

However, beyond this, results suggest marked differences in pore blockage phenomena for pore sizes in the 4 to 25 nm and 25 to 200 nm size ranges. This is of interest given that both the butyl and amine powders are known to by manufactured from functionalisation of the underlying silanol powder considered in the work (give or take batch-to-batch variation, see also Section 7.2.1). Further information on phenomena in each of these size ranges are discussed separately below.



(a)



(b)

Figure 7.10: Relationship of pore size and effective pore blockage associated with adsorbent powders modified with (a) amine and (b) butyl surface chemistries

Results for pore blockage in the 4 to 25 nm size range show clear differences between the amine powder compared to the butyl and amine powders. Firstly, it is observed over this range that powders with surfaces modified using amine chemistry show a far more consistent extent of pore blockage within the size range (round 20 vol%) when compared to the butyl chemistry, which display a positive linear correlation between pore size and pore blockage within the size range. Reasons for lowered blockage of amine surfaces may be due to any of the following factors:

1) Differences in the natural ability of organosilane reagent to diffuse into pores in this size range,

2) Reduced diffusion of organosilane into the pores due to blockage occurring as part of silanization procedure
3) Differences in tendency for silanization reagents to self-assemble, aggregate and block pores.
4) Inability for packing of nitrogen into the pores, given that the size range considered covers pores approximately 10 times the size of nitrogen and therefore packing effects are unlikely to be significant.

Points 1, 2 and 3 would require further research and understanding of the methods of silanization use, which are not available for these commercially purchased powders. Consequently, they are not considered further in this work. This is justified given the motivation for research is primarily on life cycle assessment of adsorbent design, and therefore awareness of differences in powder are satisfactory rather than deep mechanistic understanding.

Results the contrary, results for pore blockage in the 25 to 200 nm size range show more consistent tendency for all powder considered. Particularly, a reduction of approximately 20 vol% is observed for all pores of size roughly 50 nm radius.

Finally, it is worth noting that all three powders exhibit a shared, common depression in the amount of pore volume associated with a pore size of approximately 10 nm, which corresponds with a roughly consistent extent of pore blockage of 50 vol%. This is curious considering the otherwise large differences in in pore blockage phenomena identified for each powdered in the 2 to 25 nm pore radius size range (as above).

Moreover, it may be added that the rough extent of blockage for butyl in the pore size range of 20 nm to 200 nm also appear to display a relatively consistent, irregular trend. Particularly, it appears as though a consistent drop pore size of 10 nm occurs relative to unfunctionalized silica for all three powders. The reason for this reduction in pore size is unknown but may hold information associated with the interconnectivity of pores of carrying sizes within the porous network of each powder.

Reasons for differences may include:

1) underlying differences in powder used for each surface modification arising from natural production variations,
2) differences in off-gassing performance due to different adsorption affinities of each powder
3) differences in the extent of wettability of functionalising agent in pores during surface modification, leading to differing extents of pore penetration/blockage.

Additionally, it is necessary when considering trends in the relationship of pore size and pore to consider that datapoints may not be statistically independent from one another. Though the underlying skeletal structure of each powder may be equivalent – owing to the creation of each powder from the same underlying silica gel.

The reasons for differences in the blockage of different systems are not yet understood and will not be considered further in this work. Nonetheless, the visualisation of differences in the size-specific blockage of pores provides useful insight into the differences of adsorbent powder porosity, which may influence adsorbent performance considered later in this work. Consequently, results in Figure 7.10 provide relevant information when considering challenges in control of differences in adsorbent design at the microscopic level. Further research into understanding of the effect of surface chemistry choice and processing choice on pore-selective blockage may be of future interest for improved design of pore with controlled pore-surface engineering. Future work could use visualisation method shown in Figure 7.10 to better understand the extent of blockage of pores as a function of processing history.

Adsorbent First Time Use Performance

Results for the first time-use oil adsorption capacity of silanol, amine and butyl powders (gravimetric method) are shown in Figure 7.11.

Results in Figure 7.11 show consistent ranking of powders based on adsorption capacity across the three vegetable oils considered. Interestingly, this includes consistent low-ranking of the butyl surface chemistry. This may seem counterintuitive given the hydrophobicity of the butyl chemical group and expected non-polarity of “oil” substances. However, chemical interactions may partly explain this effect for two reasons.

Firstly, the improved capacity of silanol and amine groups may be related to the ability of silanol and amine groups to interact strongly with carbonyl groups present within the

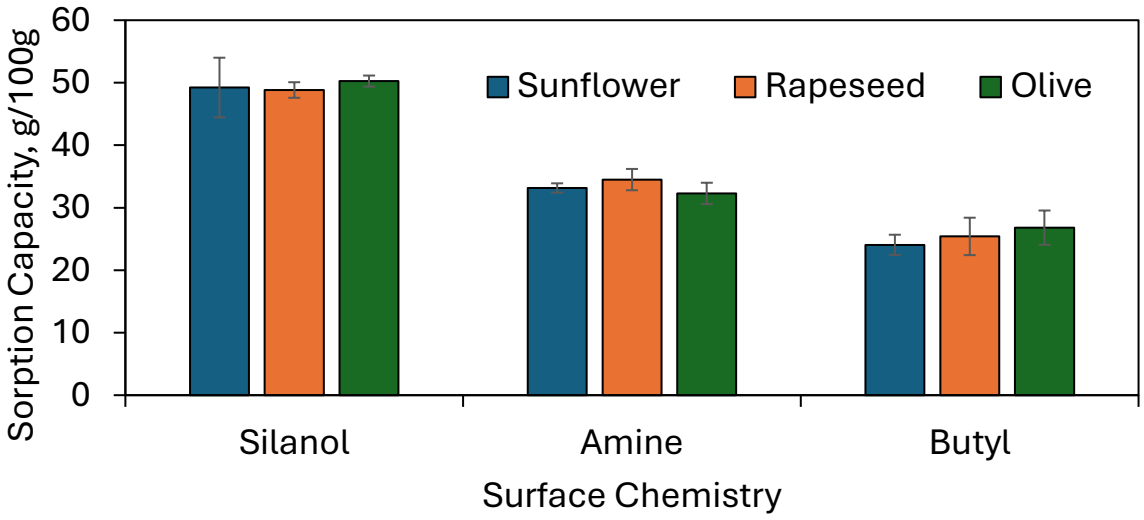


Figure 7.11: Adsorption capacity of various vegetable oils during first-time use of adsorbent according to gravimetric methods post-filtration.

triglyceride structures in vegetable oils via hydrogen bonding [192] – as shown in Figure 7.12. These stronger interactions may benefit the adsorption through increasing the driving force for the wetting of adsorbent surfaces capable of hydrogen bonding.

Secondly, the directionality of hydrogen bonding may have beneficial secondary effects on the structuring of adsorbed monolayers by causing nonpolar organic chains to oriented away from the adsorbent surface. This may benefit the formation of multilayer structures, formed on nonpolar interactions between fatty alkane chains present in triglycerides and other chemicals present in vegetable oils (see Figure 7.12b). This may improve the affinity of the "surface" over which the bulk vegetable oil liquid flows as it is imbibed into the pore network of the adsorbents, increasing the thermodynamic driving force for uptake of vegetable oil.

Adsorbent Re-use Performance

Results in Figure 7.13 illustrates the relationship between extraction solvent usage and sunflower oil extraction, as observed for powders with silanol, butyl and amine surface chemistry. Vertical lines in the figure indicate the theoretical minimum solvent amount required for complete extraction of adsorbed oil; this is based on ultimate powder adsorption capacity (taken from the maximum solvent usage considered), and the 5 wt% saturation concentration observed for the sunflower-oil system. Where observed absorbance implies an oil-in-ethanol concentration above the experimental saturation concentration (5 wt%) are plotted as at-saturation as highlighted within the plot.

Results in Figure 7.13 show reasonable agreement between solvent ratio reaching saturation and the theoretical value based on the experimentally observed oil-in-ethanol saturation concentration. This is consistent for all surface chemistries considered – suggesting that ethanol extraction may be solubility-limited rather than adsorption limited process.

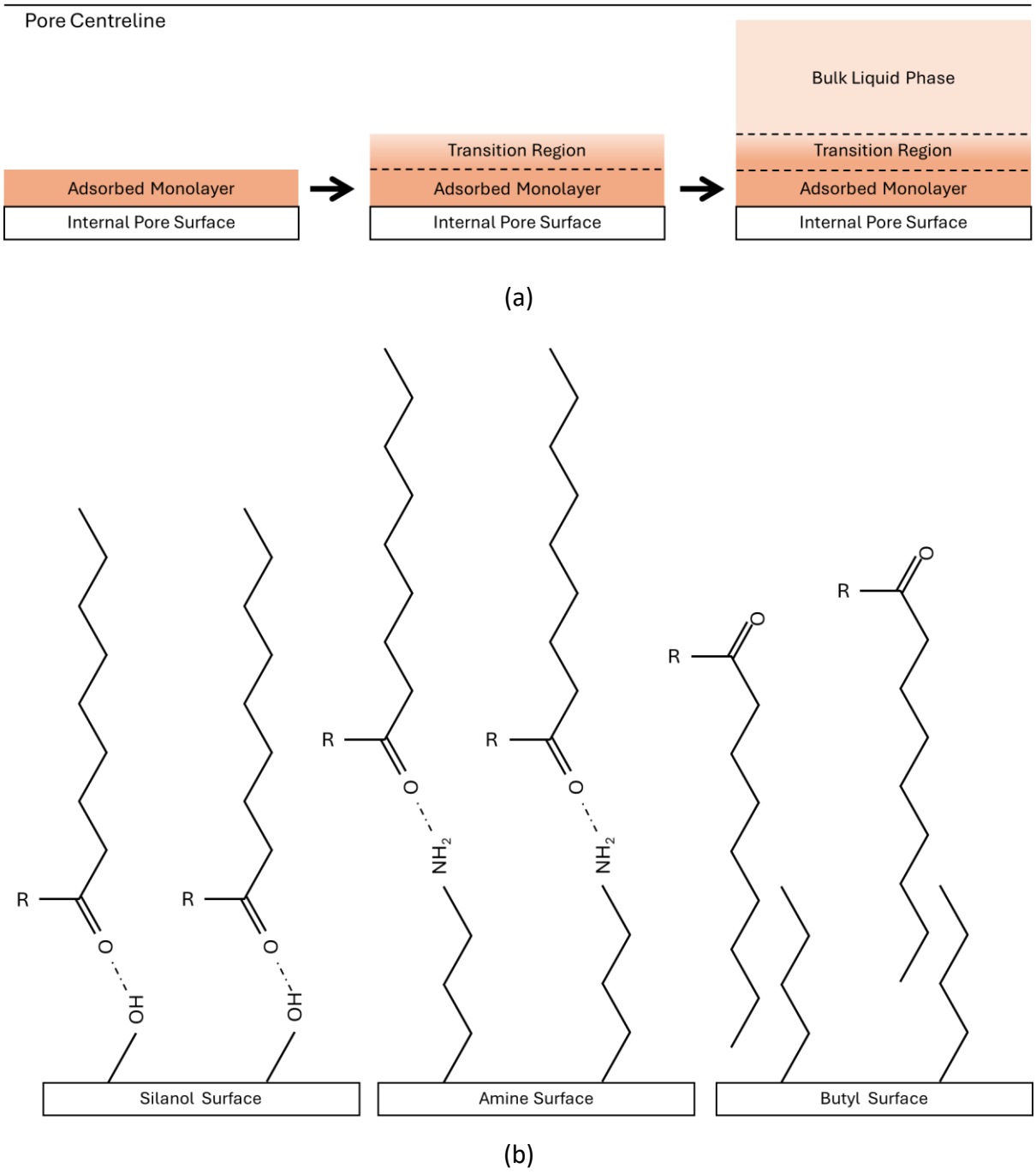


Figure 7.12: Schematic representation of key phenomena in adsorption of vegetable oil in adsorbent pores including (a) physical filling based on monolayer adsorption, transition to multilayer adsorption, and subsequent pore filling with a bulk liquid phase, and b) difference in bonding possible between adsorbents with silanol, amine and butyl surface chemistry and their effect on orientation of the monolayer structure, where dashed lines between hydrogen and oxygen groups indicate the presence of hydrogen bonding.

Interestingly, it may be observed that results for oil adsorption capacity in Figure 7.13 indicate higher oil adsorption capacities than was observes for gravimetric methods. This is believed to arise from powder loss in glass vessels during mixing, pouring and filtration according to the gravimetric method, which may reduce the mass observed for adsorbed powder.

Finally, it is noted that extraction efficiencies greater than 100% are observed for all adsorbents for the solvent use line. These results reflect overestimates for the overall amount of adsorbate likely to have been extracted, which may be attributed to combined sources in error associated with the method used. Firstly, the presence of these values near the minimum solvent requirement line (vertical lines) reflects systems with oil-in-water concentration near the solubility limit. Values in this area may be affected by unintended scattering of UV radiation, causing measurement of increased absorbance and therefore systematic overestimation of oil present in water. Scattering may have arisen from either 1) the presence of ethanol-in-oil droplets in the solution, formed by the tendency of ethanol-vegetable oil systems to undergo spinodal decomposition as a result of their mutual solubility [193]. Similarly, scattering may have arisen from unintended entrainment of powder when taking liquid samples; this is particularly plausible for the samples nearer the saturation line as these represent samples with lower solvent-to-adsorbate ratios, and therefore less head space from which to sample liquid after solid-liquid separation via centrifugation. Consequently, further work is required to refine the methods detailed within this work.

Results in Figure 7.14 then show adsorption capacity observed for silanol and butyl powders after first and second use. Values are based on oil extracted using 50kg of ethanol per kilogram of adsorbed powder reflect high extraction efficiency (as per Figure 7.13). Amine powder was not considered due to similarity in the adsorption capacity to the butyl powder observed during first-time use experiments (see Figure 7.11).

Results in Figure 7.14 show a relatively consistent adsorption capacity for the butyl chemistry after reuse. Conversely, results for the silanol surface show marked difference in the adsorption capacity after solvent extraction and reuse. This is believed to reflect the presence of ethanol residuals in the silanol powder which are not recovered during centrifugal drying stage – reducing the amount of porosity available to sorb oil upon further reuse. This finding highlights the need to consider the ease of solvent-sorbent recovery (during drying) on top of ease for adsorbate extraction when selecting the extraction solvent.

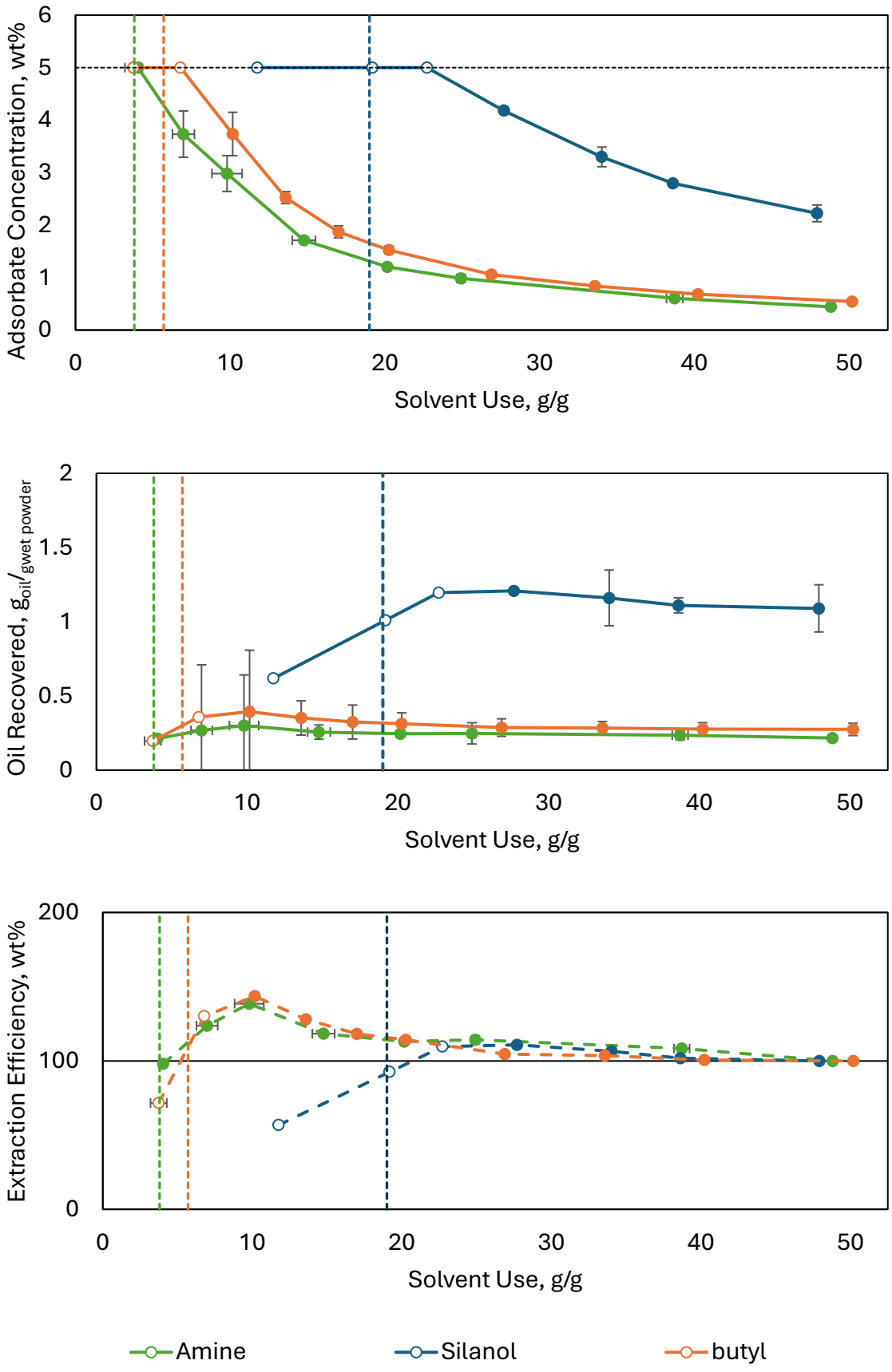


Figure 7.13: Effect of solvent use ratio on the concentration of sunflower oil present in the extraction solvent (a), implied total amount of oil extracted (b), and extraction efficiency (c). Markers with a white fill represent observations associated with a saturated oil-in-ethanol solution.

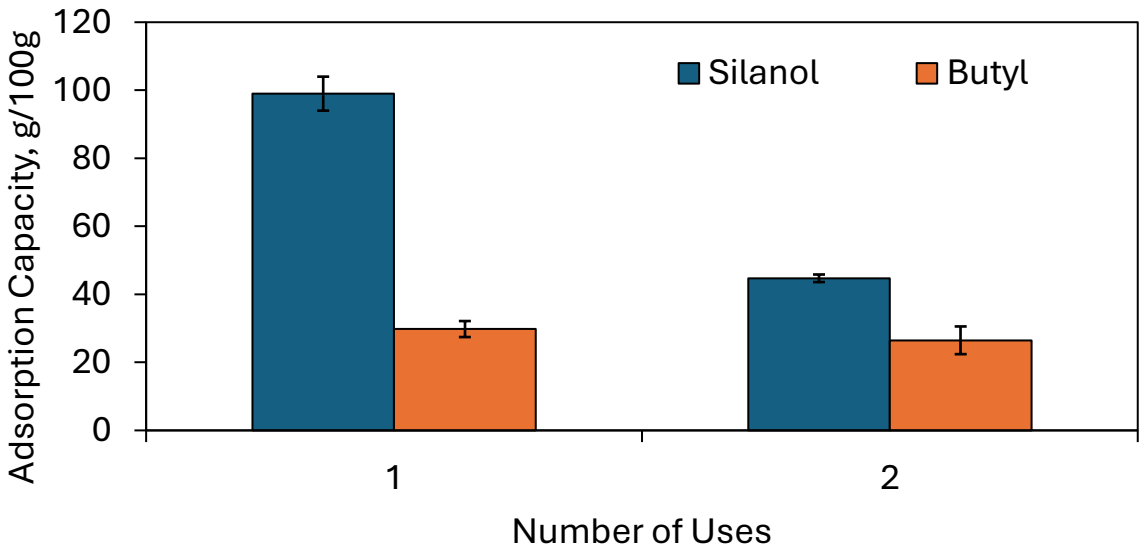


Figure 7.14: Adsorption capacity of adsorbents with silanol and butyl surface chemistry before and after re-use.

7.3.2. Environmental Impact of Adsorbent-based Oil Recovery

Impact Assessment and Contribution Analysis

Figure 7.15 summarises environmental impact associated for SBAMs based on the theoretical use case defined in Section 7.2.5 (ethanol-based solvent extraction, ethanol recovery by distillation, and powder regeneration by thermal drying). Results are based on one-time use to illustrate maximum contribution of adsorbent production to the abatement cost of using each SBAM.

Results in Figure 7.15 show carbon footprint of 12.1, 17.2, and 39.9 kg_{CO2}-eq per kilogram of oil recovered using SBAMs with silanol, butyl and amine surface chemistry respectively. This indicates the silanol SBAM as being the preferred option (of those considered) for minimising impact associated with recovering sunflower oil on a per kilogram basis. Interestingly, it is likely that this finding is likely also to agree with the cost optimal scenario (of scenarios considered) given that:

1) the silanol chemistry does not involve the additional silanization step that amine and butyl SBAMs require,
2) the amine and butyl SBAMs use the silanol powder as their underlying silica substrate,
3) energy use associated with the silanol scenario is also lowest of those considered (see Figure 7.15 or refer to Table 7.4).

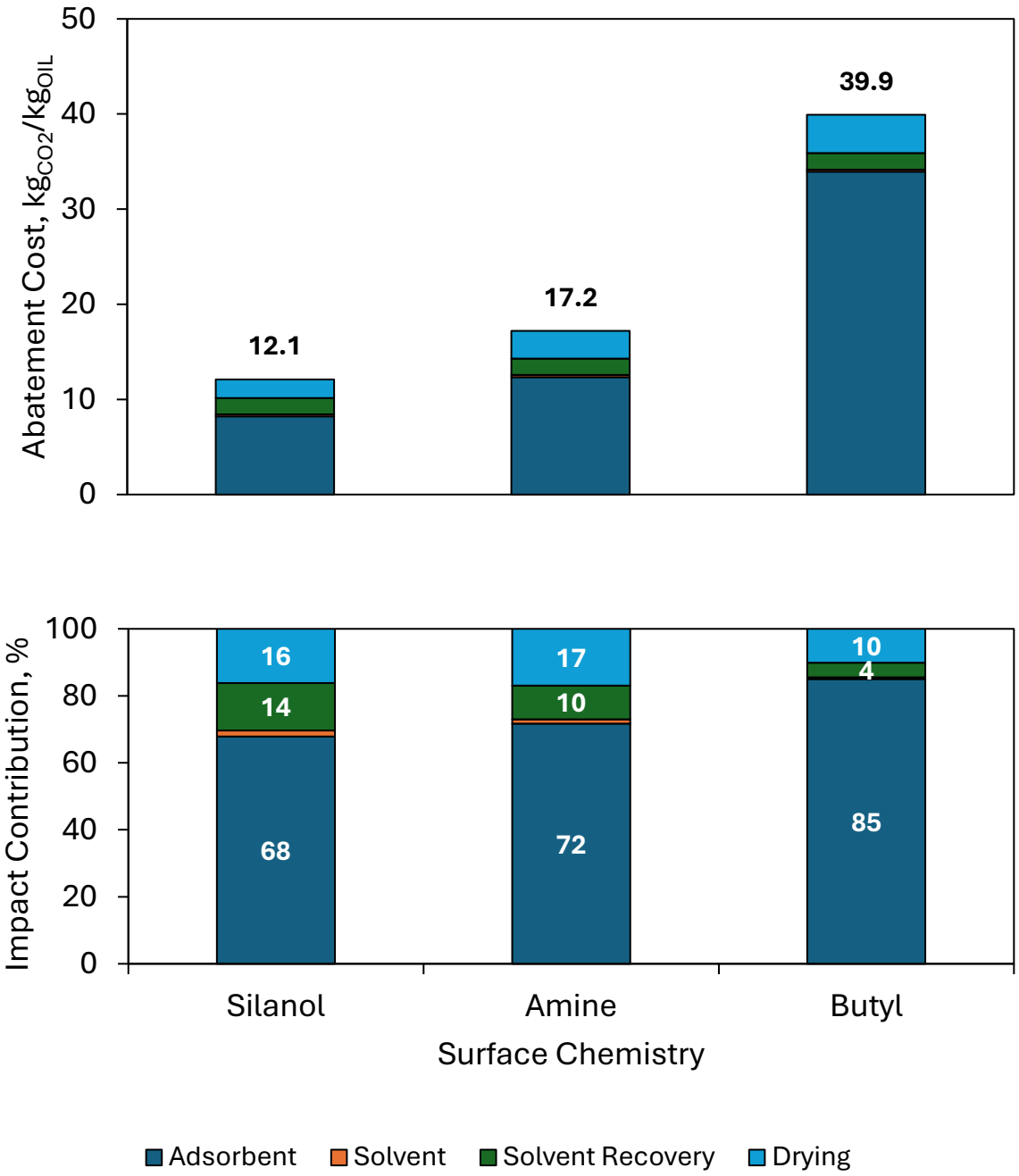


Figure 7.15: Environmental impact predictions for the recovery of sunflower oil using adsorption-solvent extraction process (top) and associated contributions based on activity category (bottom). Results are based on impact assessment assuming one time use of adsorbent.

In all cases, the SBAM is the main driver of overall impact, accounting for 68, 72, and 85% of impact associated with silanol, amine, and butyl scenarios respectively. These differences in contribution are attributed to combined factors of:

1) difference in adsorption performance associated with each chemistry (see Figure 7.13),

2) the use of silanization in producing butyl and amine SBAMs (compared to the silanol SBAM),

3) differences in processing during the silanization of amine and butyl surface chemistries.

Following adsorbent use, adsorbent drying (during regeneration) and solvent recovery (i.e. ethanol distillation) the second and third largest contributors to environmental impact (GWP) for the SBAMs considered. More specifically, drying accounts for 16, 17 and 10% of the GWP of silanol, amine and butyl scenarios, whereas solvent recovery accounts for 14, 10 and 4% respectively.

Results for adsorbent drying and solvent recovery contributions are notable as these factors (SBAM drying and solvent recovery) are the main sources of energy use in the reported LCA. Additionally, both factors are based on energy use predictions that are estimated using favourable assumptions of industrial scale thermal efficiency in the case of powder drying, and quantitative energy efficiency in the case of ethanol evaporation during distillation. Excluding consideration for any potential energy recovery during solvent recovery (which is unlikely, giving the low temperature required for ethanol distillation), this suggest that the impact contribution associated with energy use (3.6, 4.6 and 5.6 kg CO_2-eq/kg oil for silanol, amine and butyl SBAMs respectively) may reflect practical lower limits associated with the recovery method considered within the scope of the LCA.

Results also show that the contribution of solvent (i.e. ethanol) use is relatively low for the process, for 2% of the GWP of the silanol scenario and less than 1% of the GWP of the amine and butyl scenarios. This outcome is heavily related to the assumption that ethanol can be recovered and reused by the hypothesised solvent recovery method (i.e. distillation). As a result, the impact in all cases is limited to the amount of ethanol designed to be left with the residual sunflower oil – which was set as 0.2 kg ethanol per 1 kg of recovered oil (an optimal ratio for potential biodiesel production [190]) within this work. The significance of this finding should therefore be considered with a degree of scepticism based on the extent to which complete recovery of ethanol can be expected during distillation, and the extent of ethanol that is desired to be left with the extracted sunflower oil.

Finally, impact contributions associated with solvent recovery and solvent use are limited to the choice of extraction solvent used (i.e. ethanol) – which must be understood when making responsible decisions for sustainable development along this research direction in the future.

Sensitivity of Impact Predictions to Powder Reuse

Findings in Section 7.3.2 identifies the silanol SBAM as the lowest GWP option for recovery of sunflower oil under the theoretical recovery scenario considered. However, it must be noted that this is based on results that consider environmental impact predictions assuming one-time use of the SBAM materials – i.e. neglecting benefits of potential adsorbent re-use. If powders are to be reused subsequent times, this may lead to changes in the contribution of individual life cycle activities (e.g. adsorbent use,) to the overall impact of each SBAM use case, as well as the ultimate value of the impact itself. Consequently, a discussion on factors for consideration are provided below.

Adsorbent Use

The effect of adsorbent reuse may significantly change the impact predictions in multiple ways. This is due to two main reasons.

Firstly, the reuse of powder will reduce the absolute impact contribution associated with adsorbent use by increasing the amount of oil recoverable per kilogram of SBAM used. This effect will follow a consistent trend across all SBAM conditions considered, and therefore will not affect the relative ranking of impact associated with adsorbent use when comparing the across SBAM use case scenarios.

Secondly, the reuse of SBAMs may lead to an observed change in the adsorption capacity of powders as a function of number of reuses. Typically, it would be expected that this leads to an overall reduction in performance of the material over time. Nonetheless, differences in the rate of change of adsorption capacity may lead to differences in the relative ranking of each SBAM strategy. Given lack of experimental information considering a long-term adsorbent work, it is hard to account for how important this effect will be. Nonetheless, results in Figure 7.14 indicate that consideration in adsorption performance should be considered in future work.

Powder Drying

It is uncertain whether absolute contribution of powder drying to LCA results will change as a function of SBAM. In this case, the effect of reuse on the contribution of powder drying will be dependent on changes in adsorption capacity associated with the SBAM being used. If adsorption capacity on reuse remains constant, then the contribution with also remain

constant; this reflects the fact that the energy for powder drying (19.5 MJ/kg SBAM) will remain constant, but changes in adsorption capacity will change amount of oil recovered per cycle – thereby changing the amount of drying energy use per cycle. Assuming adsorption capacity decreases with SBAM reuse, the absolute value of the GWP contribution associated with powder drying may increase as a function of number of SBAM reuses. The extent of this change will be SBAM dependent and therefore may affect ranking of SBAM scenarios – suggesting a case for further research.

Solvent Recovery

The absolute contribution of solvent recovery to the impact of SBAM scenarios is not likely to change significantly with powder reuse. This is because, as discussed in Section 7.5.2, the amount of solvent used (per kilogram of oil recovered) is solubility-limited This implies that amount of ethanol recovered is constant per kilogram of oil recovered, and therefore the energy use associated with distillation is too. By extension, the energy required for drying and solvent extraction are therefore unchanging (on an amount per kg oil recovered basis) unless changes in adsorbent capacity occur.

Solvent Use

The effect of solvent use is not expected to change the impact predictions with reuse. This is because current accounting for solvent use within the LCA reflects the residual amount of ethanol left with the recovered vegetable oil in a ratio of 0.2 kg ethanol per 1 kg of sunflower oil. As the functional unit considered is per kilogram of recovered oil, the impact associated with ethanol (within the scope of this LCA) will therefore always relate to the predefined amount of 0.2 kg of ethanol.

Conclusions

Research in this chapter has aimed to develop an understanding for measuring the environmental cost associated with the use of SBAM products to capture and recover FOG material. Consideration has been made for three example SBAM products – precipitated silica gels with silanol, butyl and amine surface chemistry. This has been done in two stages: (1) experimental determination of SBAM adsorption capacities and recovery capacities, and (2) life cycle assessment of products based on implied FOG abatement cost.

Findings of the work outline clear sensitivity of adsorption performance to surface chemistry of the SBAM used. Interestingly, silanol surface chemistry SBAM is found to be best performing, having a capacity of 0.5 kg oil/kg powder first time use. This is 1.5 times better than the butyl SBAM and 2.0 times better than the amine SBAM.

Additionally, it is demonstrated how solvent choice may be critical in defining limitations to material and energy use associated with extraction and recovery of adsorbate as well as energy for powder regeneration (in this case, drying).

Findings of this work are novel in acting to demonstrate how life cycle understanding developed across the work can be applied to assess the environmental impact associated with adsorbent use. Implications of the demonstration are therefore of application to many areas of SBAM adsorbent design – including beyond direct application to FOG based adsorbents.

8. Conclusions

8.1. Key Conclusions

Current trends in consumption and pollution are increasing the risk of global environmental system failures. This has led the United Nations to establish global goals for sustainable development including clean water and sanitation (UN SDG 6), sustainable cities and communities (UN SDG 11), and responsible consumption and production (UN SDG 12).

As outlined in Chapter 1, one challenge involving these themes is the sustainable development of wastewater treatment technologies to address emerging wastewater pollutants (EWPs). This includes a significant increase in research into the use of silica-based adsorbent materials (SBAMs) as potential EWP treatments. Due to a focus on maximising technological performance (i.e. adsorption capacity) alone, this has revolved around the use of emerging technologies to generate advanced adsorbent designs targeted to recover EWPs at high separation efficiency. Typically, this is achieved through the inclusion of mesoporous properties, and/or surface chemistry modifications within the SBAM design.

However, as indicated in Chapter 2, manufacturing of SBAMs by emerging methods may be overshadowed by their environmental consequences. This is because the emerging methods often require more complex processing conditions (e.g. the use of organic solvents and other specialty chemicals), the impacts of which are still not well understood. Consequently, it is unknown whether many adsorbents SBAM designs reported in literature are being developed sustainably – i.e. balancing the need for EWP treatments, with environmental impacts introduced by the SBAM lifecycle (i.e. production, use, and disposal).

Given current gaps in literature, this thesis has been developed with the goal of providing information necessary to enable modelling the environmental impact of SBAMs. As outlined in Chapter 3, this has been done by integrating methods of process understanding, process modelling and life cycle assessment to develop life cycle understanding from which environmental impact predictions can be made.

To develop a reliable environmental impact assessment of SBAMs, a more thorough understanding is required for many points in the manufacture and use stages of the SBAM life cycle. As illustrated in Figure 8.1 (previously Figure 1.5) this includes: 1) the production of solid

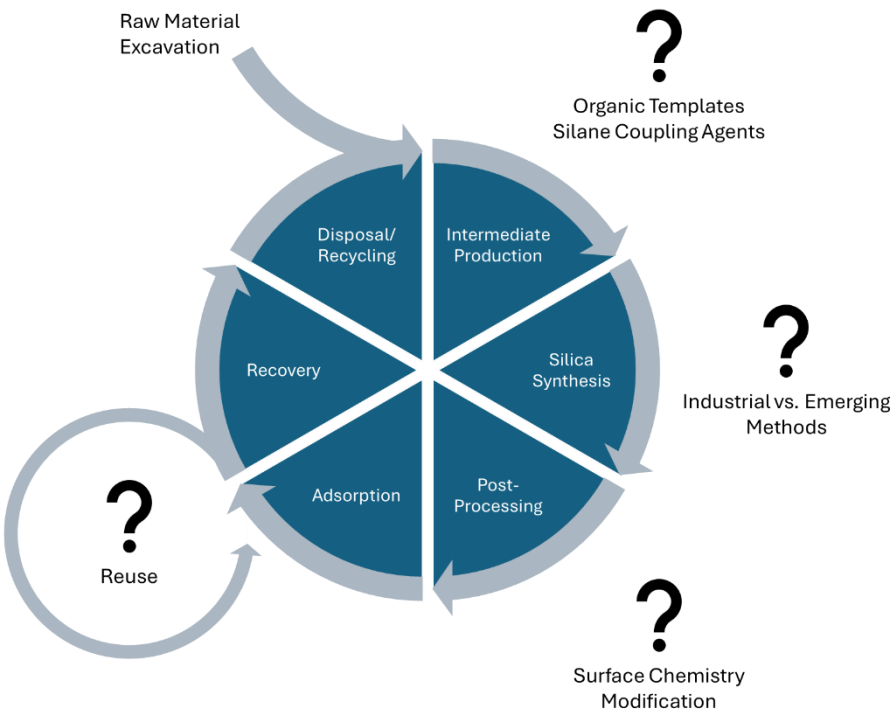


Figure 8.1: Addressing key questions in understanding across the life cycle of silica-based adsorbent materials.

adsorbent substrates, 2) the production of silane coupling agents (used in surface chemistry modification/post-processing), and 3) the use of SBAMs for recovery of FOG-like materials. Consequently, the work in this thesis has been structured in the form of 4 separate case studies (Chapters 4 to 7), considering the activities present in an individual life cycle stage in a way that is transparent and generalisable to the manufacture of a many SBAM designs.

In Chapter 4, an overview is provided for silica adsorbent substrates produced according to commercial methods within the silica synthesis life cycle stage (see Figure 8.1). Particularly, a focus is provided for precipitated and pyrogenic silica products produced using industrial "wet" and "dry" synthesis methods. This has led to generation of new life cycle inventory models for the average precipitated silica and pyrogenic silica industrial products, from which impact assessment has been carried out. Key findings of the analysis show:

1) The carbon footprint (global warming potential, ReCiPe 2016 Hierarchical method) of precipitated silica (wet method) and pyrogenic silica (mass basis) are similar, their impacts vary in a range of other impact categories including land use, marine eutrophication, ozone depletion, and water consumption.

2) Product impacts are driven by silica precursor use (sodium silicate or silicon tetrachloride) – accounting for between 69 and 100% of product impact across all impact categories considered.
3) Energy contributions are of secondary importance contributing between <0.1 and 26% of overall impact depending on the impact category considered.
4) The contribution of silica feedstock (silica sand/quartz) to product impact is insignificant (i.e. less than 3%) in all impact categories excluding land use.
5) The environmental return of producing silica from alternate feedstocks are likely to be minimal unless they 1) provide reductions in silica reagent processing, or 2) provide co-products that otherwise reduce the impact (e.g. from impact allocation or avoided activities) attributable to the silica product.

Findings of the work are crucial in providing a foundational understanding for the impact associated with the SBAM life cycle for multiple reasons. Firstly, results represent impact predictions based on commercial, industrial scale processes, providing initial benchmarks from which SBAMs (including those produced by non-commercial, emerging methods) can be compared. Secondly, results highlight the importance of silica precursor choice in governing the environmental impact of products, and therefore sustainable SBAM design. Thirdly, the low contribution of silica sand indicates that most of the impact derives from intermediate processing within the silica precursor lifecycle, suggesting alternate feedstock materials are unlikely to provide significant reduction in impact without fundamental changing the nature of intermediate processing.

Consequently, while not providing further detail into other silica products, Chapter 4 raises significant questions regarding the extent to which reagent choice and processing conditions may contribute to the impact of emerging silica products (e.g. Stöber, SBA, MCM and bio-inspired silica) – many of which use silicon tetrachloride derived alkoxysilane reagents and petrochemical derived surfactants in their production, and all of which are likely to act as additional sources of life cycle impact in comparison to the commercial silica synthesis methods.

In Chapter 5, an assessment is provided of the impacts of the silica synthesis life cycle stage according to emerging sol-gel methods (i.e. Stöber, SBA, MCM and bio-inspired silica). Owing to lack of existing information, this involves additional life cycle assessment of the Pluronic

123 (P_{123}), cetyltrimethylammonium chloride (CTAC) and pentaethylenehexamine (PEHA) surfactants involved in providing substrate porosity for SBA, MCM and BI silicas respectively. Key findings of the work show:

1) Products produced by emerging methods tend to have greater impacts in comparison to those produced by commercial methods across a range of impact categories.
2) The carbon footprint of the worst performer (Stöber silica, 92 kg CO_2-eq/kg) is roughly 30 times that of the silicas produced according to commercial methods, and 1.8 times that of the next worst performer (MCM-41) per kilogram of product.
3) Bio-inspired processes are hindered by the contribution of acid use, which is larger than in the case of equivalent commercial methods.
4) Additive use is important in contributing to the impact of all methods incorporating porosity control (SBA, MCM, BI) – including for the case of MCM-41 products, where use of CTAC material may account for 50% or more (depending on impact factor considered).
5) Significant reductions may be achieved in the impact of SBA and MCM products simply by use of sodium silica reagent in place of alkoxysilane reagents.

These findings reaffirm the importance of silica precursor use in governing the impact of products (as for commercial products in Chapter 4). However, for emerging methods, this is because of additional implications of reagent choice (especially the use of alkoxysilanes) on wider processing factors including the need for organic solvents and additives. This indicates that silica synthesis stages using sodium silicate as a precursor are likely to reduce the environmental impact of SBAMs.

Having provided consideration for major silica substrate products in Chapters 4 and 5, the focus is then turned toward understanding the impact of silane coupling agents (used in surface chemistry modification of SBAMs) in Chapter 6. This is done by considering the production of two SCA products: 1) 3-aminopropyltriethoxysilane (APTES), the most common SCA produced in industry; and 2) octyltrimethoxysilane (OTMS), a product used extensively within the Heng research group. Key findings of the work show:

1) Trichlorosilane (TCS, the platform chemical from which most SCAs are manufactured) contributes 40% or more to overall impact of APTES, OTMS, and their intermediate products.
2) The impact of TCS is heavily linked to energy demand of its production, which accounts for 60 to 80 % of product impact across carbon footprint, fossil depletion, terrestrial acidification and water depletion impact categories.
3) The impact of alkoxylation on the carbon footprint varies with SCA product, accounting for 6 and 30 % for OTMS and APTES respectively (mass basis).

Crucially, a potential reduction to the impact of SCA materials through reduced energy consumption associated with TCS is likely a low-return avenue due to thermodynamic and technological limits to the energy intensity of the Siemens process in which it is co-produced. The low impact of alkoxylation also appears to be driven by the material efficiency of alcohol use in the production stage, which is near the stoichiometric limit. This suggests, perhaps surprisingly, that a focus on clean energy associated with the Siemens process (for silicon metal manufacturing) may therefore be a more significant lever for improving the impact of SCAs than any change present in the conversion of TCS to the relevant SCA products.

Having provided all information necessary to model the silica synthesis and post-processing life cycle stages in Chapters 4 through 6 (see Figure 8.1), Chapter 7 then provides a final investigation into the impact associated with use of SBAMs as a treatment for EWPs. This is done considering the use-case of recovering FOG-type materials – using vegetable oil as a model substance. Given the demonstrative nature of the work, this is done using three SBAM materials derived from a silica gel type substrate with surface chemistries of silanol, propylamine, and butyl chemistry. Results of work show:

1) The silanol surface chemistry (i.e. substrate without modified surface chemistry) outperforms butyl and amine surface with regards to oil adsorption capacity.
2) Powder re-use is possible when using solvent-extraction methods to recover adsorbent FOG material.
3) The adsorption capacity of the silanol surface chemistry is reduced by 50% on reuse owing to difficulty in removing the extraction solvent (ethanol) from the powder – illustrating issues of adsorbent-solvent property matching.

4) When using ethanol, solvent extraction is limited by low solubility (~5wt%) of FOG material, requiring high material usage for the extraction process.
5) The low solubility of adsorbent in the extraction solvent causes abatement cost (kg CO_2-eq/kg FOG) of adsorbents to be heavily dependent on use of low-impact solvent recovery methods.
6) The abatement cost associated with adsorbents is heavily driven both by impact associated with the SBAM used, and reliability of the FOG recovery process being used.

Results of the chapter therefore act as a demonstration of how life cycle assessment models generated throughout the thesis may be applied to assess the environmental performance of SBAMs. Importantly, this approach is readily generalisable to SBAMs used in other adsorption applications – maximising the impact of the work developed. Nonetheless, for the FOG-specific case study considered, results also show that future work is required to consider the use of extracted FOG-solvent mixture as a product in further processing – e.g. in biodiesel production. The need for use of more material efficient solvent extraction process is also particularly clear, which may come through use of other solvents, or solvent recovery approach in which excess ethanol (relevant as an extraction solvent for potential biodiesel manufacturing) is recovered. Moreover, application of adsorbents in more realistic wastewater environments is imperative.

In summary, this thesis has set out to increase the understanding of environmental impacts associated with producing and using SBMAs. This has been done by considering stages in the entire SBAM production lifecycle (see Figure 8.1) into distinct case-studies under which scrutiny of sustainable development could be most clearly developed. This includes: 1) the synthesis of silica substrates by either commercial (Chapter 4) or emerging (Chapter 5) methods, 2) the production of silane coupling agents necessary for surface chemistry modification (Chapter 6), and 3) the post-processing and use of SBAMs to address EWPs (Chapter 7).

Results across the thesis identify the presence of significant levers through which the sustainability of SBAMs could be improved by changes in activity associated with the production life cycle stage. This includes:

1) improving the sustainability of product at the silica synthesis stage through informed choice of silica precursor chemistry used (Chapter 4 and 5),
2) acknowledging inherent limitations associated with additive and solvent use present in certain silica synthesis manufacturing (Chapter 5),
3) understanding fundamental limitations to the TCS platform chemical from which silane coupling agents are currently manufactured.

By considering the adsorption of FOG-like material as a use-phase case study (Chapter 7), a more holistic overview is also provided for how life cycle understanding generated throughout the work may be applied practically to the sustainable development of SBAMs as EWP treatments. A key outcome of this, is that impact of surface chemistry modification may significantly contribute to overall impacts of SBAM-based EWP treatments. This suggests that the impact added by surface chemistry modification may possibly outweigh the improvement to adsorption performance that it creates depending on the use case being considered. This finding significantly challenges the direction of existing SBAM design research literature, which focusses heavily on adsorption capacity as the main performance metric in adsorbent design.

Finally, by reporting impacts associated with silica products in standalone studies, results are provided in a way that is generalisable to wider industries. This has already been evidenced by the thesis author being approached by members of international academia and industry interested in implications of published research on topics outside of the remit of traditional SBAMs related to Chapter 4 and 5.

8.2. Recommendations for Future Work

Several areas for continued research and systematic change in research culture have become apparent throughout the course of this work. These topics discussed briefly in the following.

8.2.1. Research Themes

Consolidated Life Cycle Models

Research in Chapter 4, 5 and 6 have demonstrated significant gaps present within understanding of the mass and energy use associated in manufacturing SBAMs. Nonethless, the work has been limited in the number of manufacturing methods that have been considered in each case-study. Large opportunities are therefore still available for

development of more rigorous understanding of SBAM life cycles using this work as a foundation. This could begin by further establishing understanding for other major silane coupling agents used in surface chemistry modification – including octadecyl-functional silanes used in superhydrophobic coatings, poly(amine) SCAs, and the mercaptan SCAs used for cross-linking surfaces.

Relation to Planetary Boundaries

The information developed in this work provides life cycle models that can act as a foundation of future impact assessment of the most significant SBMA products. Nonetheless, these results fall short of considering impact in the context of planetary boundaries. Future work may expand into this area by considering the implication of SBAM production scales on the overall challenge that SBAM industries pose to ensuring sustainable growth within planetary boundaries.

Alternative Materials, Feedstocks, and Processes

The extent of research into the generation of silica powder from alternate feedstocks is already massive. Yet, results in Chapter 4 and 5 suggest that the contribution of feedstock source pales in significance when compared to the contribution of silica precursors (e.g. sodium silicate, silicon tetrachloride, and alkoxy-silicates). This suggests that further studies are required to identify the benefit that alternative feedstocks reported in literature provide to the overall environmental impact of silica products, if any.

8.2.2. Cultural Changes

Incentivising Transparent Synthesis Results

A major challenge during the investigations in this thesis has been the lack of information available on mass and energy balances associated with production stages in the SBAM life cycle. This severely limits the quality and speed at which impact assessments can be generated for SBAMs.

For reliable assessment of environmental impact, LCA must be carried out using information that is complete, accurate, and transparent. This may be addressed by introducing cultural changes which incentivise researchers to report the information necessary for mass and energy balance analysis (and therefore life cycle assessment).

Awareness/Accountability in Material Use

Extreme material and energy use is highlighted as a recurring feature across existing SBAM research in this work (see Chapter 2). For example, this includes:

1) excessive solvent use – e.g. during silica synthesis (see Chapter 2 and Chapter 5) and during surface chemistry modification (see Chapter 2 and Chapter 7)
2) the use of impact-intensive alkoxy-silicate silica precursors for emerging silica synthesis methods (see Chapter 2 and Chapter 5).

In many ways, such practice appears to have become accepted within literature. Consequently, the need for justification of extreme material use is typically overlooked. This risks the establishment of a research culture that enables acceptance of irresponsible material use as new researchers enter and learn from developments in the field. Effort should therefore be to tackle this by incentivising researcher to acknowledge the unsuitability of inefficient materials use as and when it arises.

8.3. Contribution to knowledge

Contributions of this work to wider literature can be summarised as the following:

1) A comprehensive review of life cycle understanding to producing silica substrates, including:
   - **Review of manufacturing paradigms** in commercial and emerging technologies (Chapter 1 and 2).
   - **Life cycle inventory models for two major industrial silica products** based on expert judgement of academic and patent literature (Chapter 2),
   - **Impact assessment of two major industrial silica products**
   - **Identification of silica precursor as a major impact contributor** to commercial silica products

2) A comprehensive review of life cycle understanding to produce silane coupling agents, including:
   - **Review of existing technology** for producing organosilane materials
   - **Life cycle inventory models for 7 organosilane products** - 3-aminopropyltriethoxysilane (APTES), 3-chloropropyltriethoxysilane (CPTES), 3-

chloropropyltrichlorosilane (CPTCS), octyltrimethoxysilane (OTMS), and octyltrichlorosilane (OTCS) (Chapter 7).

- **Life cycle inventory models for 2 trichlorosilane products** according to production via a dedicated direct chlorination process and as co-products of silicon metal manufacturing.

3) A review of life cycle understanding to produce surface-chemistry modified SBAMs and metal oxides, including:
   - **A review of technology** for surface chemistry modification of metal oxide surfaces (Chapter 2).
   - **Life cycle inventory models for two methods** of surface chemistry modification of silica substrates (Chapter 7)

4) High-level scoping of major hotspots present in the development of SBAMs to be used for addressing FOG pollution in wastewaters, including:
   - **A review of stages in adsorbent use and reuse** (Chapter 2 and 7).
   - **Outline of methods for adsorption performance assessment** (Chapter 7).
   - **Demonstrative life cycle assessment of adsorbent performance** (Chapter 7)**.**
   - **Highlighting abatement cost** as a key metric for adsorbent design (Chapter 7).

Finally, findings in all chapters are reported in a way that breaks down life cycle information into clearly defined life cycle stages. This makes understanding more readily transferable to the use of silica in wider industrial applications, and other metal oxide materials. This increases the potential scope of impact of the thesis to industries and applications far beyond the topic of SBAMs as treatments for wastewater pollution considered as part of this work.

References

1. Richardson, K., et al., *Earth beyond six of nine planetary boundaries*. Science Advances, 2023. **9**(37).
2. World Health Organisation, *Progress on wastewater treatment: global status and acceleration needs for SDG indicator 6.3. 1*. 2021.
3. Geissen, V., et al., *Emerging pollutants in the environment: A challenge for water resource management*. International Soil and Water Conservation Research, 2015. **3**(1): p. 57-65.
4. UK Government Department for Health and Social Care, *Sewage in water: a growing public health problem*. 2022.
5. Stallard, E. and J. Fisher, *Raw sewage spills into England rivers and seas doubles in 2023*, in *BBC News*. 2023.
6. Chaplin, P., *Combined Sewer Overflows Explained*, E. Agency, Editor. 2020.
7. Tudor, S., *In Focus: Storm overflows discharge reduction plan*, H.o. Lords, Editor. 2022: House of Lords Library.
8. Environment Agency, *Environment Agency publishes storm overflow spill data for 2023*. 2024.
9. Li, J.B., et al., *Climate change impacts on wastewater infrastructure: A systematic review and typological adaptation strategy*. Water Research, 2023. **242**.
10. Botturi, A., et al., *Combined sewer overflows: A critical review on best practice and innovative solutions to mitigate impacts on environment and human health*. Critical Reviews in Environmental Science and Technology, 2021. **51**(15): p. 1585-1618.
11. Yusuf, H.H., et al., *Tackling fat, oil, and grease (FOG) build-up in sewers: Insights into deposit formation and sustainable in-sewer management techniques*. Science of the Total Environment, 2023. **904**.
12. Ducoste, J.J., et al., *Fats, roots, oils, and grease (FROG) in centralized and decentralized systems*. 2009: IWA Publishing.
13. Williams, J.B., et al., *Fat, oil and grease deposits in sewers: Characterisation of deposits and formation mechanisms*. Water Research, 2012. **46**(19): p. 6319-6328.
14. Thames Water. *Thames Water's fatberg fight rages on a year after infamous whitechapel best defeated*. 2019; Available from: https://www.thameswater.co.uk.
15. Zeb, S., et al., *Silica-based nanomaterials as designer adsorbents to mitigate emerging organic contaminants from water matrices*. Journal of Water Process Engineering, 2020. **38**.

16. Min, B., A. Santra, and D. Goodman, *Understanding silica-supported metal catalysts: Pd/silica as a case study.* Catalysis Today, 2003. **85**(2-4): p. 113-124.

17. Schulz-Ekloff, G., J. Rathouský, and A. Zukal, *Controlling of morphology and characterization of pore structure of ordered mesoporous silicas.* Microporous and mesoporous materials, 1999. **27**(2-3): p. 273-285.

18. Cashin, V.B., et al., *Surface functionalization and manipulation of mesoporous silica adsorbents for improved removal of pollutants: a review.* Environmental Science: Water Research & Technology, 2018. **4**(2): p. 110-128.

19. Gosiamemang, T. and J.Y. Heng, *Superhydrophobic cotton for addressing fatbergs through oily wastewater treatment.* International Journal of Biological Macromolecules, 2024. **277**: p. 133863.

20. Cherukupally, P., et al., *Surface-engineered sponges for recovery of crude oil microdroplets from wastewater.* Nature Sustainability, 2020. **3**(2): p. 136-143.

21. Gibson, L.T., *Mesosilica materials and organic pollutant adsorption: part B removal from aqueous solution.* Chemical Society Reviews, 2014. **43**(15): p. 5173-5182.

22. Proctor, A., P. Clark, and C. Parker, *Rice hull ash adsorbent performance under commercial soy oil bleaching conditions.* Journal of the American Oil Chemists' Society, 1995. **72**(4): p. 459-462.

23. Onn, M., et al., *Free Fatty Acid Reduction in Used Frying Oil via Bio Adsorbent: A Short Review.* Chemical Engineering Transactions, 2023. **106**: p. 139-144.

24. Baccile, N., et al., *Introducing ecodesign in silica sol-gel materials.* Journal of Materials Chemistry, 2009. **19**(45): p. 8537-8559.

25. Gérardin, C., et al., *Ecodesign of ordered mesoporous silica materials.* Chemical Society Reviews, 2013. **42**(9): p. 4217-4255.

26. Lehman, S.E. and S.C. Larsen, *Zeolite and mesoporous silica nanomaterials: greener syntheses, environmental applications and biological toxicity.* Environmental Science-Nano, 2014. **1**(3): p. 200-213.

27. Pal, N., J.H. Lee, and E.B. Cho, *Recent Trends in Morphology-Controlled Synthesis and Application of Mesoporous Silica Nanoparticles.* Nanomaterials, 2020. **10**(11).

28. European Commission, *Commission Communication - Chemicals Strategy for Sustainability Towards a Toxic-Free Environment*. 2020.

29. Environmental Protection Agency, *Waste Water Treatment Manuals: Preliminary Treatment*. 1995.

30. Wallace, T., et al., *International evolution of fat, oil and grease (FOG) waste management - A review.* Journal of Environmental Management, 2017. **187**: p. 424-435.

31. Huynh, L.-H., N.S. Kasim, and Y.-H. Ju, *Biodiesel production from waste oils*, in *Biofuels*. 2011, Elsevier. p. 375-396.

32. Food and Agriculture Organization of the United Nations, *FAOSTAT: Food and agriculture data*. 2024.

33. Abdellatif, M., et al., *Quantitative assessment of sewer overflow performance with climate change in northwest England*. Hydrological Sciences Journal-Journal Des Sciences Hydrologiques, 2015. **60**(4): p. 636-650.

34. Arthur, S. and J. Blanc, *Management and Recovery of FOG (fats, oils and greases)*. CREW Project CD2013/6. Available online at:< crew. ac. uk/publications>.(Aug. 2015), 2013.

35. He, X., F.L. de los Reyes, and J.J. Ducoste, *A critical review of fat, oil, and grease (FOG) in sewer collection systems: Challenges and control*. Critical Reviews in Environmental Science and Technology, 2017. **47**(13): p. 1191-1217.

36. Mattsson, J., et al., *Fat, Oil, and Grease Accumulation in Sewer Systems: Comprehensive Survey of Experiences of Scandinavian Municipalities*. Journal of Environmental Engineering, 2014. **140**(3).

37. Foodservice Equipment Association, *Foodservice – Fat, Oil and Grease Management Guide*. 2023.

38. Stoll, U. and H. Gupta, *Management strategies for oil and grease residues*. Waste Management & Research, 1997. **15**(1): p. 23-32.

39. Water Resources Research Institute, *Wastewater system managers struggle with fat, oil, and grease*. 2002.

40. Sanghamitra, P., D. Mazumder, and S. Mukherjee, *Treatment of wastewater containing oil and grease by biological method-a review*. Journal of Environmental Science and Health, Part A, 2021. **56**(4): p. 394-412.

41. Sultana, N., et al., *Understanding the properties of fat, oil, and grease and their removal using grease interceptors*. Water Research, 2022. **225**.

42. Quevatre, C. *War on fatbergs: Can this 21st Century peril be blitzed?* 2019; Available from: https://www.bbc.co.uk/news/uk-england-46836867.

43. Gibbons, D. and T. Curran, *Assessing the efficacy of Dublin City Council's Fat, Oil and Grease (FOG) Programme through the quantification of FOG waste recovered*. no. April, 2015.

44. Husain, I.A.F., et al., *Problems, Control, and Treatment of Fat, Oil, and Grease (FOG): A Review*. Journal of Oleo Science, 2014. **63**(8): p. 747-752.

45. Long, J.H., T.N. Aziz, and J.J. Ducoste, *Anaerobic co-digestion of fat, oil, and grease (FOG): A review of gas production and process limitations*. Process Safety and Environmental Protection, 2012. **90**(3): p. 231-245.

46. Ragauskas, A.M.E., Y.Q. Pu, and A.J. Ragauskas, *Biodiesel from grease interceptor to gas tank*. Energy Science & Engineering, 2013. **1**(1): p. 42-52.

47. Stauffer, C.E., *Fats and Oils*. 1996, St. Paul, Minnesota., USA: USA : Eagan Press.

48. Awogbemi, O., E.I. Onuh, and F.L. Inambao, *Comparative study of properties and fatty acid composition of some neat vegetable oils and waste cooking oils*. International Journal of Low-Carbon Technologies, 2019. **14**(3): p. 417-425.

49. Leung, D.Y.C. and Y. Guo, *Transesterification of neat and used frying oil: Optimization for biodiesel production*. Fuel Processing Technology, 2006. **87**(10): p. 883-890.

50. Dalai, A.K., et al., *FUEL 30-Biodiesel production from canola oil and waste fryer grease and conversion of glycerol to value-added liquid chemicals*. Abstracts of Papers of the American Chemical Society, 2007. **234**.

51. Chhetri, A.B., K.C. Watts, and M.R. Islam, *Waste Cooking Oil as an Alternate Feedstock for Biodiesel Production*. Energies, 2008. **1**(1): p. 3-18.

52. Wen, Z.Z., et al., *Biodiesel production from waste cooking oil catalyzed by TiO*

-MgO mixed oxides. Bioresource Technology, 2010. **101**(24): p. 9570-9576.

53. Liu, L., et al., *Esterification of free fatty acids in waste cooking oil by heterogeneous catalysts*. Transactions of Tianjin University, 2014. **20**(4): p. 266-272.

54. Henriksson, J., *Characterization of composition of the fat-rich residues from grease separators*. 2016.

55. Suresh, K.S., P. Suresh, and T.G. Kudre, *Prospective ecofuel feedstocks for sustainable production*, in *Advances in eco-fuels for a sustainable environment*. 2019, Elsevier. p. 89-117.

56. Wang, Z.M., et al., *Optimization of biodiesel production from trap grease via acid catalysis*. Korean Journal of Chemical Engineering, 2008. **25**(4): p. 670-674.

57. Suto, P., et al. *Innovative anaerobic digestion investigation of fats, oils, and grease*. in *Residuals and Biosolids Conference 2006*. 2006. Water Environment Federation.

58. Keener, K.M., J.J. Ducoste, and L.M. Holt, *Properties Influencing Fat, Oil, and Grease Deposit Formation*. Water Environment Research, 2008. **80**(12): p. 2241-2246.

59. He, X., et al., *Evidence for Fat, Oil, and Grease (FOG) Deposit Formation Mechanisms in Sewer Lines*. Environmental Science & Technology, 2011. **45**(10): p. 4385-4391.

60. He, X., et al., *Mechanisms of Fat, Oil and Grease (FOG) deposit formation in sewer lines*. Water Research, 2013. **47**(13): p. 4451-4459.

61. Iasmin, M., et al., *Factors that influence properties of FOG deposits and their formation in sewer collection systems*. Water Research, 2014. **49**: p. 92-102.

62. Shin, H., S. Han, and H. Hwang, *Analysis of the characteristics of fat, oil, and grease (FOG) deposits in sewerage systems in the case of Korea*. Desalination and Water Treatment, 2015. **54**(4-5): p. 1318-1326.

63. Benecke, H.P., S.K. Allen, and D.B. Garbark, *Efficient Fractionation and Analysis of Fatty Acids and their Salts in Fat, Oil and Grease (FOG) Deposits*. Journal of Oleo Science, 2017. **66**(2): p. 123-131.

64. Iasmin, M., L.O. Dean, and J.J. Ducoste, *Quantifying fat, oil, and grease deposit formation kinetics*. Water Research, 2016. **88**: p. 786-795.

65. Kröpfl, K., et al., *Study of biofilm formation by total-reflection X-ray fluorescence spectrometry*. Microchemical Journal, 2003. **75**(2): p. 133-137.

66. Del Mundo, D.M.N. and M. Sutheerawattananonda, *Influence of fat and oil type on the yield, physico-chemical properties, and microstructure of fat, oil, and grease (FOG) deposits*. Water Research, 2017. **124**: p. 308-319.

67. Pryshlakivsky, J. and C. Searcy, *Fifteen years of ISO 14040: a review*. Journal of Cleaner Production, 2013. **57**: p. 115-123.

68. Marsmann, M., *Editorial: ISO 14040-The First Project*. International Journal of Life Cycle Assessment, 1997. **2**(3): p. 122-123.

69. International Organization for Standardization, *ISO 14040: Environmental Management-Life Cycle Assessment-Principles and Framework*. 2006: Geneva, Switzerland.

70. International Organization for Standardization, *ISO 14044: Environmental Management – Life Cycle Assessment – Requirements and Guidelines*. 2006: Geneva, Switzerland.

71. Huijbregts, M.A.J., et al., *ReCiPe2016: a harmonised life cycle impact assessment method at midpoint and endpoint level*. International Journal of Life Cycle Assessment, 2017. **22**(2): p. 138-147.

72. Santos, A., A. Barbosa-Póvoa, and A. Carvalho, *Life cycle assessment in chemical industry - a review*. Current Opinion in Chemical Engineering, 2019. **26**: p. 139-147.

73. Blömer, J., et al., *Assessment of Chemical Products and Processes: Green Metrics and Life Cycle Assessment - A Comparison*. Chemie Ingenieur Technik, 2024. **96**(5): p. 561-574.

74. Thonemann, N., A. Schulte, and D. Maga, *How to conduct prospective life cycle assessment for emerging technologies? A systematic review and methodological guidance*. Sustainability, 2020. **12**(3): p. 1192.

75. Cucurachi, S., C. van der Giesena, and J. Guinée, *Ex-ante LCA of emerging technologies*. 25th Cirp Life Cycle Engineering (Lce) Conference, 2018. **69**: p. 463-468.

76. Jobson, M., *Short-cut evaluation of distillation sequences.* Computers & chemical engineering, 1997. **21**: p. S553-S557.

77. Bhosekar, A. and M. Ierapetritou, *Advances in surrogate based modeling, feasibility analysis, and optimization: A review.* Computers & Chemical Engineering, 2018. **108**: p. 250-267.

78. Yang, X.-S., *Nature-inspired optimization algorithms*. 2020: Academic Press.

79. Service, T.C. and D.R. Tauritz. *A no-free-lunch framework for coevolution*. in *GECCO*. 2008.

80. Ioannou, I., et al., *Process modelling and life cycle assessment coupled with experimental work to shape the future sustainable production of chemicals and fuels.* Reaction Chemistry & Engineering, 2021. **6**(7): p. 1179-+.

81. Zhuravlev, L.T., *The surface chemistry of amorphous silica. Zhuravlev model.* Colloids and Surfaces a-Physicochemical and Engineering Aspects, 2000. **173**(1-3): p. 1-38.

82. European Commission, *Reference Document on Best Available Techniques for the Manufacture of Large Volume Inorganic Chemicals - Solids and Others Industry*, in *Integrated Pollution Prevention and Control*. 2007.

83. Stöber, W., A. Fink, and E. Bohn, *Controlled growth of monodisperse silica spheres in the micron size range.* Journal of colloid and interface science, 1968. **26**(1): p. 62-69.

84. Ghimire, P.P. and M. Jaroniec, *Renaissance of Stober method for synthesis of colloidal particles: New developments and opportunities.* Journal of Colloid and Interface Science, 2021. **584**: p. 838-865.

85. Green, D.L., et al., *Size, volume fraction, and nucleation of Stober silica nanoparticles.* Journal of Colloid and Interface Science, 2003. **266**(2): p. 346-358.

86. Patwardhan, S.V. and S.S. Staniland, *Green nanomaterials: from bioinspired synthesis to sustainable manufacturing of inorganic nanomaterials*. 2019: IOP Publishing.

87. Manning, J.R.H., C. Brambila, and S.V. Patwardhan, *Unified mechanistic interpretation of amine-assisted silica synthesis methods to enable design of more complex materials.* Molecular Systems Design & Engineering, 2021. **6**(3): p. 170-196.

88. Wang, J., Y. Tu, and C.-h. Yang, *Research status of MCM-41 mesoporous molecular sieves.* JOURNAL-UNIVERSITY OF PETROLEUM CHINA NATURAL SCIENCE EDITION, 2003. **27**(1; ISSU 135): p. 126-131.

89. Stevens, W.J.J., et al., *Investigation of the morphology of the mesoporous SBA-16 and SBA-15 materials.* Journal of Physical Chemistry B, 2006. **110**(18): p. 9183-9187.

90. Huo, Q.S., D.I. Margolese, and G.D. Stucky, *Surfactant control of phases in the synthesis of mesoporous silica-based materials.* Chemistry of Materials, 1996. **8**(5): p. 1147-1160.

91. Reato, P.T., et al., *Mesoporous Materials of the MCM Type: Synthesis, Application, use of Ionic Solids and Functionalization with Graphene: A Review.* Silicon, 2023. **15**(10): p. 4345-4364.

92. Patwardhan, S.V., *Biomimetic and bioinspired silica: recent developments and applications.* Chemical Communications, 2011. **47**(27): p. 7567-7582.

93. Brambila, C., et al., *A Comparison of Environmental Impact of Various Silicas Using a Green Chemistry Evaluator.* Acs Sustainable Chemistry & Engineering, 2022. **10**(16): p. 5288-5298.

94. Drummond, C., R. McCann, and S.V. Patwardhan, *A feasibility study of the biologically inspired green manufacturing of precipitated silica.* Chemical Engineering Journal, 2014. **244**: p. 483-492.

95. Siddharth Vijay Patwardhan, R.H.M., *Silica synthesis. Patent WO2017037460A1.*, W.I.P. Organization, Editor. 2015.

96. Roes, A.L., et al., *Influence of using nanoobjects as filler on functionality-based energy use of nanocomposites.* Journal of Nanoparticle Research, 2010. **12**(6): p. 2011-2028.

97. Osterwalder, N., et al., *Energy consumption during nanoparticle production: How economic is dry synthesis?* Journal of Nanoparticle Research, 2006. **8**(1): p. 1-9.

98. Middlemas, S., Z.Z. Fang, and P. Fan, *Life cycle assessment comparison of emerging and traditional Titanium dioxide manufacturing processes.* Journal of Cleaner Production, 2015. **89**: p. 137-147.

99. Rodríguez-Carrillo, C., et al., *Solid-state microwave assisted batch and flow synthesis, and life cycle assessment, of titanium containing UVM-7 mesoporous silica.* Microporous and Mesoporous Materials, 2024. **380**: p. 113314.

100. Errington, E., M. Guo, and J.Y. Heng, *Synthetic amorphous silica: Environmental impacts of current industry and the benefit of biomass-derived silica.* Green Chemistry, 2023. **25**(11): p. 4244-4259.

101. Jessop, P.G., *The use of auxiliary substances (solvents, separation agents) should be made unnecessary wherever possible and innocuous when used.* Green Chemistry, 2016. **18**(9): p. 2577-2578.

102. Kresge, C.T. and W.J. Roth, *The discovery of mesoporous molecular sieves from the twenty year perspective.* Chemical Society Reviews, 2013. **42**(9): p. 3663-3670.

103. Kabanov, A.V., E.V. Batrakova, and V.Y. Alakhov, *Pluronic block copolymers for overcoming drug resistance in cancer.* Advanced Drug Delivery Reviews, 2002. **54**(5): p. 759-779.

104. da Silva, F.D.M., et al., *Functionalization methods of SBA-15 mesoporous molecular sieve: a brief overview.* SN Applied Sciences, 2019. **1**(6).

105. Zhao, D.Y., et al., *Triblock copolymer syntheses of mesoporous silica with periodic 50 to 300 angstrom pores.* Science, 1998. **279**(5350): p. 548-552.

106. Schmolka, I.R., *A review of block polymer surfactants.* Journal of the American Oil Chemists' Society, 1977. **54**(3): p. 110-116.

107. Wegener, G., et al., *Trends in industrial catalysis in the polyurethane industry.* Applied Catalysis a-General, 2001. **221**(1-2): p. 303-335.

108. Lee, S.H., et al., *Multi-metal cyanide catalysts for ring-opening polymerization of propylene oxide.* Catalysis Today, 2008. **132**(1-4): p. 170-177.

109. de Lucas, A., et al., *Production of polyether polyols using caesium as catalyst.* Polymer International, 2002. **51**(10): p. 1041-1046.

110. Manning, J.R., et al., *Quality-by-Design Approach to Process Intensification of Bioinspired Silica Synthesis.* ACS Sustainable Chemistry & Engineering, 2024. **12**(12): p. 4900-4911.

111. Malveda, M.P., Kälin, T. & Kishi,, *Ethyleneamines*. Chemical Economics Handbook. 2003.

112. Lloyd M. BurgessArthur R. Doumaux, J.S.W.K.J.S., *Selective production of pentaethylenehexamine and hydroxyethyltriethylenetetramine. Patent US5220071A.*, U.S. Patent, Editor. 1990, Union Carbide Chemicals and Plastics Technology LLC.

113. Eghbali, H., et al., *Molecular weight distribution characterization of reactive higher ethyleneamines using size-exclusion chromatography with conventional calibration.* Journal of Chromatography A, 2019. **1603**: p. 141-149.

114. Winters, J.R., *Process for the preparation of polyethylene polyamines. Patent US4404405A.*, U.S. Patents, Editor. 1981, Union Carbide Corp.

115. de la Iglesia, O.s., et al., *Mesoporous Sn-In-MCM-41 Catalysts for the Selective Sugar Conversion to Methyl Lactate and Comparative Life Cycle Assessment with the Biochemical Process.* ACS Sustainable Chemistry & Engineering, 2022. **10**(9): p. 2868-2880.

116. Feijoo, S., et al., *Fenton and photo-fenton nanocatalysts revisited from the perspective of life cycle assessment.* Catalysts, 2019. **10**(1): p. 23.

117. Seth, A. and W. Van Ooij, *Silane coupling agents as corrosion fatigue inhibitors*. Silanes and Other Coupling Agents. Vol. 3. 2004. 119.

118. Jarkin, V.N., O.A. Kisarin, and T.V. Kritskaya, *Methods of trichlorosilane synthesis for polycrystalline silicon production. Part 1: Direct synthesis.* Modern Electronic Materials, 2021. **7**(1): p. 1-10.

119. Global Market Insights. *Trichlorosilane Market Size - By Production Process (Hydrochlorination, Direct Chlorination), By Application (Silane Coupling Agent,*

Polycrystalline Silicon), & Global Forecast, 2023 – 2032. 2022 02 Jan 2025]; Available from: https://www.gminsights.com/industry-analysis/trichlorosilane-market.

120. Long, N.V.D., Y. Kwon, and M. Lee, *Design and optimization of thermally coupled distillation schemes for the trichlorosilane purification process.* Applied Thermal Engineering, 2013. **59**(1-2): p. 200-210.

121. Yan, D., *Siemens Process.* Handbook of Photovoltaic Silicon, 2019: p. 37-68.

122. Fabry, L. and A. Grossmann, *Continuous production of (3-chloropropyl)-trichlorosilane comprises reacting trichlorosilane with allyl chloride in the presence of a homogeneous catalyst containing platinum in a reactive distillation column. Patent DE102012210308A1*. 2012, Wacker Chemie AG.

123. Weston, C.W., J.R. Papcun, and M. Dery, *Ammonium Compounds.* Ullmann's Encyclopedia of Industrial Chemistry, 2003.

124. Schinabeck, A., et al., *Continuous process for preparing silanes and siloxanes having SiOC groups. Patent US4298753A*. 1980, Wacker Chemie AG.

125. Stanjek, V., et al., *Continuous process for preparing SiOC-containing compounds. Patent US8933259B2*. 2011, Wacker Chemie AG.

126. Shilling, C.L.J., et al., *High Yield Hydrosilation Process. Patent KR100651094B1*. 1998.

127. Gelest, *Silane Coupling Agents - Connecting Across Boundaries*. 2014: Gelest.

128. Engelsberger, G.A., *Process for the preparation of organosilicon compounds. Patent DE2851456C2*. 1978, Wacker Chemie AG.

129. Geisberger, G., F. Baumann, and A. Daniels, *Continuous hydrosilylation process. Patent US7145028B2*. 2004, Wacker Chemie AG.

130. Schuster, C.H. and X. Cui, *Recoverable and Cost-Effective Platinum Catalysts for Hydrosilylation Applications.* Chemical Engineering Progress, 2023. **119**(10): p. 10-10.

131. Tachikawa, M. and K. Takei, *Method for making compounds containing hydrocarbonoxysilyi groups by hydrosilylation using hydrido (hydrocarbonoxy) silane compounds. Patent US5986124A*. 1998, DuPont Toray Specialty Materials KK.

132. Bowman, M.P. and J. Curtis L. Schilling, *Process for making chloroorganosilicon compounds. Patent US5559264A*. 1995, General Electric Co.

Osi Specialties Holding Co.

133. Chuang, V.T., *The reaction of chlorosilanes with unsaturated organic compounds.Patent US3925434A*. 1975, Union Carbide Corp.

134. Baumann, F., et al., *Process for continuous polymer-analogous reactions. US6350824B1*. 1998, Wacker Chemie AG.

135. LANG, J.E., et al., *System and process for continuous industrial preparation of alkylalkoxysilanes. Patent WO2008017562A1*. 2007.

136. Geisberger, G., M. Auer, and A. Großmann, *Continuous production of organosilanes. Patent DE102006039191A1*. 2006, Wacker Chemie AG.

137. Ahangaran, F. and A.H. Navarchian, *Recent advances in chemical surface modification of metal oxide nanoparticles with silane coupling agents: A review.* Advances in Colloid and Interface Science, 2020. **286**: p. 102298.

138. Fomitchev, D., J.K. Floess, and W.R. Williams, *Surface-treated metal oxide particles. Patent US8435474B2*. 2007, Cabot Corp.

139. Gottschalk-Gaudig, T. and M. Dreyer, *Rheology control of strongly basic liquids. Patent EP1845136A1*. 2006, Wacker Chemie AG.

140. Zhang, Y., et al., *Schiff base functionalized silica aerogels for enhanced removal of Pb (II) and Cu (II): Performances, DFT calculations and LCA analysis.* Chemical Engineering Journal, 2023. **462**: p. 142019.

141. Frischknecht, R., et al., *The ecoinvent database: overview and methodological framework (7 pp).* The international journal of life cycle assessment, 2005. **10**: p. 3-9.

142. Voll, M. and P. Kleinschmit, *Carbon, 6. Carbon Black.* Ullmann's encyclopedia of industrial chemistry, 2000.

143. Resalati, S., et al., *Comparative life cycle assessment of different vacuum insulation panel core materials using a cradle to gate approach.* Building and Environment, 2021. **188**: p. 107501.

144. Benítez, M., et al., *Scaled-up microwave-assisted batch and flow synthesis and life cycle assessment of a silica mesoporous material: UVM-7.* Green Chemistry, 2024. **26**(2): p. 785-793.

145. Toussaint, H., W. Schroeder, and W. Franzischka, *Preparation of amines. Patent US4234727A*. 1978, BASF SE.

146. Jianxing, Q., et al., *New synthesis method of high purity quaternary ammonium salt. Patent CN104163763A*. 2014, Anhui Benma Pioneer Technology Co. Ltd.

147. Gengsheng, Z. and L. Lin, *Process system and method for continuously preparing long chain alkyl dimethyl tertiary amine. Patent CN101538205A*. 2008, Zhuzhou Shanlin Technology Co. Ltd.

148. Abe, H., et al., *Studies on the Catalyst for the Production of N, N-Dimethyl (Long-chain Alkyl Amines).* Journal of Japan Oil Chemists' Society, 1988. **37**(7): p. 519-523.

149. Abe, H., H. Taniguchi, and T. Fukushima, *Process for producing N,N-dimethyl-N-alkylamine or N,N-dimethyl-N-alkenylamine. Patent US5696294A*. 1995, Kao Corp.

150. Qian , X. and G.Y. Zhang *Theory and practice of the amination of fatty alcohol by using a fixed-bed reactor* China Surfactant Detergent & Cosmetics 1997. **27**(2): p. 4-8.

151. Kimura, H., *Progress in One-step Amination of Long-chain Fatty Alcohols with Dimethylamine-Development of Key Technologies for Industrial Applications, Innovations, and Future Outlook.* Catalysis Reviews-Science and Engineering, 2011. **53**(1): p. 1-90.

152. Strauss, J., et al., *Process for the preparation of tertiary aliphatic amines. Patent US4138437A.* 1977, Hoechst AG.

153. Jianxing, Q., Z. Jing, and H. Lin, *Synthetic method for high-purity quaternary ammonium salt. Patent CN103351301A.* 2013, ANHUI BENMA PIONEER TECHNOLOGY Co Ltd.

154. Gerber, C., et al., *Method for batch cleaning of alkylene oxide polyols. Patent DD230537A3.* 1983.

155. Ostrowski, T., et al., *Method for producing polyether alcohols. Patent US7968754B2.* 2003, BASF SE.

156. Hinz, W. and E. Dexheimer, *Process for removing and regenerating a double metal cyanide (DMC) catalyst from a polymer polyol. Patent US20040158032A1.* 2003, BASF Corp.

157. Wernet, G., et al., *The ecoinvent database version 3 (part I): overview and methodology.* The International Journal of Life Cycle Assessment, 2016. **21**: p. 1218-1230.

158. Wang, S.G., et al., *The synthesis of MCM-48 with high yields.* Materials Research Bulletin, 2001. **36**(9): p. 1717-1720.

159. von der Assen, N. and A. Bardow, *Life cycle assessment of polyols for polyurethane production using CO as feedstock: insights from an industrial case study.* Green Chemistry, 2014. **16**(6): p. 3272-3280.

160. Pati, S.G. and W.A. Arnold, *Comprehensive screening of quaternary ammonium surfactants and ionic liquids in wastewater effluents and lake sediments.* Environmental Science-Processes & Impacts, 2020. **22**(2): p. 430-441.

161. Eckelman, M.J., J.B. Zimmerman, and P.T. Anastas, *Toward green nano: E-factor analysis of several nanomaterial syntheses.* Journal of Industrial Ecology, 2008. **12**(3): p. 316-328.

162. Rösch, L., P. John, and R. Reitmeier, *Silicon compounds, organic.* Ullmann's Encyclopedia of Industrial Chemistry, 2000.

163. Yin, M., et al., *Design and Control of Pressure-Swing Heat Integration Distillation for the Trichlorosilane Purification Process.* Acs Omega, 2022. **7**(11): p. 9254-9266.

164. Chen, W.Q., et al., *Surface hydrophobicity: effect of alkyl chain length and network homogeneity.* Frontiers of Chemical Science and Engineering, 2021. **15**(1): p. 90-98.

165. Gosiamemang, T. and J.Y.Y. Heng, *Sodium hydroxide catalysed silica sol-gel synthesis: Physicochemical properties of silica nanoparticles and their post-grafting using C8 and C18 alkyl-organosilanes.* Powder Technology, 2023. **417**: p. 118237.

166. Ramírez-Márquez, C., et al., *Process design and intensification for the production of solar grade silicon.* Journal of cleaner production, 2018. **170**: p. 1579-1593.

167. Kotzsch, H.J., H.J. Vahlensieck, and W. Josten, *Process for the hydrochlorination of elemental silicon. Patent US4044109.* 1977.

168. Sinnott, R. and T. Gavin, *Chemical engineering design*. Vol. 6. 2014: Elsevier.

169. Guthrie, K.M., *Process plant estimating, evaluation, and control*. 1974: Craftsman Book Company of America.

170. van Amsterdam, M., *Factorial techniques applied in chemical plant cost estimation: A comparative study based on literature and cases.* TU Delft, 1918.

171. *The Chemical Engineering Plant Cost Index*, Chemical Engineering, Editor. 2024.

172. Ulrich, G.D. and P.T. Vasudevan, *Chemical Engineering Process Design and Economics: a Practical Guide*. 2004, Process Publishing.

173. UK Government Department for Energy Security and Net Zero, *International industrial energy prices: Industrial electricity prices in the IEA*. 2024, UK Government.

174. Chee, Y. and T. Kunimune, *Hybrid TCS-siemens process equipped with 'turbo charger' FBR; method of saving electricity and equipment cost from TCS-siemens process polysilicon plants of capacity over 10,000 MT/YR. Patent US20120114546A1*. 2010.

175. Nguyen, T.A.-N. and T.-A. Nguyen. *Genetic Algorithms for Chemical Engineering Optimization Problems*. in *Genetic Algorithms*. 2022. IntechOpen.

176. Bade, S., et al., *Process for the continuous preparation of 3-halopropylorganosilanes. Patent US6242630B1*. 1996, Evonik Operations GmbH.

177. Fabry, L. and A. Grossmann, *Continuous production of (3-chloropropyl)-trichlorosilane comprises reacting trichlorosilane with allyl chloride in the presence of a homogeneous catalyst containing platinum in a reactive distillation column. Patent DE102012210308A1*. Wacker Chemie AG.

178. Schwarz, C., et al., *Manufacturing process for aminoalkyl silanes. Patent US6423858B1*. 2000, Evonik Operations GmbH.

179. Zhejiang Yuanjin Chemical Co. Ltd. *Trichlorosilane 99.5% Colourless clear liquid*. 2024; Available from: https://www.echemi.com/produce/pr2201192033-trichlorosilane-995-colourless-clear-liquid-yuanjinchem.html.

180. Jiansu Kaimei Electronic Materials Co. Ltd. *Silicon Tetrachloride for Selling Sicl4*. 2024; Available from: https://jiangsukaimei.en.made-in-china.com/product/SOFxrdVlMzhc/China-Silicon-Tetrachloride-for-Selling-Sicl4.html.

181. Boulamanti, A. and J.A. Moya, *Production costs of the chemical industry in the EU and other countries: Ammonia, methanol and light olefins*. Renewable and Sustainable Energy Reviews, 2017. **68**: p. 1205-1212.

182. Orjuela, A. and J. Clark, *Green chemicals from used cooking oils: Trends, challenges, and opportunities*. Current opinion in green and sustainable chemistry, 2020. **26**: p. 100369.

183. Diagboya, P.N.E. and E.D. Dikio, *Silica-based mesoporous materials; emerging designer adsorbents for aqueous pollutants removal and water treatment*. Microporous and Mesoporous Materials, 2018. **266**: p. 252-267.

184. Jiang, N., et al., *High-silica zeolites for adsorption of organic micro-pollutants in water treatment: A review*. Water Research, 2018. **144**: p. 145-161.

185. Rouquerol, J., et al., *Adsorption by powders and porous solids: principles, methodology and applications*. 2013: Academic press.

186. Chen, W., et al., *Surface hydrophobicity: Effect of alkyl chain length and network homogeneity*. Frontiers of Chemical Science and Engineering, 2021. **15**: p. 90-98.

187. Gosiamemang, T. and J.Y. Heng, *Sodium hydroxide catalysed silica sol-gel synthesis: Physicochemical properties of silica nanoparticles and their post-grafting using C8 and C18 alkyl-organosilanes*. Powder Technology, 2023. **417**: p. 118237.

188. Iacomi, P. and P.L. Llewellyn, *pyGAPS: a Python-based framework for adsorption isotherm processing and material characterisation*. Adsorption, 2019. **25**(8): p. 1533-1542.

189. Issariyakul, T. and A.K. Dalai, *Biodiesel from vegetable oils*. Renewable & Sustainable Energy Reviews, 2014. **31**: p. 446-471.

190. Kuwornoo, D.K. and J.C. Ahiekpor, *Optimization of factors affecting the production of biodiesel from crude palm kernel oil and ethanol*. Journal homepage: www IJEE IEEFoundation org, 2010. **1**: p. 675-682.

191. Gunstone, F., *Vegetable oils in food technology: composition, properties and uses*. 2011: John Wiley & Sons.

192. Proctor, A., C. Adhikari, and G. Blyholder, *Lipid adsorption on commercial silica hydrogels from hexane and changes in triglyceride complexes with time*. Journal of the American Oil Chemists' Society, 1996. **73**: p. 693-698.

193. Follegatti-Romero, L.A., et al., *Mutual solubility of pseudobinary systems containing vegetable oils and anhydrous ethanol from (298.15 to 333.15) K*. Journal of Chemical & Engineering Data, 2010. **55**(8): p. 2750-2756.

194. Bowman, R.G., *Method of producing amines. Patent US4806690A*. 1985, Huntsman Ethyleneamines Ltd.

195. Wang, H., *Comprehensive Organic Name Reactions*. Vol. 2. 2010: Wiley New York, NY, USA:.

196. Di Serio, M., R. Tesser, and E. Santacesaria, *Comparison of different reactor types used in the manufacture of ethoxylated, propoxylated products.* Industrial & Engineering Chemistry Research, 2005. **44**(25): p. 9482-9489.

197. Lundsted, L.G., *Polyoxyalkylene compounds. Patent US2674619A*. 1953, Wyandotte Chemicals Corp.

198. Ostrowsky, T., et al., *Process for producing reactive polyether polyols having ethylene oxide end blocks. Patent JP4664970B2*. 2004.

199. Andruzzi, F., S. Suradi, and G. Pilcher, *Enthalpy of polymerisation of ethylene oxide and of copolymerisation of ethylene oxide with 7-oxabicyclo [2.2. 1] heptane.* Die Makromolekulare Chemie: Macromolecular Chemistry and Physics, 1982. **183**(9): p. 2183-2190.

200. Chee, Y. and T. Kunimune, *Method of producing trichlorosilane (TCS) rich Chlorosilane product stably from a fluidized gas phase reactor (FBR) and the structure of the reactor. Patent US20100264362A1*. 2010.

201. Cocco, R., S.R. Karri, and T. Knowlton, *Introduction to fluidization.* Chem. Eng. Prog, 2014. **110**(11): p. 21-29.

202. Maurits, J., *Reducing polysilicon materials costs.* Labour, 2011. **3**: p. 5.

203. Díez, E., et al., *Distillation assisted heat pump in a trichlorosilane purification process.* Chemical Engineering and Processing-Process Intensification, 2013. **69**: p. 70-76.

204. Guthrie, K., *Data and techniques for preliminary capital cost estimating.* Chemical Engineering, 1969. **76**: p. 114-142.

205. Dinh, P.C. and K.P. Kaufman, *Process for preparation of primary aminoorganosilanes. Patent EP1229039B1*. 1991, Dow Silicones Corp.

206. Bade, S., et al., *Process for the continuous production of 3-halopropyl-organosilanes. Patent EP0823434B1*. 1996.

207. Lydersen, A.L., *Estimation of critical properties of organic compounds.* Univ. Wisconsin Coll. Eng., Eng. Exp. Stn. Rep. 3, 1955.

208. Benson, S.W., et al., *Additivity rules for the estimation of thermochemical properties.* Chemical Reviews, 1969. **69**(3): p. 279-324.

209. Vetere, A., *Methods to predict the vaporization enthalpies at the normal boiling temperature of pure compounds revisited*. Fluid Phase Equilibria, 1995. **106**(1-2): p. 1-10.

210. Luyben, W.L., *Distillation design and control using Aspen simulation*. 2013: John Wiley & Sons.

211. Jianfeng, D., et al., *Clean production method of 3-chloropropyltrialkoxysilane. Patent CN104086582A*. 2014, Jiangxi Chenguang New Materials Co. Ltd.

212. ChemSpider. *(3-Chloropropyl)triethoxysilane*. 2024; Available from: https://www.chemspider.com/Chemical-Structure.71110.html.

213. HURST Jr, J.E. and B. Keith Harrison, *Estimation of liquid and solid heat capacities using a modified Kopp's rule.* Chemical Engineering Communications, 1992. **112**(1): p. 21-30.

214. Kappler, F.-R., C.-D. Seiler, and H.-J. Vahlensieck, *Method of preparing gamma aminopropyl alkoxy silanes. Patent US4234503A*. 1978, Dynamit Nobel AG.

215. Balduf, T., et al., *Continuous method of producing γ-aminopropyltrialkoxysilanes. Patent US5808123A*. 1996, Evonik Operations GmbH.

216. Schilling, C.L., et al., *Hydrosilation reaction process with recycle. Patent US6015920A*. 1998, General Electric Co. Lanxess Solutions US Inc. Osi Specialties Holding Co.

217. Stanjek, V., et al., *Continuous process for preparing sioc-containing compounds*. 2011.

218. Walsh, R., *Bond dissociation energies in organosilicon compounds.* Silicon Compounds: Silanes and Silicones, 3rd ed.; Arkles, B., Larson, G., Eds, 2013: p. 163-166.

219. Blanksby, S.J. and G.B. Ellison, *Bond dissociation energies of organic molecules.* Accounts of chemical research, 2003. **36**(4): p. 255-263.

Appendix A: Life Cycle Assessment of Commercial Silicas

Data in this section relates to LCA modelling carried out in Chapter 4. Data quality scores are given from 1 (low uncertainty) to 5 (high uncertainty) for all flows modelled using the data quality pedigree matrix method using scoring definitions were based on the ecoInvent data quality system, using the score values provided by Frischknecht *et al*. [141].

A.1. Data Quality Scores of Life Cycle Inventory Flows for Pyrogenic Silica

Data quality scores for the dry mineral-derived synthetic amorphous silica are shown in Tables A.1 to A.11.

Table A.1: Data quality score card for Silicon Tetrachloride. Model: Silicon Tetrachloride - GLO

Data Quality Indicator	Score	Justification
Reliability	1	Reliable data source.
Completeness	3	Data not based on observation of all sites in the EU-15 region.
Temporal Correlation	5	Data reported in 2007, therefore minimum age at time of assessment is 14. Score of 5 chosen instead of 4 on this basis.
Geographical Correlation	5	Data intended to represent global geography.
Technological Correlation	2	Data is correct for the processes considered, but may not reflect all enterprises

Table A.2: Data quality score card for hydrogen. Model: market for hydrogen, liquid - RER

Data Quality Indicator	Score	Justification
Reliability	1	Reliable data source.
Completeness	3	Data not based on observation of all sites in the EU-15 region.
Temporal Correlation	5	Data reported in 2007, therefore minimum age at time of assessment is 14. Score of 5 chosen instead of 4 on this basis.
Geographical Correlation	5	Data intended to represent global geography.
Technological Correlation	3	Data lacking on the source (i.e. production method) of hydrogen production used.

Table A.3: Data quality score card for electricity. Model: market group for heat, district or industrial, natural gas - RER

Data Quality Indicator	Score	Justification
Reliability	1	Reliable data source.
Completeness	3	Data not based on observation of all sites in the EU-15 region.
Temporal Correlation	5	Data reported in 2007, therefore minimum age at time of assessment is 14. Score of 5 chosen instead of 4 on this basis.
Geographical Correlation	5	Data intended to represent global geography.
Technological Correlation	3	Lack of information on energy carrier used in process means that energy use could be from a different technology.

Table A.4: Data quality score card for hazardous waste. Model: market for hazardous waste, for incineration - Europe without Switzerland.

Data Quality Indicator	Score	Justification
Reliability	1	Reliable data source.
Completeness	3	Data not based on observation of all sites in the EU-15 region.
Temporal Correlation	5	Data reported in 2007, therefore minimum age at time of assessment is 14. Score of 5 chosen instead of 4 on this basis.
Geographical Correlation	5	Data intended to represent global geography.
Technological Correlation	4	Model selected based on those used to model equivalent titanium dioxide processes [a] within the ecoInvent database.

[a] Model: Titanium Dioxide model: titanium dioxide production, chloride process | titanium dioxide | APOS, U

Table A.5: Data quality score card for landfill. Model: process-specific burdens, sanitary landfill, (product flow).

Data Quality Indicator	Score	Justification
Reliability	1	Reliable data source.
Completeness	3	Data not based on observation of all sites in the EU-15 region.
Temporal Correlation	5	Data reported in 2007, therefore minimum age at time of assessment is 14. Score of 5 chosen instead of 4 on this basis.
Geographical Correlation	5	Data intended to represent global geography.
Technological Correlation	4	Model selection based on description of burden as “landfill” within the source text.

Table A.6: Data quality score card for carbon dioxide. Model: carbon dioxide, fossil.

Data Quality Indicator	Score	Justification
Reliability	1	Reliable data source.
Completeness	3	Data not based on observation of all sites in the EU-15 region.
Temporal Correlation	5	Data reported in 2007, therefore minimum age at time of assessment is 14. Score of 5 chosen instead of 4 on this basis.
Geographical Correlation	5	Data intended to represent global geography.
Technological Correlation	1	Technological criteria not considered relevant to emissions.

Table A.7: Data quality score card for chlorine. Model: emission to air

Data Quality Indicator	Score	Justification
Reliability	1	Reliable data source.
Completeness	3	Data not based on observation of all sites in the EU-15 region.
Temporal Correlation	5	Data reported in 2007, therefore minimum age at time of assessment is 14. Score of 5 chosen instead of 4 on this basis.
Geographical Correlation	5	Data intended to represent global geography.
Technological Correlation	1	Technological criteria not considered relevant to emissions.

Table A.8: Data quality score card for hydrogen chloride. Model: emission to air

Data Quality Indicator	Score	Justification
Reliability	1	Reliable data source.
Completeness	3	Data not based on observation of all sites in the EU-15 region.
Temporal Correlation	5	Data reported in 2007, therefore minimum age at time of assessment is 14. Score of 5 chosen instead of 4 on this basis.
Geographical Correlation	5	Data intended to represent global geography.
Technological Correlation	1	Technological criteria not considered relevant to emissions.

Table A.9: Data quality score card for nitrogen oxides. Model: emission to air

Data Quality Indicator	Score	Justification
Reliability	1	Reliable data source.
Completeness	3	Data not based on observation of all sites in the EU-15 region.
Temporal Correlation	5	Data reported in 2007, therefore minimum age at time of assessment is 14. Score of 5 chosen instead of 4 on this basis.
Geographical Correlation	5	Data intended to represent global geography.
Technological Correlation	1	Technological criteria not considered relevant to emissions.

Table A.10: Data quality score card for particulates. Model: emission to air

Data Quality Indicator	Score	Justification
Reliability	1	Reliable data source.
Completeness	3	Data not based on observation of all sites in the EU-15 region.
Temporal Correlation	5	Data reported in 2007, therefore minimum age at time of assessment is 14. Score of 5 chosen instead of 4 on this basis.
Geographical Correlation	5	Data intended to represent global geography.
Technological Correlation	1	Technological criteria not considered relevant to emissions.

Table A.11: Data quality score card for Volatile organic carbons. Model: emission to air

Data Quality Indicator	Score	Justification
Reliability	1	Reliable data source.
Completeness	3	Data not based on observation of all sites in the EU-15 region.
Temporal Correlation	5	Data reported in 2007, therefore minimum age at time of assessment is 14. Score of 5 chosen instead of 4 on this basis.
Geographical Correlation	5	Data intended to represent global geography.
Technological Correlation	1	Technological criteria not considered relevant to emissions.

A.2. Data Quality Scores of Life Cycle Inventory Flows for Precipitated Silica

Data quality scores for the wet mineral-derived synthetic amorphous silica are shown in Tables A.12 to A.23.

Table A.12: Data quality score card for Sodium Silicate. Model: market for sodium silicate, without water, in 37% solution state - RER

Data Quality Indicator for	Score	Justification
Reliability	1	Reliable data source.
Completeness	3	Data not based on observation of all sites in the EU-15 region.
Temporal Correlation	5	Data reported in 2007, therefore minimum age at time of assessment is 14. Score of 5 chosen instead of 4 on this basis.
Geographical Correlation	5	Data intended to represent global geography.
Technological Correlation	2	True solution state (i.e. wt%) may vary slightly different to that present in the model.

Table A.13: Data quality score card for electricity. Model: market group for heat, district or industrial, natural gas - RER

Data Quality Indicator for	Score	Justification
Reliability	1	Reliable data source.
Completeness	3	Data not based on observation of all sites in the EU-15 region.
Temporal Correlation	5	Data reported in 2007, therefore minimum age at time of assessment is 14. Score of 5 chosen instead of 4 on this basis.
Geographical Correlation	5	Data intended to represent global geography.
Technological Correlation	3	Lack of information on energy carrier used in process means that energy use could be from a different technology.

Table A.14: Data quality score card for Sulfuric Acid. Model: market for sulfuric acid - RER

Data Quality Indicator for	Score	Justification
Reliability	1	Reliable data source.
Completeness	3	Data not based on observation of all sites in the EU-15 region.
Temporal Correlation	5	Data reported in 2007, therefore minimum age at time of assessment is 14. Score of 5 chosen instead of 4 on this basis.
Geographical Correlation	5	Data intended to represent global geography.
Technological Correlation	1	Model provides estimates based on a blend of sources in the region.

Table A.15: Data quality score card for Deionised Water. Model: market for water, deionised - Europe without Switzerland

Data Quality Indicator for	Score	Justification
Reliability	1	Reliable data source.
Completeness	3	Data not based on observation of all sites in the EU-15 region.
Temporal Correlation	5	Data reported in 2007, therefore minimum age at time of assessment is 14. Score of 5 chosen instead of 4 on this basis.
Geographical Correlation	5	Data intended to represent global geography.
Technological Correlation	1	Model reflects reasonably expected technology, impact from deionised water already known to be negligible from prior investigation so no further thought required.

Table A.16: Data quality score card for non-hazardous waste. Model: process-specific burdens, sanitary landfill, (product flow).

Data Quality Indicator for	Score	Justification
Reliability	1	Reliable data source.
Completeness	3	Data not based on observation of all sites in the EU-15 region.
Temporal Correlation	5	Data reported in 2007, therefore minimum age at time of assessment is 14. Score of 5 chosen instead of 4 on this basis.
Geographical Correlation	5	Data intended to represent global geography.
Technological Correlation	4	Model selection based on description of burden as "landfill" within the source text.

Table A.17: Data quality score card for wastewater. Model: wastewater, average.

Data Quality Indicator for	Score	Justification
Reliability	1	Reliable data source.
Completeness	3	Data not based on observation of all sites in the EU-15 region.
Temporal Correlation	5	Data reported in 2007, therefore minimum age at time of assessment is 14. Score of 5 chosen instead of 4 on this basis.
Geographical Correlation	5	Data intended to represent global geography.
Technological Correlation	1	Based on reasonable fitting of model description with reported waste type.

Table A.18: Data quality score card for carbon monoxide. Model: emission to air

Data Quality Indicator	Score	Justification
Reliability	1	Reliable data source.
Completeness	3	Data not based on observation of all sites in the EU-15 region.
Temporal Correlation	5	Data reported in 2007, therefore minimum age at time of assessment is 14. Score of 5 chosen instead of 4 on this basis.
Geographical Correlation	5	Data intended to represent global geography.
Technological Correlation	1	Technological criteria not considered relevant to emissions

Table A.19: Data quality score card for chemical oxygen demand (COD). Model: emission to water

Data Quality Indicator	Score	Justification
Reliability	1	Reliable data source.
Completeness	3	Data not based on observation of all sites in the EU-15 region.
Temporal Correlation	5	Data reported in 2007, therefore minimum age at time of assessment is 14. Score of 5 chosen instead of 4 on this basis.
Geographical Correlation	5	Data intended to represent global geography.
Technological Correlation	1	Technological criteria not considered relevant to emissions

Table A.20: Data quality score card for dissolved solids. Model: emission to water

Data Quality Indicator	Score	Justification
Reliability	1	Reliable data source.
Completeness	3	Data not based on observation of all sites in the EU-15 region.
Temporal Correlation	5	Data reported in 2007, therefore minimum age at time of assessment is 14. Score of 5 chosen instead of 4 on this basis.
Geographical Correlation	5	Data intended to represent global geography.
Technological Correlation	1	Technological criteria not considered relevant to emissions

Table A.21: Data quality score card for nitrogen oxides. Model: emission to air

Data Quality Indicator	Score	Justification
Reliability	1	Reliable data source.
Completeness	3	Data not based on observation of all sites in the EU-15 region.
Temporal Correlation	5	Data reported in 2007, therefore minimum age at time of assessment is 14. Score of 5 chosen instead of 4 on this basis.
Geographical Correlation	5	Data intended to represent global geography.
Technological Correlation	1	Technological criteria not considered relevant to emissions

Table A.22: Data quality score card for particulates. Model: emission to air

Data Quality Indicator	Score	Justification
Reliability	1	Reliable data source.
Completeness	3	Data not based on observation of all sites in the EU-15 region.
Temporal Correlation	5	Data reported in 2007, therefore minimum age at time of assessment is 14. Score of 5 chosen instead on this basis.
Geographical Correlation	5	Data intended to represent global geography.
Technological Correlation	1	Technological criteria not considered relevant to emissions

Table A.23: Data quality score card for sulfate. Model: emission to water

Data Quality Indicator	Score	Justification
Reliability	1	Reliable data source.
Completeness	3	Data not based on observation of all sites in the EU-15 region.
Temporal Correlation	5	Data reported in 2007, therefore minimum age at time of assessment is 14. Score of 5 chosen instead of 4 on this basis.
Geographical Correlation	5	Data intended to represent global geography.
Technological Correlation	1	Technological criteria not considered relevant to emissions

Appendix B: Process Modelling of Cetrimmonium Chloride

Modelling of mass and energy balances for CTAC have been carried out assuming production according to the commercially practiced two-stage alcohol alkylation route (see Chapter 2). Each stage has been modelled as a distinct chemical process. In all cases, this has been carried out in the using the Aspen Plus V11 process simulation software. Vapour-liquid equilibria were modelled using the NRTL-RK method. Further information follows.

B.1. Production of cetyldimethylamine, CDMA

Production of CDMA was modelled based on reductive amination of CA with dimethylamine. A continuous process design was assumed based on previous patent literature [147]. As per Figure B.1, the process is split generally into three main stages: 1) pretreatment, 2) reaction, 3) gas separation, and 4) product purification. Further assumptions are provided below.

Pretreatment Stage

Pretreatment of materials was modelled to include heating material to the reactor operating conditions (170 C and 1.1 bar) [145]. This was done using the “heater” and “compressor” equipment modules in the Aspen V11 Software.

Reaction Stage

Reaction of materials was modelled assuming reaction conditions (170 C and 1.1 bar) reported in wider literature [145]. Reactions considered included formation of the cetyldimethylamine product (Equation B.1) and common by-products (Equation B.2) [148]. The overall conversion of dimethylamine was assumed to be 99 % [149], with a selectivity of 95 and 2 % for each reaction respectively [150, 151].

$$\mathrm{ROH} + \mathrm{NH(CH_3)_2} \rightarrow \mathrm{RN(CH_3)_2} + \mathrm{H_2O} \quad \text{(B.1)}$$

$$2\mathrm{RCH_3OH} + \mathrm{DMA} \rightarrow (R)_2N(\mathrm{CH_3}) + TMA \quad \text{(B.2)}$$

Alcohol:DMA molar feed ratio was set at 1:1.4 [145] and hydrogen was fed with DMA in a volume ratio of 570:28 [145] to act to reduce by-product formation [145, 194]. Reagents were

preheated to a temperature of 250 C prior to reaction to offset endothermic enthalpy of reaction [145].

Gas Separation

Reactor exhaust gas is passed through a single-stage flash condenser, F1, to separate water and dimethylamine at a temperature of -10 C and 1.1 bar pressure [145]. Water is then condensed in flash condenser F2 at a temperature of -40 C and 1.1 bar [145]. DMA and hydrogen is assumed to be recycled [145].

Product Recovery

Liquid recovered from F1 was passed through a 3-phase separator at standard conditions (25 C and 1 bar pressure) to recover individual organic gas, fatty organic, and water products [152]. The final product was then recovered from the organic phase by vacuum distillation at 2 mbar. This produced a product of roughly 98 wt% purity.

A breakdown of energy flows associated with process modelling equipment is provided in Table B.1.

Table B.1: Predicted energy flows for equipment used in the production of 1 kg of cetyldimethylamine (CDMA).

Equipment	Description	Amount	Unit
H1	Hydrogen Heat Duty	0.20	kWh
H2	Dimethylamine Heating	0.03	kWh
H3	Cetyl Alcohol Heating	0.16	kWh
R1	Reactor Heating	-0.16	kWh
F1	Gas Separation	-0.35	kWh
F2	Water Condensation	-0.03	kWh
F3	Off-gassing	0.02	kWh
S1	Solid-Liquid Filtration	[a] -	kWh
C1	Distillation Duty	0.17	kWh
H4	Recycle Heating	0.26	kWh

[a] no heat duty associated with filtration.

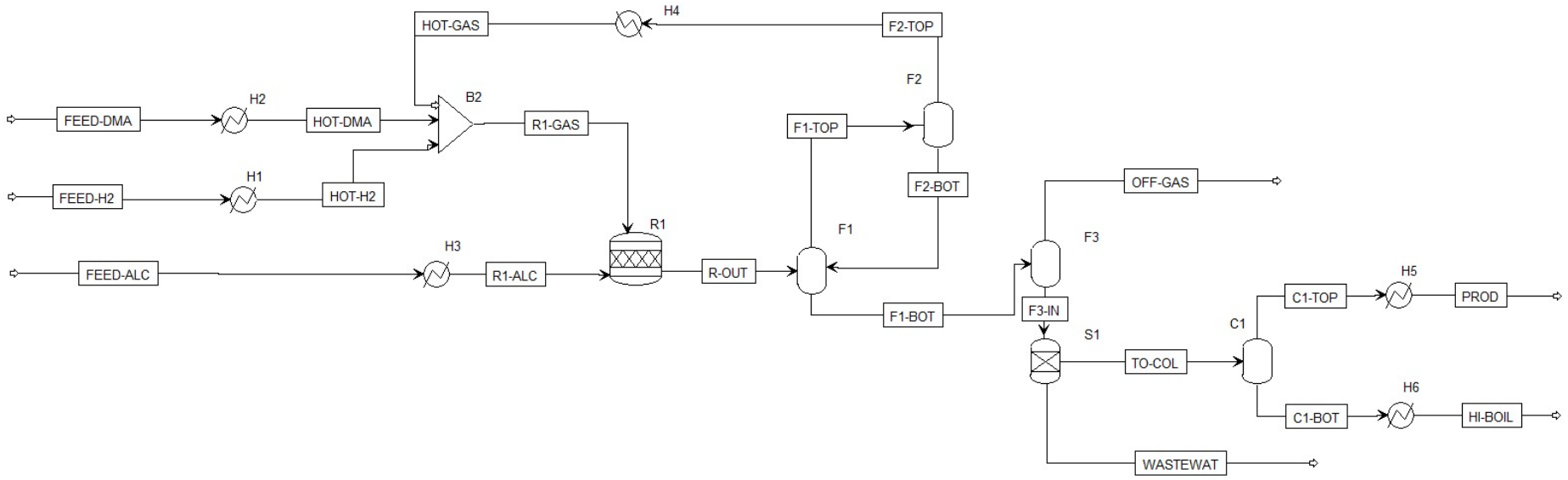


Figure B.1: Process flow diagram of Aspen Plus model approximating the production of cetyldimethylamine from cetyl alcohol.

B.2. Production of cetrimmonium chloride, CTAC

Production of CTAC was modelled based on reductive alkylation of CDMA with methyl chloride. A one-pot, batch-wise process design was assumed [146]. As per Figure B.2, this involved major production stages: 1) reaction, 2) crystallization, and 3) filtration.

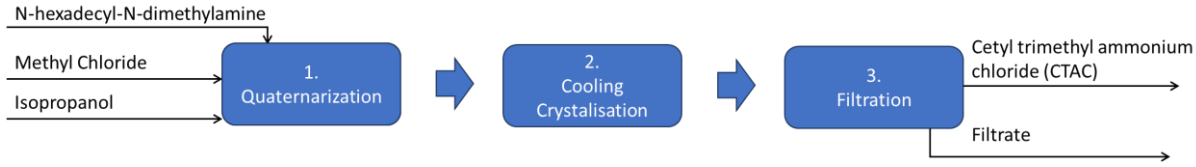


Figure B.2: Process flow diagram for model approximating the production of cetrimmonium chloride (CTAC). Dotted lines represent transitions in conceptual processing stage within the same single batch process equipment.

Reaction stage

Reaction was assumed to occur at 75C and 1 bar [146] . Only product formation reaction (Equation B.3) was considered to occur. Reaction yield was assumed to be 95% with negligible undesired co-products based on a 2014 patent [146]. CDMA and methyl halide were introduced into the reactor in molar feed ratio of 1:1.1 respectively. Isopropanol solvent [123] was used in a ratio of 0.4 mole per mol of CDMA based on a 2014 patent [146].

$$\mathrm{RN(CH_3)_2 + CH_3Cl \rightarrow R[(CH_3)_3N]^+Cl^-} \qquad \text{(B.3)}$$

Crystallisation and Filtration Stage

Cooling crystallisation was done by cooling the liquor to 25 C [153]. 100 % of the CTAC product was assumed to be crystallised, and heat of crystallisation was neglected. The enthalpy of formation of CTAC was estimated from a heat of reaction of 435 kJ/mol [195].

The process flow diagram used to model heat flows in the process is shown in Figure B.3. A breakdown of energy flows from process modelling equipment is shown in Table B.2.

Table B.2: Predicted energy flows for equipment used in the production of 1kg of cetrimmonium chloride (CTAC).

Equipment	Description	Amount	Unit
H1	Solvent Heating	0.06	kWh
H2	Cetyldimethylamine Heating	0.03	kWh
H3	Methyl Chloride Heating	<0.01	kWh
R1	Reactor Cooling	0.06	kWh
F1	Solution Cooling	-0.06	kWh
H4	Gas Cooling	<0.01	kWh
H5	Product Cooling	-0.06	kWh

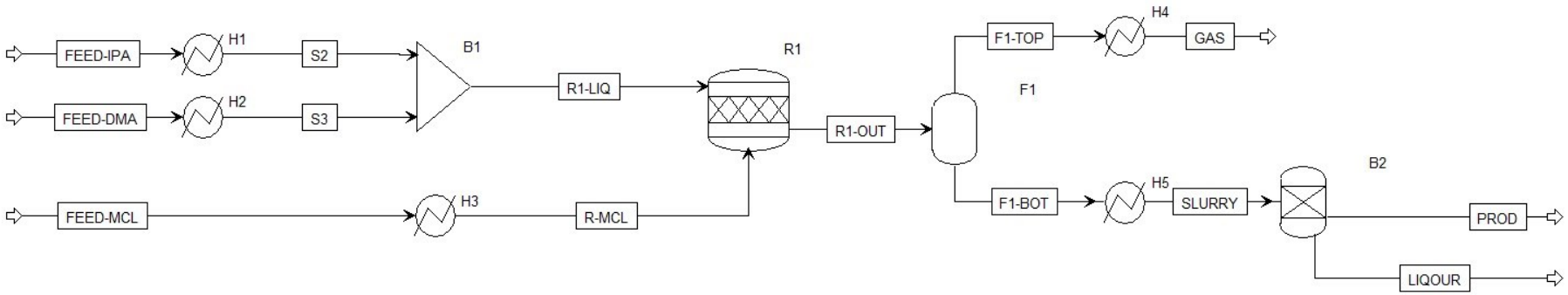


Figure B.3: Process flow diagram of Aspen Plus model approximating the production cetrimmonium chloride.

Appendix C: Process Modelling of Pluronic 123

Production of Pluronic 123 has been modelled according to the three-stage approach of: 1) PPO_{17} (1005 g/mol) synthesis, 2) PPO_{70} synthesis (4084 g/mol), and 3) P_{123} synthesis.

In all cases, this has been carried out in the using the Aspen Plus V11 process simulation software Vapour-liquid equilibria were modelled using the NRTL-RK method. Further information on modelling each stage follow.

C.1. Production of poly(propylene oxide)$_{17}$, PPO_{70}

Production of the PPO_{17} block polymer was assumed to occur according to KOH catalysed PO polymerisation using PG as a starter. A batch-wise process design was assumed based on patent literature [107]. As shown in Figure C.1, this included stages of 1) polymerisation, 2) neutralisation, and 3) product filtration.

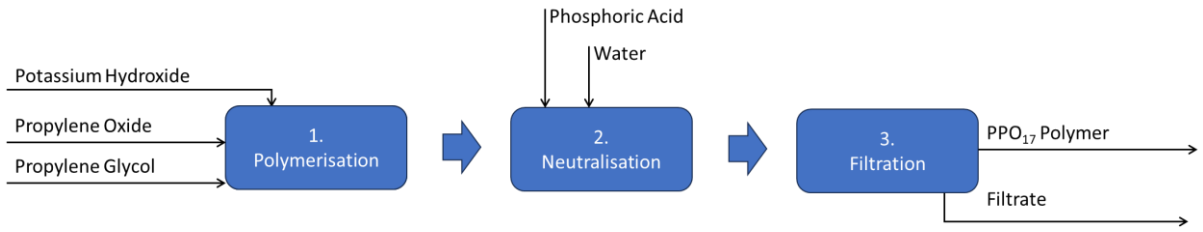


Figure C.1: Process flow diagram for production of PPO17 according to a batch-wise process. Dotted lines represent transitions in conceptual processing stage within the same single batch process equipment.

Polymerisation Stage

Reaction was assumed to occur at 115 C and 3.5 bar [107]. Reaction yield was taken as 95 %. Sodium hydroxide (KOH) base use was assumed to reflect 1 wt% of the reaction fluid [196], and supplied in 85 wt% solution state. Heat of polymerisation assumed to be -105 kJ/mol PPO [197].

Neutralisation and Filtration Stages

Neutralization was done using phosphoric acid [154] in a 1:1 molar ratio to the amount of potassium hydroxide. Salts were dissolved by adding water in an amount equivalent to 5 wt%

of the crude polyol product [154]. The alkali neutralisation was assumed to be complete, following the stoichiometry in Equation C.1.

$$H_3PO + KOH \rightarrow KH_2PO + H_2O \quad \text{(C.1)}$$

Salts were crystallised by evaporation of water at 115 C and atmospheric pressure [154], the remaining liquor was then cooled to 25 C and salts were assumed to be separated from the PPO_{17} product by filtration. A recovery of 100 % of PPO_{17} was assumed.

The process flow diagram used to model heat flows in the process is shown in Figure C.2. A breakdown of energy flows associated with process modelling equipment is provided in Table C.1.

Table C.1: Predicted energy flows for equipment used in the production of 1kg of poly(propylene oxide)$_{17}$.

Equipment	Description	Amount	Unit
P1	Propylene Oxide Pumping	<0.01	kWh
P2	Potassium Hydroxide Pumping	<0.01	kWh
P3	Propylene Glycol Pumping	<0.01	kWh
H1	Propylene Oxide Heating	0.16	kWh
H2	Potassium Hydroxide Heating	0.01	kWh
H3	Propylene Glycol Heating	<0.01	kWh
R1	Polymerisation Reaction Cooling	0.46	kWh
P4	Phosphoric Acid Pumping	<0.01	kWh
H4	Phosphoric Acid Heating	0.11	kWh
R2	Neutralisation Reaction Cooling	0.01	kWh
F1	Water Evaporation	0.62	kWh
H5	Cooling Crystallization	<0.01	kWh
B1	Slurry Filtration	[a] 0.00	kWh

[a] no heat duty associated with filtration.

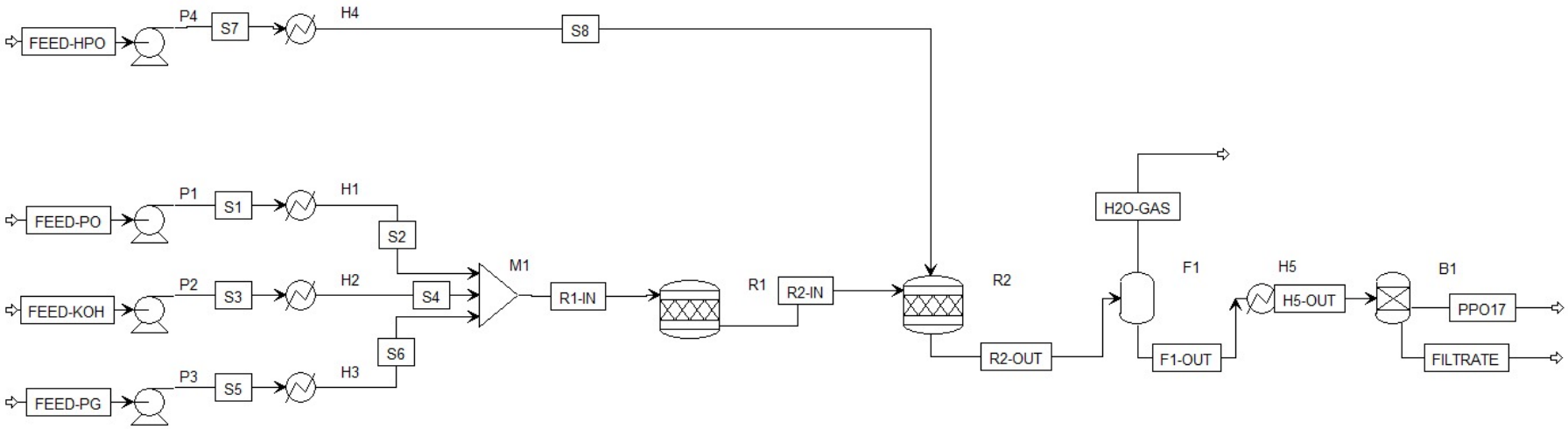


Figure C.1: Process flow diagram of Aspen Plus model approximating the production of poly(propylene oxide)$_{17}$.

C.2. Production of poly(propylene oxide)$_{70}$, PPO$_{70}$

Production of PPO$_{70}$ was assumed to occur according to the DMC-catalysis using PPO$_{17}$ as a starter [155]. A continuous flow method was assumed based on reports from BASF [155]. As shown in Figure C.2, this involves: 1) polymerisation, 2) catalyst coagulation, and 3) product separation by filtration.

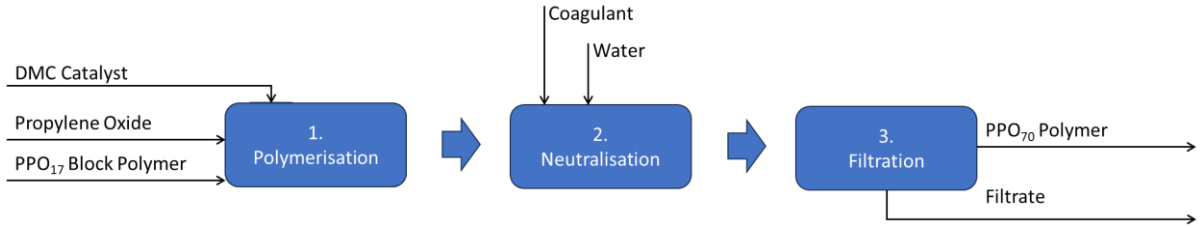


Figure C.1: Process flow diagram for model approximating the production of a 4000 g/mol polypropylene oxide polymer block, PPO$_{70}$. Bold arrows represent transitions in processing stage occurring within the same process vessel.

Reaction Stage

Reaction was modelled to occur at a temperature of 115 C at atmospheric pressure [155]. Reaction conversion of PPO$_{20}$ to PPO$_{70}$ was assumed to be 100% .The catalyst slurry (suspended in PPO$_{20}$) was assumed to be 100 wt% PPO$_{20}$ block polymer – given the low concentration of the DMC catalyst typically used [155]. Mass feed ratios of PPO$_{17}$ starter, propylene oxide, and catalyst slurry were assumed to be 2.3:7.5:0.2 based on the reported steady state operation conditions [155]; additional mass use associated with reaching reactor steady state were neglected given their relatively low mass contribution over the entire period for which the reactor is typically run [155]. The heat of polymerisation was assumed to be -105 kJ/mol PO [197].

Coagulation Stage

It was assumed that an amount of water equal to 0.5 wt% of the new mixture was added during coagulation [156]. Coagulant addition was not modelled explicitly within the Aspen Software owing to low use amounts and lack of relevant data. The heat of catalyst coagulation was neglected.

The process flow diagram used to model heat flows in the process is shown in Figure C.2. A breakdown of energy flows associated with process modelling equipment is provided in Table C.2.

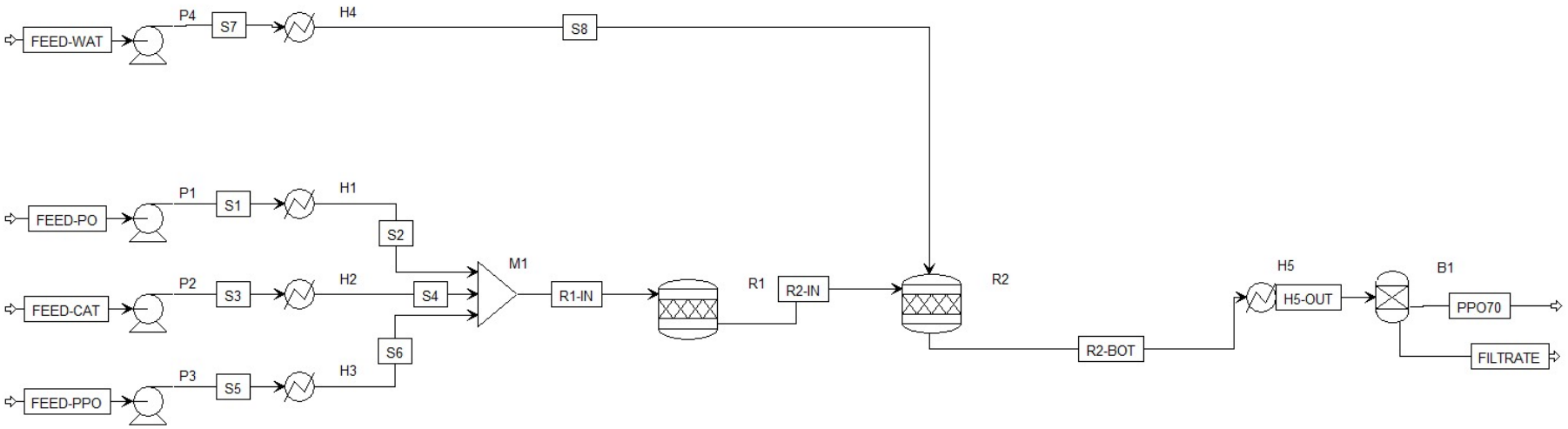


Figure C.2: Process flow diagram of Aspen Plus model approximating the production of poly(propylene oxide)$_{70}$.

Table C.2: Predicted energy flows for equipment used in the production of 1kg of poly(propylene oxide)$_{70}$.

Equipment	Description	Amount	Unit
P1	Propylene Oxide Pumping	<0.01	kWh
P2	Catalyst Slurry Pumping	<0.01	kWh
P3	poly(propylene oxide)$_{17}$ Pumping	<0.01	kWh
H1	Propylene Oxide Heating	0.13	kWh
H2	Catalyst Slurry Heating	<0.01	kWh
H3	poly(propylene oxide)$_{17}$. Heating	<0.00	kWh
R1	Polymerisation Reaction Cooling	[a]0.38	kWh
P4	Phosphoric Acid Pumping	<0.01	kWh
H4	Phosphoric Acid Heating	<0.01	kWh
R2	Coagulant Addition	<0.01	kWh
H5	Cooling Crystallization	<0.01	kWh
B1	Slurry Filtration	[a]0.00	kWh

[a] no heat duty associated with filtration.

C.3. Production of Pluronic 123, P_{123}

Production of the Pluronic 123 was modelled to occur according to KOH-catalysed addition polymerisation of ethylene oxide to a PPO_{70} starter. A batch-wise production process was assumed based on patent literature [198]. As shown in Figure C.3, this involved a three-stage process including: 1) polymerisation reaction, 2) neutralisation, and 3) filtration.

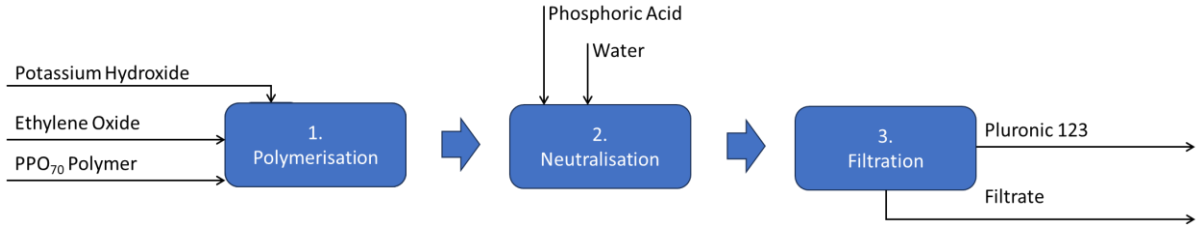


Figure C.3: Process flow diagram for model approximating the production of Pluronic 123. Bold arrows represent transitions in processing stage occurring within the same process vessel.

Reaction Stage

Reaction conditions and yield were assumed to be the same as described in producing PPO_{17} (see above). Heat of polymerisation was calculated using the -102 kJ/mol [199]..

Neutralisation and Filtration Stages

Neutralization was done using phosphoric acid [154] in a 1:1 molar ratio to the amount of potassium hydroxide initially added alongside. Salts were dissolved by adding water in an amount equivalent to 5 wt% of the crude polyol product [154].

The heat of alkali neutralisation was calculated assuming complete neutralisation according to the stoichiometry in Equation A.4. Salts were crystallised by evaporation of water at 115 C and atmospheric pressure [154], the remaining liquor was then cooled to 25 C and salts were assumed to be separated from the PPO_{17} product by filtration. A recovery of 100 % of PPO_{17} was assumed.

The process flow diagram used to model heat flows in the process is shown in Figure C.4. A breakdown of energy flows associated with process modelling equipment is provided in Table C.3 C.3Table C.2.

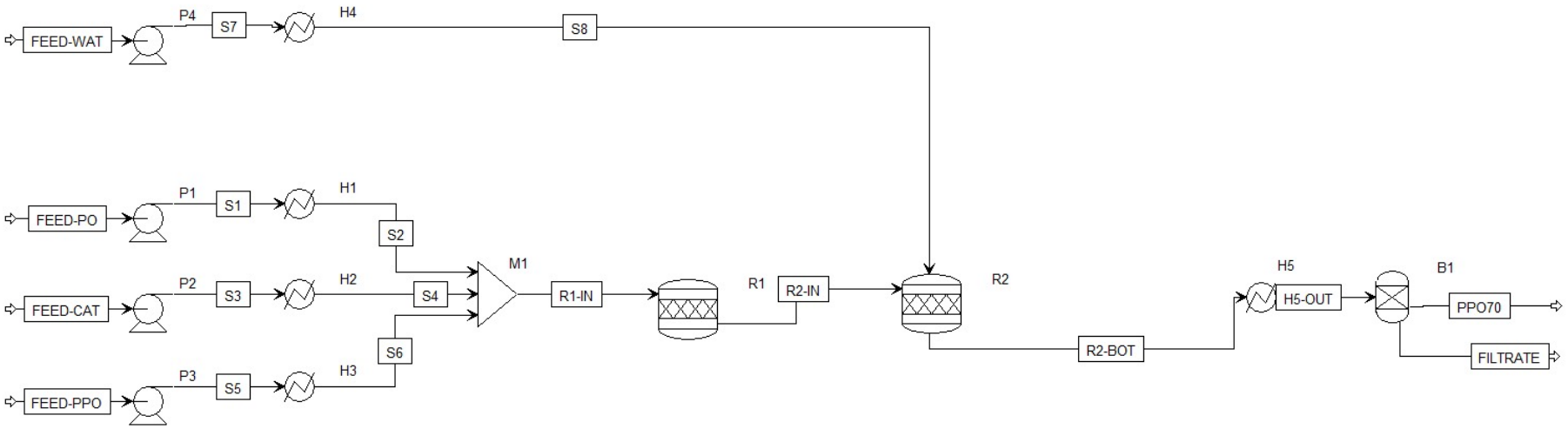


Figure C.4: Process flow diagram of Aspen Plus model approximating the production of Pluronic 123.

Table C.3: Predicted energy flows for equipment used in the production of 1kg of Pluronic 123.

Equipment	Description	Amount	Unit
P1	Ethylene Oxide Compression	0.01	kWh
P2	Potassium Hydroxide Pumping	<0.01	kWh
P3	poly(propylene oxide)$_{70}$. Pumping	<0.01	kWh
H1	Ethylene Oxide Heating	0.01	kWh
H2	Potassium Hydroxide Heating	<0.01	kWh
H3	poly(propylene oxide)$_{70}$. Heating	<0.01	kWh
R1	Polymerisation Reaction Cooling	0.19	kWh
P4	Phosphoric Acid Pumping	<0.01	kWh
H4	Phosphoric Acid Heating	<0.01	kWh
R2	Neutralisation Cooling	<0.01	kWh
H5	Water Evaporation	0.01	kWh
B1	Slurry Filtration	[a]0.00	kWh

[a] no heat duty associated with filtration.

Appendix D: Process Modelling of Trichlorosilane

D.1. Process Modelling

Estimates for mass and energy use produced in this section by modelling chemical process thermodynamics. In all cases, this has been carried out in the using the Aspen Plus V11 process simulation software. Vapour-liquid equilibria were modelled using the NRTL-RK method. Further information on the production of trichlorosilane is provided in the following.

Production of TCS has been modelled based on the direct chlorination of silicon metal with hydrogen chloride. This is done according to a continuous process. As per Figure D.1, the process is split into a total of three conceptual stages: 1) pretreatment, 2) reaction, and 3) flash separation, and 4) product distillation. Further information on the modelling of each stage is provided below.

Reaction Stage

Reactor operation was assumed to be isobaric, with inlet conditions of approximately 5 bar and 350 C [174]. Hydrogen chloride was fed in molar ratio of 3.1:1 to ensure complete conversion of Si fed. A reaction yield of 95% Si to TCS was assumed [174], with the remaining silicon forming STC. Temperature of hydrogen chloride fed to the reactor was assumed to be 100 C to help control exothermicity of the process [200].

Pressure drop across the entire reactor, ΔP_r, was assumed to be 0.5 bar based on assumption a minimum pressure drop over the gas distribution grid, ΔP_d, of one third the pressure drop of powder fluidization (the minimum recommended to ensure good mixing [201], and assuming pressure drop of powder fluidization, ΔP_f, was arising from hydrostatic forces only - see Equations D.1 and D.2).

$$\Delta P_r = \Delta P_f + \Delta P_d = \frac{4}{3}\Delta P_f \quad \text{(D.1)}$$

$$\Delta P_f = g H_{bed}(\rho_p[1-\varepsilon] - \rho_g) \quad \text{(D.2)}$$

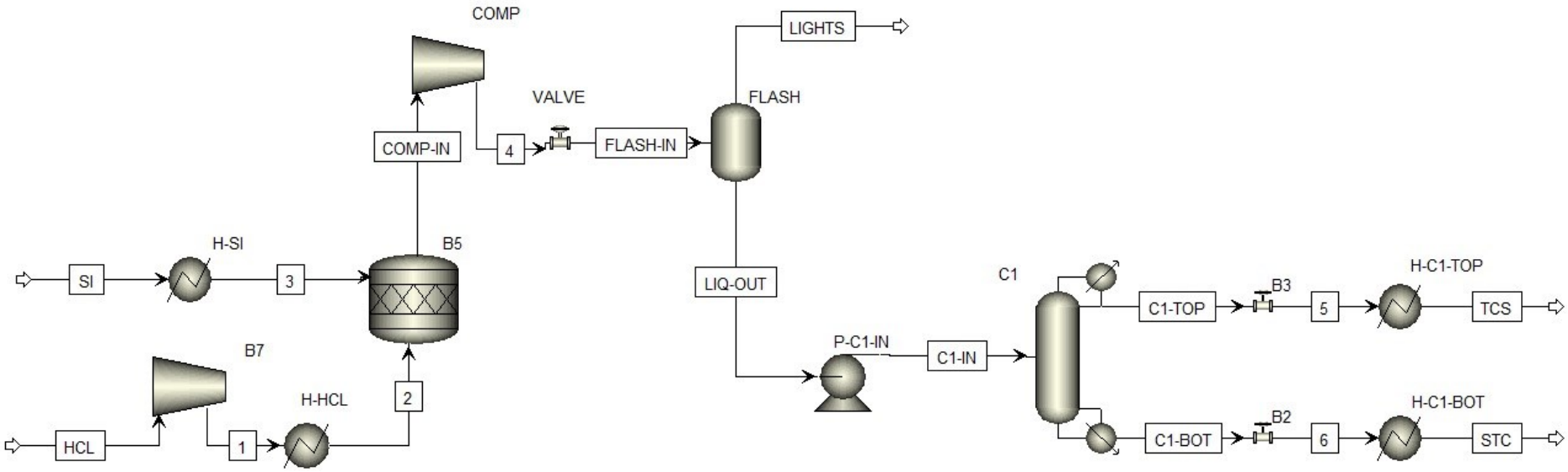


Figure D.1: Process flow diagram of Aspen Plus model modelling the production of trichlorosilane by direct chlorination.

Where g is gravitational acceleration due to gravity, H_{bed} is the height of the bed at onset of fluidization, ρ_p is the particle density, and ε is the powder porosity [201].

Associated geometry for the reactor was calculated based on a scaled version of geometry described in patent literature [174] set to an inlet gas velocity of 20 cm/s [174] – a typical speed for silicon bed fluidization [202].

Flash Separation Stage

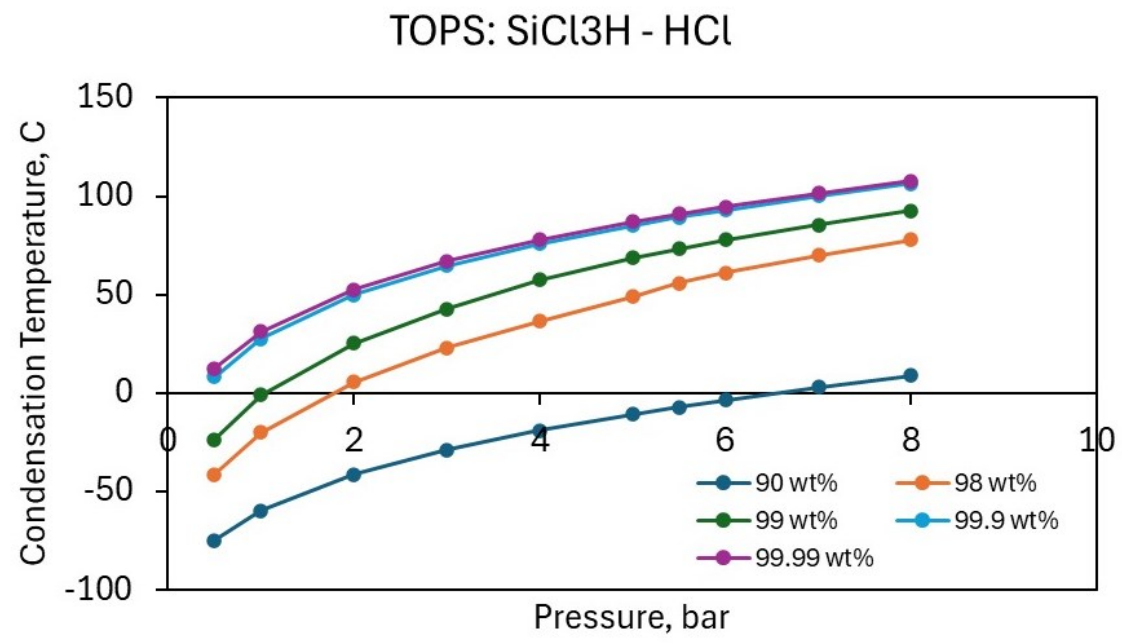
Operation of the flash condenser was assumed to focus on condensation of a chlorosilane rich distillate. Operating conditions were assumed to occurs within a temperature range of -40 to 0 C and pressure range of 1.1 to 5 bar. The lower pressure limit (1.1. bar) was set to avoid suction of atmospheric oxygen into a hydrogen-rich gases.

Product Distillation Stage

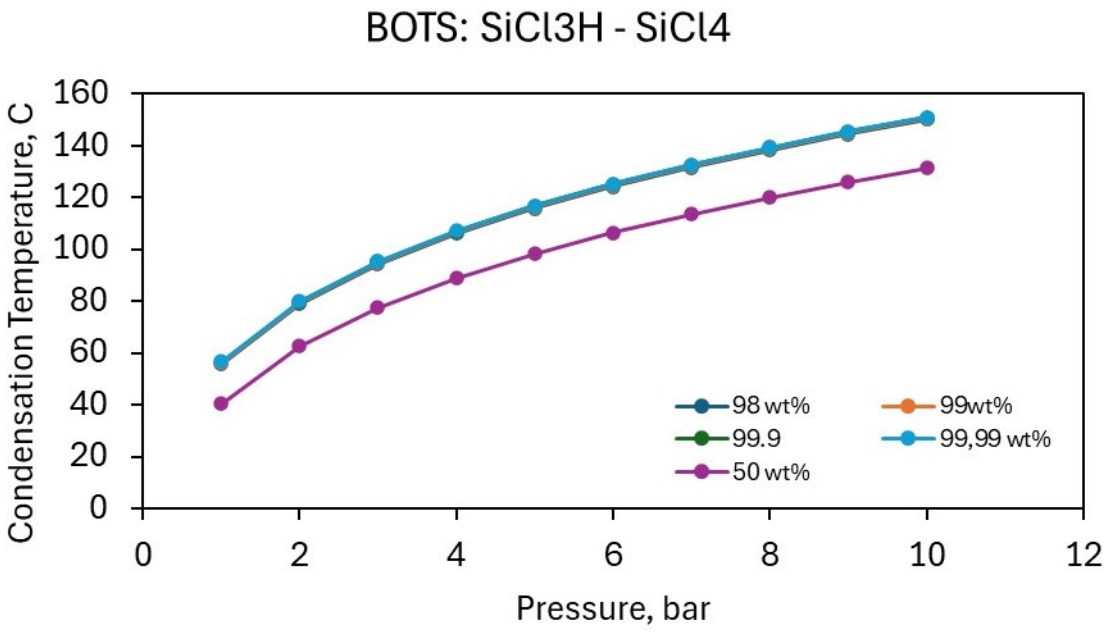
Distillation column operation was defined to achieve production of TCS and STC products at 99 wt% purity while operating the vapor condenser under the total reflux. Operating pressure at all points within the column were was assumed to be within the range of 1.1 to 6 bar to reflect operating temperatures corresponding to use of economically preferable reboiler and condenser utilities – see Figure D.2.

The number of stages present within the column were assumed to be within the range of 15 to 105 based to safely cover the typical number of 40-70 stages reported in literature [120, 163, 166, 203] for producing TCS at higher purity grades. Pressure drop across each stage in the distillation column was assumed to be 0.02 bar per stage. Modelling of the distillation column was carried out using the Aspen Plus software separators>RADFRAC module.

A breakdown of energy flows associated with process modelling equipment is provided in Table D.1.



a)



b)

Figure D.2: Relationship of pressure and purity of trichlorosilane ($SiCl_3H$) (a) and silicon tetrachloride ($SiCl_4$) (b) products on temperature of condensation. Results taken from preliminary modelling with the Aspen Plus V11 software.

Table D.1: Predicted energy flows for equipment used in the production of 1kg of trichlorosilane.

Equipment	Description	Amount	Unit
B7	HCl Compression	0.058	kWh
H_HCL	HCl Heating	0.010	kWh
H-Si	Si Heating	0.005	kWh
B5	Reactor Cooling	0.473	kWh
FLASH	Flash Cooling	-0.158	kWh
COMP	Reactor Effluent Compression	[a]0.000	kWh
C1	Reboiler Heating	0.109	kWh
C1	Condenser Cooling	0.090	kWh
H-C1-TOP	TCS Cooling	0.004	kWh
H-C1-BOT	STC Cooling	0.001	kWh

[a] reactor effluent compression not included in optimal design identified.

D.2. Process Optimization

Solution of the optimization formulation was carried out using a hybrid algorithm developed in-house. The algorithm uses two-stage approach based on use of an “inner” and “outer” iteration step. The outer step was designed to handle selection of new trial conditions for the entire process. The inner step then refines trial conditions relating to distillation column to enforce the 99wt% product purity constraint constraints. This is shown in Figure D.3.

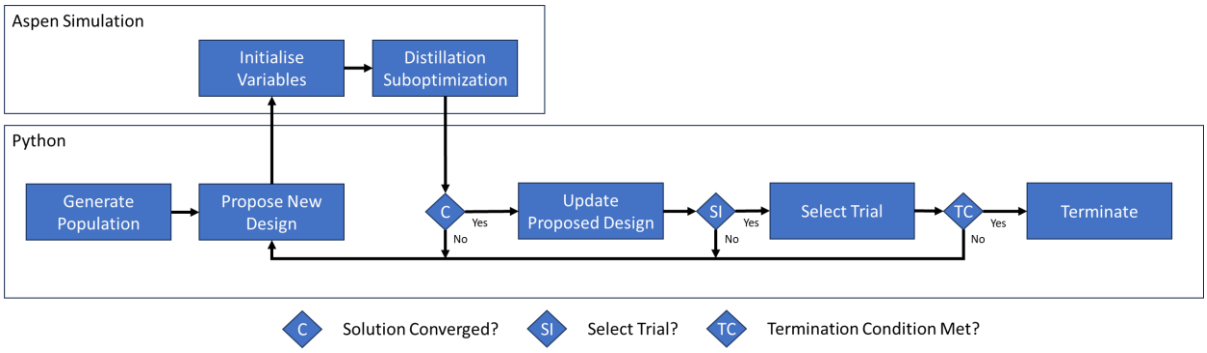


Figure D.3: Illustration of major stages of the hybrid solution method employed during optimization of the TCS process.

Master Problem Solver

Generation of new trial conditions for the entire process (outer step) was done using a Differential Evolution method. A population of 200 individuals was used. Offspring were generated according to the BEST\1\bin method and the mutation rate of each generation was selected randomly from a uniform distribution between 0.5 and 1.0. The crossover rate was held constant at 0.7. Selection of the initial population was done in a way that ensured coherence with the inequality constraints set in the objective formulation.

Subproblem Solver

Distillation column conditions were adjusted using the derivative-based solver in Aspen V11 software. A maximum of 200 iterations were allowed to achieve convergence and the principle of Lamarckian Inheritance was used to update genetic information of trial candidates following successful convergence. Convergence was defined as conditions with purity within an absolute tolerance of 0.0001 wt% of the equality conditions.

D.3. More on Cost Calculation Parameters

A summary of parameters used to calculate operational costs is provided in Table C.1. Parameters associated with the calculation of equipment capital cost associated with purchasing is provided in Table D.2, information on calculations of bare module cost associated with equipment is then provided in Table D.3, and information on bare module factor values is provided in Table D.4.

Table D.2: Parameters for calculating utility costs using the cost correlations of Ulrich and Vasudevan [172]

Utility	Cost Coefficients		Definitions
	a	b	
Process Steam, $/kg	$2.3 \times 10^{-5} \dot{m}_s{}^{-0.9}$	$3.6 \times 10^{-3} p_g$	m_s steam capacity (kg/s) p_g is process steam gauge pressure (bar)
Hot Media, $/kJ	$6.0 \times 10^{-7} \dot{Q}_H{}^{-0.9} T^{0.5}$	$6.0 \times 10^{-7} \dot{Q}_H{}^{-0.9} T^{0.5}$	$\dot{Q}_H$ is the heating capacity (kJ/s)
Cooling Water, $/m³	$2.3 \times 10^{-5} + 2.3 \times 10^{-5} \dot{q}^{-1}$	3×10^{-3}	$\dot{q}$ is the total water capacity (m^3/s)
Refrigeration, $/kJ	$0.5 \times \dot{Q}_c{}^{-0.9} T^{-3}$	$1.1 \times \dot{Q}_c{}^{-0.9} T^{-3}$	$\dot{Q}_c$ is the cooling capacity (kJ/s) T operating temperature (K)

Table D.3: Parameters used in calculating purchase costs of equipment using the cost correlations of Sinnott and Towler [168]

Equipment	Capacity Information			Cost Coefficients			Use
	Unit	Lower Limit	Upper Limit	a	b	n	
Pressure Vessel, vertical [a]	Shell mass, kg	160		10,000	29	0.85	Distillation columns Reactors Flash condensers
Sieve Trays	Diameter, m			110	380	1.80	Distillation Column
Compressor, centrifugal	Driver power, kW	75	30,000	490,000	16,800	0.60	Gas compressor
U-Tube Shell and Tube Heat Exchanger	Area, m^2	10	500	24,000	46	1.20	Heat exchanger Distillation condenser
U-tube kettle reboiler	Area, m^2	10	500	25,000	340	0.90	Distillation reboiler

[a] based on stainless steel unit.

Table D.4: Parameters used for calculating the bare module cost of individual equipment according to Guthrie's method [204]. Values taken from those listed by van Amsterdam [170].

Equipment	Factor, F_{BM}
Compression Unit	2.15
Heat Exchanger, shell and tube	3.17
Heat Exchanger, U-tube kettle reboiler	3.17
Pressure Vessel, vertical	4.16

Appendix E: Process Modelling of Aminopropyltriethoxysilane

Production of APTES has been assumed to occur using trichlorosilane as a feedstock reagent by following three-stage reaction of hydrosilylation followed by alkoxylation and ammoniation. All stages are modelled using information exclusively from patent literature. Operating conditions have been set based on a mixture of subprocess optimization and engineering judgement.

In all cases, this has been carried out in the using the Aspen Plus V11 process simulation software. In all cases, vapour-liquid equilibria were modelled using the NRTL-RK method. Further information on modelling of each stage is provided in the following subsections.

E.1. Production of 3-chloropropyltrichlorosilane, APTCS

Production of 3-chloropropyltrichlororsilane (CPTES) was modelled according to continuous production via hydrosilylation of trichlorosilane with allyl chloride (e.g. [122, 205, 206]). A conceptual process flow diagram of the entire process is shown in Figure E.1.

Reaction Stage

Reaction was assumed to involve use a reactive distillation column using a platinum-based catalyst solvent solvated in 1-dodecene [136]. Reaction conditions and duties were taken directly from those values reported in [136]; for simplicity, materials were assumed to be fed to the reactor at a pressure of 2.5 bar and 100 C [136]. Catalyst recycling was not considered [136]. Purification of crude product was assumed to occur using a three-stage direct distillation sequence based on prior art [176].

$$C_3H_5Cl + Cl_3SiH \rightarrow Cl_3Si(C_3H_6Cl) \quad \text{(E.1)}$$

Property Estimation

Property estimation was required for the propyltrichlorosilane (PTCS) co-product. Critical temperature, pressure, and volume of PTCS were estimated by the method of Lyderson [207]; these values were used to calculate the critical compressibility factor of PTCS. Ideal gas heat capacity of PTCS was estimated using the method of Benson [208]. Heat of vaporisation was

estimated using the method of Vetere [209]. All models were based on implementations available in the Aspen Plus V11 software.

Distillation Column Specifications

Modelling of all columns was done using the Fenske-Underwood-Gillian-Kirkbride (FUGK) shortcut method [76]. Conditions for columns C1 to C3 were set at 1 bar pressure, while pressure of column C4 was set to 0.05 bar. A reflux ratio of 1.2 times the theoretical minimum was targeted for all columns based on common heuristic that this reflects financially optimal conditions [210].

Operation of column C1 was set to ensure that: 1) recycle of all chloride and trichlorosilane at a rate that caused purity of the reactor inlet stream of 99 wt%, and 2) mass ratio of 99:1 for combined allyl chloride and trichlorosilane compared to silicon tetrachloride entering column C2.

Operation of column C2 was set to achieve a recovery of silicon tetrachloride and propyltrichlorosilane in proportions that enabled 1) their recovery as sellable products in column C3, and 2) 99 wt% recovery of CPTCS in the bottoms. Operation of column C3 was set to achieve production of silicon tetrachloride and CPTCS of 99 wt% each. Operation of column C4 was set to produce CPTCS distillation and dodecene residual bottoms at product purities of 99 wt% each.

Performance specifications for each column was achieved according to minimizing the quadratic error associated with each design specification (see Equation E.2) using heavy and light key split of each distillation column as decision variables.

$$\min \sum_{i} (x_i - y_i)^2 \tag{E.2}$$

Where x_i is the observed product purity and y_i targeted product purity.

The process flow diagram used to model heat flows in the process is shown in Figure E.2. A breakdown of energy flows associated with process modelling equipment is provided in Table E.1.

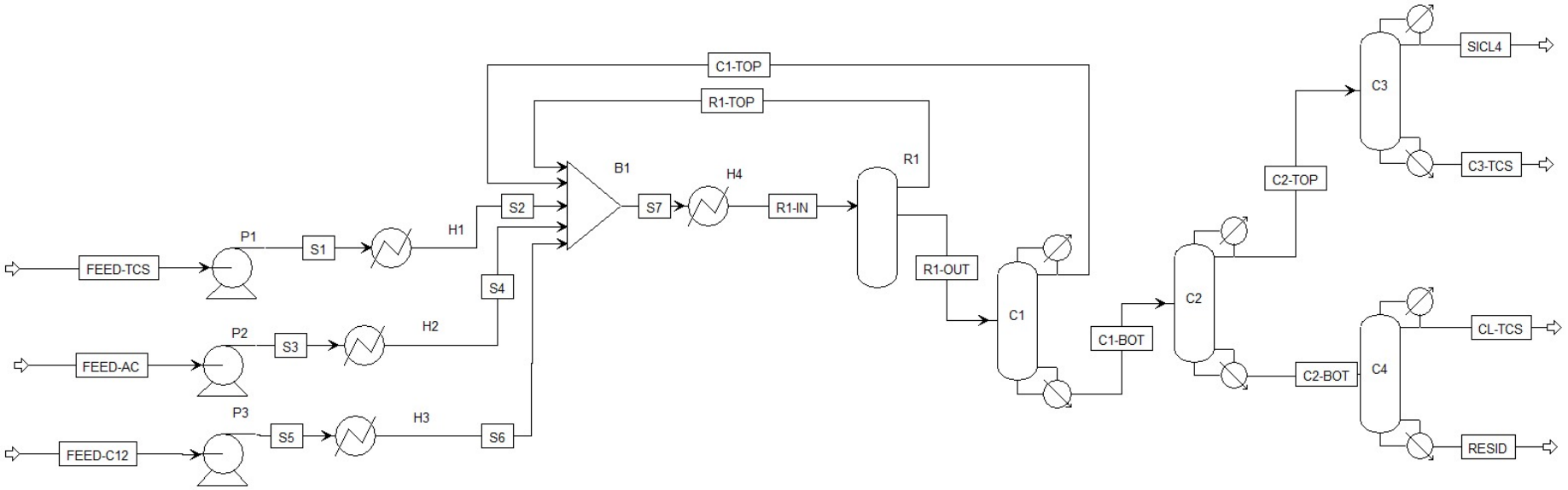


Figure E.1: Conceptual process flow diagram of the process used to model production of 3-aminopropyltriethoxysilane.

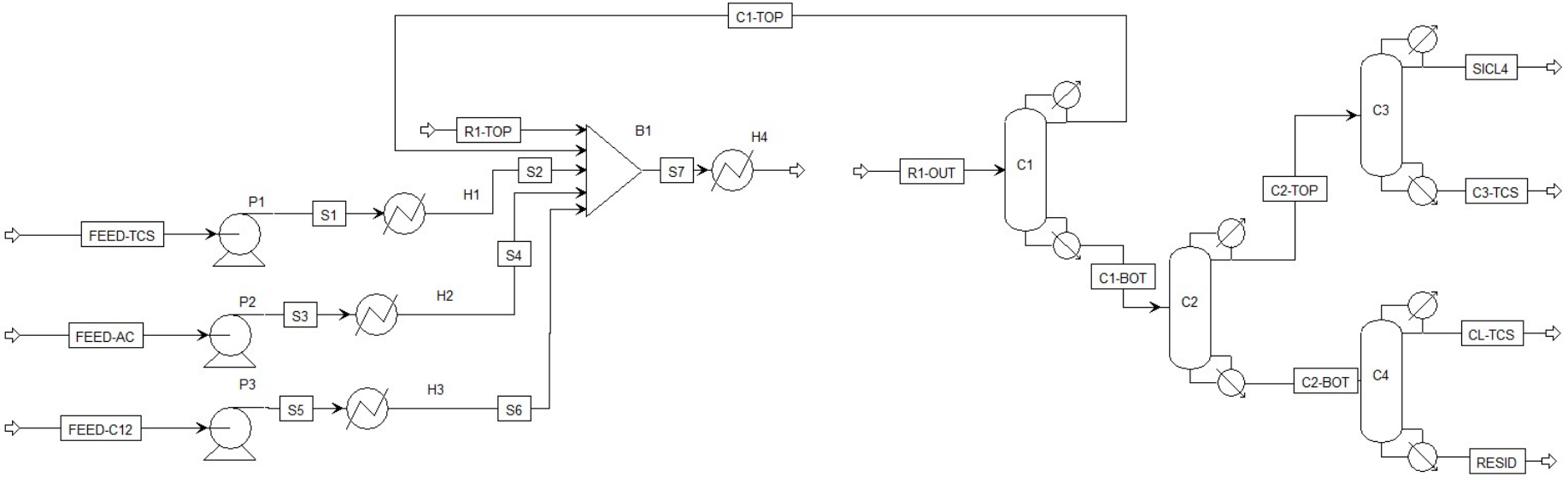


Figure E.2: Process flow diagram of Aspen Plus model approximating the production of 3-chloropropyltrichlorosilane. Note: Reactor R1 is not modelled explicitly to reflect reaction conditions, mass flows and duties being taken as values reported in [136].

Table E.1: Predicted energy flows for equipment used in the production of 1kg of 3-chloropropyltrichlorosilane.

Equipment	Description	Amount	Unit
P1	Trichlorosilane Pumping	<0.001	kWh
P2	Allyl chloride pumping	<0.001	kWh
P3	Dodecene pumping	<0.001	kWh
H1	Trichlorosilane heating	0.031	kWh
H2	Allyl chloride heating	0.116	kWh
H3	Dodecene heating	0.075	kWh
H4	Reactor inlet heating	0.008	kWh
R1	Reactor condenser	0.002	kWh
R1	Reactor reboiler	0.002	kWh
C1	Distillation condenser	0.023	kWh
C1	Distillation reboiler	0.057	kWh
C2	Distillation condenser	0.027	kWh
C2	Distillation reboiler	0.040	kWh
C3	Distillation condenser	0.007	kWh
C3	Distillation reboiler	0.008	kWh
C4	Distillation condenser	0.086	kWh
C4	Distillation reboiler	0.059	kWh

E.2. Production of 3-chloropropyltriethoxysilane, CPTES

Production of 3-chloropropyltriexthoxysilane, $(C_2C_5O)_3Si(C_3H_6Cl)$, was assumed to occur according to the alkoxylation of 3-chloropropyltrichlorosilane, $Cl_3Si(C_3H_6Cl)$, with ethanol (Equation E.3).

$$Cl_3Si(C_3H_6Cl) + 3C_2C_5OH \rightarrow (C_2C_5O)_3Si(C_3H_6Cl) + 3HCl \quad \text{(E.3)}$$

A stoichiometric molar ratio (3:1) of CLTCS to ethanol assumed [211]. Conversion was assumed to complete, producing a CPTES product requiring no further purification, which was cooled and stored. CPTES was assumed to condense upon formation, separating naturally from the gas-phase reaction. Subsequent processing therefore involved cooling of the reactor products. No side reactions were considered. Separation of hydrogen chloride by product was done using a single flash condensation stage. A summary of the process is shown in Figure E.3. Property estimation was also required for some information.

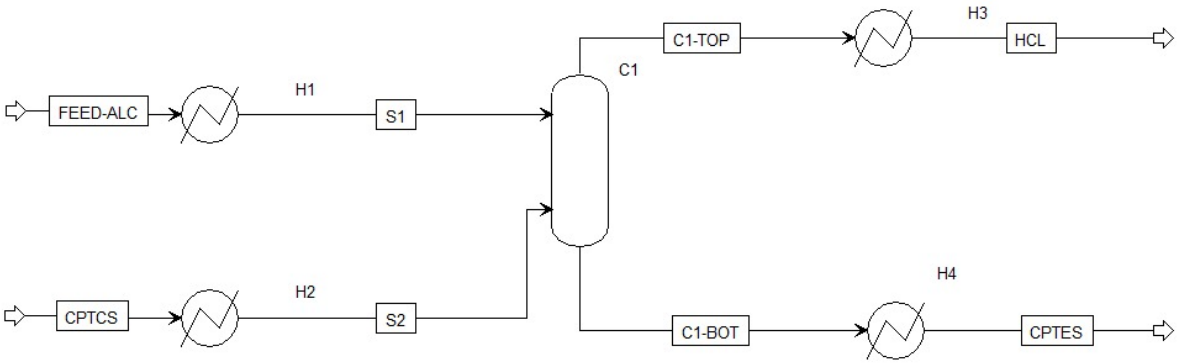


Figure E.3: Process flow diagram of the used to model production of 3-chloropropyltriethoxysilane. CPTCS: 3-chloropropyltrichlorosilane, HCl: hydrogen chloride, CPTES: 3-chloropropyltriethoxysilane

Reactor heating duty was estimated based on contributions from the heat of reaction (-162 kJ/mol) and the heat of vaporization (57 kJ/mol) to reflect the boiling point of APTES (230 C) being higher than operating conditions of the column (100 C).

Property Estimation

Property estimation was required for CPTES. Heat of vaporisation was estimated as 47 kJ/mol based on use of the Clausius-Clapeyron equation with boiling points of 250 and 100 C at pressures of 1atm and 1.3158×10^{-2} atm reported on ChemSpider [212] . Heat of reaction was estimated as 54 kJ/mol. Duty associated with cooling the CPTES product to room temperature was estimated based on a specific heat capacity of 417 J/mol·K; this value is an estimate based on a modified form Kopp's rule [213].

A breakdown of energy flows associated with process modelling equipment is provided in Table E.2.

Table E.2: Predicted energy flows for equipment used in the production of 1kg of 3-chloropropyltriethoxysilane.

Equipment	Description	Amount	Unit
H1	3-chloropropyltrichlorosilane heating	0.019	kWh
H2	Ethanol heating	0.188	kWh
R1	Reactor cooling	0.137	kWh
H3	Hydrogen chloride cooling	0.009	kWh
H4	3-chloropropyltriethoxysilane cooling	0.041	kWh

E.3. Production of 3-aminopropyl triethoxysilane, APTES

Model Assumptions

Production of APTES was modelled as occurring from the ammoniation of 3-chloropropyltriethoxysilane (Equation E.4). The reaction and initial separation stages were assumed to occur under batch processing conditions typical of patent art [178, 214] as shown in Figure E.4.

$$(C_2C_5O)_3Si(C_3H_6Cl) + 2NH_3 \rightarrow (C_2C_5O)_3Si(C_3H_6H_2) + NH_4^+Cl^- \quad \text{(E.4)}$$

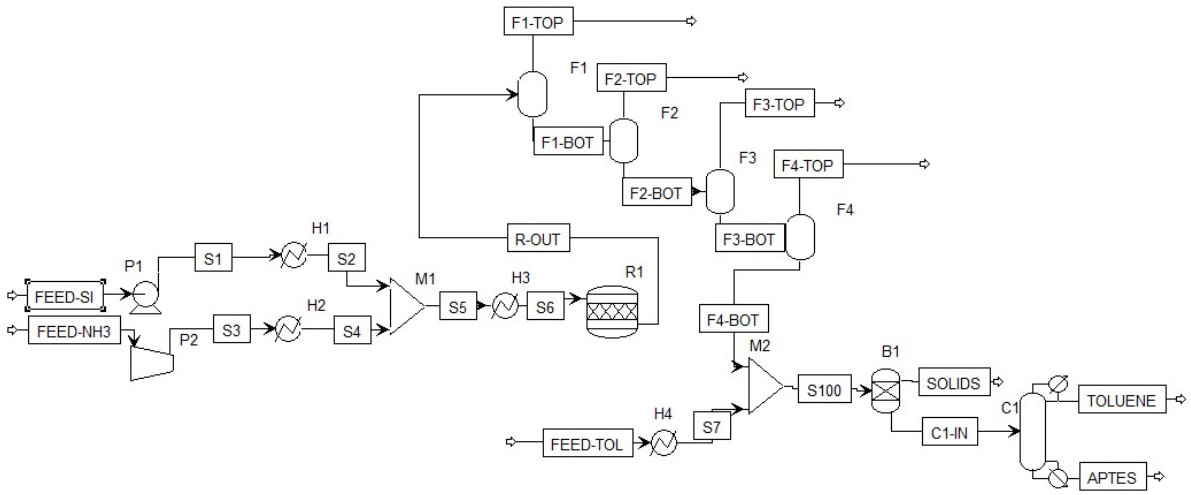


Figure E.4: Process flow diagram of the used to model production of 3-aminopropyltriethoxysilane in Aspen V11 software.

Reaction was assumed to occur at conditions of 100 C and 50 bar pressure. Ammonia and CPTES were introduced in mole ratios of 30:1 [178]. Total conversion of CPTCS was assumed to be 95 % with a selectivity of 100% [215]. Separation of ammonia was modelled as occurring by a four-stage off-gassing based separation based on the patent of Evonik Operations GmBH [178].

Subsequent separation of ammonium chloride from the crude stream was carried out according to precipitation induced by a toluene solvent wash. Solvent washing was done using 1 L (~0.870 kg) of toluene per batch [214]. Mass recovery of the APTES crude product by the washing procedure was assumed to be 97% [215].

Separation of the toluene and APTES reagent was assumed to be done by distillation at 1 bar. Modelling of the distillation process was done using the Fenske-Underwood-Gillian-Kirkbride shortcut method shortcut method [76]. Assuming a reflux ratio of 1.2 times the theoretical

minimum required to achieve product purities of 99 wt% and 99.5 wt% for APTES and toluene respectively.

A breakdown of energy flows associated with process modelling equipment is provided in Table E.3.

Table E.3: Predicted energy flows for equipment used in the production of 1kg of 3-aminopropyltriethoxysilane.

Equipment	Description	Amount	Unit
P1	3-chloropropyltriethoxysilane pumping	0.004	kWh
P2	Ammonia compression	0.777	kWh
H1	3-chloropropyltriethoxysilane heating	0.068	kWh
H2	Ammonia heating	0.743	kWh
H3	Reactor inlet heating	0.54	kWh
R1	Reactor cooling	0.270	kWh
F1	Off gassing stage 1	0.135	kWh
F2	Off gassing stage 2	<0.000	kWh
F3	Off gassing stage 3	<0.000	kWh
F4	Off gassing stage 4	<0.000	kWh
H4	Toluene heating	0.007	kWh
B1	Solids filtration	[a]0.000	kWh
C1	Distillation condenser	0.155	kWh
C1	Distillation reboiler	0.068	kWh

[a] no duty associated with filtration.

Appendix F: Process Modelling of Octyltrimethoxysilane

Production of octyltrimethoxysilane (OCTMS) was modelled assuming a two-stage process in which trichlorosilane undergoes methoxylation to form trimethoxysilane (TMS) followed by hydrosilylation with 1-octene to form OTMS. Modelling of the methoxylation stage is based on the patent art of Schinabeck *et al*. [124]; hydrosilylation was modelled according to patent art reported by action information of Tachikawa and Takei [131]. In all cases, vapour liquid equilibria were modelled according to the NRTL-RK method.

F.1. Production of octyltrichlorosilane, OTCS

Production of octyltrichlorosilane (OTCS) was assumed to according to hydrosilylation of trichlorosilane with 1-octene (Equation F.1) followed by distillation separation. This has been carried out using the using the Aspen Plus V11 process simulation software. The process model used is shown in Figure F.1.

$$C_8H_{21} + Cl_3SiH \rightarrow Cl_3Si(C_8H_{21}) \quad \text{(F.1)}$$

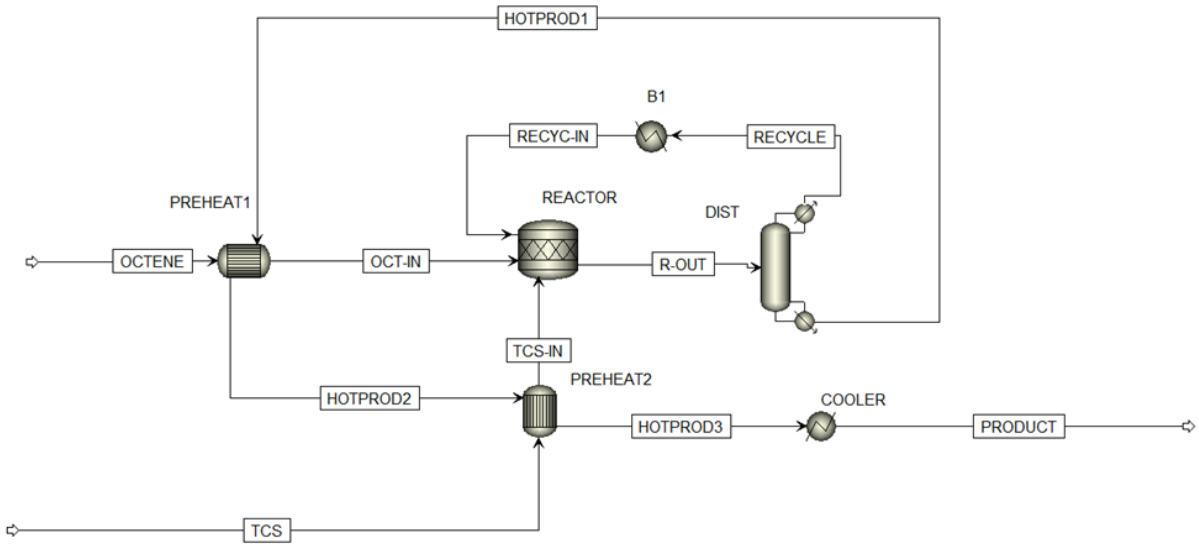


Figure F.1: Process flow diagram of the process used to model the production of octyltrichlorosilane in the Aspen V11 software. TCS: trichlorosilane

Reaction conditions were taken as 70 C and 1 bar, with 1-octene being provided in a 25% molar excess [129]. A TCS conversion of 95% with no side reaction product formation was assumed.

It was assumed that catalyst was suspended within the 1-octene fluid without need of a separate solvent [129]. Synthetic products of the reaction were separated by evaporation of residual alkene within a distillation column operating at 1 bar. The separated alkene was recycled to the reactor [216]. Operating conditions of the column were set to achieve a product purity of 98wt%

Modelling of the distillation column was done using the Fenske-Gillian-Underwood-Kirkbride method. This is justified given significant differences in the boiling point of octene and octyltrichlorosilane product. The heat of reaction was assumed to be 160 kJ/mol [162].

Property Estimation

Property estimation was required to model some aspects of production. The heat of reaction was assumed to be 160 kJ/mol. Specific heat capacity of the liquid phase was estimated using a modified form Kopp's rule [213]. NRTL binary parameters for octyltrichlorosilane were taken from parameters estimated for 1,1,1-trichlorononane (the carbon analogue of OTCS) using the UNIFAC method. A summary of estimated parameters is provided in Table F.1

A breakdown of energy flows associated with process modelling equipment is provided in

Table F.21.Table E.1

Table F.1: Binary interaction parameters used for modelling liquid equilibria via the NRTL method while modelling the production of octyltrichlorosilane.

Component 1	Component 2	Interaction Parameters				
		A_{ij}	A_{ji}	B_{ij}	B_{ji}	C_{ji}
TCS	Octene	0	0	402.922	-217.335	0.3
TCS	OTCS	0	0	-42.5218	-8.84201	0.3
Octene	OTCS	0	0	126.425	-113.573	0.3

Table F.2: Predicted energy flows for equipment used in the production of 1kg of octyltrichlorosilane.

Equipment	Description	Amount	Unit
PREHEAT1	Octene heating	0.029	kWh
PREHEAT2	Trichlorosilane heating	0.045	kWh
REACTOR	Reactor heating	0.197	kWh
DIST	Distillation condenser	0.004	kWh
DIST	Distillation reboiler	0.072	kWh
Cooler	Octyltrichlorosilane cooling (to 100 C)	0.076	kWh
H3	Octyltrichlorosilane cooling (100C to 25 C)	0.033	kWh

F.2. Production of octyltrimethoxysilane, OTMS

Production of octyltrimethoxysilane was assumed to occur according to the methoxylation of octyltrichlorosilane. It was assumed that this was done using a continuous reaction column design [217]. As per Figure F.2, this involved a use of a reaction column which acts to simultaneously produce and separate octyltrimethoxysilane and hydrogen chloride [217]. Property estimation was also required for some information.

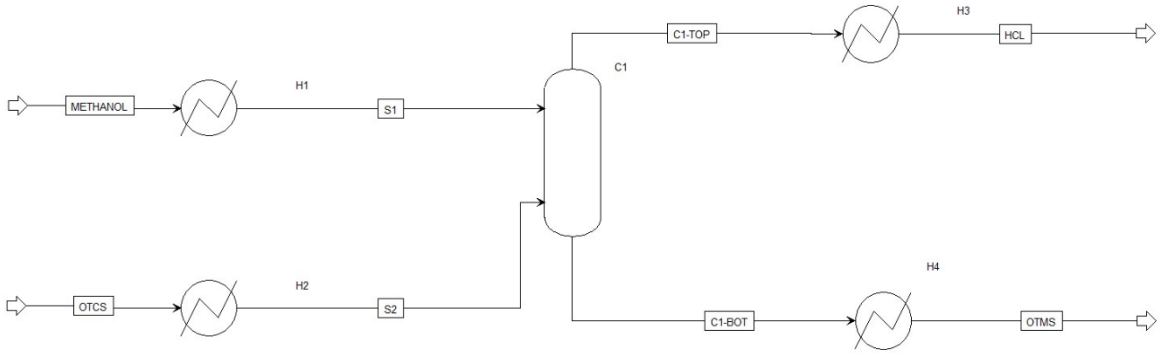


Figure F.2: Process flow diagram of the process modelled for octyltrimethoxysilane production. OTCS: octyl trichlorosilane, OTMS: octyltrimethoxysilane, HCl: hydrogen chloride.

Reaction Stage

Reaction conditions were assumed to be under atmospheric pressure and temperatures 90 C [125, 217]. A molar ratio of methanol to OTCS of 3.3:1 was assumed to be fed to the reactor [217]. Conversion of the octyltrichlorosilane was assumed to be complete and the product was assumed not to require further purification [217]. Hydrogen chloride is assumed to be recovered as a material of value [125].

Separation Stage

Separation of OTMS product was assumed to occur naturally in the column due to the high boiling point of the compound (192 C). Separation of Hydrogen chloride and residual methanol was assumed to occur under equilibrium flash-stage by cooling methanol to room temperature (25C).

Property Estimation

Heat of reaction was estimated as -54 kJ/mol based on average bond dissociation energies available in literature for silicon compounds [218], hydrogen chloride bond dissociation energies of organic molecules, and methanol [219].

A breakdown of energy flows associated with process modelling equipment is provided in Table F.3.

Table F.3: Predicted energy flows for equipment used in the production of 1kg of octyltrimethoxysilane.

Equipment	Description	Amount	Unit
H1	Ethanol heating	0.144	kWh
H2	Octyltrichlorosilane heating	0.029	kWh
R1	Reactor cooling	0.260	kWh
H3	Hydrogen chloride cooling	0.007	kWh
H4	Octyltrimethoxysilane cooling	0.049	kWh